ISTANBUL TECHNICAL UNIVERSITY ★ GRADUATE SCHOOL OF SCIENCE ENGINEERING AND TECHNOLOGY

GEOTECHNICAL RISK ASSESSMENT FOR BUILDINGS ADJACENT TO DEEP EXCAVATIONS

Ph.D. THESIS

Zeynep ASLAY
(501052303)

Department of Civil Engineering

Soil Mechanics and Geotechnical Engineering Programme

Thesis Advisor: Prof. Dr. Derin URAL

APRIL 2012

İSTANBUL TEKNİK ÜNİVERSİTESİ ★ FEN BİLİMLERİ ENSTİTÜSÜ

DERİN KAZILARA KOMŞU YAPILAR İÇİN GEOTEKNİK RİSK ANALİZLERİ

DOKTORA TEZİ

Zeynep ASLAY
(501052303)

İnşaat Mühendisliği Anabilim Dalı

Zemin Mekaniği ve Geoteknik Mühendisliği Programı

Tez Danışmanı: Prof. Dr. Derin URAL

NİSAN 2012

Zeynep Aslay, a **Ph.D.** student of ITU **Institute of / Graduate School of Science Engineering and Technology** student ID **501052303**, successfully defended the **thesis/dissertation** entitled "**GEOTECHNICAL RISK ASSESSMENT FOR THE BUILDINGS ADJACENT TO DEEP EXCAVATIONS**", which she prepared after fulfilling the requirements specified in the associated legislations, before the jury whose signatures are below.

Thesis Advisor:	**Prof. Dr. Derin URAL** Istanbul Technical University	....
Jury Members:	**Prof. Dr. Mete İNCECİK** Istanbul Technical University	....
	Prof. Dr. Kutay ÖZAYDIN Yıldız Technical University	....
	Assoc. Prof. Dr. Recep İYİSAN Istanbul TechnicalUniversity	....
	Assoc. Prof. Dr. Sami O. AKBAŞ Gazi University	....

Date of Submission : 09 January 2012
Date of Defense : 13 April 2012

To my parents and my brother,

For their support and love.

FOREWORD

I would like to thank to the respectful members of Soil Mechanics and Geotechnical Department of Istanbul Technical University for giving me the chance to study my PhD in ITU. I specially would like to tell my regards to my supervisor Prof. Derin Ural for spending their valuable time and guidance on my thesis.

I also want to thank to all colleagues in ENAR Eng. Arch. and Cons. for their support and patience. M.Sc. Civil Engineer Mehmet Altun is another person to be thanked, for his help during site investigations and for sharing his knowledge about engineering and steel complexes. Also appreciate the efforts of M.Sc. Civil Engineer Hakan Dinç and thanking him for his patience during monitoring that made this research convincing.

I am grateful for the help of Assoc. Prof. Dr. Oğuzhan Akbaş, during understanding the reliability process, performing the calculations and interpretation of the results. He helped this research to cover a noteworthy distance.

Special thanks are due to Prof. Dr. Ahmet Sağlamer for spending his precious time on this thesis, giving his knowledge and interest. Under his guidance the main idea of this thesis was born and the research was formed. I would like to thank him for believing in me on the way to be a Doctor. This research could not be completed without his support and trust.

My family deserves the most beautiful things in the life. They never left me alone and supported me in whatever I want to try. Thanking is not enough, I owe them my life.

April 2012 Zeynep ASLAY
(MSc. Civil Engineer)

TABLE OF CONTENTS

Page

ABBREVIATIONS

AFOSM	**:** Advanced First Order Second Moment
AIS	**:** Adaptive Importance Sampling
AMV	**:** Advanced Mean Value
CDF	**:** Cumulative Distribution Function
COV	**:** Coefficient of Variation
CPT	**:** Cone Penetration Test
FE	**:** Finite Element
FORM	**:** First Order Reliability Method
FOSM	**:** First Order Second Moment
FPI	**:** Fast Probability Integration
HS	**:** Hardening Soil
HSsmall	**:** Hardening Soil Small Strain
ISAMF	**:** Radius Based Importance Sampling
JPDF	**:** Joint Probability Density Function
JR	**:** Joint Rock
MC	**:** Mohr-Coulomb
MCC	**:** Modified Cam-Clay
MCS	**:** Monte Carlo Simulation
MLD	**:** Master Logic Diagram
MPP	**:** Most Probable Point
n	**:** number of samples
PDF	**:** Probability Density Function
PEM	**:** Point Estimate Method
RBD	**:** Reliability Based Design
SOF	**:** Scale of Fluctuation
SORM	**:** Second Order Reliability Method
SPT	**:** Standard Penetration Test
SSC	**:** Soft Soil Creep
SwRI	**:** Southwest Research Institute
UD	**:** User Defined
USCS	**:** Unified Soil Classification System

LIST OF TABLES

Page

LIST OF FIGURES

Page

GEOTECHNICAL RISK ASSESSMENT FOR BUILDINGS ADJACENT TO DEEP EXCAVATIONS

SUMMARY

“Which risks may appear during the project?, “How do they affect the system? (What are the results?) and How they can be prevented?” are the main questions to be asked before starting a project. As a general definition; risk is the probability of failure on the system resulting with adverse effects on health, property and environment. Risk in engineering systems may manifest itself to cracks on the structure, cause non-serviceability in some parts and even collapse of the whole system. In geotechnical engineering, risk can be explained as exceeding the earth pressures and/or bearing capacity, exceeding any limit state, losing the serviceability or collapse in the system, causing loss of money or even life.

Risk assessment and reliability analyses may be applied to any engineering projects. Reliability of a building against corrosion, poor workmanship in pouring concrete, reliability of the cover material of a spaceship against friction during atmospheric action may be subjects for reliability analyses. On the other hand, geotechnical engineers deal with earth, which is formed by various geologic processes that is impossible to “win against”. However, determining the risks before starting a project can give the contractor, the employer and the engineer/consultant, the opportunity to understand the reasons and get measures to prevent the system at least from a collapse and loss of life.

There are several methods to estimate the risk or the probability of failure such as; first order reliability method (FORM), second order reliability method (SORM), Mean value first order second moment method, the Radius-based Importance Sampling (ISAMF), Adaptive Importance Sampling (AIS), Monte Carlo method (MCS), and etc.

Reliability of a system depends on the reliability of its individual elements and the reliability of the combination as a whole. Modeling schemes for reliability analysis for a system, such as reliability block diagram, fault tree, success tree, event tree methods, failure mode and effect analysis; and master logic diagram can be created. Fault tree analyses has been used in this research in order to determine elements cause failure and identify the probability of failure of the whole retaining system of the deep excavation.

In literature, researchers are generally focused on the risk assessment of slopes and earthquake (seismic) effects. Some of them used common reliability methods, some created their own methods. The common aim of all projects is to determine the uncertainties, assess the risk due to these uncertainties, and find the reliability of the system, such as the slope, building, retaining structure for an excavation, etc. Variability and uncertainty in geotechnical engineering projects, settlement of foundations, stability of slopes, and performance of dams, off-shore platforms, and deep excavations are the main topics subjected to reliability analyses. For example,

Peck has investigated deformations of deep excavations and stands for the idea that the most effective factor that affects deformations on retaining structures is neither the rigidity of the structure nor the distance between lateral supports, but is the property of the soil surrounding the system. He classifies the displacements and settlements due to soil type. Clough and O'Rourke (1990), Liu et al. (2005), Roboski et al. (2006) and Park et al. (2007) are some of following researches studied on deep excavations and their reliability.

Performance of deep excavations is the main subject of this research. Determination of the effect of parameter variations on the reliability of a retaining system for deep excavations has been targeted. The reliability of the system has been investigated considering the settlement of neighboring structures. A correlation between the settlement of adjacent structures and the excavation system reliability has been examined.

For this purpose, a detailed monitoring has been conducted on a 24m wide, 40m long and 13.0m deep scale pit excavation in a steel complex and the excavation has been monitored from the beginning till the last level of the struts have been removed. The measured and predicted horizontal and vertical displacements and pipe loads are compared to verify the model accuracy.

The system was first modeled with the parameters obtained from soil borings during site investigations at the beginning of the project. Then the soil parameters obtained from the tests during excavation of the scale pit has been used to model the system and the results of these two FE models were compared to the monitoring readings taken during excavation and construction of the structure inside. The comparing results showed that the predicted results from the model using soil parameters obtained during excavation give more accurate results and similar deformations are gained with the monitoring results.

Following this verification, the soil profile has been idealized and the system has been modeled again in this soil profile. For the FE analysis the soil profile has been varied by the soil parameters created by point estimate method (PEM), suggested by Schweiger et al. (2001). 132 analysis were performed in order to determine the lateral displacement of the retaining structure and settlement behind it and analyze the effect of soil parameter variations on the system reliability. The target reliability index (β) has been established as 2.2 according to the monitoring results and data in literature for service limit state. NESSUS software, which was developed by Southwest Research Institute, was used for reliability analysis.

Depending on the analyses the results below have been obtained:

- Increasing wall stiffness tends to reduce system movements, but this is most effective in soft to medium clays. On the other hand, support spacing is more important than wall stiffness in defining system stiffness and helping control movements. It is important because movements in strutted systems occur just after excavation phase and cannot be reduced after placement of struts.
- Horizontal displacements on piles of excavations, which are laterally supported with struts, occur at the excavation stage at the excavation level. Thus, the settlement behind the retaining system occurs in a hyperbolic shape. The settlement increases with distance from excavation at first and lasts at a distance of twice the maximum excavation depth.
- The variation in ϕ and c with the calculated coefficient of variation (COV) of

the parameters is not that effective on the probability of failure of the system. Changing the ϕ and c and E with the maximum COV in the literature, which represents the case that the geological profile in the field vary on the edge or the soil parameters may be incorrect, helped to understand the effect of parameter fluctuations on the system displacement and reliability.

- Using point estimate method (PEM), developed by Schweiger et al. (2001), in combination with finite element analysis can help reducing budget of site investigations by creating realistic artificial models, reducing time for modeling, and can allow optimal decisions with less certainty in the properties of the layers in the soil profile.
- The magnetic column readings at the site confirmed that the ground movement lie in between $S_v(max) = 0.25S_h(max)$ and $S_v(max) = 0.5S_h(max)$ for the soil profile of Scale Pit, while it is $S_v(max) = 0.5S_h(max)$ and $S_v(max) = S_h(max)$ according to Mana and Clough (1981). The ground movements are substantially small because of the dimensions of the excavation is small and the soil profile behind the retaining system is stiff.
- The horizontal displacements and settlements conducted during analyses are less than 0.1% and 0.3% of the maximum excavation depth, respectively and are related with a ratio of $0.4S_h<S_v<1.0S_h$. While, the same range was obtained as $0.25S_h< S_v < 0.5S_h$, during the measurements on the site.
- For temporary retaining systems of deep excavations target reliability index may be chosen as 2.2, which allows a 1.1% probability of failure in the system.
- It can be said that the reliability of the system is over target reliability, where soil parameters vary at lower and upper limits of E. However, the reliability of the system is under target reliability when COV is maximum with lower limit of E. This is because; fluctuations in the soil parameters vary on the edges and its affect doubles when E is also in the lower limits.
- When the reliabilities due to S_h and S_v have been compared to the reliability of the system, it is clear that S_v is the significant criteria for the system reliability and system is weak when the lower limit of E is chosen while the COV of soil parameters is at maximum.
- When E is calculated with its upper limits and average COV the system becomes over reliable. When it is calculated with COV max in the literature, the reliability decreases sharply. This is because the uncertainties in the system increases sharply, as the fluctuations, variations in the soil conditions and soil parameters increase, causing the reliability of the parameters and system to decrease.
- In order to determine the most effective soil parameter on the system deformations, sensitivity analyses were performed by using VIPlaxis 9.2 software. The results of the analyses with different variations of soil parameters also showed that the most important soil parameter is the Young's Modulus, E. The most sensitive E is the Medium Stiff Silty Clay's, with an average 40-50% sensitivity, on the horizontal displacements on the pile. For vertical displacements behind the retaining system we can also say that E of medium stiff silty clay is most effective for the distances where heave occurs and E of dense sand-gravel layer is effective at the distance far from 0.75Hmax from the system where settlement occurs.
- In soft clay conditions the horizontal movements tend to average about 1.5% of maximum excavation depth, Hmax and vertical movements about 1.2% of

Hmax, when reached to maximum excavation depth.

- The reliability of the system in soft clay, is under target reliability and probability of failure of the system is about 90%, depending on the soft soil conditions and low, c and E values. For such soft clay conditions, rigidity of the system should be increased and the strut spacing should be closer at the horizontal and vertical directions. Also, from the FE analyses diagrams, we can say that the base of the excavation in front of the piles should be strengthened against heave and opening in the socket of the pile.
- Limit conditions, such as settlement, horizontal displacement, angular distortion limits for retaining walls or crack width limits for superstructures may be differ from site to site and even from employer to employer, of course to be under limits that are specified by the standards. The limit values for each element affecting the system reliability should be determined precisely before starting the design. This is because the limit values affect the reliability conditions and systems are specified as reliable or unreliable due to those limits.

DERİN KAZILARA KOMŞU YAPILAR İÇİN GEOTEKNİK RİSK ANALİZLERİ

ÖZET

"Proje sırasında hangi riskler oluşabilir?, "Bunlar sistemi nasıl etkiler? (Sonuçları nelerdir?) ve Nasıl engellenebilirler?" gibi sorular bir projeye başlamadan once sorulması gereken ana sorulardır. Genel olarak risk, insan hayatı, mülk ve çevre üzerinde kötü etki ile sonuçlanacak olan, sistemin göçme ihtimalidir. Mühendislik sistemlerinde, risk yapılarda çatlakların oluşması, bazı bölümlerin servis veremez hale gelmesi ve hatta tüm sistemin göçmesi olarak değerlendirilebilir. Geoteknik mühendisliğinde, bu durum, toprak basınçlarının veya taşıma kapasitesinin aşılması, limit durumlara ulaşılması, hizmet verememe veya sistemin para ve mal kaybına neden olacak şekilde göçmesi olarak tanımlanabilecektir.

Risk tahminleri ve güvenilirlik analizleri birçok mühendislik projesinde uygulanabilir. Korozyona karşı bir binanın güvenilirliği, beton dökümünde kötü işçilik, uzay gemisinin kaplama malzemesinin atmosfere girişteki sürtünmeye karşı güvenilirliği gibi konular güvenilirlik analizlerini gerektirebilir. Diğer yandan, geoteknik mühendisliği, çeşitli jeolojik süreçlerle oluşmuş doğaya karşı çalışmaktadır ki bu kazanılması imkansız bir savaştır. Ancak, projeye başlamadan önce risklerin belirlenmesi, müteahhide, işverene ve mühendise nedenleri anlayabilmek ve sonuçları en aza indirebilmek, insan hayatı için tehlike olmaktan çıkarabilmek için fırsat verecektir.

Riskin belirlenebilmesi için çeşitli yöntemler vardır. Bunlar, birinci derece güvenilirlik metodu (FORM), ikinci derece güvenilirlik metodu (SORM), ortalama değer birinci derece ikincil moment metodu, Monte Carlo metodu (MC), vd.

Bir sistemin güvenilirliği hem ayrı ayrı elemanlarının hem de bir bütün olarak tüm sistemin güvenilirliğine bağlıdır. Blok diyagramı, hata ağacı metodu, başarı ağacı metodu, olay ağacı metodu, ana neden diyagramı metodu gibi modelleme şemaları ile sistem bir bütün olarak ele alınabilir. Ve bu sayede sistemi etkileyen tüm elemanların birbirleri ile bağlantıları da tanımlanarak sistem güvenilirliği hesaplanabilir. Bu araştırmada hata ağacı şeması kullanılarak sistemde göçmeye neden olabilecek elemanlar belirlenmiş ve derin kazı sisteminin göçme ihtimali hesaplanmıştır.

Literatürde, araştırmacılar genelde şev kaymalarının ve deprem etkilerinin risk analizlerine odaklanmışlardır. Bazıları genel metotları kullanırken bazıları da kendi metodlarını oluşturmuştur. Hepsinin ortak noktası, sistemlerindeki belirsizlikleri ortaya çıkarmak, bu belirsizliklere bağlı riskleri tahmin etmek ve şev, bina, istinat duvarı gibi sistemlerin güvenilirliğini hesaplamak olmuştur.

Geoteknilk mühendisliği projelerinde çeşitlilik ve belirsizlikler, temellerin oturması, şev stabilitesi problemleri, barajların performansı ve derin kazılar, mühendislerin analizleri yaptıkları başlıca konular olmuşlardır. Örneğin, Peck (1969) derin

kazılarda oluşan deplasmanları incelemiştir. Bu çalışmasında, iksa sistemindeki deformasyonların değerini belirleyen en önemli faktörün; iksa sisteminin rijitliği ya da yatay desteklerin arasındaki mesafe değil sistemi çevreleyen zeminin özellikleri olduğunu savunur. Deplasmanları zemin cinsine göre sınıflandırır. Aynı şekilde, Clough ve O'Rourke (1990), Liu et al. (2005), Roboski et al. (2006) ve Park et al. (2007), derin kazıların güvenilirliği üzerine çalışan diğer araştırmacılardan sadece birkaçıdır.

Bu tezdeki araştırmanın amacı da derin bir kazının yapılabilmesi için inşa edilen bir iksa sisteminin güvenilirliğinin, zemin parametrelerindeki değişime bağlı olarak araştırılmasıdır. Bu yapılırken, iksa sistemine komşu yapıların oturmasına bağlı olarak sistem güvenliği tartışılmış ve yüzeydeki oturma ve iksa sistemindeki yatay deplasmanlar ile sistem güvenliği arasında bir bağlantı kurulmaya çalışılmıştır. Bu amaçla, bir demir çelik tesisi kapsamında kazısı gerçekleştirilen 24.0m genişliğinde, 40.0m uzunluğunda, 13.0m derinliğinde bir tufal çukurunun kazısı detaylı aletsel gözlem altına alınmıştır. Sistem, kazının başından son yatay desteğin demonte edilmesine, yapının inşasına kadar izlenmiş ve aletsel gözlem sonuçları kaydedilmiştir. Ölçülen ve hesaplanan yatay deplasman, oturma ve boru destek yükleri karşılaştırılarak sonlu elemanlar modelinin doğruluğu kanıtlanmıştır.

İksa sistemi ilk olarak kazı öncesinde sahada yapılan arazi araştırmaları sırasında belirlenen zemin profili esas alınarak modellenmiş ve boyutlandırılmıştır. Daha sonra, kazı sırasında alınan zemin örnekleri üzerinde yapılan laboratuar çalışmaları sonucunda elde edilen zemin parametreleri ile sistem yeniden modellenmiş ve her iki analizle elde edilen deplasmanlar ve toprak basınçları, hem birbirleri ile hem de aletsel gözlem sonuçları ile karşılaştırılmıştır. Karşılaştırma sonuçları, kazı sırasında alınan numuneler ile belirlenen zemin modeli esas alınarak yapılan modelleme sonuçlarında elde edilen hareketlerin daha gerçekçi sonuçlar verdiğini ve gözlemlenen deplasmanlar ve yatay toprak basınçları ile aynı olduğunu göstermiştir.

Söz konusu doğrulamayı takiben, zemin profili güncel verilere göre idealize edilmiş ve sonlu elemanlar modeli ile modellenmiştir. Sonlu elemanlar analizlerinde kullanmak için gerekli olan parametre varyasyonları, Schweiger et al. (2001) tarafından geliştirilen nokta tahmin yöntemi (PEM) kullanılarak türetilmiştir. İksa sistemindeki yatay deplasmanları ve gerisindeki oturmaları hesaplayabilmek ve zemin parametrelerindeki değişimin deplasmanlara etkisini belirleyebilmek için 132 adet sonlu elemanlar analizi yapılmıştır. Sahada yapılan ölçümlere ve literatürdeki verilere dayanılarak servis limit durumu için analiz edilen geçici iksa sistemi için hedef güvenilirlik indisi (β) 2.2 olarak seçilmiştir. Güvenilirlik analizleri sırasında Southwest Araştırma Enstitüsü tarafından geliştirilmiş olan NESSUS programı kullanılmıştır.

Yapılan araştırmalar sonucunda aşağıdaki sonuçlara varılmıştır:

- Duvar rijitliğinin arttırılması genelde sistemdeki hareketleri azaltmaya yardımcı olsa da, bu durum daha çok yumuşak-orta katı killi zeminlerde etkili olmaktadır. Diğer yandan, yatay desteklerin aralıkları kademe kazılarının derinliğini belirledikleri için duvar rijitliğinden daha öenemli ve etkili olmaktadır. Zira, yatay desteklerin düşey aralıkları arttıkça, kazdeme kazılarının derinlikleri ve buna bağlı olarak kademe kazısı sırasında oluşan ve geri döndürülemeyen hareketler artmaktadır.
- Yatay borular ile desteklenmiş kazıklarda oluşan yatay hareketler, kademe kazıları sırasında oluşmaktadır. Buna bağlı olarak, iksa sistemi arkasındaki

oturmalar hiperbolik şekilde oluşur. Oturmalar, iksadan uzaklıkla önce artarken, maksimum kazı derinliğinin iki katı uzaklıkta sıfırlanmaktadır.

- ϕ ve c'nin orijinal varyasyon katsayıları (VK) ile değişmeleri sistem hareketlerinde yeterli etkiyi yaratmamaktadır. Öte yandan, ϕ ve c ve onlara bağlı olarak E'nin literatürdeki maksimum VK'larında değişmesi, sahadaki jeolojik profilin uç noktalarda değişmesi ya da zemin parametrelerinin yanlış belirlenmiş olması durumlarında, sistemdeki hareketlerin ve sistem güvenilirliğinin parametre değişimlerinden nasıl etkilendiğinin anlaşılmasına yardımcı olmuştur.
- Schweiger ve diğerleri (2001) tarafından geliştirilen nokta tahmin yönteminin (PEM) sonlu elemanlar analizleri ile birlikte kullanılması, eldeki verilerin az olması durumunda az sayıda analiz yapılarak güvenilir sonuçlar elde edilmesini sağlamaktadır.
- Sahada yapılan aletsel gözlemler sırasında alınan oturma kolonu ve inklinometre okumaları oranlandığında yatay deplasman/ oturma oranı Sv(max) = 0.25Sh(max) ve Sv(max) = 0.5Sh(max) arasında çıkar. Bu orani Mana ve Clough (1981)'de Sv(max) = 0.5Sh(max) ve Sv(max) = Sh(max) arasındadır. Muhtemelen kazının boyutlarının küçük olması ve iksa sistemi arkasındaki zemin profilinin katı kıvamda olması nedeni ile hareketler az olmuştur.
- Sonlu elemanlar analizleri sırasında elde edilen yatay deplasman ve oturma değerleri maksimum kazı derinliğinin sırasıyla %0.1 ve %0.3'ünden daha azdır ve 0.4Sh<Sv<1.0Sh oranını oluşturmaktadır.
- Derin kazıların geçici iksa sistemleri için hedef güvenilirlik 2.2 olarak seçilebilecektir. Bu %1.1 göçme olasılığına tekabül etmektedir.
- Zemin tabakalarının orijinal VK ile yapılan hesaplarında, elastisite modülünün alt ve üst sınırlarında sistem güvenliği hedef güvenilirlikten büyüktür. Ancak, VK'nın maksimum değerde olması durumunda elastisite modülünün alt sınırı ile yapılan hesaplarda sistem hedef güvenilirliğin altında güvenilirlik vermektedir. Bunun nedeni, zemin parametrelerindeki dalgalanmaların VK maksimum olduğunda sınırda değişmesi ve E'nin de alt sınırda hesaplanması ile sistemdeki etkinin katlanmasıdır.
- VK'nın maksimum olduğu durumda E'nin üst sınırda hesaplanması ile orijinal VK ile E'nin üst sınırında hesap yapılması arasında keskin bir fark vardır. Bunun nedeni, VK maksimum ile zemin parametrelerindeki değişimin, dalgalanmanın artması, sistemdeki belirsizliklerin artmasına ve buna bağlı olarak da sistemin güvenilirliğinin azalmasına neden olmasıdır.
- S_h ve S_v üzerinden ayrı ayrı hesaplanan güvenilirlik ile sistem güvenilirliği karşılaştırıldığında, sistem güvenilirliğinde S_v etken parametre olduğu ve sistemin, VK'nın maksimum ve E'nin alt sınırı ile yapılan hesaplarda zayıf olduğu görülecektir.
- Sistem üzerinde en etkili parametrenin belirlenebilmesi için VIPlaxis 9.2 ile hassaslık analizleri yapılmıştır. Değişik parametre varyasyonları ile yapılan analizlerin sonucunda, zeminde en etkili parametrenin Elastisite Modülü (E) olduğu görülmüştür. Sistemde yatay deplasmanlar üzerinde en etkili E, %40-50 hassaslıkla, orta katı kilin E'sidir. Oturmalar için de yine en etkili parametre, kabarmanın oluştuğu mesafelerde orta katı kilin E'si iken oturmaların oluştuğu 0.75Hmax mesafeden sonra sıkı kum-çakıl tabakasının E'sidir.
- Yumuşak killi zemin koşullarında, maksimum kazı derinliğine ulaşıldığında

yatay deplasmanlar %1.5Hmax değerini alırken, oturmalar %1.2Hmax değerindedir.

- Yumuşak killi zemin koşullarında, sistem güvenilirliği hedef güvenilirliğin altındadır ve sistemin göçme ihtimali %90 civarındadır. Bu gibi yumuşak zemin koşullarında, sistemin rijitliği arttırılmalı ve yatay destek aralıkları hem yatayda hem de düşeyde azaltılmalıdır. Sonlu elemanlar analizlerinden de söyleyebileceğimiz gibi, kazıkların önü, soketten açmanın ve kabarmanın önlenmesi için kazı tabanının altında güçlendirilmelidir.
- Güvenilirlik analizlerinde oturma, yatay deplasman, açısal dönme, üst yapıdaki çatlakların genişlikleri gibi limit değerler, projeden projeye hatta standartlarca belirlenen değerler altında kalmak şartı ile İşveren'den İşveren'e bile değişebilmektedir. Sistem güvenilirliğini etkileyen bu tip limit değerler, projenin başında titizlikle belirlenmelidir. Zira, bu değerler güvenilirlik koşullarını etkilemekte ve sistemin güvenilir veya güvenilmez olduğunu belirlemektedir.

1. INTRODUCTION

“Which risks may appear during the project?, “How do they affect the system? (What are the results?) and How they can be prevented?” are the main questions to be asked before starting a project. Risk can be explained in different ways depending on the system and its effects. As a general definition; risk is the probability of failure on the system resulting with adverse effects on health, property and environment. A risk can be classified into two categories depending on who it affects [Individual or Societal] and how much does it affect [Acceptable or Tolerable (controllable)] or the source it is caused by, such as external (created by nature) or manufactured (created by human actions). In this research deep excavations which is a manufactured source, has been investigated.

The risk and the uncertainties in the system and its elements have to be determined at the beginning of a project and the results should be considered in order to manage the risks. The contractor, the employer and the engineer/consultant have to specify the elements at risk that will be affected by the undesired cause of the engineering activity nearby.

In order to define the mechanism of the risk and to model the system, finite element methods (FEM) are generally performed. However, modeling is not enough in defining the reliability of the system. Following the FE analyses reliability analyses should be carried out to verify if the suggested system is reliable or not. There are three methods that can be used during reliability analyses, stochastic, fuzzy set, and probabilistic methods. There are many researchers that have used stochastic and fuzzy set approach in the literature. Probabilistic approach has been used for the reliability analyses in this research.

Reliability analysis methods have been developed corresponding to limit states of different types. The limit state equation plays an important role in the development of structural reliability analysis methods. The failure occurs when performance is less than zero. Therefore, the probability of failure, P_f is given by

$P_f = \int \ldots. \int fx\ (x_1, x_2, \ldots\ldots, x_n)\ dx_1\ dx_2 \ldots\ldots\ dx_n.$

Since the solution of this equation is too complicated, by using analytical approximation the integral can be computed simpler. There are several methods, such as first order reliability method (FORM), second order reliability method (SORM), mean value first order second moment method, the radius-based importance sampling (ISAMF), adaptive importance sampling (AIS), Monte Carlo method (MCS), and etc. They are all based on the determination of failure surface (limit state surface) for estimating pf.

The minimum distance point on the limit state surface is called the design point. The distance between the design point and the origin is referred to as the reliability index. The nearer design point is to the origin, the larger is the failure probability. Thus, the minimum distance point in the limit state surface is also the most probable failure point. The design point represents the worst combination of the stochastic variables and is appropriately called the most probable point of failure (Haldar et al., 2006).

Reliability of the elements is important since the system may fail due to its elements' individual mechanisms. On the other hand, a system may fail due to the combination of the weakness of its elements. System reliability is a whole with its components. According to Riha et al. (2002), most engineering structures can fail by multiple events including multiple failure modes and/or components in which the nonperformance of one or a combination of events can lead to system failure. Every item in the system should be considered and analyzed separately of course, for the reliability of the system. However, in order to determine the system reliability, this is not enough. It is also important and necessary to model the relationships between the items and analyze the system as a whole (Modarres et al. 1999). There are several modeling schemes for reliability analysis, such as reliability block diagram, fault tree, success tree, event tree methods, failure mode and effect analysis; and master logic diagram. Fault tree analysis have been used in this research in order to determine the elements cause failure and identify the probability of failure of the whole retaining system of the deep excavation.

In literature, researchers are generally focused on the risk assessment of slopes and earthquake (seismic) effects. Some of them used common reliability methods, some created their own methods. On the other hand, all of them have modeled their systems with commercial FEM software. The common aim of all projects is to determine the uncertainties, assess the risk due to these uncertainties, and find the reliability of the system, such as the slope, building, retaining structure for an excavation, etc. Variability and uncertainty in geotechnical engineering projects, settlement of foundations, stability of slopes, performance of dams, off-shore platforms, and deep excavations have always been the main topics subjected to reliability analyses.

The objective of this study is to investigate the reliability of a retaining system of a deep excavation, depending on the variability of soil parameters. The reliability of the system has been investigated due to the settlement of neighbor structures and the correlation between the settlement of adjacent structures and excavation system reliability has been compared. For this purpose, a detailed monitoring has been conducted on a scale pit excavation, in a steel complex in Dörtyol and the excavation has been monitored from the beginning of the excavation till the last level of the struts have been removed. Following the monitoring, the system was modeled in 2D with Plaxis, by using parameter variations, created by point estimate method (PEM), suggested by Schweiger et al. (2001). More than 200 models were performed in order to determine the variation in the lateral displacement of the retaining structure and settlement behind it and analyze the effect of soil parameter variations on the system reliability. NESSUS (Southwest Research Institute) was used for reliability analysis and different reliability methods have been compared.

2. RISK AND RISK ASSESSMENT

2.1 Risk

It is important to explain the meaning of risk and risk assessment, and what they mean for geotechnical design, prior to discussing risk assessment.

For various situations and cases, risk can be defined differently. So, the main question is: What can be estimated as a risk? The Australian Geomechanics Society's Committee on Risk Assessment has the following definition for geotechnical risks: "Risk is a measure of the probability and severity of an adverse effect to environment, property or health. Risk is often estimated by the product of probability and consequences. However, a more general interpretation of risk involves a comparison of the probability and consequences in a non-product form." Following this explanation, one has to specify the elements at risk, which are the population, buildings, engineering works, economic activities, public service utilities, infrastructures and environmental features in the area potentially that will be affected by the undesired cause of the engineering activity nearby. On the other hand, risk can be defined as the potential loss resulting from the convolution of hazard and vulnerability.

Hazard is a situation or occurrence of an event that could lead to harm in particular circumstances. Mathematically hazard can be expressed as the probability of occurrence of an event of certain intensity at a specific site during a determined period of exposure. Hazard and vulnerability cannot exist on their own. A system cannot be assumed to be at risk unless it is exposed to a hazard and it is vulnerable. Risk can be expressed by the equation:

Risk = Hazard uncertainty + consequence due to the system's vulnerability to hazard (Singh et al., 2007).

Although the risk seems to be dependent to hazard and vulnerability of the system at equal levels, it is not possible to reduce risk by modifying the hazard. However, reducing the vulnerability of the system as a measure of prevention or mitigation, the risk can be reduced and this process is already known as risk reduction.

2.1.1 Classification of risk

A risk can be classified into two main categories due to the effect of it.

- To whom it affects [Individual or Societal]
- How much does it affect [Acceptable or Tolerable (controllable)]

Risks may affect only individuals or the whole community and it becomes a problem for the local and/or general administrations. So, risk will be evaluated if it is in the acceptable range, which means there is no need to manage, or tolerable, which means that the risk is important and dangerous but the society is willing to live with it and management and control is required. Acceptability of a risk depends on the context in which to assess risk and the availability of financial resources. Also, depends on whether one is taking an individual view or a much broader view. Generally, engineers deal with the tolerable risks for individuals and/or public.

Risk can also be classified into two categories due to the source of it.

- External
- Manufactured

External risks are the ones created by nature and occur in a systematic way. But, manufactured risks are created by human actions, such as constructions and excavations.

2.2 Risk Assessment and Management

How will one manage the risk? Risk management can be explained in three steps. They are (1) risk analysis, (2) risk assessment and (3) risk management (Figure 2.1). Risk assessment is a systematic, analytical method used to determine the probability of adverse effects, whereas risk management is a systematic process of making decisions to accept a known or assumed risk and/or the implementation of actions to reduce the harmful consequences or probability of occurrence. Risk assessment is the process that gathers information, prepares a hazard map and measures the damages caused to structures and lives with risk analysis which identifies the hazard or the problem, analyzes the possibility (factor of safety, settlement degree, etc.) and makes the risk estimation. Risk assessment also contains risk evaluation in it. Risk evaluation is the assessment of vulnerability (degree of loss) which means estimation of costs and benefits in economical and/or living base. After risk assessment, control of the risk and monitoring phases follow.

Risk management is also concerned with the mitigation of those risks derived from unavoidable hazards through the optimum specification of warning and safety devices and risk control procedures, such as contingency plans and emergency actions.

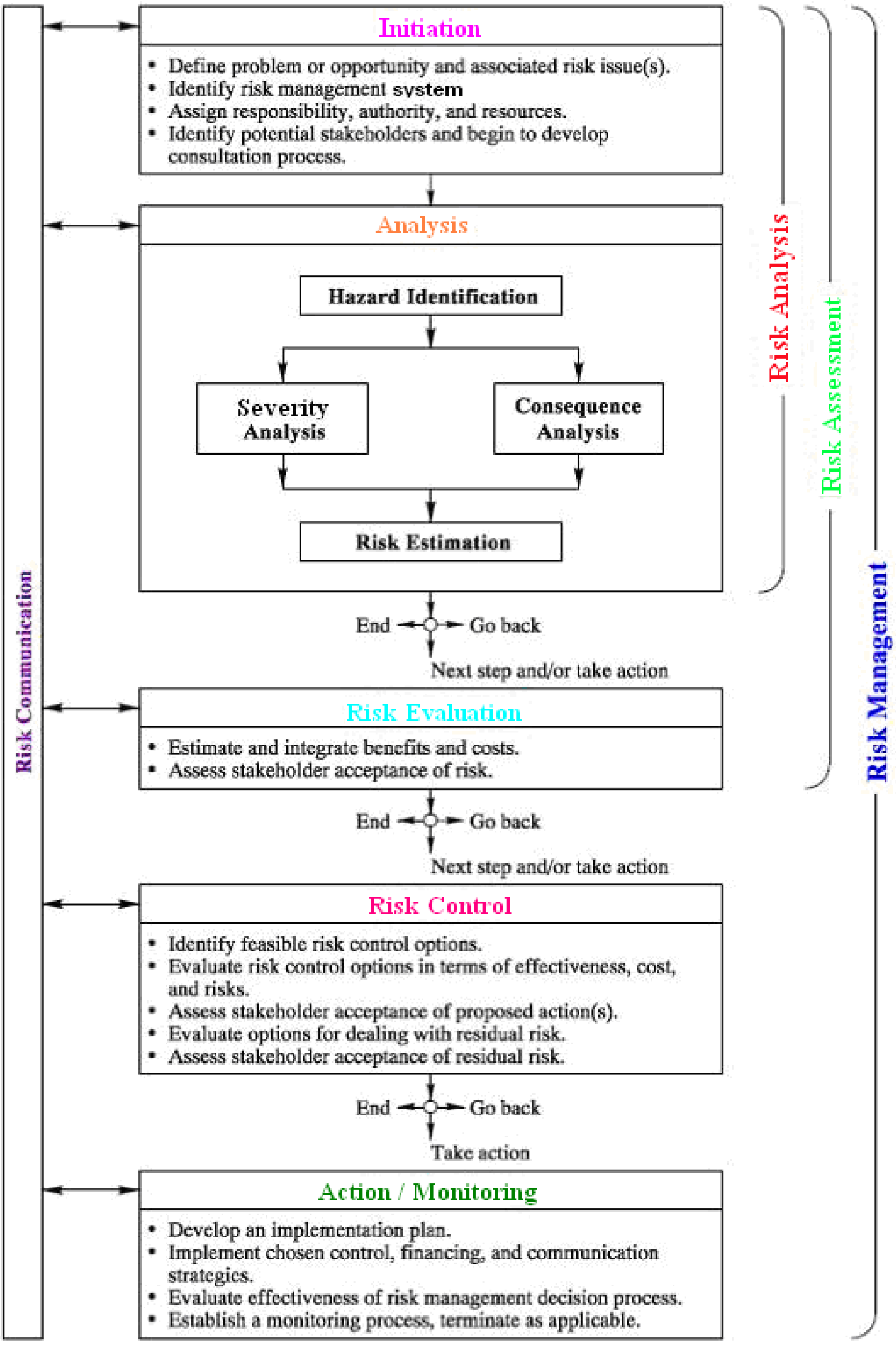

Figure 2.1: Risk Management Diagram (Horelli, J.A., 2005).

2.2.1 Uncertainty analysis

Before starting the assessment and management of risk, the uncertainties that trigger the risk and the analysis to determine these uncertainties must be established. An uncertainty can be defined as a measure of insufficient knowledge or probable error that can occur during the data collection process, modeling, and analysis of engineering systems and prediction of a random process. Uncertainty can be categorized as:

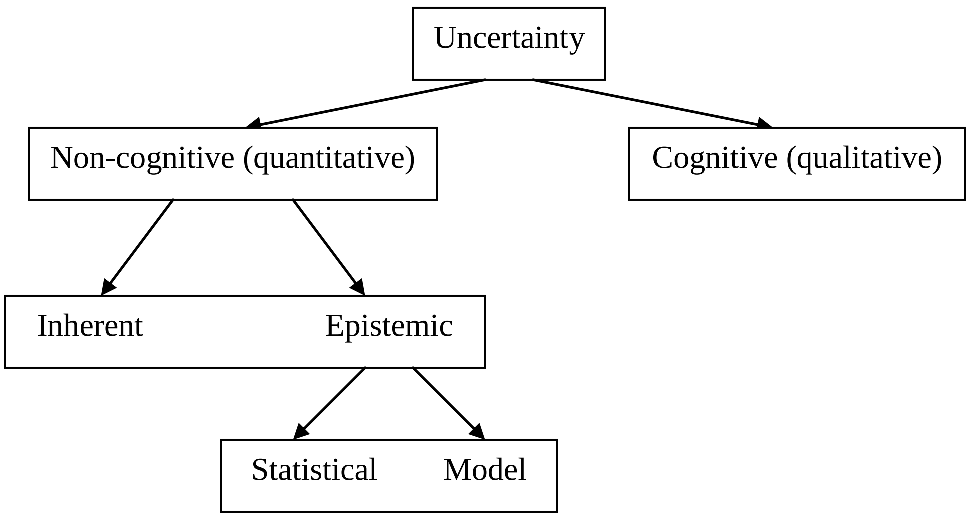

2.2.1.1 Non-Cognitive sources of uncertainty

Non-Cognitive sources of uncertainty can be classified into two types for discussion purposes. The first one is inherent randomness in all physical observations. That is, repeated measurements of the same physical quantity does not yield the same value due to numerous fluctuations in the environment, test procedures, instruments, etc. Inherent uncertainties are also caused by the randomness in nature, such as geologic, seismic and climatic actions associated with the intrinsic variability of the system. The second uncertainty is epistemic and can be subcategorized into statistical and modeling uncertainties.

Model uncertainties arise when the model is unable to closely represent the true behavior of the system, because of the inadequacy of model assumptions and hypotheses. This model uncertainty is called as model structure uncertainty. Another one is model parameter uncertainty, which reflects the variability in determining the parameters to be used in a model or design.

Statistical uncertainties arise from parameter and distribution uncertainties. Parameter uncertainties are due to lack of knowledge or inadequate method of parameter estimation. Distribution uncertainties are due to indecision in choosing distribution of a random variable; due to the vagueness in which type of a probability distribution does it follow.

2.2.1.2 Cognitive sources of uncertainty

Cognitive (qualitative) uncertainties may come from, 1- the definitions of the certain parameters, such as structural performance, quality deterioration, skill and experience of construction workers, and engineers, environmental impact of projects and conditions of existing structures; 2- other human errors; 3- definitions of the interrelationships among the parameters of the problems. Cognitive uncertainties can be sorted as data uncertainties, which arise from measurement inaccuracy and errors, inadequacy of data gauging networks, and data handling and transcription errors; computational uncertainties, which arise from truncation and rounding off errors in doing the calculations; and operational uncertainties that are associated with construction, maintenance and management of the system.

Before starting to analyze the uncertainty of a system or individual, the errors causing uncertainties must be defined. There are two types of errors that are randomness of physical phenomena and errors in data and modeling. Modeling and data errors are of two types: systematic and random. Systematic errors are frequently constant and can be evaluated experimentally and statistically. Random errors are the property that its repeated occurrence does not produce the same outcome and can be evaluated statistically.

In order to measure the error, consistency and bias are to be mentioned. When N, number of samples/observations, gets large, the arithmetic average of the measured values approach a constant value, the estimator approaches a constant value and is qualified as a consistent estimator. Thus, consistency is a measure of experimental data error and is tied to the sample size. Bias is another measure of experimental data error and also is tied to the sample size.

The systematic error is a bias in the prediction or estimation and can be corrected through a constant bias factor. The random error represents the degree of dispersiveness of the range of possible errors. It may be presented by the standard deviation or coefficient of variation of the estimated mean value. An objective determination of bias as well as the random errors will require repeated data on the sample mean.

2.2.2 Reliability analysis

In order to define the mechanism of the risk and to model it, finite element methods (FEM) can be performed. However, before modeling the system, reliability analyses have to be performed and there are three methods for this analysis: stochastic, fuzzy set, and probabilistic methods (Peschl and Schweiger, 2003). A comparison of probabilistic and fuzzy set methods can be found in Chen et.al (1999).

2.2.2.1 Stochastic approach

A stochastic process, is the opposite of a deterministic process in probability theory. Instead of dealing only with one possible 'reality' of how the process might evolve under time, in a stochastic or random process there is some indeterminacy in its future evolution described by probability distributions. This means that even if the initial condition is known, there are many possibilities the process might go through, but some paths are more probable than others.

In the simplest possible case ('discrete time'), a stochastic process amounts to a sequence of random variables known as a time series. Another basic type of stochastic process is a random field, whose domain is a region of space, in other words, a random function whose arguments are drawn from a range of continuously changing values. One approach to stochastic processes treats them as functions of one, or several deterministic arguments whose values are random variables: non-deterministic (single) quantities which have certain probability distributions. Random variables corresponding to various times (or points, in the case of random fields) may be completely different. The main requirement is that these different random quantities all have the same 'type'.

2.2.2.2 Fuzzy set approach

Fuzzy set approach is an alternative to probability approach since it is based on the possibility distributions. The main difference between the possibility and probability approach is possibility of a union of disjoint events is equal to the maximum of the possibilities of the individual events, while the probability of a union of disjoint events is equal to the sum of the probabilities of these events.

2.2.2.3 Probabilistic approach

Uncertainty is introduced into engineering systems through the variation inherent in nature, lack of understanding the causes and effects in physical systems, lack of sufficient data or inaccuracy thereof. Thus, the possibility of occurrence of an event must be considered and the likelihood of the occurrence has to be determined.

Probability theory, deals with the prediction of chance or likelihood of occurrence of an event from sampled data. As Singh et al. (2007) has defined, classical probability theory has two cornerstones. "The first is the equal likelihood of all possible outcomes in a game of chance. The other is related to the relative frequency tends to approach the ratio of the numbers of successes to the total number of trials. This is the number adopted to define probability."

The uncertainty in a random variable can be modeled by its underlying distribution, generally expressed in terms of probability density function or probability mass function and cumulative distribution function. To uniquely define these functions, its parameters need to be estimated and they are generally estimated by using the information on mean, variance and COV obtained from available data.

$$\text{Mean} = \mu x = E(X) = 1/n\ \Sigma\ xi \tag{2.1}$$

$$\text{Variance} = Var(X) = 1/\ (n-1)\ \Sigma\ (x_i - \mu_x{}^2) \tag{2.2}$$

$$\text{Standard Deviation} = \sigma_x = \sqrt{Var(X)} \tag{2.3}$$

$$\text{Coefficient of Variation} = COV\ (X) = \delta_x = \sigma_x / \mu_x \tag{2.4}$$

where, n is sample size and x_i is the i^{th} sample, $(1 < i < n)$.

As Paul Wirsching (2008) has explained; a probability can be a priori probability, a posterior probability or a subjective probability. A priori probability is the probability established by definition of the system and the ratio, which is the number of equally likely outcomes of an experiment over the total number of outcomes. A posteriori probability, can also be called as a relative frequency or empirical probability, is the limit function of the ratio, which is the number of times that an event is observed during a test that is repeated n times over n. On the other hand, subjective probability is a non-mathematical way of finding the probability. It is like; "I feel that there is a 10% chance that this system will fail in that environment." (Wirsching et al., 2008)

There are several commonly used distributions to evaluate the risk or reliability of events or systems. They can be studied in two main categories depending on the random variable used for the distributions, as continuous random variables and discrete random variables.

For discrete random variables, the item is inspected and judged to be defective or non-defective. But for continuous random variables there are not such specific two outcomes. It is the possibility of defectiveness or non-defectiveness. Continuous random variables deal with the probability of occurrence while the discrete random variables deal with the number of defective or non-defective particles. For discrete random variables the sample space is limited but for continuous random variables it goes to infinity. For continuous random variables, exact numbers for probability cannot be mentioned but the probabilities associated with intervals are to be talk about. In engineering problems we usually work with continuous variables. For that reason; the distributions for continuous random variables will be explained in this chapter.

1. Normal (Gaussian) Distribution

It is applicable for any value of a random variable from $-\infty$ and $+\infty$. The distribution is symmetric about the mean and the mean, median, and mode values are identical and can be estimated directly from the data. For example, the water content of a soil is normally distributed. It is symmetric on its optimum value and its mean, median and mode values can be estimated directly from the samples.

The probability density function of a normal distribution is

$$f_x(x) = (1/ \sigma_x\sqrt{2\pi}) \exp (-1/2 [(x-\mu_x) / \sigma_x]^2] \qquad -\infty < x < +\infty \qquad \textbf{(2.5)}$$

Where, σ_x and μ_x are the mean and standard deviation, respectively.

2. Lognormal Distribution

In geotechnical engineering problems, most of the engineering parameters of soils are greater than zero. In lognormal distribution the sample values differ from 0 to $+\infty$. So, for geotechnical problems, it is more appropriate to use lognormal distribution, because it automatically eliminates the possibility of negative values. For example, the elasticity modulus, the angle of friction or the unit weight of a soil cannot be negative.

The probability density function of a lognormal distribution is

$$f_x(x) = (1/ \zeta_x \, x \sqrt{2\pi}) \exp (-1/2 \, [(\ln x-\lambda_x) / \sigma_x]^2] \qquad 0 \le x < +\infty \qquad \textbf{(2.6)}$$

$$\lambda_x = E(\ln X) = \ln \mu_x -1/2 \, \zeta_x^2 \qquad \textbf{(2.7)}$$

$$\zeta_x^2 = Var (\ln X) = \ln [1 + (\sigma_x / \mu_x)^2] = \ln (1 + \delta_x) \qquad \textbf{(2.8)}$$

3. Beta Distribution

Beta distribution is very flexible and can be used when a random variable is known to be bounded by two limits, a and b. Beta distribution is a version of lognormal distribution when the lower boundary is zero. Such as, in geotechnical engineering, it is known that the Poisson's ratio, ν, can be between 0.3 and 0.5 for cohesive soils. So the beta distribution is suitable for analyses that use the Poisson's ratio as the parameter. Or another example is that, the friction angle ϕ has to be between 0 and 90 degrees. So the beta distribution is suitable for friction angle, also.

$$f_x(x) = [1/B(q,r)] \, [(x-a)^{q-1} (b-x)^{r-1}] / (b-a)^{q+r-1} \qquad a \le x \le b \qquad \textbf{(2.9)}$$

q, r : parameters of the function, B(q,r) : beta function

$$E(X) = a + q \, (b-a) / (q+r) \qquad \textbf{(2.10)}$$

$$Var (X) = q \, r \, (b-a)^2 / [(q+r)^2 (q+r+1)] \qquad \textbf{(2.11)}$$

If a=0, b=1 then the distribution is standard beta function

If q = r = 1, then the beta distribution is uniform.

4. Binomial Distribution

In many engineering applications, events consisting of repeated trials can be formulated in terms of occurrence or nonoccurrence, success or failure. Only two outcomes are possible, representing the behavior of a discrete random variable. If the events are statistically independent and the probability of the occurrence or nonoccurrence of events remains constant, they can be mathematically represented by binomial distribution. This distribution is not valid for soils or the geotechnical systems, since the soil parameters and every component of a system are not independent. Although they can be calculated independently, the results of their distribution affect each other and the system reliability. Also, in most cases the occurrence or nonoccurrence of events does not remain constant; they change when the soil layers change. For example, when the lateral displacement of a retaining system increases, the failure probability of the system also increases.

Binomial distribution can be used in cases that the probability of the flood only 2 out of 10 years for a drainage system of a city that has been designed for a rain fall intensity that will be exceeded on an average once in 50 years (Haldar, A. et al., 2006).

5. Geometric Distribution

If the events occur in a Bernoulli sequence and p is the probability of occurrence in each trial, then the probability that the event will occur for the first time at the i^{th} trial is given by geometric distribution.

6. Return Period

Return period deals with the probability of occurrence of periodical events such as earthquakes, flood and hurricanes.

7. Poisson’s Distribution

Poisson’s distribution is used to evaluate risk damages. Accidents can occur at any time at any location in a road or a twister can hit a building at any time during the lifetime of the house. If these events need to be modeled in Bernoulli sequence then the total space or time needs to be divided into small intervals so that only one occurrence is possible in an interval. So, modeling *X* occurrences in time t in a Bernoulli sequence as n (number of time intervals) approaches infinity will lead to the Poisson's distribution. Occurrence of floods, earthquakes, accidents in a time interval in a place can be modeled by Poisson's distribution.

The Poisson's distribution can be used as an approximation to the binomial distribution, when the parameter, p (probability of occurrence in each interval), of the binomial distribution is small, and parameter n is large.

8. Weibull Distribution

Weibull distribution is used to represent the time to failure or life duration of components as well as the systems. There are also two more continuous random variable distributions that are Exponential distribution and asymptotic distribution.

2.2.2.4 Measures of importance

During the reliability analysis or risk assessment of a system, some specific components and their arrangement may be more critical than others from the standpoint of their impact on the system reliability. In order to describe this importance, there are five methods. They are birnbaum, criticality, fussell-vesely, risk reduction worth, and risk achievement worth measures of importance (Modarres et al., 1999).

- **Birnbaum measure of importance**

In this measure reliability of the system depends on the reliability of the component, which means, the reliability of the system will change extremely even there is a small change in the reliability of the component. The method completely depends on the structure of the system. However, "the importance of the component is independent of the reliability of the component itself" (Modarres et al., 1999).

$$I_i^B (t) = \partial R_s [R(t)] / \partial R_i (t) \quad \textbf{(2.12)}$$

I_i^B : Birnbaum measure of importance
R_i (t) : reliability of individual component
R_s [R(t)] : reliability of the system as a function of R_i (t)

- **Criticality measure of importance**

On the contrary to Birnbaum method, the criticality measure of importance assigns a low importance to the component with low reliability with respect to the reliability of the system. The importance of the component depends on its reliability.

$$I_i^{CR}(t) = \{\partial R_s[R(t)] / \partial R_i(t)\} \times \{R_i(t) / R_s[R(t)]\} \qquad \textbf{(2.13)}$$

A subset of criticality importance measure is inspection importance of measure, which is used to prioritize operability test activities to ensure high component readiness and performance.

$$I_i^{W}(t) = I_i^{B}(t) \times Q_i(t) \qquad \textbf{(2.14)}$$

$Q_i(t)$: the failure probability of the component

- **Fussel-Vesely measure of importance**

It can be used, where the component contributes to system reliability but is not necessarily critical. This measure has been applied to system cut sets to determine the importance of individual cut sets to the failure probability of the whole system.

$$I_i^{FV}(t) = R_i[R(t)] / R_s[R(t)] \qquad \textbf{(2.15)}$$

$R_i[R(t)]$: the contribution of component i to the reliability of the system

- **Risk-Reduction Worth measure of importance**

The measure of the change in unreliability when an input variable is set to zero, which means the component is perfect. This measure shows how much better the system can become as its components are improved.

$$I_i^{RRW}(t) = F_s[Q(t)] / F_s[Q(t) \mid Q_i(t)=0] \qquad \textbf{(2.16)}$$

$F_s[Q(t)]$: the system unreliability

$F_s[Q(t) \mid Q_i(t)=0]$: the system reliability when unreliability of component i is zero

- **Risk-Achievement Worth measure of importance**

The input variable set to one and the effect of this change on the system unreliability is measured. By setting the component failure probability to one, RAW measures the increase in system failure probability, assuming the worst cause of failing the component.

$$I_i^{RAW}(t) = F_s[Q(t)] / F_s[Q(t) \mid Q_i(t)=1] \qquad \textbf{(2.17)}$$

Components with high I^{RAW} are the ones that will have the most impact, should their failure probability unexpectedly rise.

2.2.2.5 Reliability analysis methods

Following the explanation about the probability distributions, we can now analyze the probabilistic methods for reliability. Reliability analysis methods have been developed corresponding to limit states of different types. The limit state equation plays an important role on the development of structural reliability analysis methods. The failure occurs when performance is less than zero. Therefore, the probability of failure, P_f is given by

$$P_f = \int \ldots \int fx\,(x_1, x_2, \ldots\ldots, x_n)\, dx_1\, dx_2 \ldots\ldots dx_n \quad \textbf{(2.18)}$$

As the solution of this equation is too complicated, by using analytical approximation the integral can be computed simpler. There are several methods for estimating pf. The normal and lognormal formats, first order reliability method (FORM), second order reliability method (SORM), mean value first order second moment method, the radius-based importance sampling (ISAMF), adaptive importance sampling (AIS), Monte Carlo method (MC), and etc. They are all based on the determination of failure surface (limit state surface). The limit state surface is the surface between the safe region and the failure region. It can be either linear or nonlinear (Figure 2.2). FORM is used when the limit state function is linear and consists of uncorrelated normal variables, or when the function is represented by a first order approximation with equivalent normal variables. SORM is used when the limit state function is nonlinear, including a linear limit state function with correlated non-normal variables.

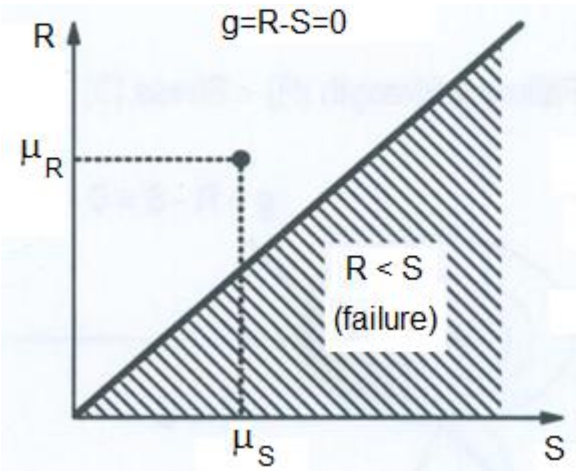

Figure 2.2: Linear Limit State Surface and Regions (SwRI, 2008).

- **Monte Carlo**

The term “Monte Carlo” was invented during the 1940’s by N.Metropolis and S. Ulaw as part the Manhattan project because of its similarity to a game of chance and the method is named after the Monte Carlo district of Monaco. Since it works for any analysis model, which does not differ whether the response function is discrete or continuous, or need to be known in analytical form or there can be a discontinuity in the model response. Another advantage of Monte Carlo Method is that it is simple to implement in existing software. However, since it requires large sample sizes, such as if the engineer needs 10^{-5} of p_f then he needs 10^6 of samples, it may take hours and even years to generate random variables or calculate the probability or sensitivities. For constant computational effort, less confidence is achieved when probability is small. On the other hand it is always good to use MC for comparing with other probabilistic models in order to have an idea.

Monte Carlo method repeatedly generates a set of random values from the joint probability density function (JPDF) and computes corresponding Z-function (response function) values. The Z values are used to construct a cumulative distribution function (CDF) for Z or compute the p_f estimate for $Z<Z_0$.

- **First Order Reliability Method (FORM)**

The development of FORM can be traced to second moment methods, which used the information on first and second moments of the random variables. These are first-order second moment (FOSM) and advanced first-order second moment (AFOSM) methods. In FOSM, information on the distribution of random variables is ignored, however, in AFOSM; the distributional information is appropriately used. In design of recent engineering problems AFOSM is being used in order to take the distribution factor into account.

- **Second Order Reliability Method (SORM)**

When the limit state function of the system is nonlinear due to the relationship between the random variables in the limit state equation or due to some variables being normal, SORM can be used.

A linear limit state in the original space becomes nonlinear when transformed to the standard normal space if any of the variables is nonnormal. Also, transformation from correlated to uncorrelated variables might induce nonlinearity. If the decay of the joint probability density function is slow and the limit state is highly nonlinear, then the geotechnical engineer has to use a higher-order approximation for failure probability computation such as SORM (Figure 2.3). If the joint probability density function decays rapidly as the geotechnical engineer moves away from the minimum distance point then the first order estimate of failure probability is quite accurate.

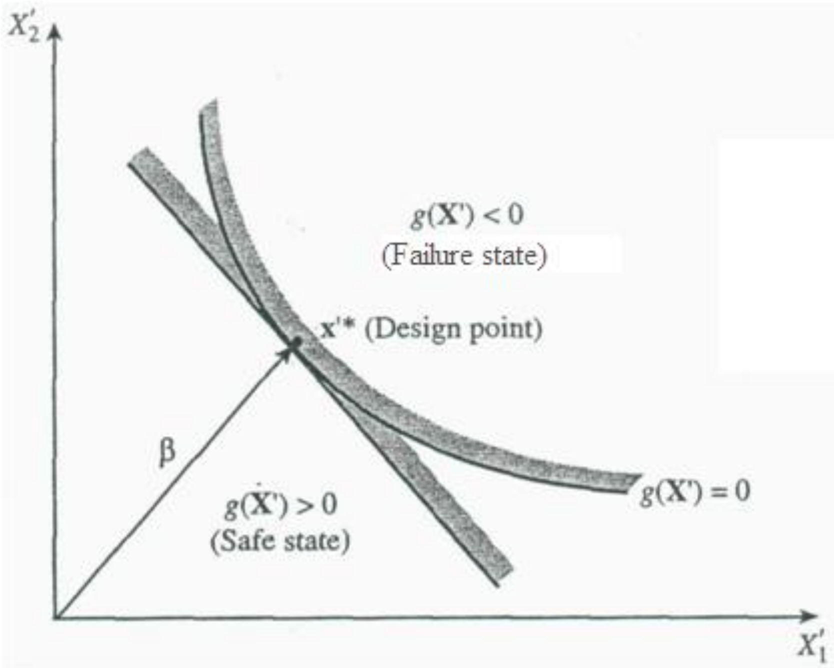

Figure 2.3: Linear and nonlinear limit states (Haldar, A. et al., 2006).

The minimum distance point on the limit state surface is called the design point. It is denoted by vector x* in the original coordinate system and by vector x′* in the reduced coordinate system. The distance between the design point and the origin is referred to as the reliability index. In general, many random variables represented by the vector X or X′, the limit state g(X′)=0 is a nonlinear function as shown in Figure 3. At this stage, $X_i^{\prime}$'s are assumed to be uncorrelated. Here, g(X′)>0 denotes the safe state and g(X′)<0 denotes the failure state. It is obvious that the nearer x′* is to the origin, the larger is the failure probability. Thus, the minimum distance point in the limit state surface is also the most probable failure point (MPP). The point x′* represents the worst combination of the stochastic variables and is appropriately called the most probable point of failure (Haldar et al., 2006). In order to define the MPP, the highest point of joint probability function of two random variables, it is easier to define minimum distance from the center at g(u)=0 line at the standard normal limit state function, that we transformed from the nonlinear function in space (Figure 2.4).

There are several methods for finding the MPP, such as standard optimization methods; reduced gradient, penalty function methods, sequential quadratic programming, etc. and Tailored methods; Hasofer-Lind, Rackwitz-Fiessler. The most commonly used one is the Rackwitz-Fiessler. In this method, an initial value for design point [$x_i^*(=\mu_i)$] is estimated and the g function for that point is computed. It is not always the MPP, but an easy way to start computation. Then the mean and standard deviation in original coordinates and the design point in reduced coordinates ($x_i^{`*}$) are computed. After computing the response sensitivities, the updated design point in reduced coordinates is computed. Then the distance from MPP to origin, β, is computed and the design point in the original coordinates is calculated. If the updated design point in the original coordinates fits the g function, then it is the MPP, if not then the steps are repeated. If the g function is a circle then there will be many MPP's. So, in order to be sure about the point, the angle between β calculated in one step and the other should be zero.

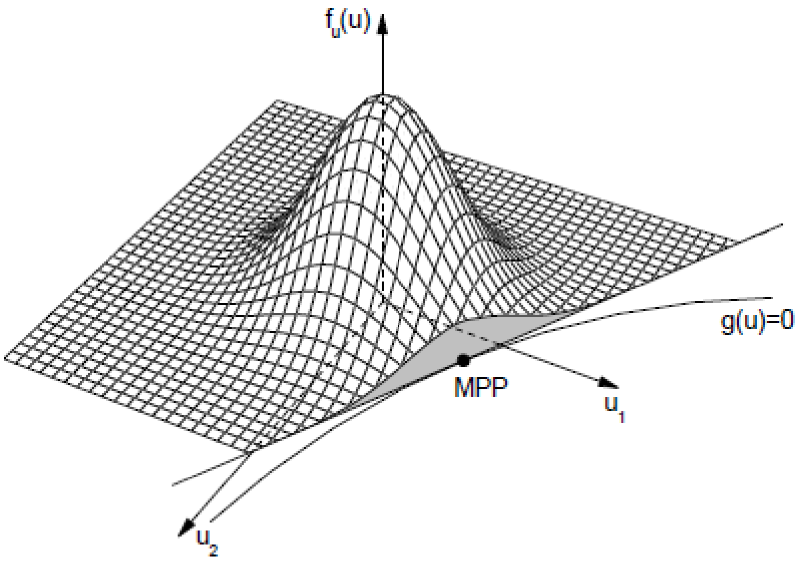

Figure 2.4: Most Probable Point on a JPDF (SwRI, 2005).

- **Radius-based Importance Sampling (ISAMF)**

In the radius-based importance sampling methods, samplings are performed in the standardized normal (u) space outside of a sphere. For each sample generated in the u-space (standardized normal space), the inverse transformation is used to generate a sample in the X space for g-function evaluations. The basic assumption is that if the MPP is correct then according to the MPP definition g>0 within the sphere.

In ISAMF, failure probability index first search for MPP to define the reference radius, then use the reduction factor to reduce the radius and increase sampling region. Reduction factor can be used to check accuracy of β. If β is correct, reducing the sampling radius will not generate any further g<0 samples. p_f estimate is;

$$p_f = (N_f / N)\, P_{\text{sampling region}} \tag{2.19}$$

where N is the total number of samples (outside the sphere), N_f is the number of samples with negative g values and $P_{\text{sampling region}}$ is the probability outside the sphere.

By specifying an error bound and a confidence interval, the number of samples can be computed as follows:

$$\%\ \text{error} = 100\ \Phi^{-1}(1\text{-}a/2)\ \sqrt{[(1\text{-}p) / N_p]} \tag{2.20}$$

where the probability p is the (conditional) probability of failure in the sampling region, such as

$$p = N_f / N \tag{2.21}$$

In ISAMF, sampling efficiency is always better than MC, except for the special cases of zero radiuses, which is equivalent to the MC.

- **Adaptive Importance Sampling (AIS)**

The Adaptive Importance Sampling (AIS) methods minimize sampling in the safe region by adaptively and automatically adjusting the sampling space from an initial approximation of the failure region. The sampling space is defined using a limit-state surface (boundary). The performance of AIS depends on the quality of the initial failure region approximation. Even though the AIS method cannot totally replace the standard Monte Carlo method, it provides efficient accuracy improvement or checking to the MPP-based approximation methods (FORM, SORM, AMV+) for component reliability analysis.

There are two AIS methods (AIS1, AIS2) available in fast probability integration (FPI) for selecting the sampling limit-state boundaries. AIS1 uses planes and AIS2 uses parabolic surfaces. Both surfaces are constructed in the u-space and use the MPP to define the beginning sampling limit state. AIS1 changes the distance to the plane and AIS2 changes the MPP curvature. For most problems tested to date, both methods performed equally well with AIS2 having a slight edge. AIS1 is less sensitive to the accuracy of the initial MPP but may require more samples. AIS2 is more sensitive to the accuracy of the initial MPP but is generally more efficient.

For user-defined g-functions, AIS is highly recommended because of its overall effectiveness in accuracy and efficiency. It should be cautioned, however, that the performance of AIS depends on the accuracy of the MPP. If the starting MPP is far away from the true MPP, AIS may either require a larger number of samples than usually required or may miss a failure region. Therefore, if FPI fails to find the MPP, AIS may not be efficient or may converge incorrectly.

2.2.2.6 System reliability

System reliability is a whole with its components. According to Riha (2002), most engineering structures can fail by multiple events including multiple failure modes and/or components in which the nonperformance of one or a combination of events can lead to system failure. Every item in the system should be considered and analyzed separately of course, for the reliability of the system. However, in order to determine the system reliability, this is not enough. It is also important and necessary to model the relationships between the items and analyze the system as a whole (Modarres et al. 1999).

The concept used to consider multiple failure modes and/or multiple component failures is known as system reliability analysis includes both the component level and system level estimates. System reliability evaluation depends on, for example for a retaining system:

- The contribution of the component failure events to the system’s (in this research it will be the retaining structure of a deep excavation) failure
- The redundancy in the retaining structure
- The post failure behavior of a component, such as the anchorages or the soil nails or the piles of a retaining structure and the rest of the system
- The statistical correlation between failure events
- The progressive failure of components

There are several modeling schemes for reliability analysis, such as reliability block diagram, fault tree, success tree, event tree methods, failure mode and effect analysis; and master logic diagram. In this research, the tree methods are used.

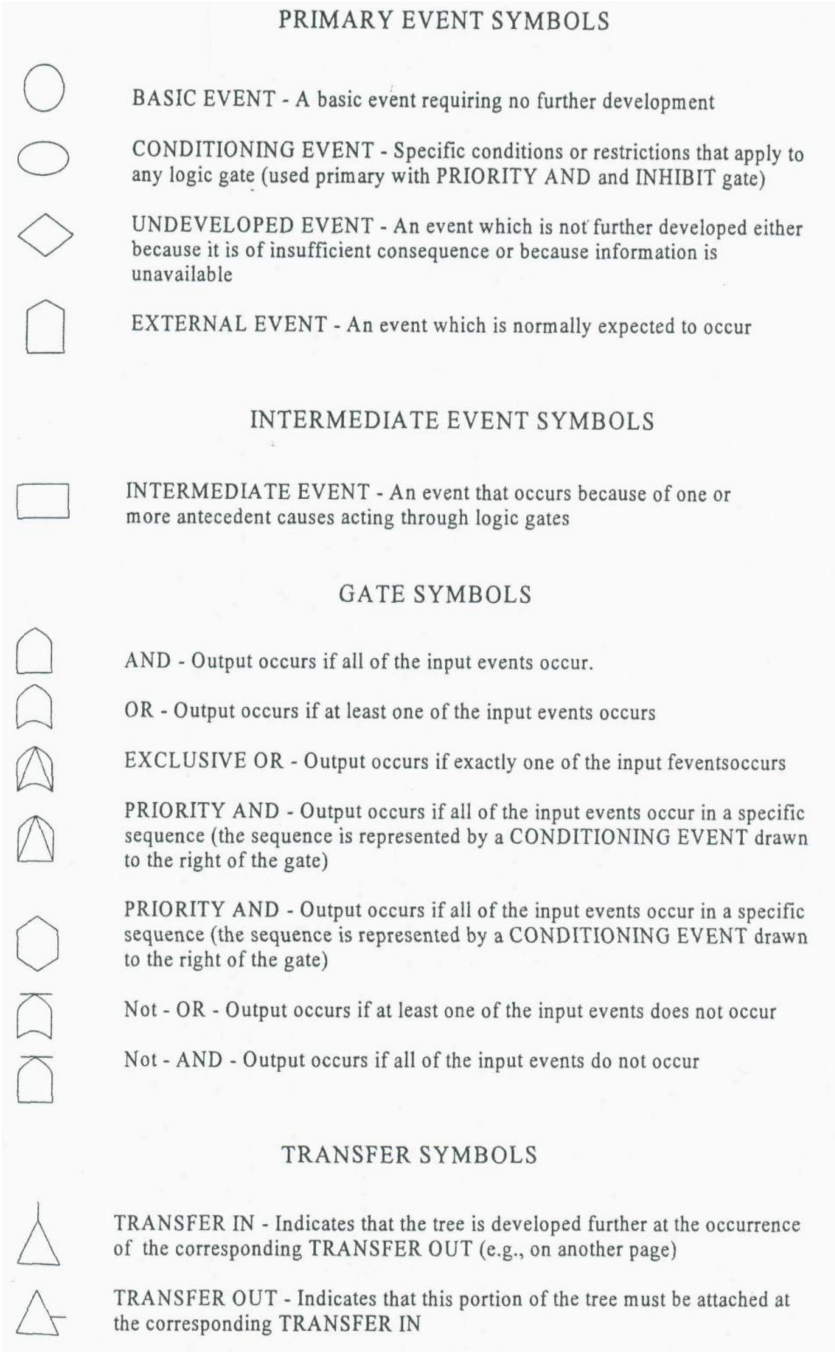

Figure 2.5: Primary Event, gate, and transfer symbols used in logic trees (Modarres et al. 1999).

- **Fault Tree Method**

In this method, an undesirable event is described first and the possible ways for occurance of this event are systematically deduced. The fault tree is a graphical presentation of the various combinations of failures that lead to the occurrence of the top event. A fault tree consists of only the failure modes that contribute to the occurrence of the top event, but not all the possible modes. However, the decision for inclusion of failure events is not arbitrary; it is influenced by the fault tree construction procedure, system design and operation, operating history, available failure data, and the experience of the analysts.

When complex logical relationships are required, other logical representations by combining AND and OR gates, such as K-out-of-N and exclusive OR logics can be described (Figure 2.6).

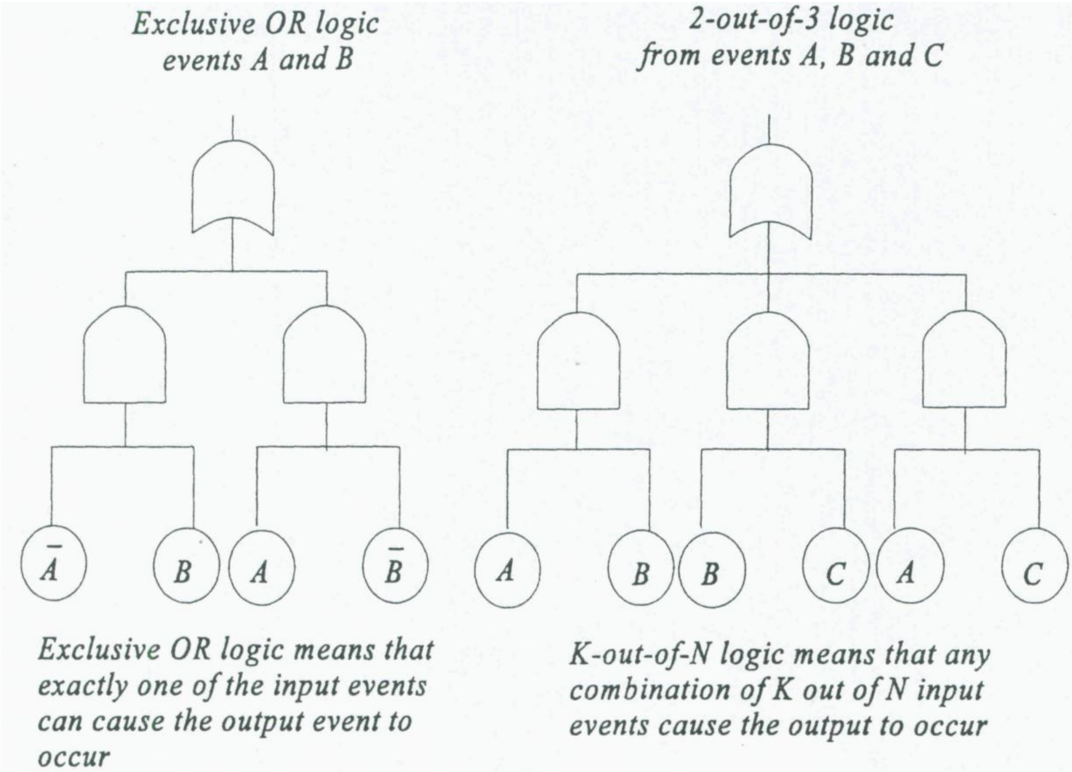

Figure 2.6: Exclusive OR and K-out-of-N logics (Modarres et al. 1999).

In order to calculate system failure by FPI, the system failure is defined using a fault tree, which provides a way to manage multiple failure modes. The limit state functions are defined in the bottom events. Sequential failures can be modeled using the PRIORITY AND gate. A sequence of g-functions, corresponding to a sequence of updated structural configurations with load redistribution can be explicitly or implicitly defined in the bottom events.

Through a fault tree, all the failure modes can be defined. A failure mode can involve one or more limit states. By adding all the failure modes, and therefore all the limit states, the system limit state surface can be constructed piece by piece. The AIS procedure for system reliability analysis requires the construction of multiple parabolic surfaces. In principle, it is a straightforward extension of the concept for one limit state. The difficult part is to develop a procedure to add failure regions.

The probability of failure statement is

$$pf = P\ \{(g1 < 0) \cup (g2 < 0) \cap (g3 < 0)\ldots\ldots\} \quad \textbf{(2.22)}$$

The above adaptive approach for system reliability can be easily modified for use with the radius-based and plane-based methods. However, the curvature-based AIS is recommended for its overall performance in efficiency and robustness.

- **Success Tree Method**

This method is similar to fault tree, except in this method, by defining the desirable top event, all intermediate and primary events that guarantee the occurrence of this desirable event are deductively postulated. The difference between the representations of fault tree and success tree is viewed in Figure 2.7.

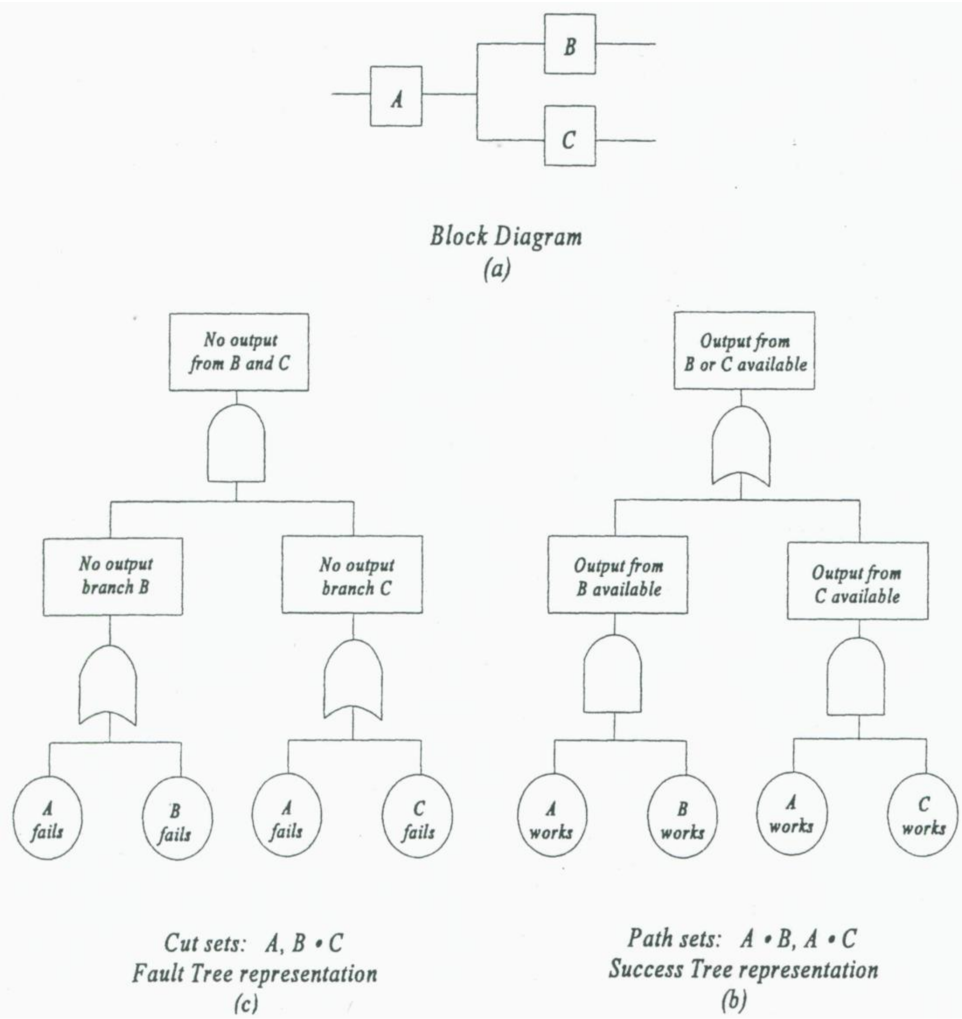

Figure 2.7: A correspondence between fault and success trees (Modarres et al. 1999).

- **Event Tree Method**

If success of the operation of a system depends on an approximately chronological, but discrete, operation of its items, then an event tree is more appropriate. Event tree method is more appropriate for complex systems than the other tree methods.

- **Master Logic Diagram (MLD)**

In complex systems, there are always several functionally separate subsystems that interact with each other, each of which can be modeled independently. However, it is necessary to find a logical representation of the overall systems. The MLD clearly shows interrelationships among the independent support function (Figure 2.8). The MLD can show the manner in which various functions, subfunctions, and hardware interact to achieve the overall system objective.

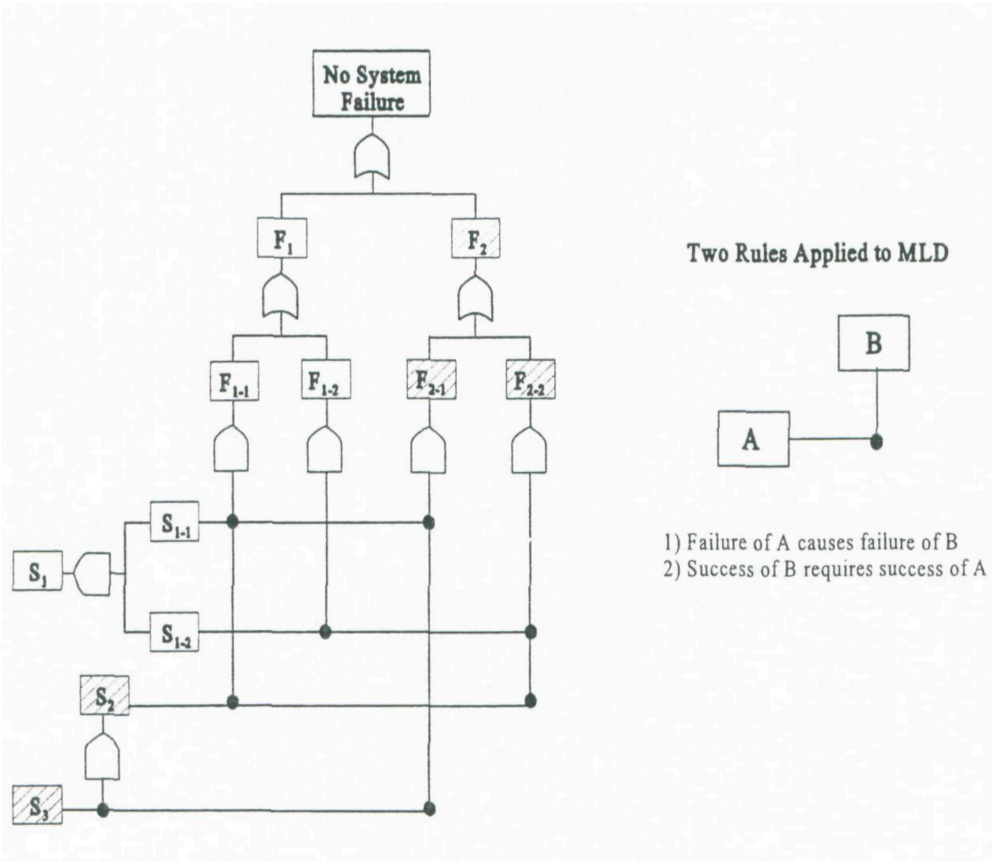

Figure 2.8: Master Logic Diagram (Modarres et al. 1999).

3. LITERATURE REVIEW

In literature, researchers are generally focused on the risk assessment of slopes and earthquake (seismic) effects, such as Australian Geomechanics Society (2000), Ferris et al. (2003), Horelli (2005), Whittlestone et al. (1995) and Wislocki et. al (1991). Some of them used common reliability methods, some created their own. On the other hand, systems have been modeled with commercial FE software, in most recent researches. The common aim of all projects is to determine the uncertainties, assess the risk due to these uncertainties, and find the reliability of the system, such as the slope, building, retaining structure for an excavation, etc. Some of the main topics are examined and explained in the paragraphs below.

3.1 Variability and Uncertainty in Geotechnical Engineering

Uncertainty in the soil structure and variability depending on the depth and distance is unavoidable for soil mechanics and geotechnical engineering issues. However, although it is more common in structural engineering since mid 1970's, geotechnical engineers are familiar to reliability based design (RBD), meaning taking uncertainties into account during design, since 1980's. The major difference between the disciplines comes from the difficulty in correctly estimating the variability of design properties of geomaterials, which vary vertically and horizontally, even in homogeneous called soil layers. As Phoon et al. (1995) has indicated by his studies, the resistance factors in RBD equations are functions of the coefficient of variation (COV) of the design soil property. In the study conducted by Akbaş (2008), the COV of inherent variability is evaluated for geotechnical properties of Ankara clay and proved that RBD is more realistic to use than the traditional design with factor of safety. By taking soil variability in calculations, more economical and realistic results is obtained.

In order to reduce the effect of the variability of soil parameters on the design, more site investigations should be done more accurately. However, the numbers of the laboratory and in-situ tests are determined by the budget and time of the project. On the other hand, the number of the borings is also an issue during site investigations. It is never enough to bore an additional well. The engineer can never be sure about the number of the investigations, because of the variability of the nature of the soil.

Therefore, it is necessary to plan locations of such tests to provide the most suitable information for the design. Goldsworthy et al. (2007), presented the errors associated with using soil properties from a single sample location and the relative benefits of taking soil samples closer to the center of the foundation to be designed.

As the sample located increasingly further from the foundation, the average design error increases at a rate that is influenced by the scale of fluctuation (SOF) of the elastic modulus. The maximum average design error is a function of both COV and SOF of the elastic modulus field. The worst case appears to occur when SOF is approximately 16m.

By using a simple linear relationship between expected cost savings and the average design error, Goldsworthy et al. (2007), estimated a measure of savings due to sample location. They proved that if the distance between the sample location and the center of the footing or foundation system is reduced to as little as 5m, where Westergaard and Timoshenko and Goodier, relationships yielded designs that were close to the optimal design when sampling occurred further than 10m from center of the footing, the best information is required for design (Goldsworthy et al., 2007).

In order to minimize the uncertainties in geotechnical investigations Reznik (1996), suggested two approaches. One is correlating laboratory and in-situ tests and the other is mathematical modeling. It is possible to increase efforts in development of statistical correlations between relatively inexpensive in-situ tests and bearing plate test.

Alternatively, Bourdeau and Amundaray (2006) suggested the application of bootstrap resampling, a non-parametric simulation technique, to the analysis of uncertainty associated with geotechnical statistical data. Bootstrap re-sampling is an unordered collection of n items drawn randomly from a population of samples, with replacement, so that each item has the same probability 1/n of being equal to any of y_j's. For each individual re-sample, statistics are computed in order to obtain estimates of unknown population parameters and the results are summarized to obtain empirical parameter estimators as well as their standard errors and confidence intervals. As the number of re-samples increases, the approximation improves.

In the paper they had correlated cone penetration test (CPT) and dilatometer test results of Heber Road in Imperial Valley, CA, by bootstrap simulation. The averaged value of the bootstrap samples were compared with the standard deviation of sample autocorrelation values calculated from the tests, in order to test the accuracy of standard error estimates for autocorrelation functions.

Bootstrapping has the advantage that standard error estimates are lower even with a small number of investigations, if the quality of the initial sampling is high, the statistical estimators of geotechnical properties and associated confidence levels can be computed directly from empirical data without parametric assumptions.

The bootstrap simulation is accurate in general, over large series of simulations. However, as every method have limitations, bootstrap sampling has too. Although statistical homogeneity of the data population is necessary for the bootstrap to provide realistic results, the most important requirement is the representativeness of the data sample. Also, estimation based on a single sample is not necessarily improved by bootstrapping when the sample is biased, because bootstrap estimates are conditioned to the initial sample drawn from the population.

3.2 Settlement of Foundations

Assessment of settlements of a structure is an important problem in geotechnical engineering. Settlements may be caused by deformations induced during excavations, ground water control (pumping) and due to soil type (settlement under structures' own load).

In a probabilistic approach, reliability of a foundation or footing against serviceability limit state failure in the form of excessive differential settlements can be calculated. For this purpose, Fenton and Griffiths (2002) have investigated the relation between the distribution of elastic modulus, the total and differential settlements. The results showed that if E is log-normally distributed then the settlement under one footing is also log-normally distributed. However, it is not the same for differential settlements under two footings. They are normally distributed while E is log-normally distributed. For very deep soil layers underlying the footings, it is recommended that the depth of the averaging region does not exceed about 10 times its width due to the stress reduction with depth.

Groundwater control during an excavation or watering in a nearby farm may cause settlements or heave on the foundations. Especially in metropolitan areas, due to need for space, deep excavations are necessary to build multi-storey car parks under residences, hotels and shopping malls. Lowering of groundwater level by pumping during excavation, increases vertical stress in the soil and results with ground settlements that may cause damage to surrounding structures, if large enough. Preene (2000), has suggested a risk assessment method to determine whether such settlements should be of concern. The principle steps in this method are: 1. To develop a simplified ground profile for the site, consisting of layers categorized as aquifer, aquitard and aquiclude; 2. To assign parameters, D and E_o' for layers below initial groundwater level and k_h for aquifers and k_v for aquitards, to each soil layer; 3. To assess the parameters of the groundwater control works, such as maximum period of pumping, dimensions and geometry of the ground water control system, target drawdown and correction factor for effective stress; 4. Calculate the ground settlement at a given distance with $\rho_{total} = \rho_{(corr)\ all\ aquifers} + \rho_{(corr)\ all\ aquitards}$,where $\rho_{(corr)\ all\ aquifers}$ and $\rho_{(corr)\ all\ aquitards}$ are corrected compression of all aquifer and aquitard layers, respectively. As a result the calculated settlements at various distances give the risk zones that will help to determine the structures at risk.

Another excavation induced problem is deformations on the retaining system and settlements on the nearby structures. Maximum lateral displacements on the retaining wall and settlements behind the wall can be categorized between S_{hm}/H=0.2% and S_{hm}/H=0.5% and S_{vm}/H=0.5% and S_{vm}/H=0.15%, respectively as reported in Clough and O’Rourke (1990). S_{hm}, S_{vm} and H are maximum horizontal displacement, maximum vertical displacement and Excavation depth, respectively. On the contrary Hashash, et al.,2008, reported smaller deformations than those listed above. They supported their idea with high stiffness of the support system, difference in the soil profile, which consists of glacial till instead of clay like in Clough and O’Rourke; and embedment of the wall into the rock layer.

As can be seen from the examples above, it is possible to control deformations of the retaining system, depending on the soil profile and rigidity of the system. Estimation of the displacements can be done by using figures used by Clough and O’Rourke (1990), Hashash et al. (2008) and Peck (1969).

3.3 Performance of Dams

Reliability analysis is also performed to estimate potential for failure of dams. Mostly earthquake effects (Barneich et al., 1996 and Von Thun, 1996) and rock fall during and after construction (Kandaris and Euge, 1996) have been investigated. During the reliability analysis logic tree and fault tree diagrams have been used in order to investigate the probability of failure of the system. Since there is limited empirical data, about the probability of failure of the whole system, the probability of failure of the system is very small to calculate. Therefore, it is more suitable to calculate first the probability of failure of each component of the system and pass to the system failure. It is easier to estimate the failure of each element by using the obtained data or engineering judgment. When the components are connected properly to each other, the system reliability can be achieved.

While modeling the system and performing risk assessment: 1. Potential failure scenarios should be determined, 2. The effect of individual failure phases to system failure should be estimated, 3. The order of magnitude of overall probability of failure for each dam should be estimated, 4.Critical factors and considerations related to the filed investigations, design, construction and operation should be determined.

Simulation programs, reliability and finite element analysis software may be used to model the system correctly and precisely. All research in the literature shows that a qualitative planning and investigation prior to modeling and construction, prevent failure or help failure to be acceptable.

3.4 Deep Excavations

In urban areas there is risk when performing deep excavations. To determine the risk factors and their effects on the system, fault tree method as explained in Clause 2.2.2.6, can be used. As an example, Chen et al. (2009), used fault tree analysis in a soil nail wall. They had calculated the probability of failure of the system and the most dangerous events in the fault tree. By this method, which is reasonably consistent with the real failure of the system, they had identified the potential dangerous events that help avoiding unsafe designs and construction procedures and proposing the most important items to be monitored.

In a retaining system design, all the excavation and construction phases should be modeled and the reliability should be determined. It is important to analyze the reliability of the elements of the system and system as well. The system reliability based on the risk assessment of stability and/or serviceability failure of an excavation support system through the entire construction process should be demonstrated as done by Park et al. (2007). Fault tree analysis has been used in this study, too. According to the authors the serviceability performance for braced excavation problems can be assessed based on the system reliability index. In reliability based design, the parameters that may affect the system reliability, chosen to be random variables and the others remain constant. For the fault tree analysis there are several methods, such as the adaptive importance sampling (AIS) method, Monte Carlo simulation (MCS) method, etc.

System reliability sensitivity analyses are more complex than single limit state sensitivity analyses, because there are multiple ‘most probable’ points. The sensitivity factors derived from the individual limit state function cannot be used to derive the system reliability sensitivities because the contribution from the individual limit function cannot be quantified easily. For the system reliability calculation, the sensitivity should be checked to judge which limit state function most influences the probability of failure of the whole system. The adjacent structure damage potential limit state function is the dominant factor for determining excavation system reliability. The system reliability approach always gives higher probability of failure than any other component reliability approach, since it is the combination effects of all failure modes.

In all case studies in literature for reliability analysis, the most important idea is to analyze the reliability of the system. Probabilistic approaches based on the distribution of the parameters were determined. The effects of the parameters on the reliability of the contents and the whole system were examined. The safety factors, material properties such as φ, γ, ν, c, E^{ref}_{50} and E^{ref}_{ur} were used. They had correlated the samples and their mean and standard deviations in order to evaluate reliability index and to simulate the system. By using the standard simulation and reliability methods or by creating their own methods, the authors aimed to assess the risk that the studied system is under.

4. METHODOLOGY

In order to analyze the effects of the deep excavations on the adjacent buildings and analyze the reliability of a system, the stability equation of the system is required. This equation may contain soil parameters or parameters of the elements of the retaining structure or the deformation parameters or all. It depends on the parameters the engineer is interested in. Such as, Il'ichev (2001) used an equation with the soil parameters, ϕ and c, the difference between the embedment depth of the adjacent building foundation and the bottom of the trench and also the structural condition category of the building nearby.

$$(H-h)/L \leq tg\ \phi_1 + c_1/p \qquad \textbf{(4.1)}$$

where H/L is the relative distance between buildings and excavation, (H-h) is the difference between the embedment depth of the building foundations and the bottom of the trench, ϕ_1 and c_1 are the computed values of the angle of friction and specific cohesion of the soil and p is the average pressure beneath the lower surface of the foundation of the existing structure due to design loads.

On the other hand, Roboski and Finno (2006) used the error function equation consisting of the depth and length of the excavation, and the horizontal and vertical displacements of the system.

$$\delta(x)=\delta_{max}\ \{1-1/2\ \mathrm{erfc}\ [2.8\ (x-A)/\ (0.5L-A)]\}\ \text{or} \qquad \textbf{(4.2)}$$

$$\delta(x)=\delta_{max}\{1-1/2\mathrm{erfc}[2.8\{x+L[0.015+0.035\ln(He/L)]/0.5L-L[0.015+0.035\ln(He/L)]\} \qquad \textbf{(4.3)}$$

$$\text{max. distorsion} = 2.8\ \delta_{max}\ /\ [(0.5L-A)\sqrt{\pi}] \qquad \textbf{(4.4)}$$

where A is the inflection point of the erfc at the location where the movement is $\delta_{max}/2$, L is the length of the excavation, He is the excavation height and $\delta(x)$ is the horizontal displacement. While creating the equations Roboski and Finno (2006) assumed that the maximum δ occurs at the center of the excavation, L/2 and the results showed that A is approximately constant with increasing distance behind the wall, but decreases with increasing depth of excavation (Figure 4.1).

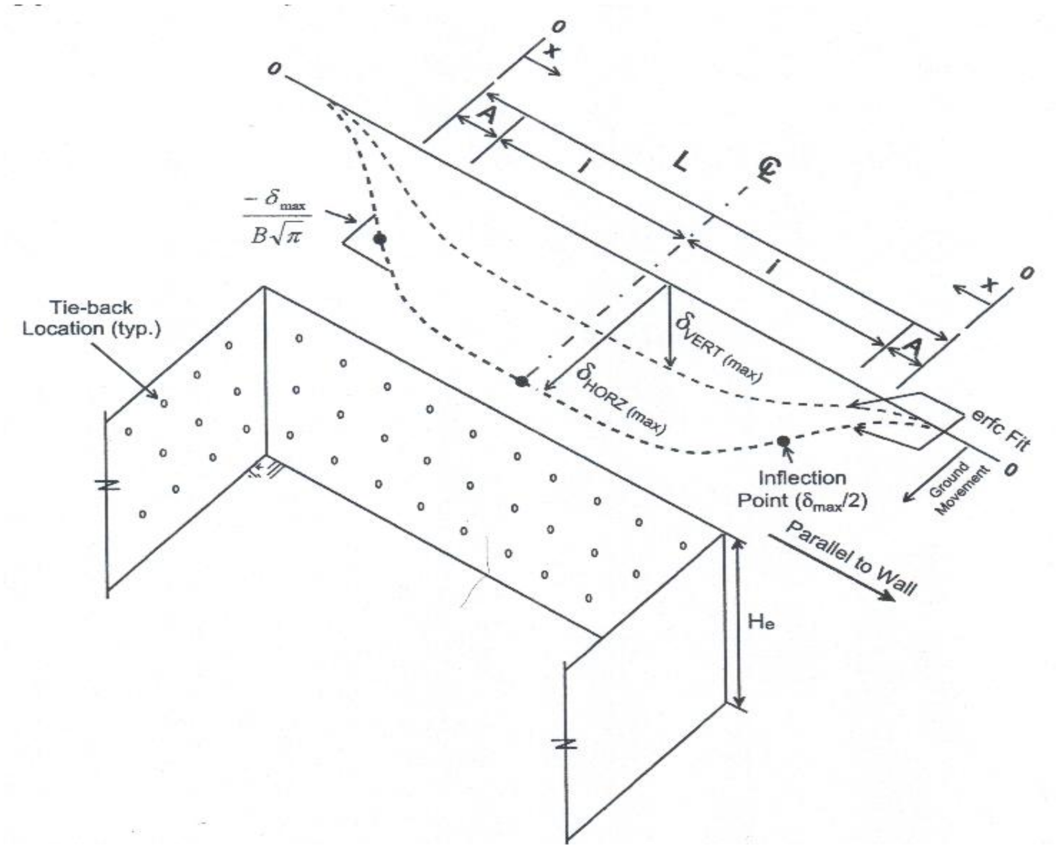

Figure 4.1: Derived Fitting Parameters For The Complementary Error Function δVERT, Settlement; δHORZ, Lateral Movement (Roboski and Finno, 2006).

Hence, the same A value is used for all distances behind the wall for each excavation stage, only the δ_{max} values change as a function of distance behind the wall. Liu et al.(2005) also supports this idea, that the settlements due to excavation decreases as the distance between excavation and the building increases (Figure 4.2).

Liu et al.(2005) also investigated the distribution of surface and subsurface settlements due to the horizontal displacement of a multi-strutted retaining wall. They used the inclinometer and extensometer readings and draw diagrams in order to be able to realize what's going on. The results showed that for the soil profile of Shanghai metro station, probably because of excavating the system in short sections, the ground movements are substantially small and the measured data lie in between δv(max) = 0.4δh(max) and δv(max) = 0.5δh(max), while it is δv(max) = 0.5δh(max) and δv(max) = δh(max) according to Mana and Clough (1981).

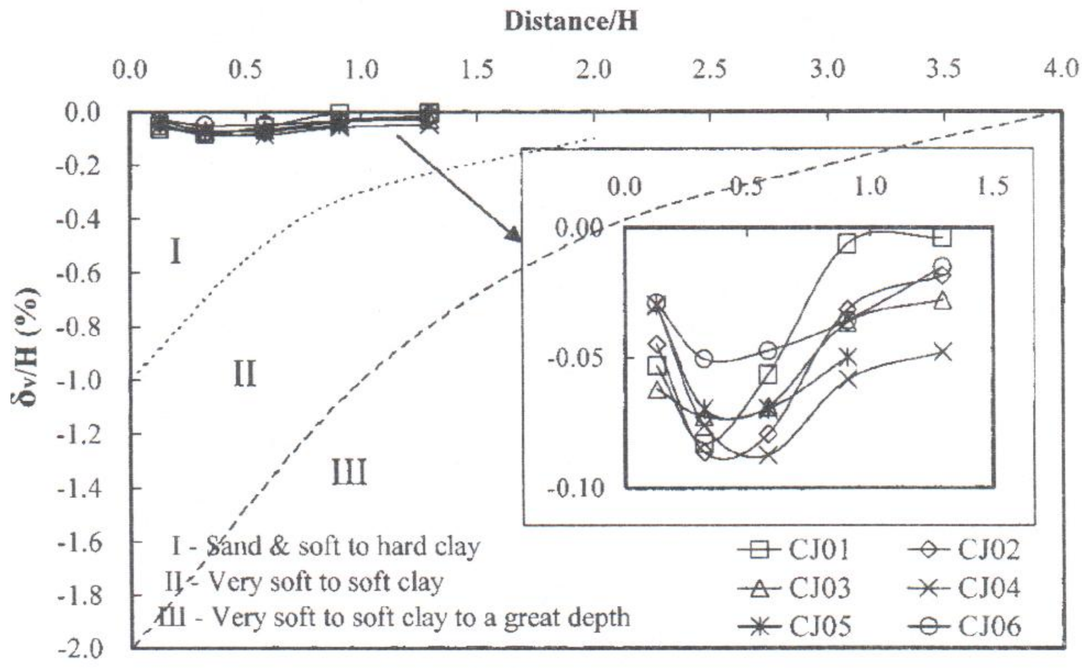

Figure 4.2: Normalized Settlement Profiles Adjacent to Excavations (Liu et al. 2005).

For the purpose of describing the behavior of the retaining structure and its effect on the buildings adjacent to the excavation, Peck (1969) has created his own diagrams for various soils as function of distance from edge of excavation (Figure 4.3).

Peck advocates that the settlements vary considerably with the type of the soil. He says the most important factor that "determines the amount of movement" is not the rigidity of the retaining structure or the vertical space between the lateral struts but the characteristic of the soil behind the wall, under the adjacent structures. That is why Peck (1969) classified the settlements and lateral movements in accordance with the subsurface materials, such as cohesionless sands, cohesive granular soils, soft medium clays, stiff clays and the saturated plastic clays which give the settlements appreciably greater than other soils.

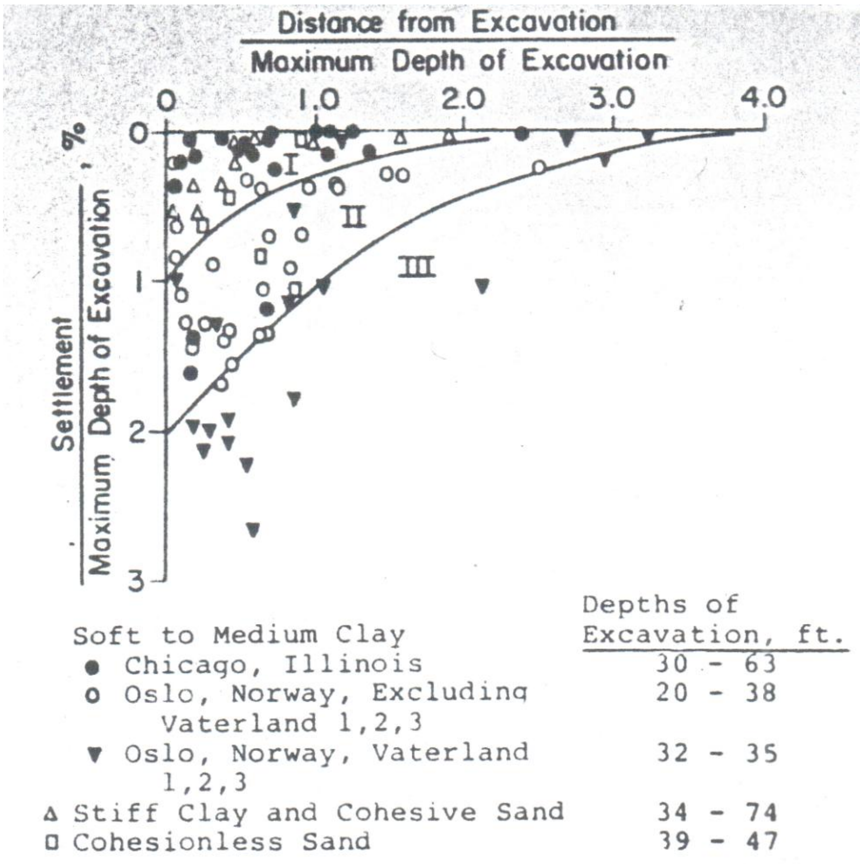

Figure 4.3: Summary of Settlements Adjacent to Open Cuts in Various Soils, as Function of Distance from Edge of Excavation (Peck, 1969).

Figure 4.3 shows the settlements of the buildings adjacent to the excavations in Chicago and Oslo, with respect to distance from the excavation. In Zone I; the soil profile consists of sand and soft to hard clay and an average workmanship is used during the construction of wall, in Zone II; very soft to soft clay layers are in the soil profile and the depth of clay below bottom of excavation is either limited or significant with $N_b<N_{cb}$, and in Zone III; there lays very soft to soft clay below the bottom of the excavation with $N_b>N_{cb}$.

4.1 Numerical Analyses

The reliability analysis of the retaining system of a deep excavation and the risk assessment for the settlement of structures neighboring that deep excavation is important for the stability for both the adjacent structures and the excavation. The effect of the excavation system reliability on the settlements of the adjacent structures can be measured during and after the excavation, which is risky, or can be analyzed before the construction process during design phase. Unquestionably, it is better to model the system at the design phase and analyze the reliability of the retaining system and indirectly the safety of the buildings nearby.

The system can be modeled with many programs, either in 2D or 3D. In this thesis the system is modeled in 2D with a finite element (FE) program (Plaxis) and a reliability program (NESSUS).

Plaxis is the most used geotechnical software in Europe and Turkey for deep excavations and foundation analysis. Plaxis is developed by Delft University of Technology as an initiative of Dutch Department of Public Works and Water Management, for 2D FE code for the river embankments analysis on soft soils and in years it covered most areas of geotechnical engineering. Plaxis can be used to compute lateral displacements of elements in a deep excavation, settlements of a footing, the displacements due to tunnel construction or the effects of a road or river embankment. The analysis may be computed with eight different models, Mohr-Coulomb model (MC), Jointed Rock model (JR), Hardening Soil model (HS), Hardening Soil model with Small-Strain Stiffness (HSsmall), Soft Soil Creep model (SSC), Soft Soil model (SS), Modified Cam-Clay model (MCC), and User Defined (UD) model. In this research, Mohr Coulomb model is used.

Mohr-Coulomb model is a linear elastic-perfectly plastic model. It includes a limited number of soil parameters, E, ν, φ, c, and ψ, and estimates a constant average stiffness. The initial soil conditions play an important role on the results, so a proper K_0 has to be selected for initial horizontal soil stresses. Like every other model, Mohr-Coulomb model also has limitations. Although the increase in stiffness can be taken into account, the Mohr Coulomb model does neither include stress dependency nor stress path dependency of stiffness or unisotropic stiffness (Brinkgreve et al., 2009). The model represents a first order approximation of soil behavior and the results give a first impression on the deformations of the system.

In this research, a deep excavation in a soil profile consisting of gravely sand layers underlained by medium to stiff clay layers will be analyzed. The Mohr Coulomb model is used for the determining the deformations, in order to get the results faster.

After creating the FE model in Plaxis and computing the lateral displacements and settlements the reliability and the sensitivity analysis will be performed with NESSUS. NESSUS is a general purpose tool, which is developed by Southwest

Research Institute (SwRI) for NASA, for computing the probabilistic response or reliability of engineering systems (Riha, 2002). NESSUS can be used to simulate uncertainties in loads, geometry, material behavior (soil parameters), and any user defined random variables to forecast the reliability and probabilistic sensitivity of the variable and the system. The program can compute the cumulative distribution function (CDF) of the system to calculate the reliability. By providing a general g function and linking the function to different analysis codes and analytical functions, NESSUS computes the performance of the system. The results of the analysis give a point reliability value or cumulative distribution function and importance factors that indicate which variables affect the reliability of the system, most. System reliability is calculated by the probabilistic fault tree analysis in NESSUS.

The system how NESSUS works can be expressed as: (SwRI, 2001)

- Compute the probability of failure for each event using FPI methods
- Create a polynomial failure function at MPP.
- Combine the failure functions based on the logic of fault tree.
- Then compute the system reliability using adaptive importance sampling (AIS), which can sample the fast running functions developed for each event or the actual response model.
- Account the correlation between events due to common random variables
- Compute the probabilistic sensitivities with respect to means and standard deviations of the random variables and rank the importance of each event on the probability of failure.

NESSUS allows the use of commercial finite element models in order to reduce the time elapsed for modeling and running the probability analysis and to be able to use the data directly from the finite element model. However, it does not have an interface with Plaxis, so the modeling in this research had been created and run in Plaxis and the results were used in the analytical equation in NESSUS.

4.2 Deep Excavation of a Scale Pit

Since there is lack of space in metropolitan areas, deep excavations are usually necessary for both public and private constructions. Even local failure of an excavation slope in urban areas causes irreversible damages on nearby existing structures and public utilities. It is possible to prevent such failures with an adequate earth retaining system design and construction and careful monitoring with sufficient instrumentation. Before starting the construction, it is very important to confirm the applicability of the preferred retaining system and to verify the carrying capacity of struts and pre-stressed ground anchors regarding the soil profile at the site. As the design of all earth retaining systems is done with engineering judgment to some extent, it is very important to verify the design assumptions before construction by conducting tests on site. The engineer or the client also has to be informed in advance that allowable deformations or stress limits are to be exceeded. So, proper instrumentation and correct monitoring has significant importance. Also, the reliability of the retaining system has to be analyzed and before starting the construction, the client and the engineer has to be aware of the limits and the risks.

A steel plant consisting of 4 main buildings has been constructed on south of Turkey. The main buildings are the melt shop, cold mill, hot mill, slitting cutting package service buildings and supportive buildings are the neutralization building and air separation and air compressed plant, emergency water tower and electricity distribution center. The total construction area of the plant is 440 000 m^2. The plant will also have a 1 300m long pier on steel piles. When construction is completed, the plant will be the largest steel and iron plant that is constructed by private sector and the second of all in Turkey.

In order to collect all scrap from melt shop and hot mill buildings, two scale pits has been constructed. The pits are 17.00 m deep. Dimensions of the scale pit in plan are 42.0m x 24.0m. This scale of deepness is required to collect all scrap from all over the plant with a minimum inclination. The case in this research is the hot mill scale pit. The site investigations, model created based on the soil profile observed during the investigations and monitoring phases are explained in details and the results of the model and the monitoring have been compared with each other.

4.2.1 The site and the engineering characteristics of the scale pit

The steel plant is being constructed on a 550 000 m^2 region with a construction area of 440 000 m^2. The area is next to the Mediterrenian sea and the elevation of the construction site is at +8.00m from sea level.

A hot mill complex has been constructed in the steel plant. The building contains heavy equipments and the superstructure and equipment loads reach 350kPa. The dimensions of the main building of hot mill are 33.0m x 276.0m on plan. It has been constructed on single foundations. Foundations of the building and equipments are deep and the depth may reach up to 12.00m from the surface (elevation +8.00m).

A scale pit is designed next to the hot mill building to collect all scrap coming from hot mill area. The scale pit is 17.00m deep and is constructed with reinforced concrete. The structure does not have any floors or horizontal supports for side walls. It is designed without any floors for getting the collected scrap out with equipments like clam shells, scrapers, etc. The outside walls of the scale pit are 1.50m thick. There are two inside walls, one perpendicular to long side, separating the scale part and pumping room and another perpendicular to short side, dividing the scale pit into two parts (Figure 4.4). The thickness of the inside walls are 60cm. The pit has been constructed on a raft foundation, whose thickness is 1.50m.

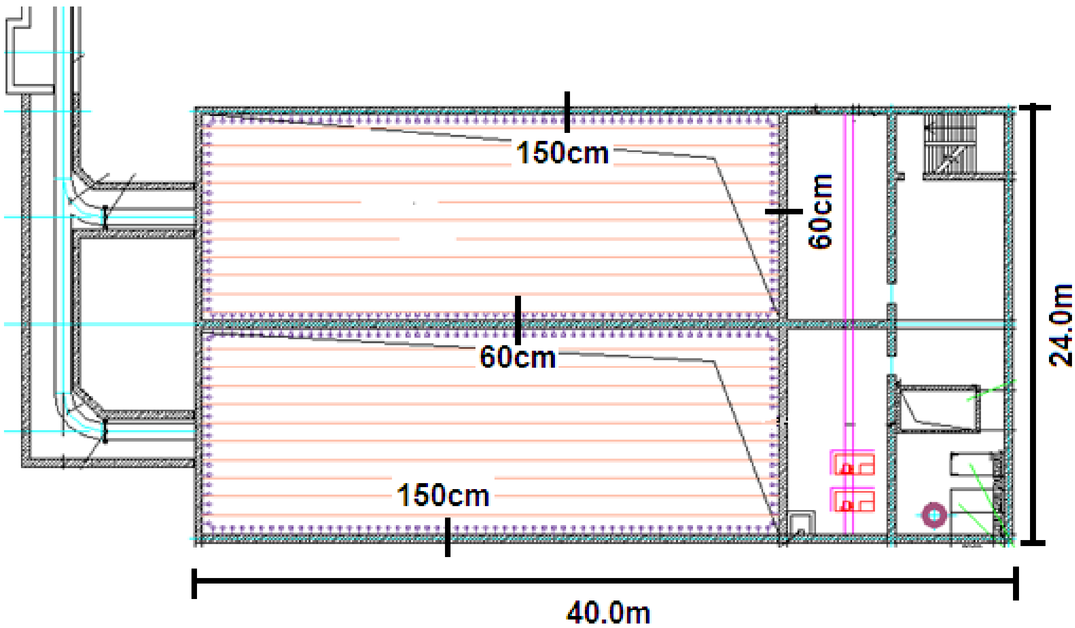

Figure 4.4: Layout of the Scale Pit.

4.2.2 Site investigation and soil profile

4.2.2.1 Investigations prior to construction of retaining system

In order to determine the soil profile and obtain the soil properties to design soil models for geotechnical analysis, extensive soil investigations were conducted. 70 borings having 20m to 50m depth are performed at the construction site of steel plant. Locations of the borings are shown in Figure 4.5. In-situ and laboratory tests are conducted on disturbed and undisturbed samples taken during borings. The soil profile has been determined based on the results of the borings and laboratory tests.

The soil profile under the foundations of the buildings changes from building to building depending on the distance from the sea. However, it mainly consists of soft-medium stiff silty clay layer at the surface, medium dense to dense sandy gravel below and stiff silty clay layer at deep levels. At some parts of the site fill with dense gravel material was made in order to fill the sea and gain space and elevation. The accepted surface elevation is ±8.00m at most of the region at present. The SPT values for the medium stiff-stiff silty clay layers at the surface are N_{30}= 6-11. The clay layers get stiffer with depth and the SPT values become N_{30}= 15-20. SPT values for fill layers and gravelly sand layers do not give specific and correct values because of coarse grains. According to the laboratory tests the silty sand-gravel layers are classified as SM, GM and GC due to USCS and they are non-plastic. On the other hand silty clay-clayey silt layers are classified as SC, CL and CL-ML with a plasticity index of Ip=4-7 at the surface and Ip=8-17 at deeper layers.

The groundwater at the site is balanced by sea and the depth of ground water changes from 2.00m to 6.00m.

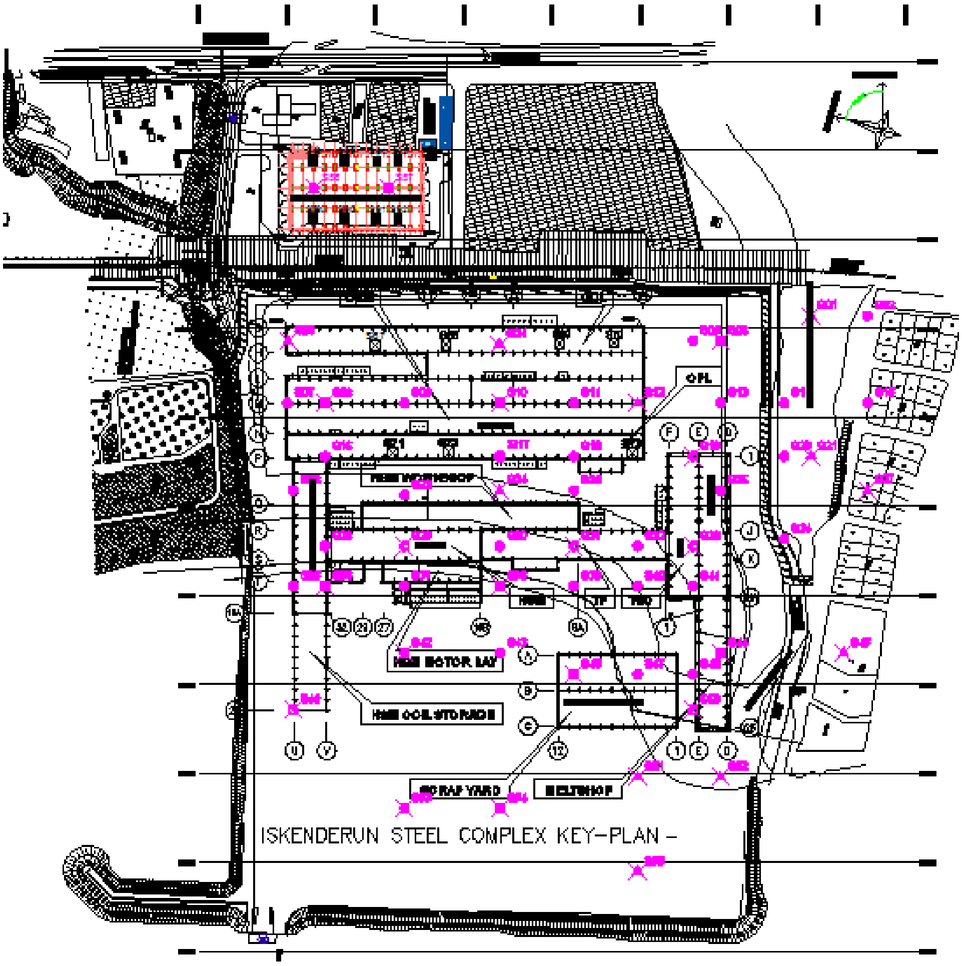

Figure 4.5: Locations of borings on the general layout of the site (ENAR, 2009a).

As already been mentioned above, the soil profile varies from building to building with small changes in the properties, depth and thickness of the layers. But the engineering parameters for the analyses are accepted as shown in Table 4.1. The idealized soil model is given in Figure 4.6.

Table 4.1: Average Engineering Parameters of the Layers in the Soil Profile (ENAR,2009a).

Engineering Property	Sand-Gravel Fill	Sand-Gravel (I)	Silty Clay-Clayey Silt (I)	Sand-Gravel (II)
Natural Unit Weight (γ: kN/m^3)	20	20	18	20
Average SPT Value (N_{30})	30-50	30-R	12	30-50+
Internal Friction Angle (ϕ:°)	32.5-35	37.5	-	40
Undrained Cohesion (c_u:kPa)	-	-	55	-
Deformation Modulus (Es or Mc:MPa)	15	30	5	30
Vertical Subgrade Coefficient (kv: kN/m^3)	50 000	50 000	10 000 - 20 000	60 000

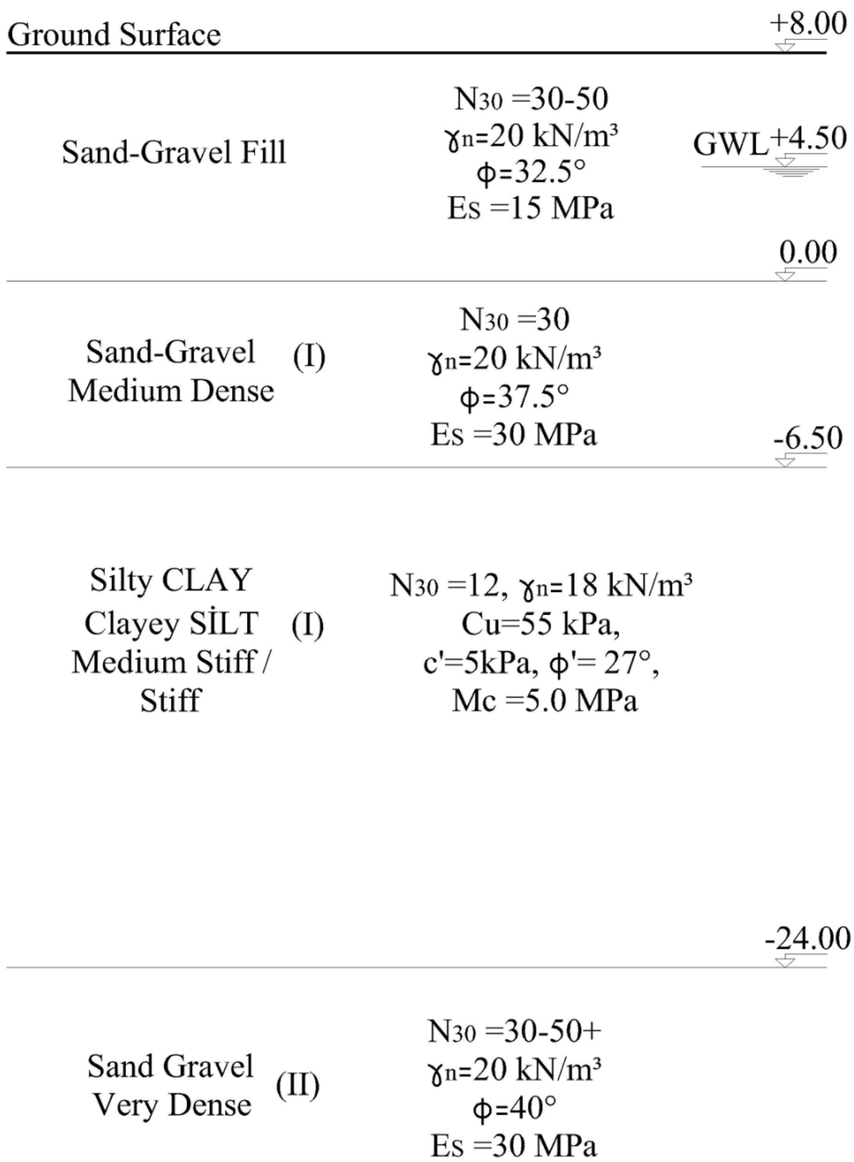

Figure 4.6: Idealized Soil Model for the Analysis (ENAR, 2009a).

4.2.2.2 Investigations during excavation of the scale pit

While excavating the scale pit, it was easy to see the soil profile from the excavation facades. The layers seemed to differ from the soil layers obtained by the site investigations, prior to construction of retaining system, thus undisturbed ring samples were taken from the excavated layers and laboratory tests were conducted.

- Laboratory Tests

8 samples were taken from the clay and sandy layers with D=20cm and H=25cm ring samplers, and 38 laboratory tests, such as Atterberg limits, water content, sieve analysis, oedometer, triaxial compression (CU), shear box, unconfined compression

test were conducted. The results of the tests are discussed in details, at the paragraphs below. Soil parameters (average), obtained from the test results are summarized in Table 4.2.

Table 4.2: Engineering Parameters obtained from Laboratory Tests.

Depth (m)	Soil Type	γ	w	LL	PL	Ip	c	ϕ	c'	ϕ'	E(MPa)
5.50	CL	22	24	26	16	10	25	-		11	20
6.00	CL	20	24	27	15	12	16	-		8	22
7.50	CL	19	26	35	18	17	40	22	65	15	16
8.00	CL	20	21~28	34	18	16	40	20	65	12	18
9.00	CL-ML	21	18	24	18	6	-	-			
9.50	CL	21	21	25	13	12	-	-			
22.50	CL	22	26	30	18	12	60	-		22	15

- Soil Profile

The soil profile at the excavation site is determined to be different from one used for the pre-analyses. During excavation, 4.0m thick, gravel-sand fill layer has been encountered at the surface. This fill layer is created to fill the sea to gain more space for buildings. Below the fill layer there lays a medium dense sand-gravel layer, whose thickness is 2.0m. Below the fill layer there lays a soft-medium stiff clay layer, whose thickness is 5.0m. Clay layer is low-medium plastic and contains sandy levels at 9.00m. The plasticity index of this clay layer is between Ip=6-17 and layer can be classified as CL, CL-ML. Sand-gravel layer starts right below clay layer. It is 9.0m thick. According to the laboratory tests the silty sand-gravel layers are classified as SM, GM and GC due to USCS and they are non-plastic.

The groundwater level at the site is 8.00m deep from the top of the retaining system (+4.00m elevation). The engineering parameters for the analyses are accepted as shown in Table 4.3. The idealized soil model is given in Figure 4.7.

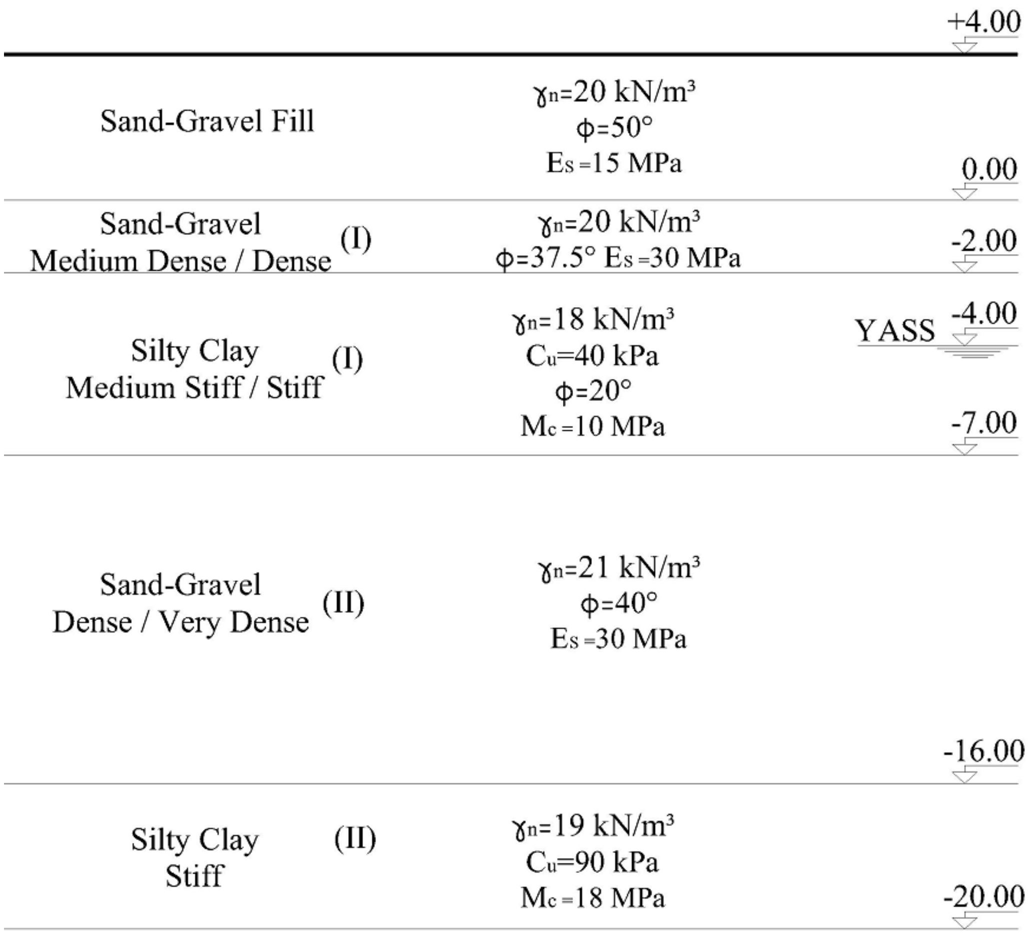

Figure 4.7: Idealized Soil Model for the Analysis (obtained during excavation).

Table 4.3: Average Engineering Parameters obtained during Sampling from Excavation

Engineering Property	Sand-Gravel Fill	Sand-Gravel (I)	Silty Clay-Clayey Silt (I)	Sand-Gravel (II)	Silty Clay-Clayey Silt (II)
Natural Unit Weight (γ: kN/m^3)	20	20	18	20	19
Internal Friction Angle (ϕ:°)	50	37.5	20	40	15
Undrained Cohesion (c_u:kPa)	-	-	40	-	90
Deformation Modulus (Es or Mc:MPa)	15	30	16	30	18

4.2.3 Earth retaining system

The scale pit is 17.00m deep. However, the site has been excavated for 4.0m prior to foundation excavation in order to reduce the depth of the excavation and retaining system. While determining the retaining system for the excavation; soil profile, the depth and high ground water level, soft clays and loose sands in the soil profile with high permeability were taken into consideration. Other factors affecting the predetermination of the retaining structure were the available techniques that can be readily employed by the geotechnical contractor and since the structure does not have any floors or horizontal supports for side walls, the safety of the system at the construction phase at each construction stage. Limitations in the time schedule of the whole project and the budget allocated for the retaining system construction also restricted the alternatives in the retaining structure.

As the construction site was adjacent to sea, high water pressures and impermeability of the retaining wall had a major role in the design. Site survey showed that the thickness of the clay layer under the gravel fill is 5.0m. The existence of the hot mill adjacent to scale pit and the construction sequence of the single foundations of the building had a serious effect on the decision and modeling phases. For the excavation of the scale pit, bored piles with D =1.20m diameter, spacing s =1.40m center to center were designed. D = 80cm jet grout columns were decided to be drilled outside the retaining system, between the bored piles with s=1.40m spacing. This would avoid the ingress of water into the excavated area and avoid erosion of granular deposits between piles until the reinforced concrete walls of the pit were constructed. The horizontal supports of the retaining system has been chosen as D = 914mm pipes. The thickness of the pipes were t = 12mm. Since the piled foundations of the hot mill building were close and deep, use of pre-stressed anchors was out of the list. On the other hand, decision of the diameter and thickness of the pipes were generally based on the steel and pipe stocks of the employer. The plan and section of the system are shown in Figure 4.8 and Figure 4.9, respectively.

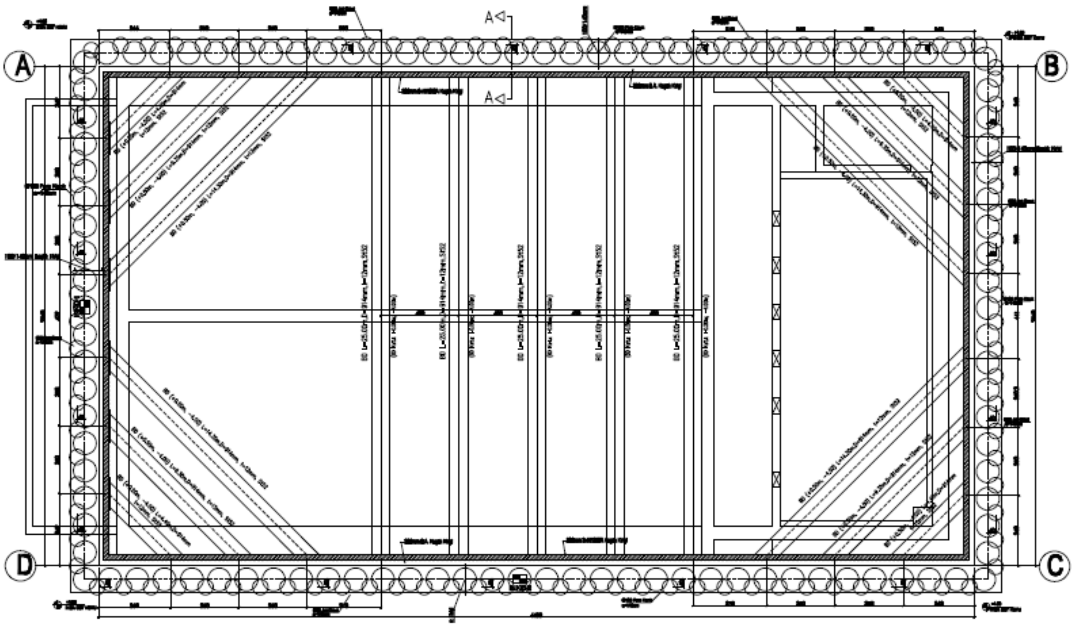

Figure 4.8: Plan of the Retaining System (ENAR, 2009b).

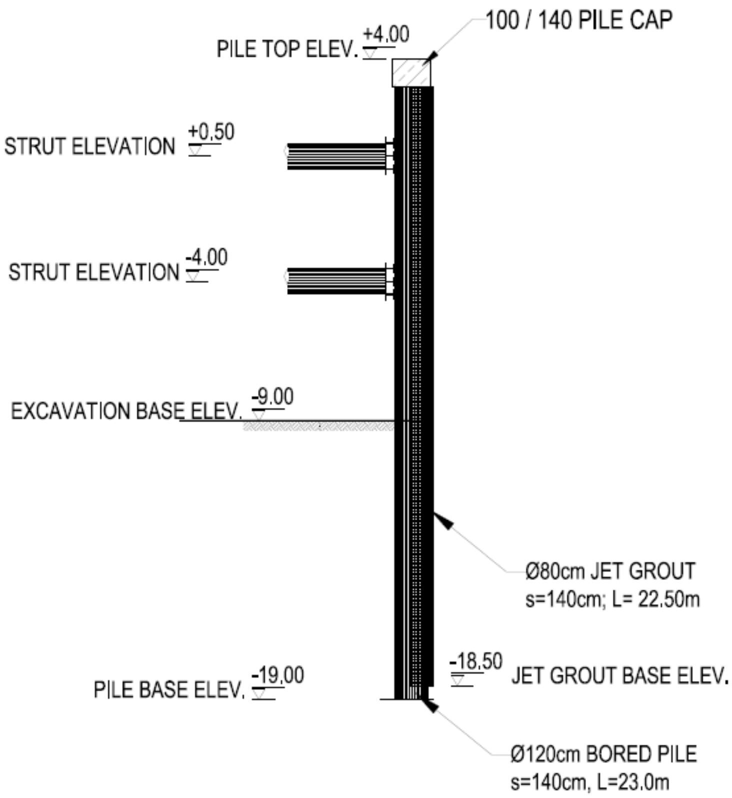

Figure 4.9: Section of the Retaining System (ENAR, 2009b).

4.3 Finite Element Analyses

4.3.1 Defining the problem

The retaining system of the deep excavation explained above was analyzed for uniform soil conditions. The aim of analyzing the system with FE model was to ensure the system stability during excavation and construction phases, step by step and determine the horizontal and vertical deformations on and behind the retaining system.

The retaining structure consists of D=1.20m, L=23.0m bored piles and 914mm, 12mm steel pipes. The external wall thickness of the scale pit and thickness of foundation are accepted as 1.50m. The parameters of the retaining system elements and scale pit walls/foundation are assumed to be uniform and rigid. The properties of the elements of retaining wall and scale pit are set as constant and do not vary with distance or depth. Sketch of the system analyzed is shown in Figure 4.10.

Finite Element Analyses are performed in twelve phases:

Phase 1: Installation of the bored piles at +4.00m, with surcharge load of hot mill foundations behind the piles

Phase 2: Excavation to (-1.50)

Phase 3: Installation of First Level 914mm pipes at +0.50 (s=4.00m)

Phase 4: Excavation to (-6.00)

Phase 5: Installation of Second Level 914mm pipes at -4.00 (s=4.00m)

Phase 6: Excavation to (-9.00)

Phase 7: Construction of the foundation (t = 1.50m)

Phase 8: Construction of the First Stage of pit wall till (-4.50)

Phase 9: Uninstallation of Second Level of Pipes

Phase 10: Construction of the Second Stage of pit wall till (0.00)

Phase 11: Uninstallation of First Level of Pipes

Phase 12: Construction of the Third Stage of pit wall till (+4.00)

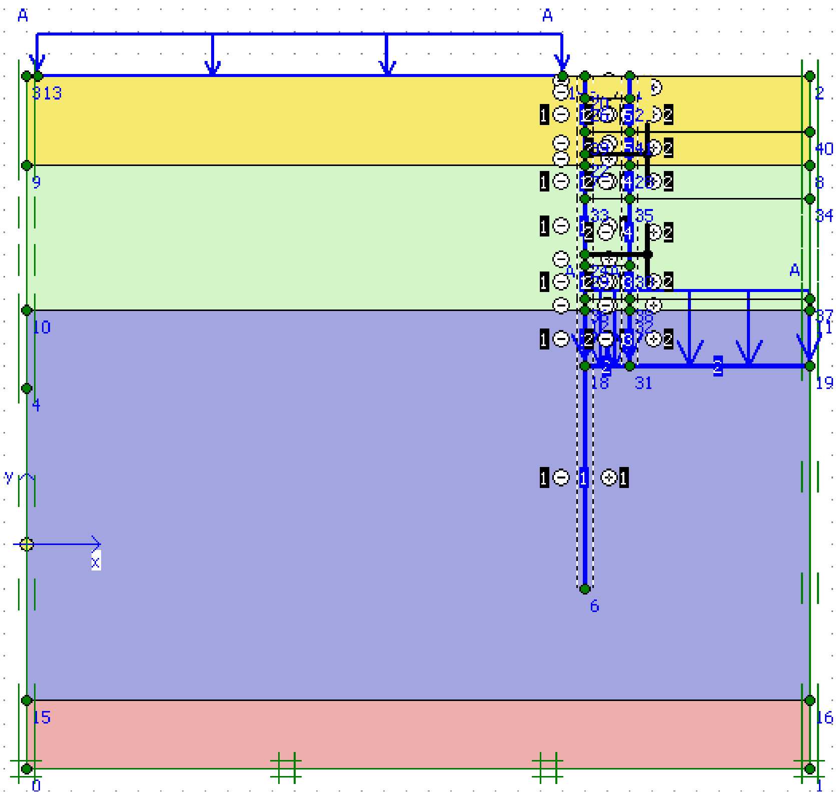

Figure 4.10: Sketch of the System used in the Analysis.

4.3.2 Numerical modeling with Mohr-Coulomb model with first parameters

4.3.2.1 Mesh design and boundary conditions

The retaining structure was first analyzed with Mohr-Coulomb Model with Finite Element Program Plaxis. In the analyses soil and bored piles are considered as fully bounded. The system is modeled as half, depending on the symmetrical shape of the scale pit. Plain strain model with 15 node elements has been used. Global coarseness has set to fine. 845 elements and 7290 nodes were used in total to define the piles and soil layers. The boundaries of the system is fixed by “standard fixities”, to generate a full fixity at the base of the geometry and roller conditions at vertical sides (ux=0, uy=free) (Brinkgreve et. al. 2006).

4.3.2.2 Materials for 1st model

Mohr Coulomb Model has been issued for FE analyses, to accept soil material behavior as elasto-plastic, in order to simulate the deformations on the system and shear failure of soil layers. Four different types of soils, fill consisting of sand and gravel, dense sand-gravel, medium stiff silty clay and very dense sand-gravel, have been modeled as they appear in the soil profile.

On the other hand, linear elastic material model has been used for the retaining system elements; bored piles, foundation, reinforced concrete walls and steel pipes. The parameters used in the analyses are summarized in Table 4.4.

4.3.2.3 Results of the FE analyses

FE analysis with Mohr-Coulomb model has showed that the horizontal deformations on the bored piles change between 12mm (min.) and 50mm (max.). The results are shown in Figure 4.11. The maximum horizontal deformation at pile cap level is 20mm. Also, the maximum vertical displacement behind the pile cap is 40 mm and this value decreases with distance from excavation (Figure 4.12).

Table 4.4: Material Parameters.

Model	Material	Modulus of Elasticity (E=3*Es) (kN/m^2)	Poisson's Ratio (υ) (-)	Unit Weight (γ) (kN/m^3)	Cohesion (c) (kPa)	Friction Angle (ϕ) (°)	Dilation Angle (φ) (°)
MC	Sand-Gravel Fill	50000	0.30	20	5	32.5	1
	Dense Sand Gravel	90000	0.30	20	5	37.5	7.5
	Medium Stiff Silty Clay	25000	0.30	18	5	27	0
	Very Dense Sand Gravel	90000	0.30	20	1	40	10
		EA (kN/m)	EI (kNm^2/m)	Weight (w) (kN/m^2)	Poisson's Ratio (υ) (-)	-	-
Elastic	D=120cm Bored Pile	2.422E7	2.1801E6	4.3	0.15	-	-
	d=150cm Foundation	6.4E7	2.1333E7	50.0	0.15	-	-
	d=150cm RC Walls	4.8E7	9E6	37.5	0.15	-	-
	914mm Steel Pipes	7.137E7	-	-	-	-	-

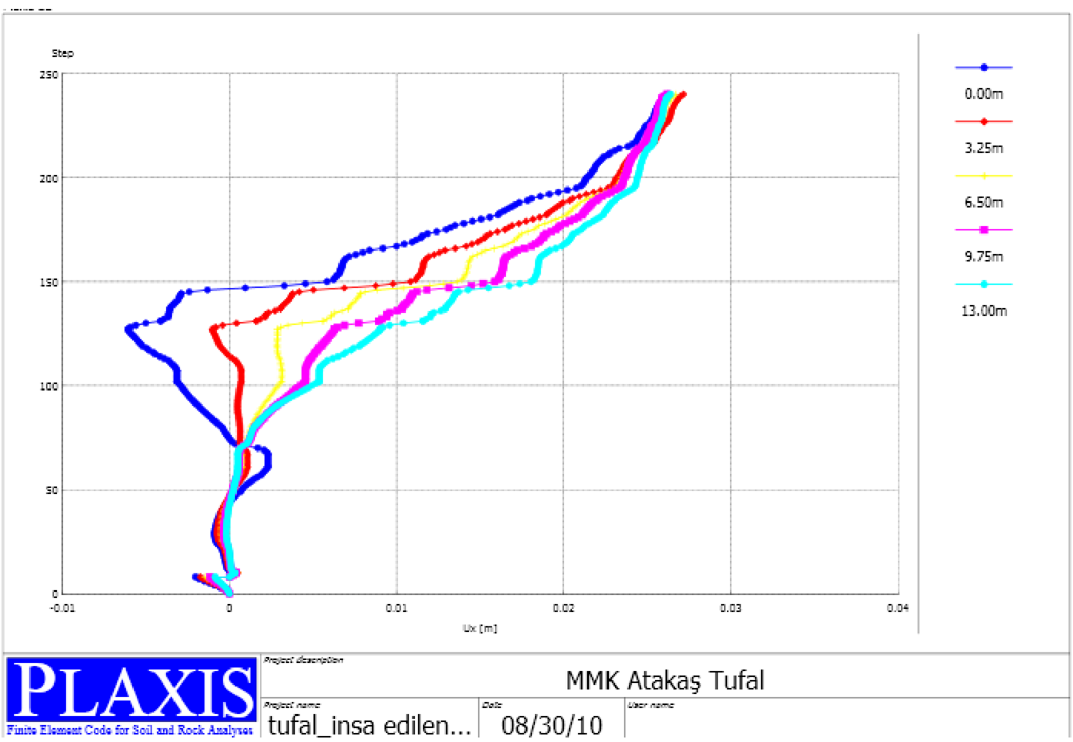

Figure 4.11: Variation of Horizontal Displacement behind Pile Cap with the Distance from the Excavation.

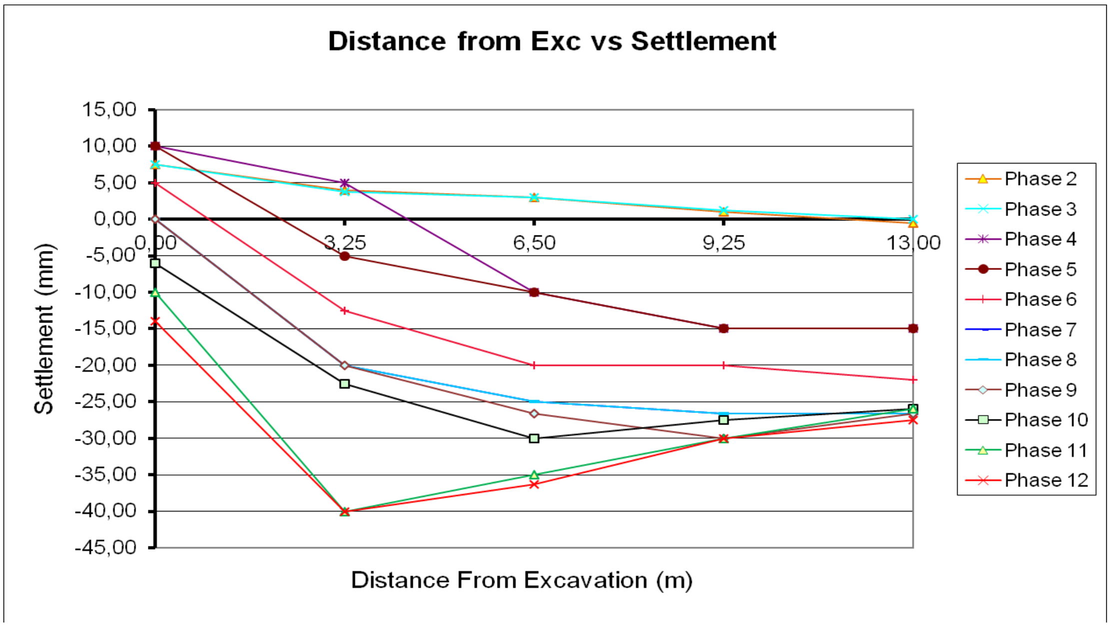

Figure 4.12: Settlement Behind the Wall Due to the Distance from the Excavation.

Also, the axial loads on the steel pipes were calculated, by the increasing excavation depth and the results showed that the pipes are loaded till 80 tons/m. Since the system is designed as 1pipe/4m, the pipes will be loaded to 320 tons. The 914mm steel pipes are strong enough to bear this value of tons, easily. The maximum shear force on the piles is 73 ton/m and maximum moment is 228 tonm/m.

4.3.3 Numerical modeling with Mohr-Coulomb model by using recent soil data obtained from samples taken during excavation

The soil investigations; borings, ring sampling and laboratory tests were re-performed during excavation. Results of the investigations had showed that the soil profile has different layers than the idealized soil model used at first analysis, and the engineering properties of the layers also differ. So, the system modeled and analyzed again with the new parameters, using the same Mohr-Coulomb method before.

4.3.3.1 Mesh design and boundary conditions

The system is modeled as half in this analysis too. Plain strain model with 15 node elements has been used. Global coarseness has set to fine and 845 elements and 7290 nodes were used in total to define the piles and soil layers. The boundary conditions were also the same with the first Mohr-Coulomb Analysis.

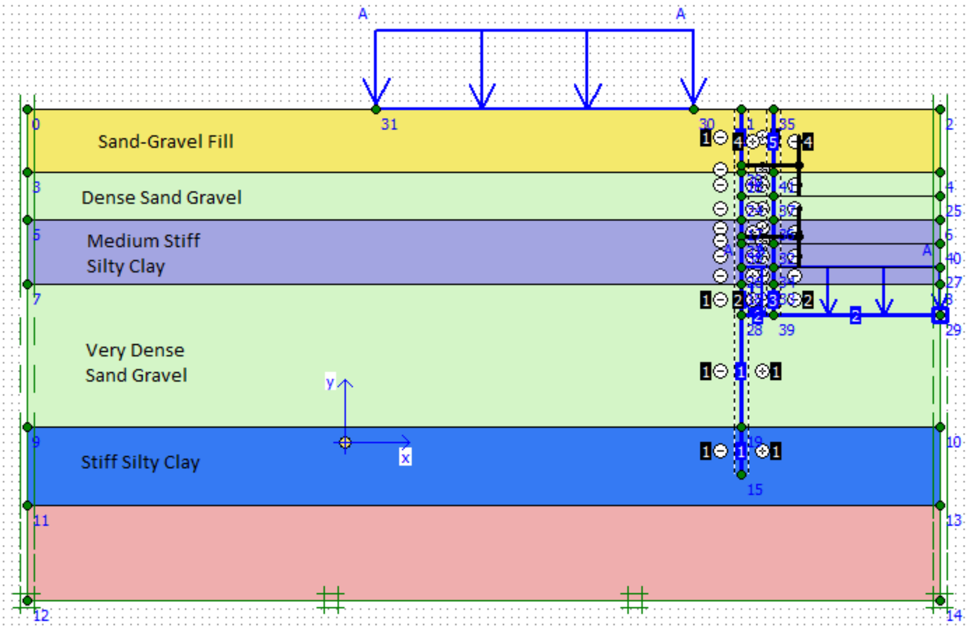

Figure 4.13: Soil Model Used in the Analysis with Recent Soil Data Obtained during Excavation.

4.3.3.2 Materials for 2nd model

The properties of the soil layers have been summarized in Table 4.5. Properties of the elements of retaining system have not changed. Four different types of soils consisting of sandy-gravel fill layer at the surface, dense sand-gravel below with medium stiff silty clay as successor and very dense sand-gravel as the deepest layer below 25.00m (Figure 4.13).

On the other hand, linear elastic material model has been used for the retaining system elements as used before. The parameters for these elastic materials are as given in Table 4.4.

Table 4.5: Material Parameters.

Model	Material	Modulus of Elasticity (E=3*Es) (kN/m^2)	Poisson's Ratio (υ) (-)	Unit Weight (γ) (kN/m^3)	Cohesion (c) (kPa)	Friction Angle (ϕ) (°)	Dilation Angle (φ) (°)
MC	Sand-Gravel Fill	50000	0.30	20	10	40	10
	Dense Sand Gravel	90000	0.30	20	10	37.5	7.5
	Medium Stiff Silty Clay	25000	0.30	18	40	20	0
	Very Dense Sand Gravel	90000	0.30	20	5	40	10

4.3.3.3 Results of the FE analyses

The Mohr-Coulomb Model Analysis with new parameters has showed that the horizontal deformations on the bored piles change between 6mm (min.) and 14mm (max.). The results are shown in Figure 4.14. The maximum horizontal deformation at pile cap level is 7.5mm. Also, the maximum vertical displacement behind the pile cap is 4.5 mm and this value decreases with distance from excavation (Figure 4.15).

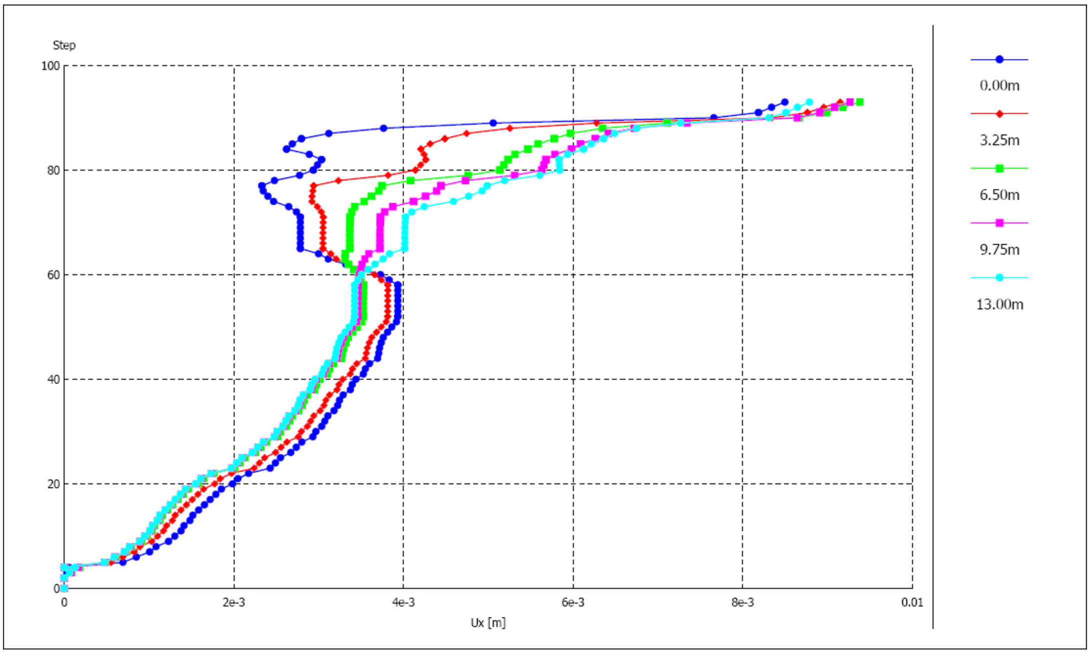

Figure 4.14: Variation of Horizontal Displacement behind Pile Cap with the distance from the excavation.

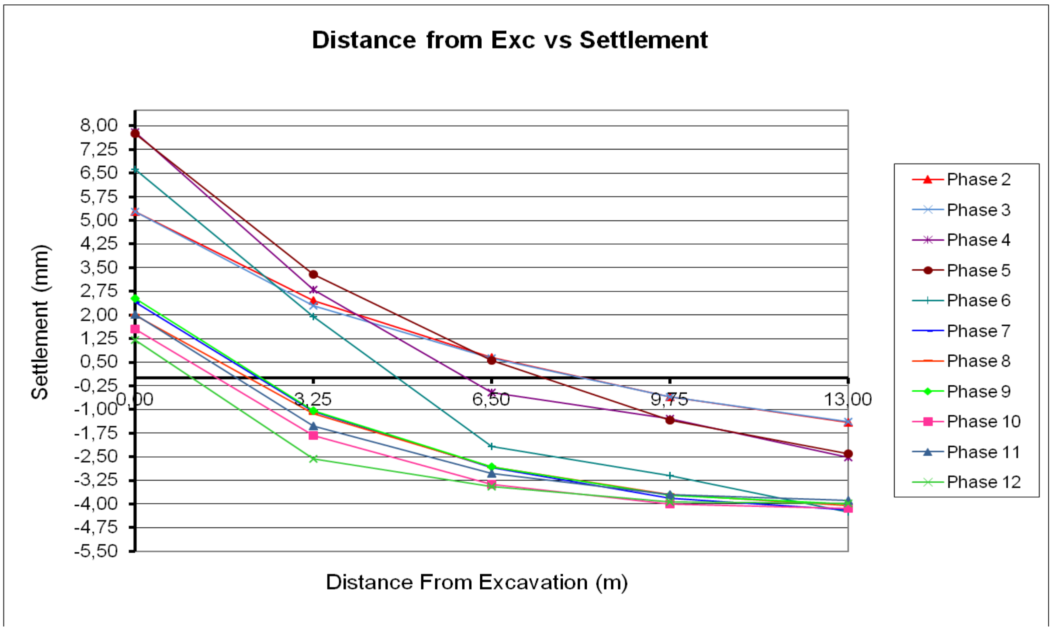

Figure 4.15: Settlement behind the wall due to the distance from the excavation.

Also, the axial loads on the steel pipes were calculated, by the increasing excavation depth and the results showed that the pipes are loaded till 40 tons/m. Since the system is designed as 1pipe/4m, the pipes will be loaded to 160 tons. The maximum shear force on the piles is 32 ton/m and maximum moment is 75 tonm/m.

4.3.4 Comparing the analyses results

When the results of the two analyses are compared, the differences between them are clearly obtained from comparison tables. As can be seen from Table 4.6 the results of two analyses are as half of each other. The differences between results depend on the difference between soil parameters used in the analyses (Table 4.4 and Table 4.5). The soil parameters used in the new analyses show a stiffer soil profile than the first ones so the horizontal displacements and settlements behind the retaining system and the moment and shear stress effecting on the piles are less than the ones in the first analyses. This shows that the soil parameters (c, ϕ) are effective on the FE analyses, although the rigidity of the system has not changed.

Table 4.6: Comparison Table for First Analyses and Second Analyses.

Analyses Type	Total Horizontal Displacement of the System	Maximum Horizontal Displacement at the Pile Cap	Settlement just behind the Pile Cap	Loads on Steel Struts	Maximum Shear Stress at the Piles	Maximum Moment at the Piles
First	12~50mm	20mm	40mm	80 t/m	73 t/m	228 tm/m
Second	6~14mm	7.5mm	4.5mm	40 t/m	32 t/m	75 tm/m

While the soil parameters encountered during excavation is more representative of the soil profile, it is obvious that the results of the FE analyses with the parameters from investigation during excavation are more reliable. That is why the monitoring results will be compared to the new analyses in the next clauses.

4.4 Monitoring at the Scale Pit

The scale pit is 24.0m x 42.0m in plan and 13.0m deep from surface (+4.00m) elevation. In such deep excavation, it was necessary to monitor the system. In order to measure the horizontal displacements at the bored piles and behind, inclinometers are placed, 1 in the mid-pile at long façade at the sea side and 4 behind with a distance of 3.25m (1/4 of the excavation depth) from center to center (Figure 4.16 and Figure 4.17).

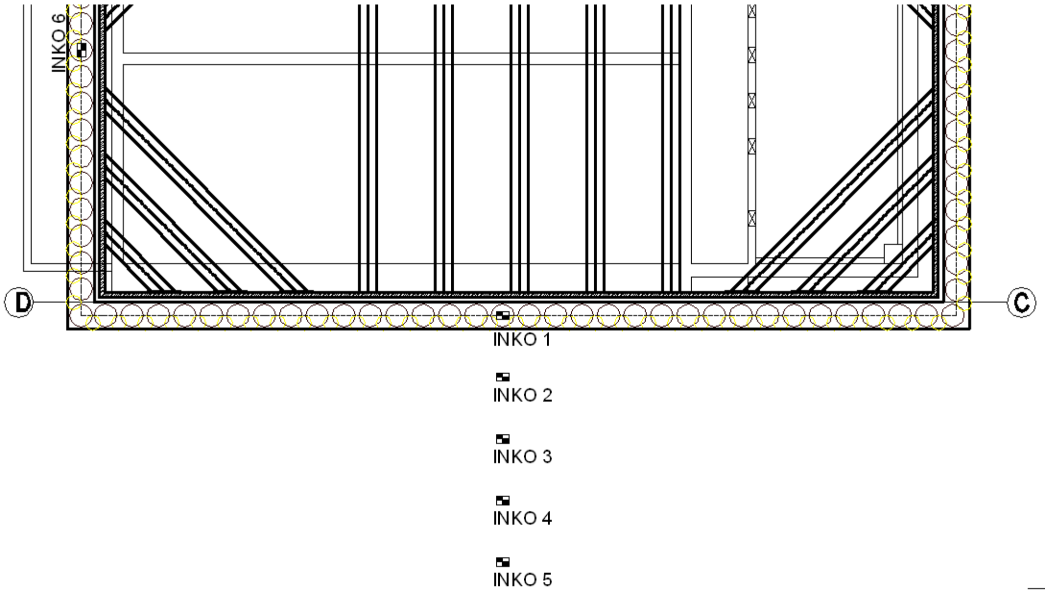

Figure 4.16: Locations of Inclinometers on plan.

Figure 4.17: Location of the Inclinometers behind Retaining System.

Spider magnet, magnetic settlement columns were installed in each inclinometer behind the retaining wall, at every steel pipe level and one at bottom for reference. In order to record the forces on the pipes at each excavation and construction level, vibrating wire solid load cells and vibrating wire arc welding strain gauges are installed on 3 of pipes at the middle of the system. Two of the load cells are installed at first level pipes and one at the second level. Four strain gauges are placed at each pipe carrying a load cell. The measurements are recorded by a FLEXDAQ CR1000 data logger (Figure 4.18), and logger net program has been used to decode the measurements to SI units.

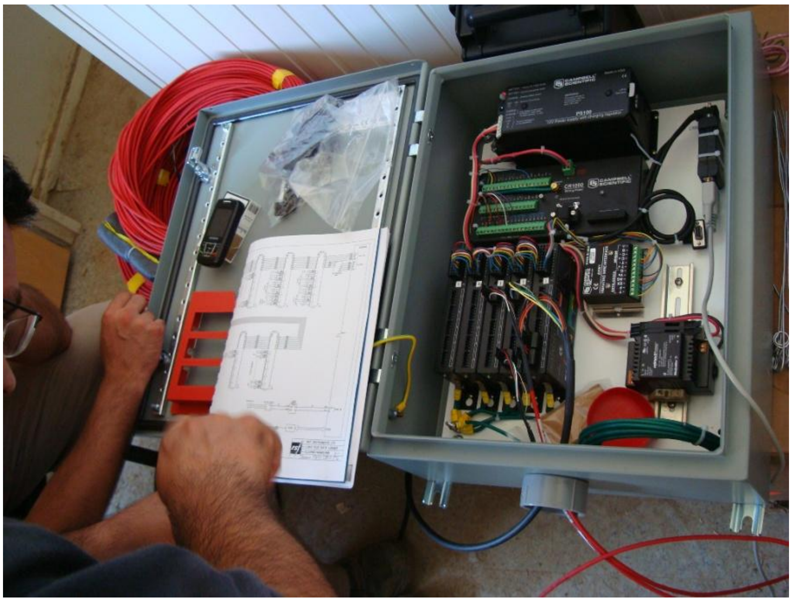

Figure 4.18: FLEXDAQ Data Logger CR1000.

4.4.1 Inclinometers

Inclinometers are instruments that measure the horizontal displacement at the ground. They are generally used for monitoring deep excavations. Inclinometers consist of 3 main parts. A pocket PC to record the data obtained from wells, a probe, which senses the movements in the inclinometer well, a cable connected to probe to let it in the well (Figure 4.19).

The digital inclinometer probe consists of two force-balanced servo accelerometers, which measure tilt in two axes. Proper installation of the inclinometer casing attempts to align one set of grooves in line with the axis of expected movement. This is called the A axis. The perpendicular set of grooves is the B axis (Figure 4.20).

Figure 4.19: Parts of a Digital Inclinometer.

1.Soft Shell Case

2.Reel Battery Charger

3.Digital Inclinometer Probe

4.85mm/3.34´´OD Cable Grip

5.70mm/2.75´´OD Cable Grip

6.iPAQ hx2410 Pocket PC w/Rugged Case

7.Spare Reel Battery

8.9-Pin to USB Cable

9.12V DC Adapter for Pocket PC

10. AC Adapter for Reel Battery Charger

11. AC Adapter for Pocket PC

12. 12V DC Adapter for Reel Battery Charger

13. Silicon to protect Probe connection

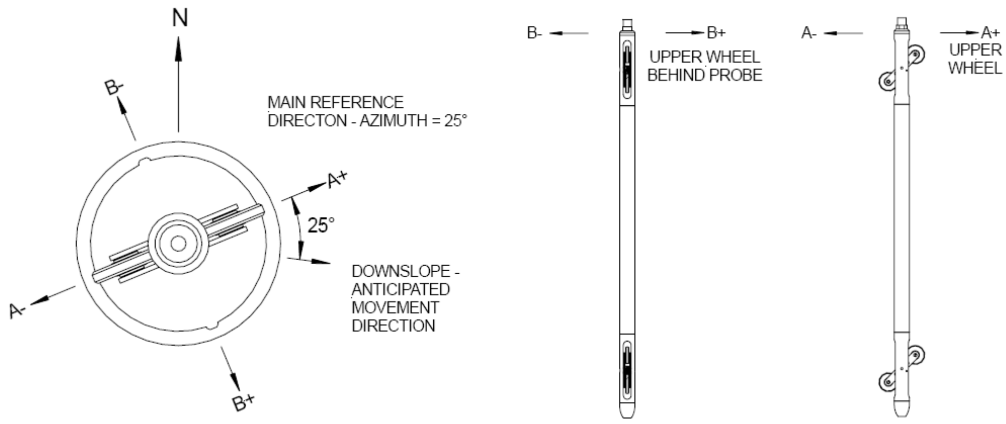

Figure 4.20: Probe Axes.

4.4.2 Spider magnet – magnetic settlement columns

Spider magnets are systems to monitor either heave or settlement in the ground. A spider magnet can be installed either by itself or with inclinometer casing as performed in our case. Installation is generally vertical but there are some examples about horizontal installation.

Spider magnets are anchored to the inclinometer casing; however the anchors are not coupled to the access pipe and are free to move with soil (Figure 4.21). Spider magnets are utilized in borehole installations, employing two different methods. The simplest method requires a cased borehole, whereby the greased access pipe/casing is installed and drill casing is pulled to the first anchor elevation. A 3-legged spider anchor as seen in Figure 4.22 is then pushed down over the access casing, exiting the drill casing, allowing the spring legs of the spider magnet to bite into the soil. The casing is pulled to the next anchor location and the procedure is repeated until all anchors are placed.

Magnets are made of plastic and magnetic tapes. When the probe is lowered down the casing, when it reaches the magnet level, an electrical circuit is completed and a light in the read out unit flashes and a sharp sound occurs. Magnet level is then read directly from the cable connecting the probe to the circuit board (Figure 4.23).

Magnetic settlement system utilizes the bottom of the borehole as a reference datum. It assumes that the bottom magnet never moves, since it is fixed on the inclinometer casing. Settlement or heave is determined by comparing subsequent readings to the initial datum reading.

Figure 4.21: Spider Magnet attachment detail for Inclinometer Casing.

Figure 4.22: 3-Legged Spider Magnets.

Figure 4.23: Magnet Reading Unit – Reed Switch Probe.

4.4.3 Vibrating wire load cells

There are two types of load cells available, solid and annular (Figure 4.24a and Figure 4.24b). Solid style of cells is used in the project (Figure 4.25). The diameters of the platens of the solid cells are 20cm and the length of the three parts (upper and lower platen and load cell) is 30cm in total. They incorporate 6 vibrating wire strain sensing elements mounted parallel to the longitudinal axis of the cell. Each sensor is read individually and a switch box is used to sequentially switch between them. The outer protective cover is outfitted with O-Ring seals, providing the internal strain elements with shielding from demanding geotechnical conditions and the elements. Load cells also take thermal measurements, which allow classification of the readings and comparing due to changes in the weather conditions.

Figure 4.24a: Annular Load Cell. **Figure 4.24b:** Solid Load Cell.

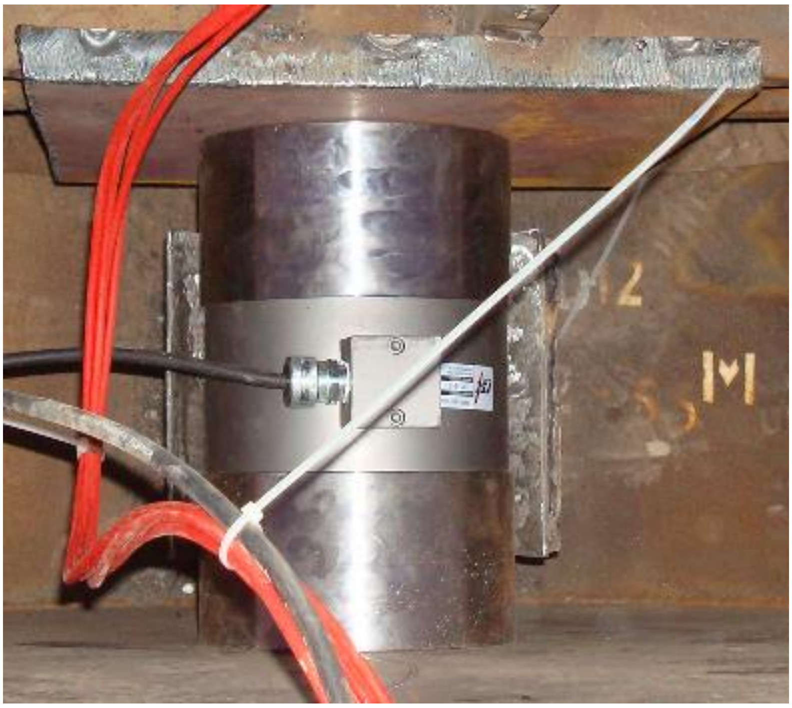

Figure 4.25: Load Cell used in the Project.

Each load cell is calibrated before starting the measurement. The calibration is as follows; 1. Each load cell is cycled 3 times, taking 10 equally spaced readings each cycle, to load capacity, 2. The readings are then averaged, and a regression is done with Applied Load vs. the Averaged Readings to get the load cell constants for scale "B" and zero "A". The constants are used for calculating the current load in formulation:

$$F = (A\text{-average of readings}) * B \quad \textbf{(4.5)}$$

Load cells are used in measuring loads in tie-backs, struts, ground anchors and steel pipes. They are also used during load tests of piles.

4.4.4 Vibrating wire strain gauges

Vibrating wire strain gauges are designed to measure strains in civil and structural engineering works. They consist of two end blocks with a tensioned steel wire between them. As steel or concrete surface that encompasses the strain gauge undergoes strain, the end blocks will move relative to each other. The tension in the wire between blocks will change accordingly, thus altering the resonant frequency of the wire. Vibrating wire readout is utilized to generate voltage pulses in the magnet/coil assembly plucks the wire and measures the resulting resonant frequency of vibration.

Each gauge is fitted permanently with an encapsulated pair of electromagnetic coils, one is used to excite the wire and cause it to vibrate at it resonant frequency and the other is used to detect the resonant frequency and generate an output frequency. This output frequency is recorded with either a vibrating wire read out unit or a data logger.

The advantages of vibrating wire strain gauges are that the frequency output is immune to electrical noise, able to tolerate wet wiring common to geotechnical application and capable of several kilometers without loss of signal.

There 3 types of strain gauges; arc welded, spot welded and embedment (Figure 4.26). Arc welded strain gauges are used in the project (Figure 4.27).

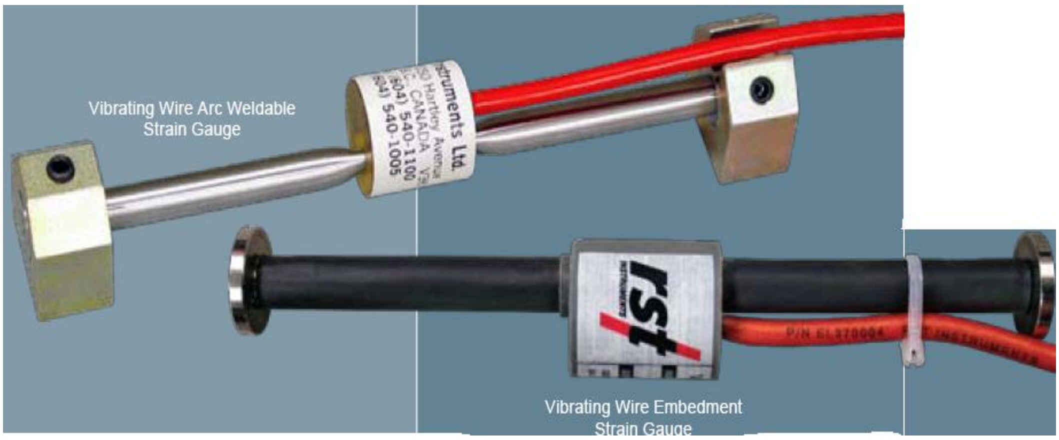

Figure 4.26: Vibrating Wire Arc Welded and Embedment Strain Gauge.

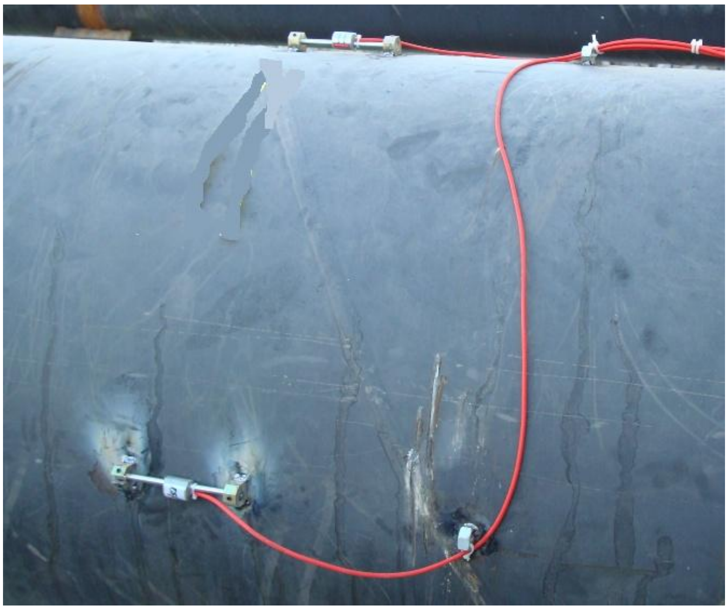

Figure 4.27: Strain Gauges used in the Project.

4.4.5 Installation process

4.4.5.1 Installation of the inclinometers and spider magnets

The inclinometer installation consists of drilling, installing the casing and grouting the well. In our case, first a hole with 15cm has been bored in order to be able to place inclinometer casing and spider magnets together in the well. Then, spider magnets are attached on the casings (Figure 4.28) and 3.0m long casings are attached to each other, 2 by 2, with polyethylene based mastic and plastic fiber tapes, to prevent grout leakage into the casing during grouting of the well (Figure 4.29a~Figure 4.29d). Then, coupled casings are lowered down the wells and attached to the other casing couples (Figure 4.30 and Figure 4.31). During and after the installation and attachment of all casings the well has been grouted (Figure 4.32). While lowering the casings, they are filled with water to bear uplift force of the grout in the well.

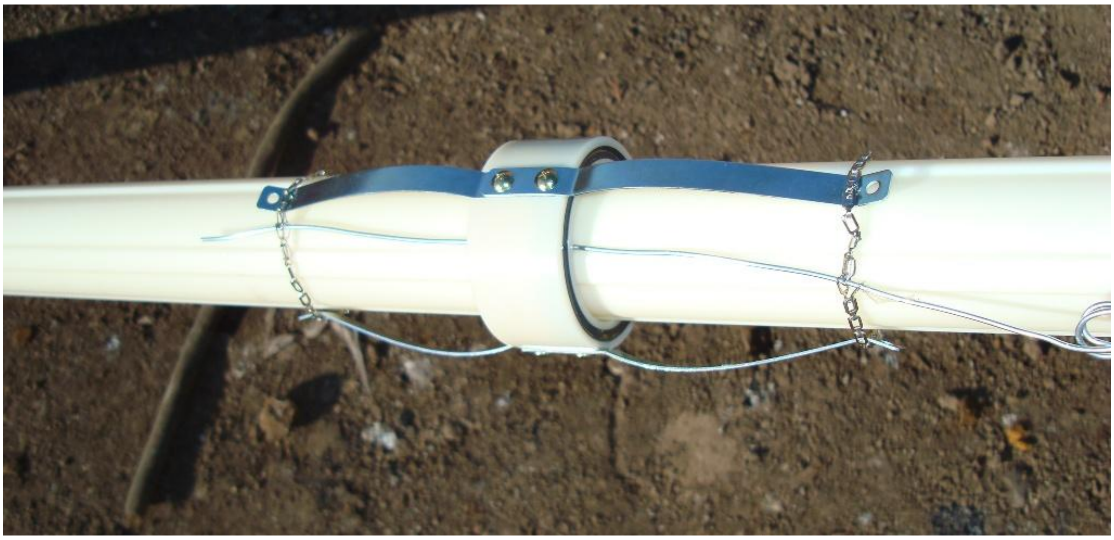

Figure 4.28: Magnets on the Inclinometer Casing.

Figure 4.29a: Installation Process Step1.

Figure 4.29b: Installation Process Step2.

Figure 4.29c: Installation Process Step3.

Figure 4.29d: Installation Process Step4.

Figure 4.30: Installation Process Step5.

Figure 4.31: Installation Process Step6.

Figure 4.32: Grouting the Well during Installation of the Casings.

4.4.5.2 Installation of the load cells and strain gauges

The strain gauges were arc welded on the steel pipes. Four strain gauges would be placed on the pipes at a cross location (Figure 4.33). However, the load cells were smaller than the pipes in diameter, so a bed should be welded for them, on the pipe and on the cross beam. As can be seen from Figure 4.34, a 3.0cm thick plate has been arc welded on the cross, which is already welded on the pipe. It will be the bed between load cell upper platen and the pipe. The other bedding has been welded on the bedding of steel pipes, to carry the load cell and platens during installation, before pre-stressing (Figure 4.35).

Figure 4.33: Views of Load Cell and Strain Gauges on the Steel Pipe.

Figure 4.34: Plate between Load Cell and Steel Pipe.

Figure 4.35: Bedding for Load Cell.

When the first excavation depth has been reached, the reinforced concrete cross beam was constructed and steel cross beam was welded on it. Then a 135cm x 135cm x 3cm plate has been welded on the steel cross beam. Then the bedding for pipes, which is used to carry the pipes during installation prior to welding, has been welded to this plate. This bedding also contains the bedding for load cells (Figure 4.35). After all this welding process is completed, the pipe with strain gauges already welded on it, has been lowered down the excavation and settled on the bed. Then the load cell with its upper and lower platens has been settled in the load cell bed. Following this installation, a pre-stress of 5-10 tons has been applied on the steel pipe to compress the load cell (Figure 4.36). This procedure is repeated for the second level pipes.

Figure 4.36: Application of the Pre-stress to the Load Cell.

4.4.6 Excavation and monitoring results

There are 3 excavation levels; 3.80m depth from surface, right below the 1st level of pipe, 7.80m depth from surface right below the 2nd level of pipe and 13.00m depth the base of excavation. Monitoring results will be discussed depending on the excavation depth and pipe installation dates. Table 4.7 gives the dates for excavation depths and pipe installation.

Table 4.7: Excavation Depth and Pipe Installation Dates.

Date	Excavation Depth	Pipe Level
01.09.2009	3.80	-
14.09.2009-30.09.2009	3.80	1
10.10.2009	7.80	1
19.10.2009-22.10.2009	7.80	2
11.11.2009	13.00	2

4.4.6.1 Inclinometer measurements

As explained in the paragraphs above, inclinometers were installed in and behind the mid-pile of the retaining system at long façade at sea side. There are 4 inclinometers behind the wall spacing 3.25m (1/4 of excavation depth) from center to center. Inclinometer readings are taken every week and the results are graphed by excavation depth. The graphs are categorized due to dates/excavation depths given in Table 4.7.

As can be seen from Figure 4.37 and Figure 4.38, horizontal displacement of the pile and behind the pile increases, while the excavation depth increases. Also, the elevation of lateral displacement changes from pile cap level to below the half of the excavation depth. The maximum lateral displacement in the retaining system is 10.75mm at the pile cap and 17.5mm at 9.0m deep from the surface. These values decrease as the inclinometers move away from the retaining system, and they reduce to 11.0mm and 3.5mm, respectively (Figure 4.38 and 4.39a~4.39c).

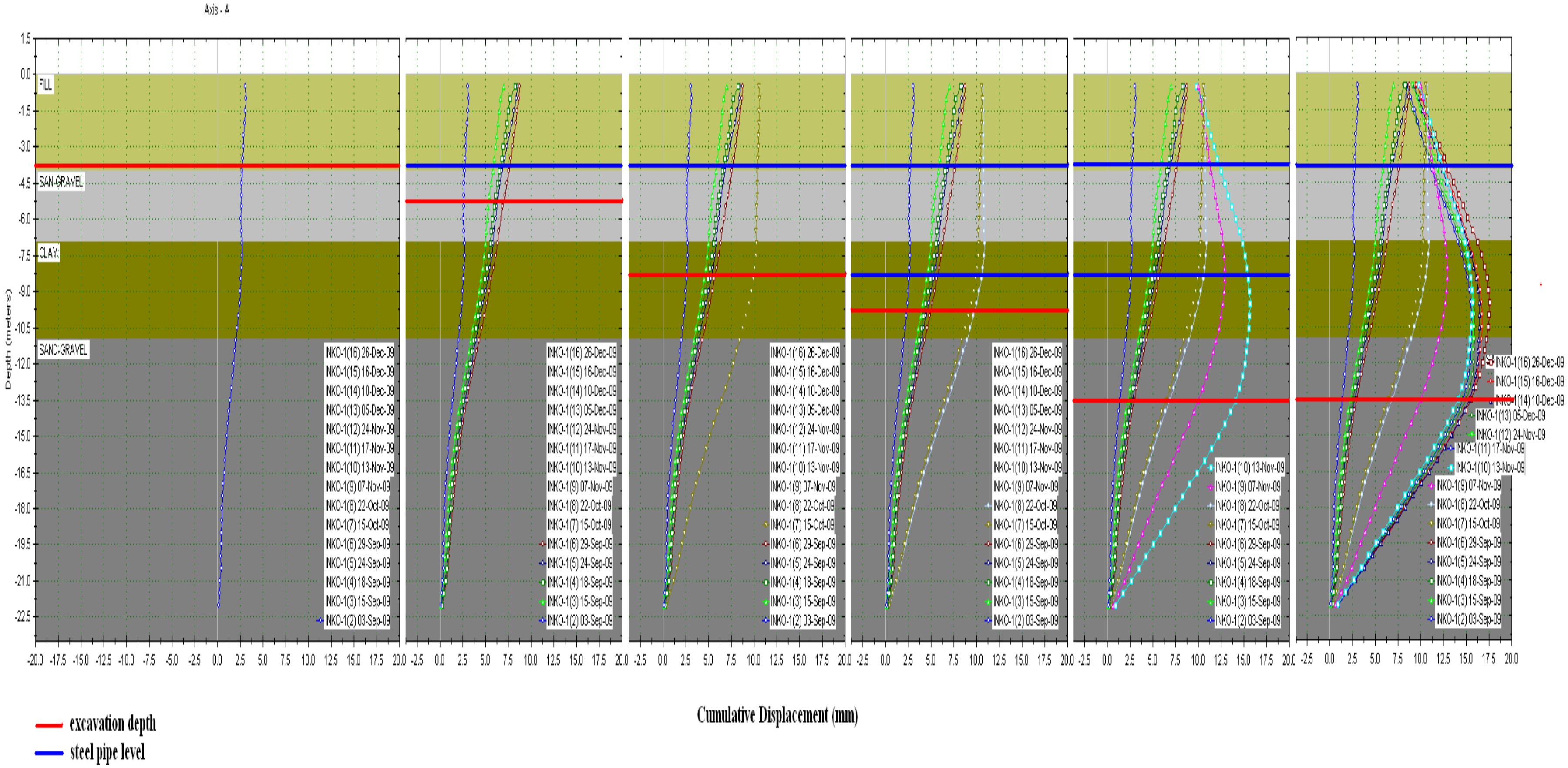

Figure 4.37: Lateral Displacement of the Pile vs Excavation Depth (Inco-1 Readings).

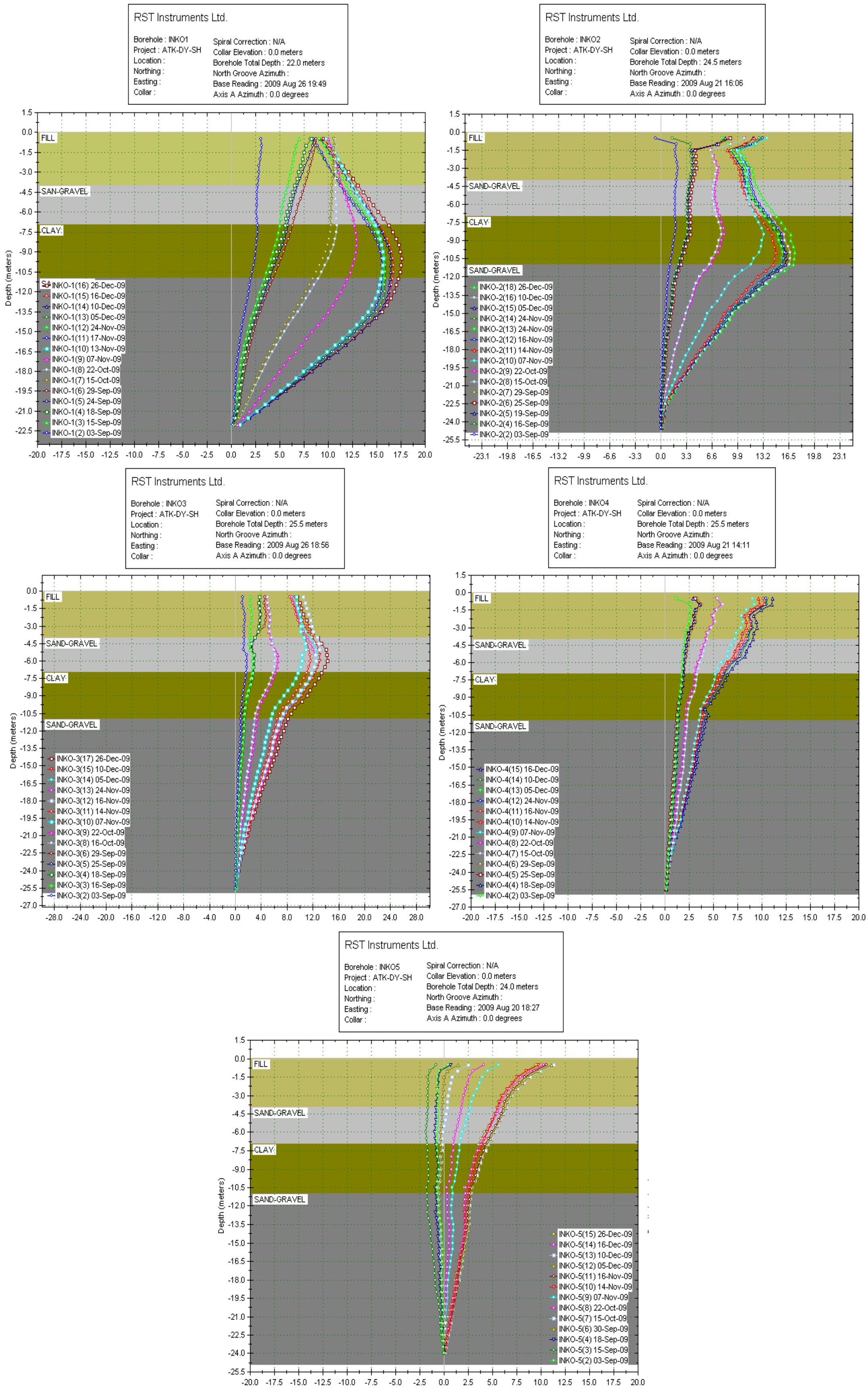

Figure 4.38: Lateral Soil Displacement vs Depth Variations with the Distance from Excavation (Inco-1, Inco-2, Inco-3, Inco-4 and Inco-5 Readings).

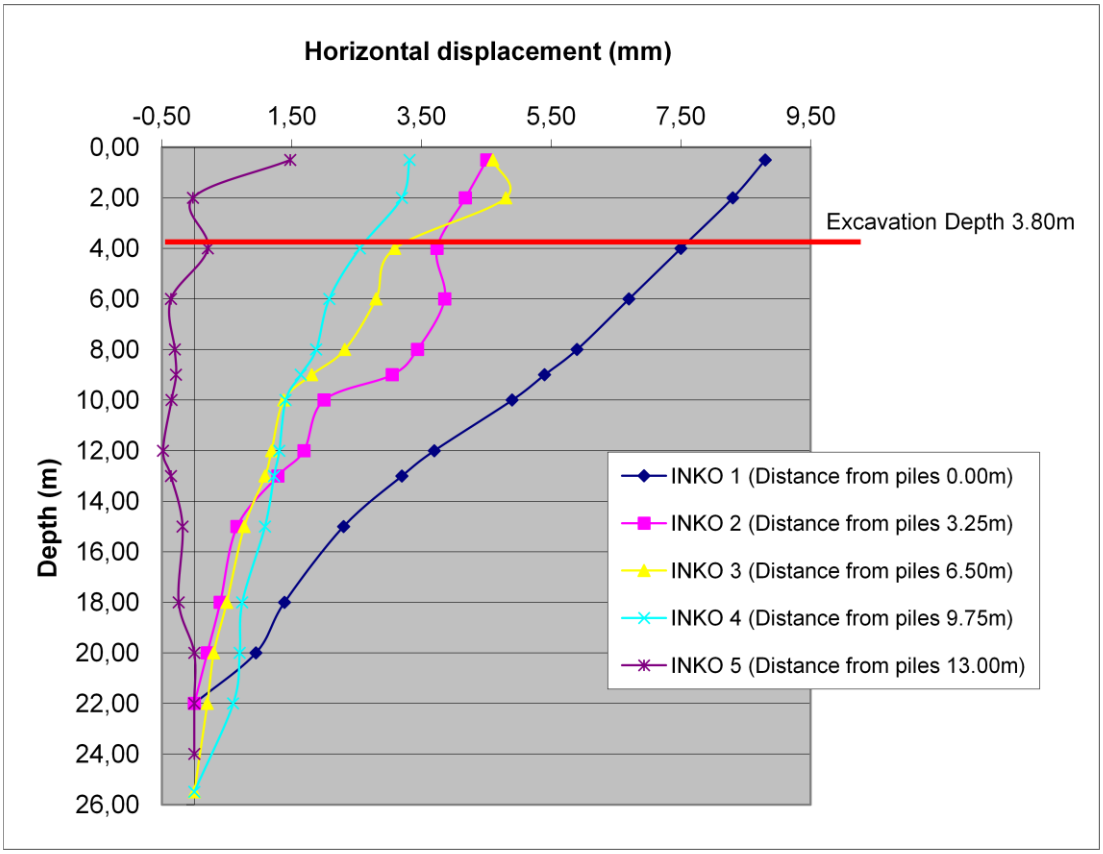

Figure 4.39a: Horizontal Displacement vs Depth (When Excavation Base at 3.80).

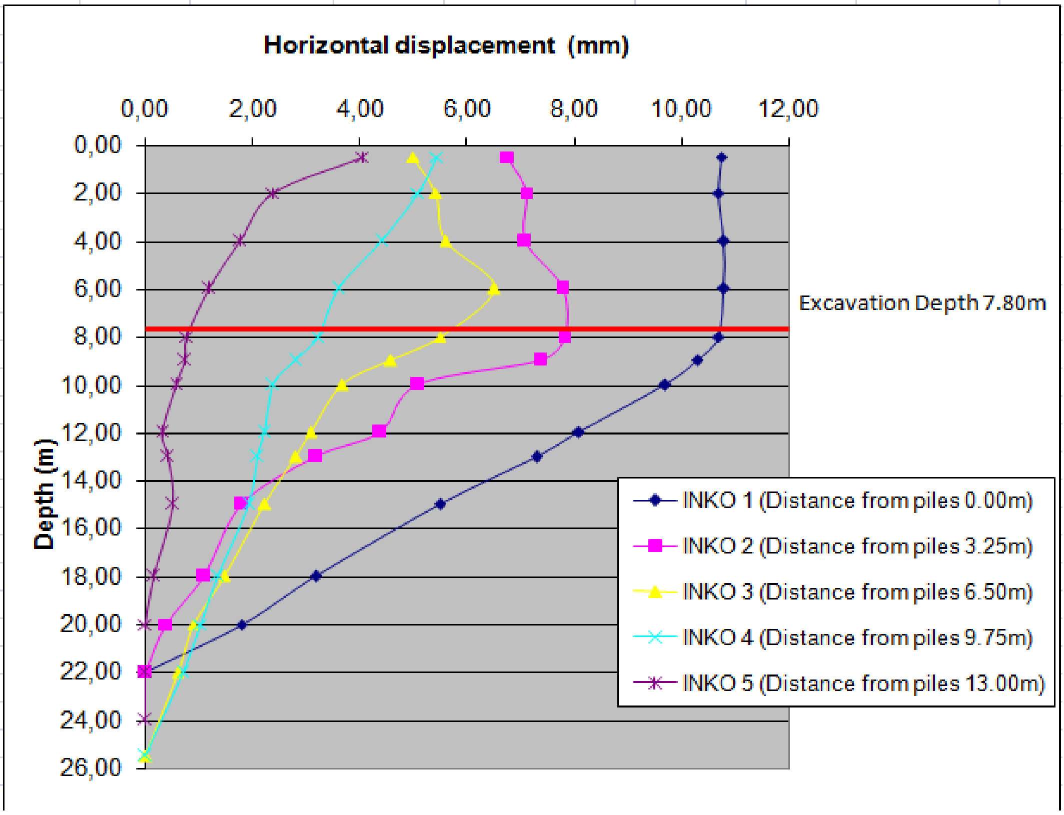

Figure 4.39b: Horizontal Displacement vs Depth (When Excavation Base at 7.80).

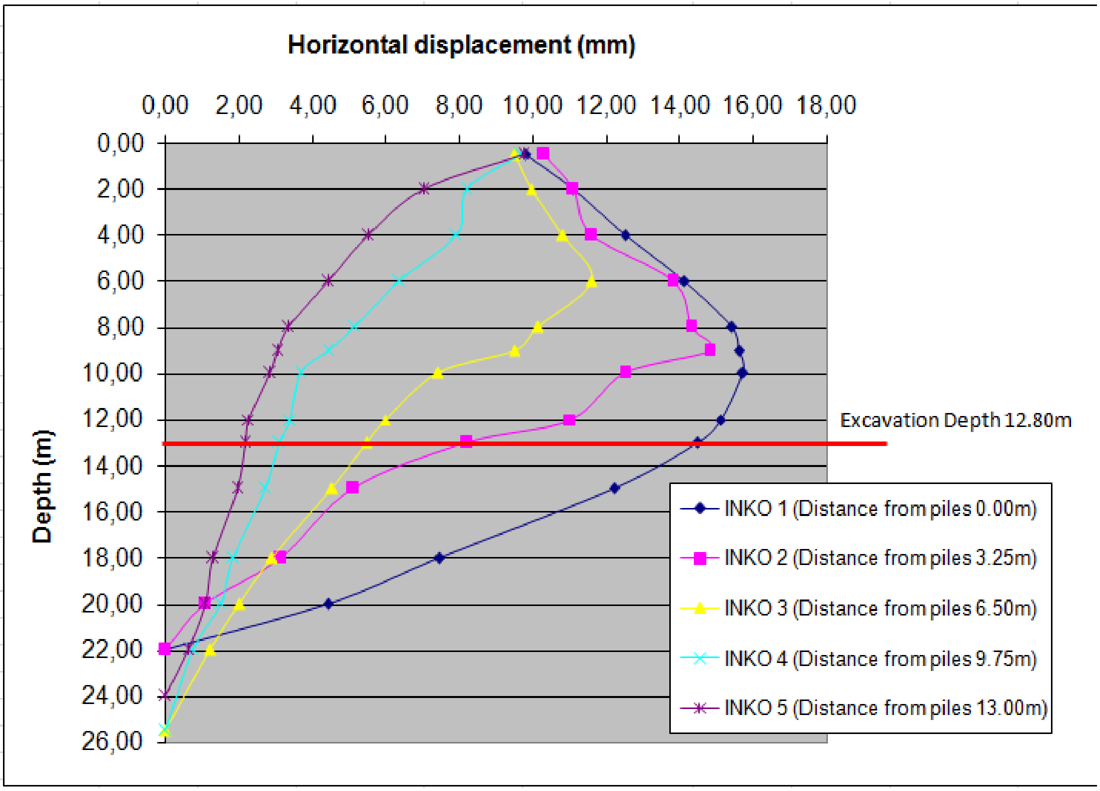

Figure 4.39c: Horizontal Displacement vs Depth (When Excavation Base at 12.80).

4.4.6.2 Magnetic column measurements

Spider magnet magnetic settlement columns are placed on the inclinometers behind the retaining system. Spider magnets are tried to be placed at the excavation and pipe levels and their numbers change from 5 to 7. The bottom magnets, No.1, are assumed to be unable to move, since they are glued on the inclinometer casing by polyethylene based mastic, which means if there is a movement on the bottom magnet, there is a movement at the whole casing. Depths of the magnets in each inclinometer are given in Table 4.8.

Magnet readings were taken once every week, similar to the inclinometer readings. The settlement records of the magnets of one inclinometer are compared to the bottom magnet and the cumulative settlement graphs are draw in reference with the bottom magnet. The results are depicted in Figure 4.40, Figure 4.41, Figure 4.42 and Figure 4.43. The positive values denote settlement and negative values denote heave.

Table 4.8: Magnet Levels at each Inclinometer.

Depth (mm)	INKO 2	INKO 3	INKO 4	INKO 5
Inclinometer	2490	2585	2590	2448
Magnet 1	2473.40	2585.45	2570.00	2448
Magnet 2	1515.60	1674.00	1729.40	1798.00
Magnet 3	945.40	1054.05	1222.80	1227.25
Magnet 4	505.30	687.95	840.15	506.10
Magnet 5	159.00	317.33	537.90	307.90
Magnet 6	-	133.65	339.55	120.00
Magnet 7	-	-	149.75	-

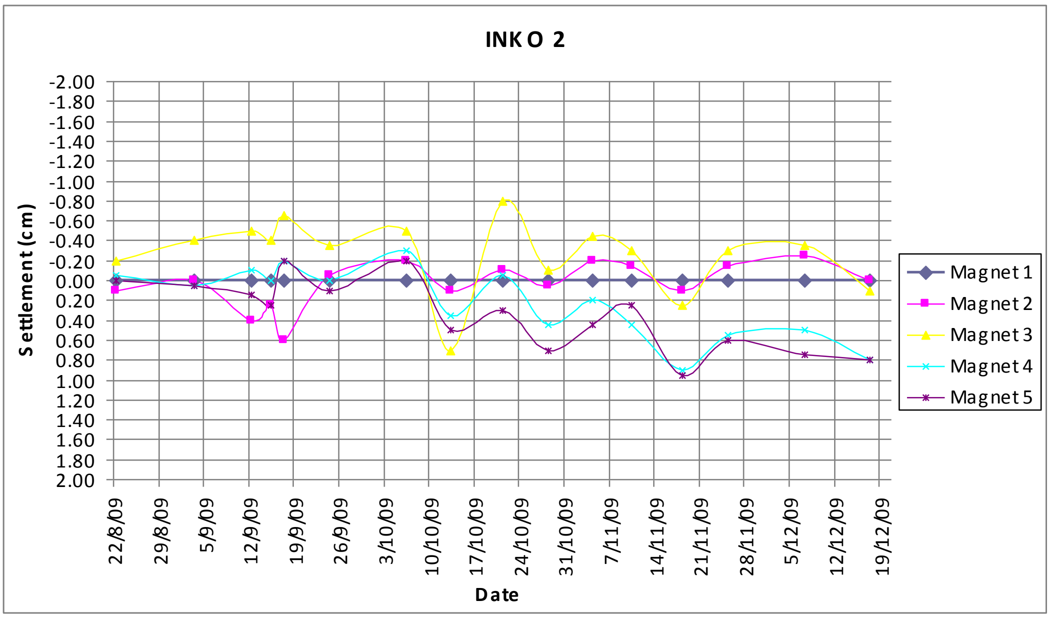

Figure 4.40: Cumulative Settlement vs Date for Inclinometer 2.

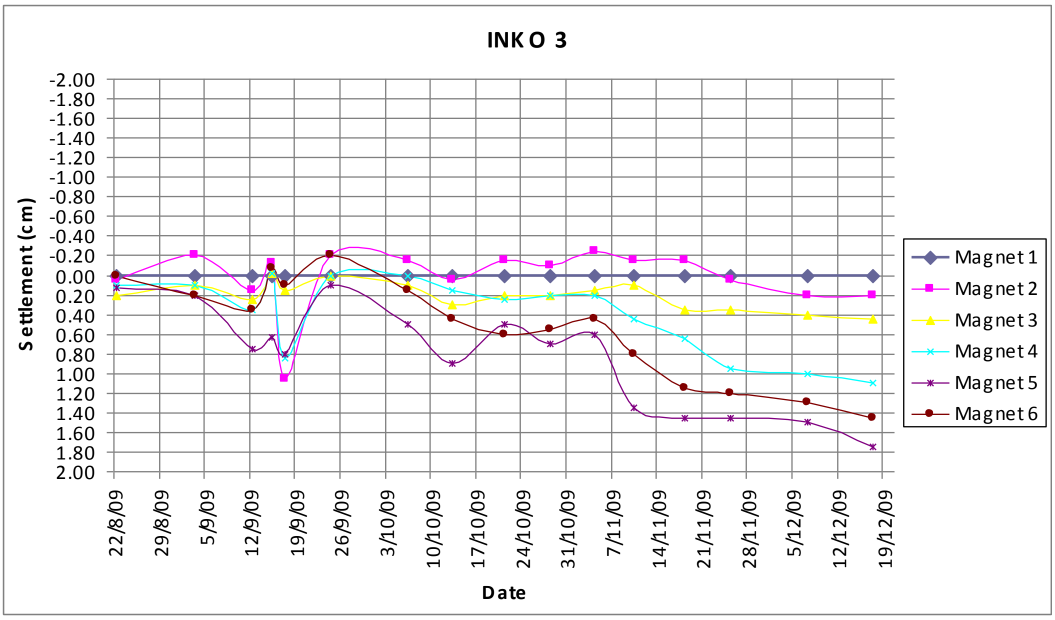

Figure 4.41: Cumulative Settlement vs Date for Inclinometer 3.

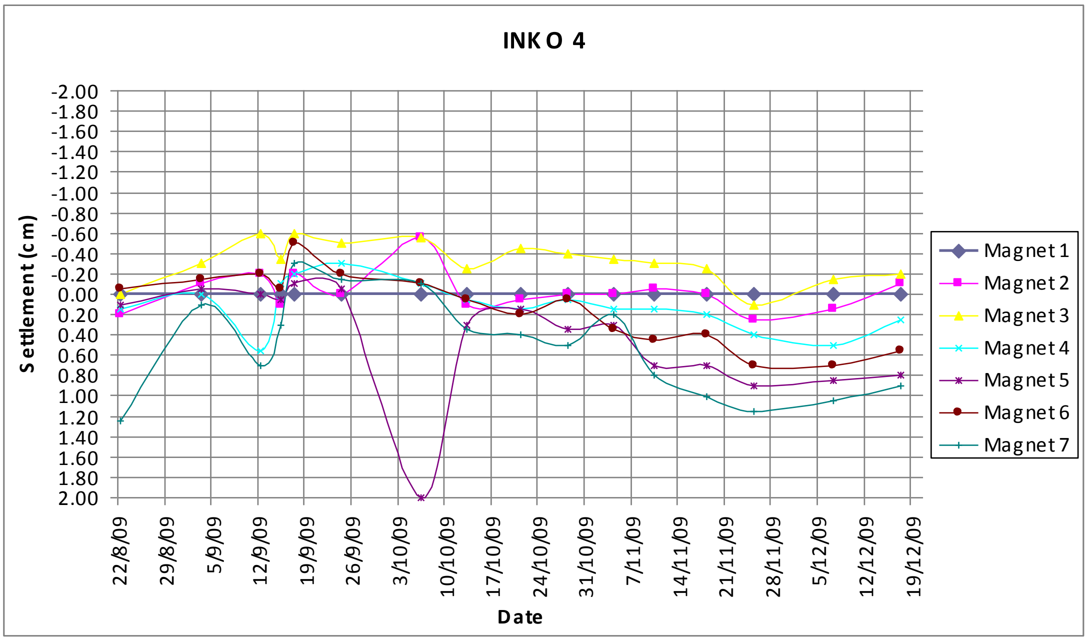

Figure 4.42: Cumulative Settlement vs Date for Inclinometer 4.

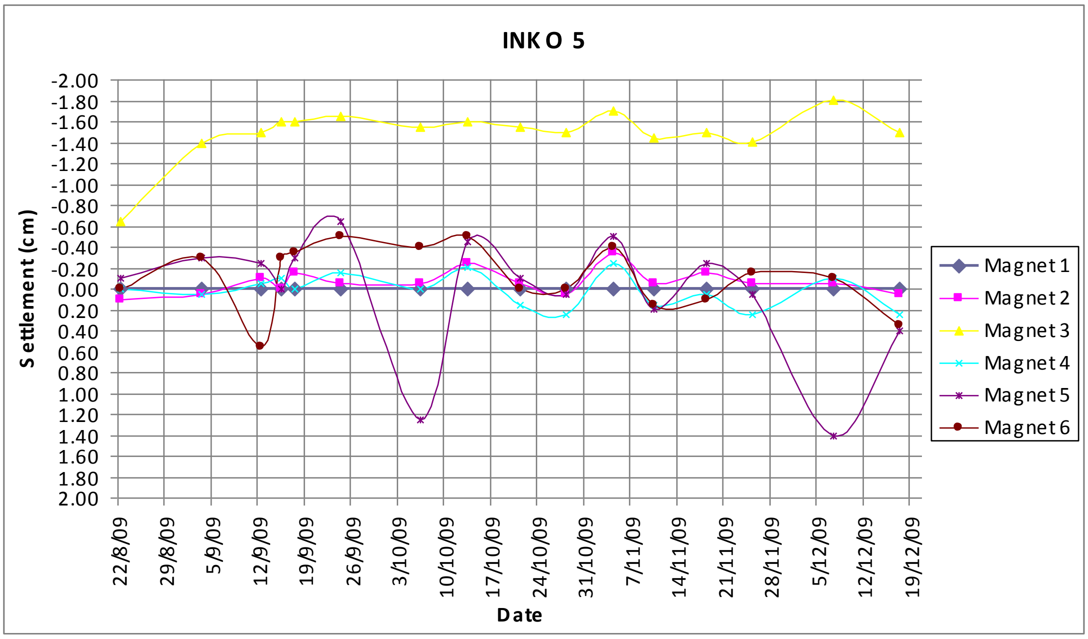

Figure 4.43: Cumulative Settlement vs Date for Inclinometer 5.

Figure 4.44 summarizes the settlements adjacent to excavation as a function of distance from excavation. It is clear that the settlements are low at the closest inclinometer and increases by distance first then decreases at the furthest inclinometer. This path has proved the soil profile diagram given by Peck (1969) in Figure 4.3 and the path modified by Liu et al. (2005) in Figure 4.2. The path also modified in this research with the data obtained during monitoring as in Figure 4.45.

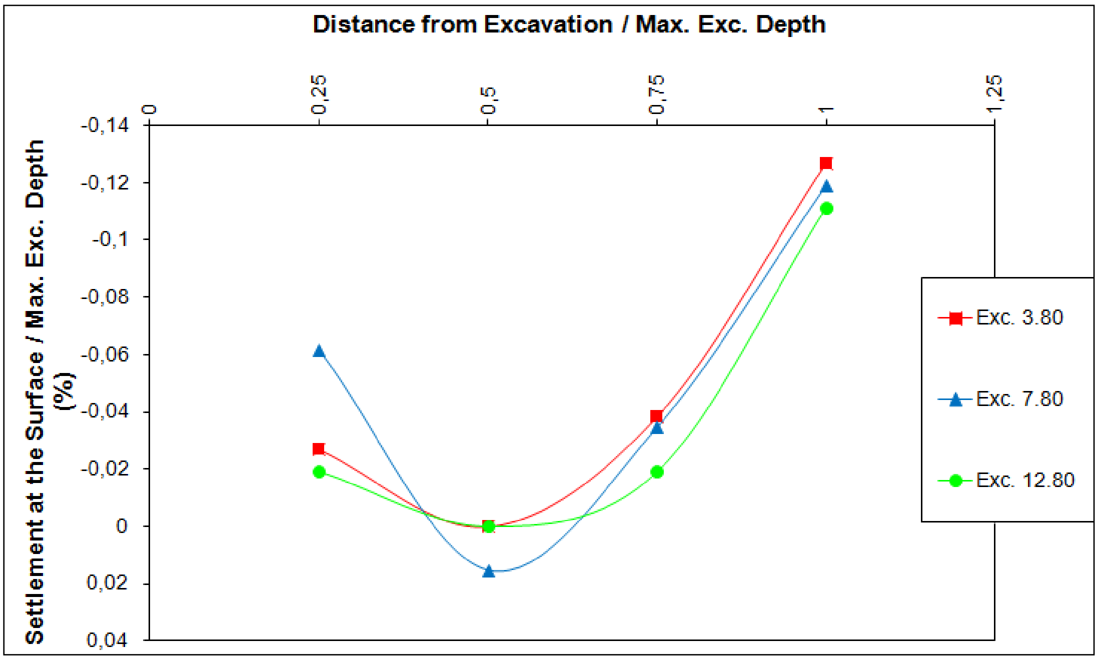

Figure 4.44: Settlements Adjacent to Excavation as Function of Distance from Excavation.

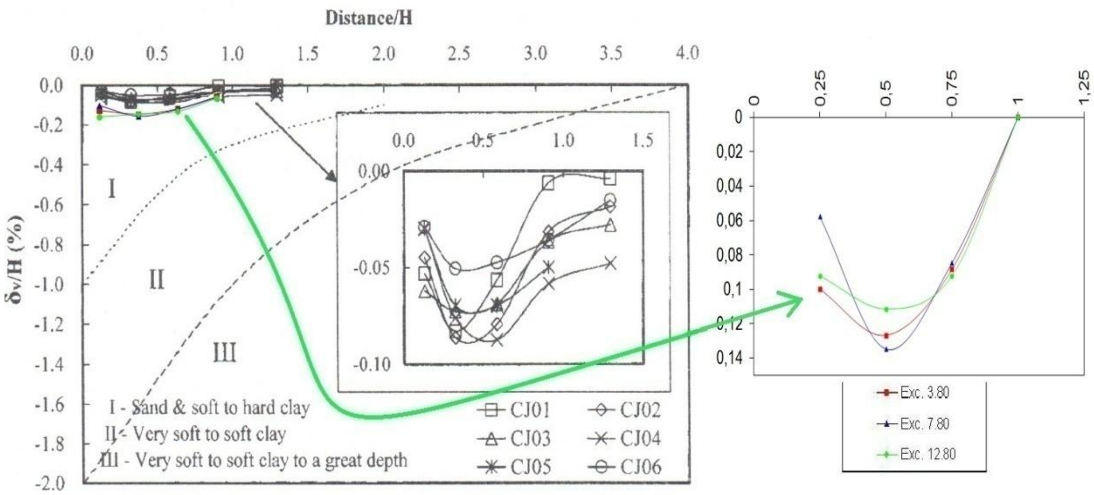

Figure 4.45: Normalized Settlement Profiles Adjacent to Scale Pit Excavation.

The magnetic column readings at the site confirmed that the ground movement data lie in between δv(max) = 0.25δh(max) and δv(max) = 0.5δh(max) for the soil profile of scale pit as shown in Figure 4.45, while it is δv(max) = 0.5δh(max) and δv(max) = δh(max) according to Mana and Clough (1981). The ground movements are substantially small probably because of the dimensions of the excavation is small.

4.4.6.3 Load cell measurements

Load cells are installed between steel pipes and cross beams at two lateral support levels. There are totally 3 load cells, two at the first pipe level and one at the second pipe level (Figure 4.46). Load cell readings were taken automatically and recorded by Flexdaq data logger at every 5 minutes. Thermal measurements were also recorded, which helped us to categorize the readings due to thermal changes. Because the pipes were steel, they were sensitive to the changes in weather and there appears to be elongation and shrinkage at the pipes.

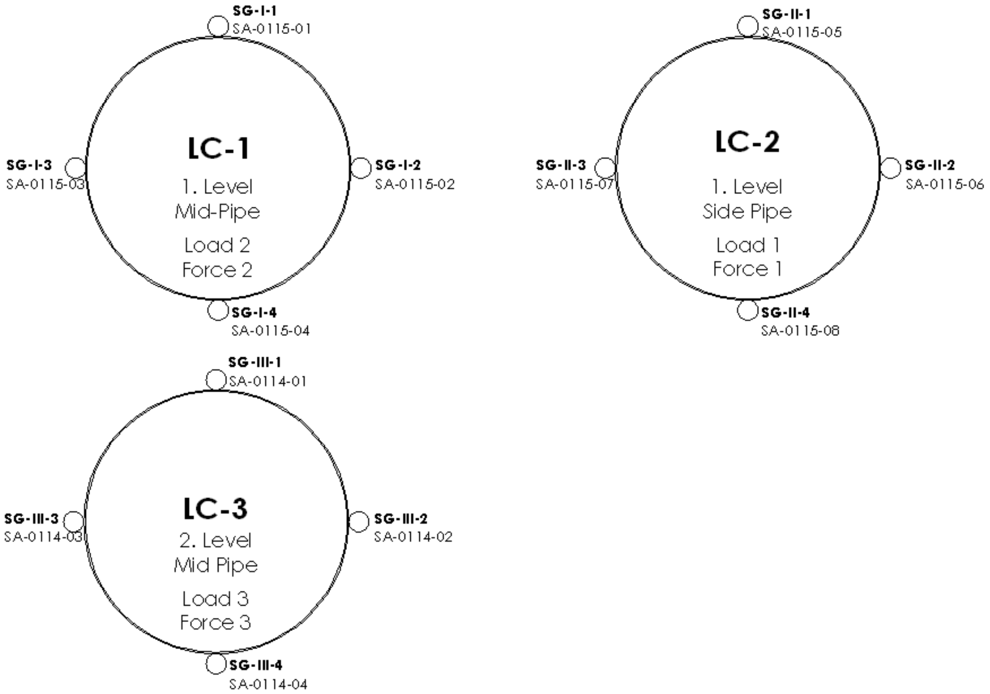

Figure 4.46: Locations of the Load Cells at Pipe Levels – Front View.

Load cell, load graph Figure 4.47, is scattered depending on the excavation process and the depth of the excavation has been applied on the graphic. As can be seen easily, load on the first level pipe increases as the excavation depth increases till the second level is installed and the load values get in a balance together within time. The maximum load at the site was recorded as 120 tons at the maximum excavation depth at an average temperature of 22°C.

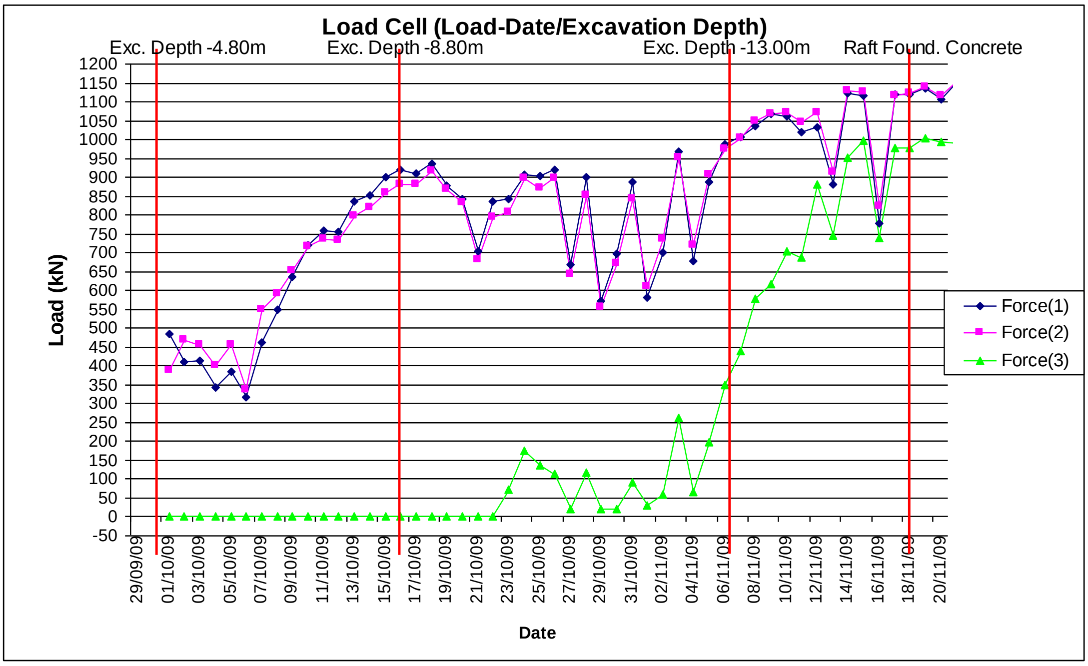

Figure 4.47: Maximum Load vs Date Graph including Excavation Depth.

4.5 Comparing the Predicted and Monitored Results

As can be seen from Table 4.9 the predicted and monitored results are nearly same. This means that the soil parameters chosen at the new analyses are likely close to the real in-situ parameters and correct enough to design the system realistically. If we need to see the exact parameters that would give the exactly same results with monitored system, then a back analysis should be performed to determine the soil parameters.

Table 4.9: Comparison Table for Predicted and Monitored Results

	Total Horizontal Displacement of the System	Maximum Horizontal Displacement at the Pile Cap	Settlement just behind the Pile Cap	Loads on Steel Struts
Predicted	6~14mm	7.5mm	4.5mm	40 t/m
Monitored	17.5mm	10.75mm	2.6mm	30 t/m (*)

(*)Because the temperature differences between day and night and mid-day differ in a wide range at the construction site, readings at 22° C have been taken into account for load-cells, for the comparison of computed and monitoring results. 22° C was the average temperature during whole day.

Also Figure 4.48a~4.48c and Figure 4.49~4.51 show the comparison of measured and predicted horizontal displacements at the pile and soil behind the retaining structure.

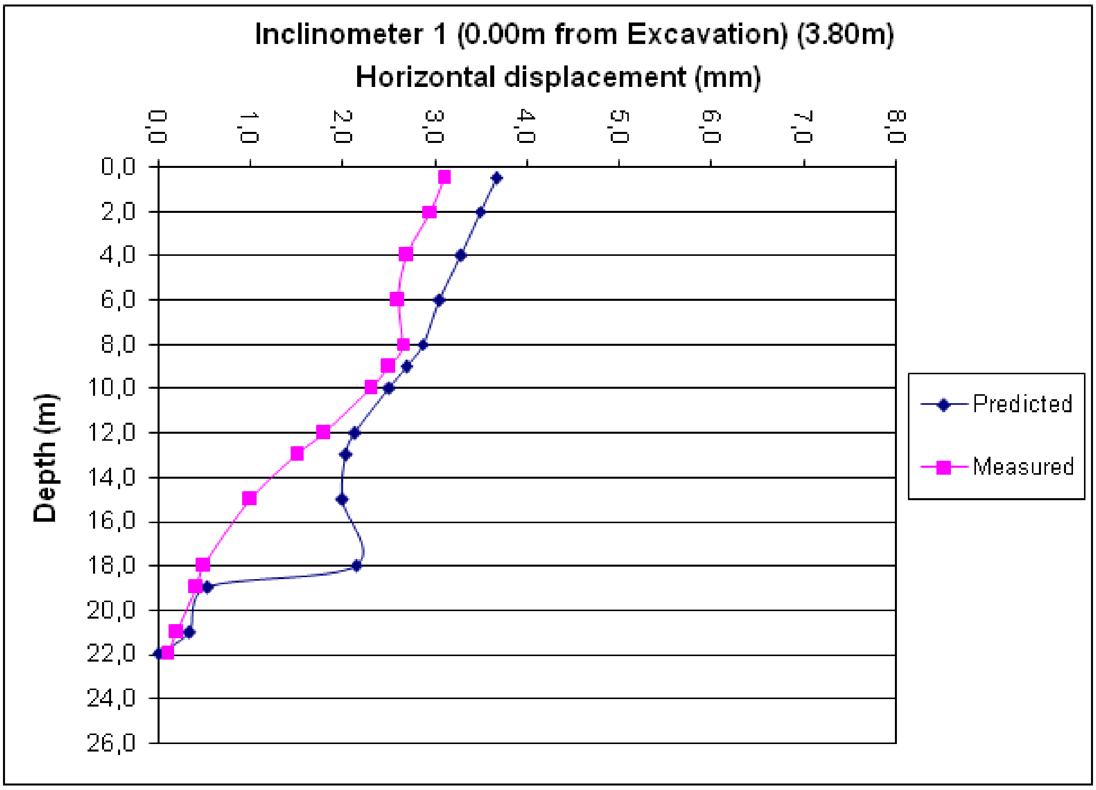

Figure 4.48a: Horizontal Displacement vs Depth Graph for Inco 1 when Exc. Depth is 3.80m.

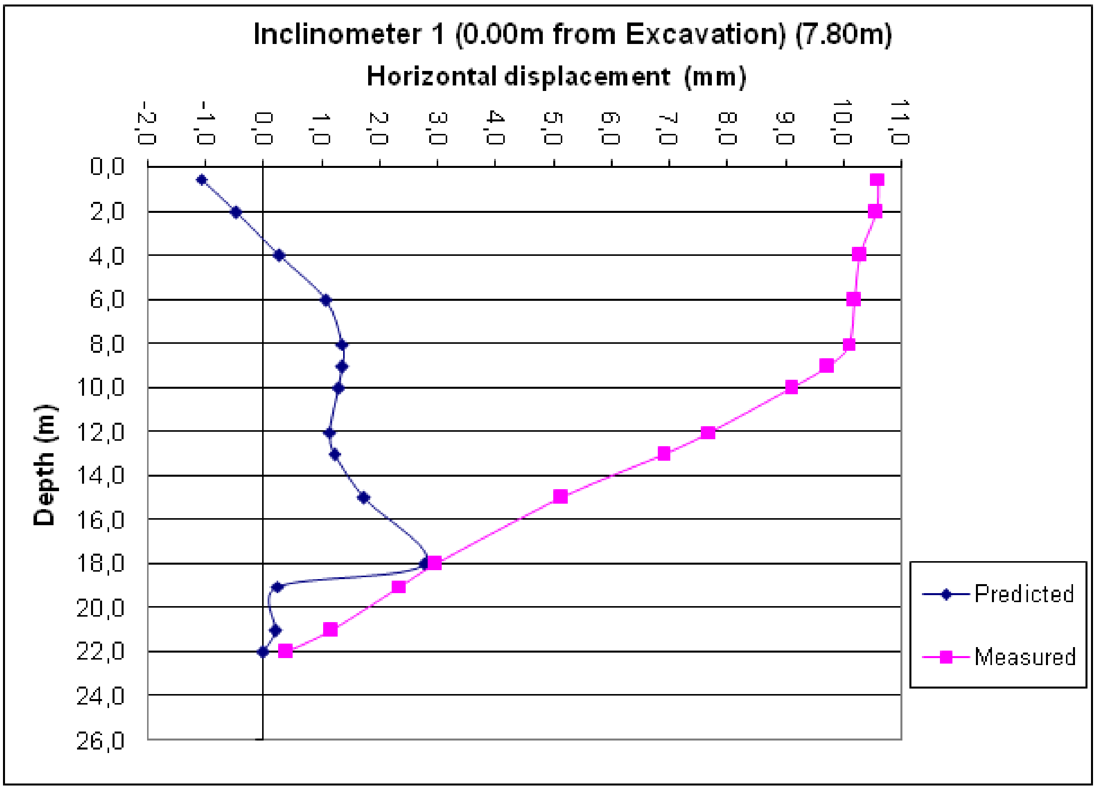

Figure 4.48b: Horizontal Displacement vs Depth Graph for Inco 1 when Exc. Depth is 7.80m.

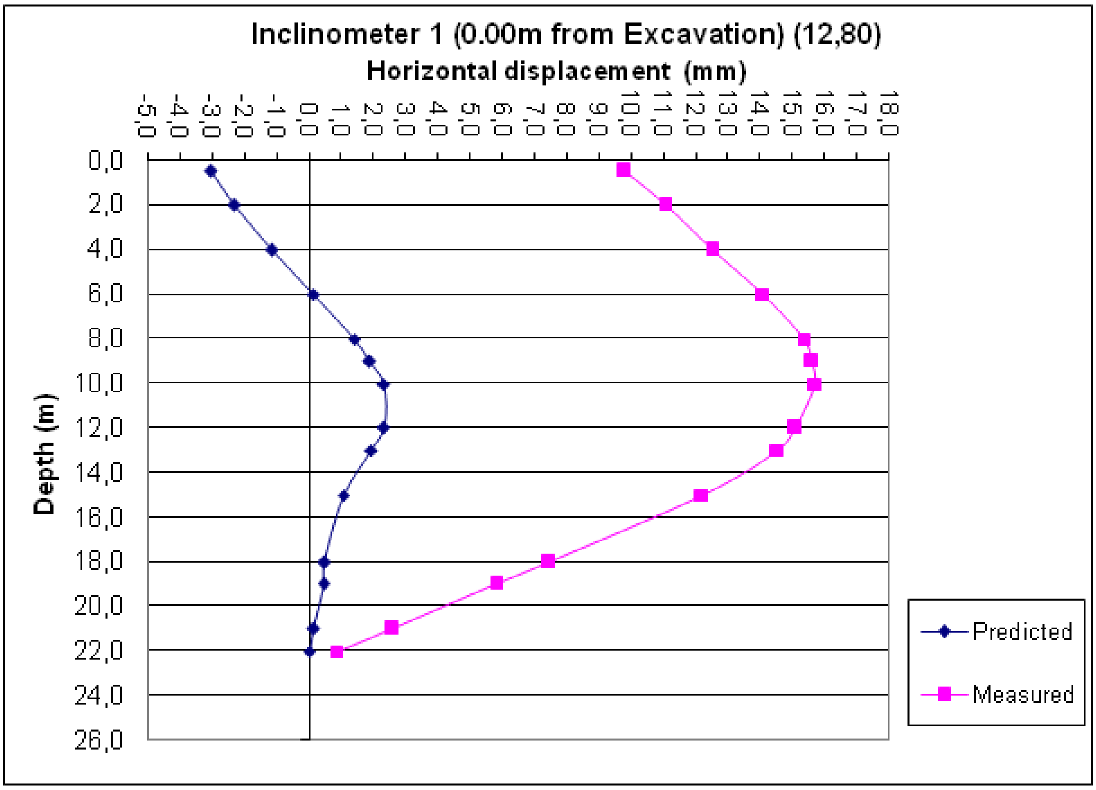

Figure 4.48c: Horizontal Displacement vs Depth Graph for Inco 1 when Exc. Depth is 12.80m.

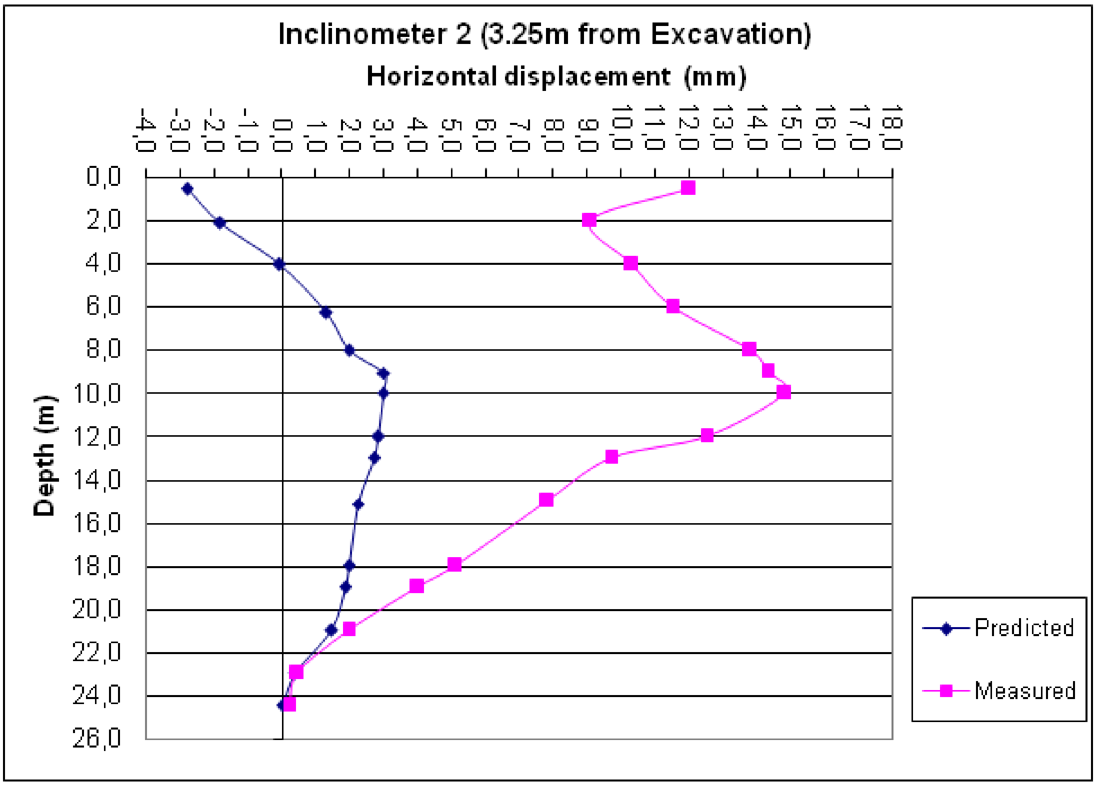

Figure 4.49: Horizontal Displacement vs Depth Graph for Inco 2 when Exc. Depth is 12.80m.

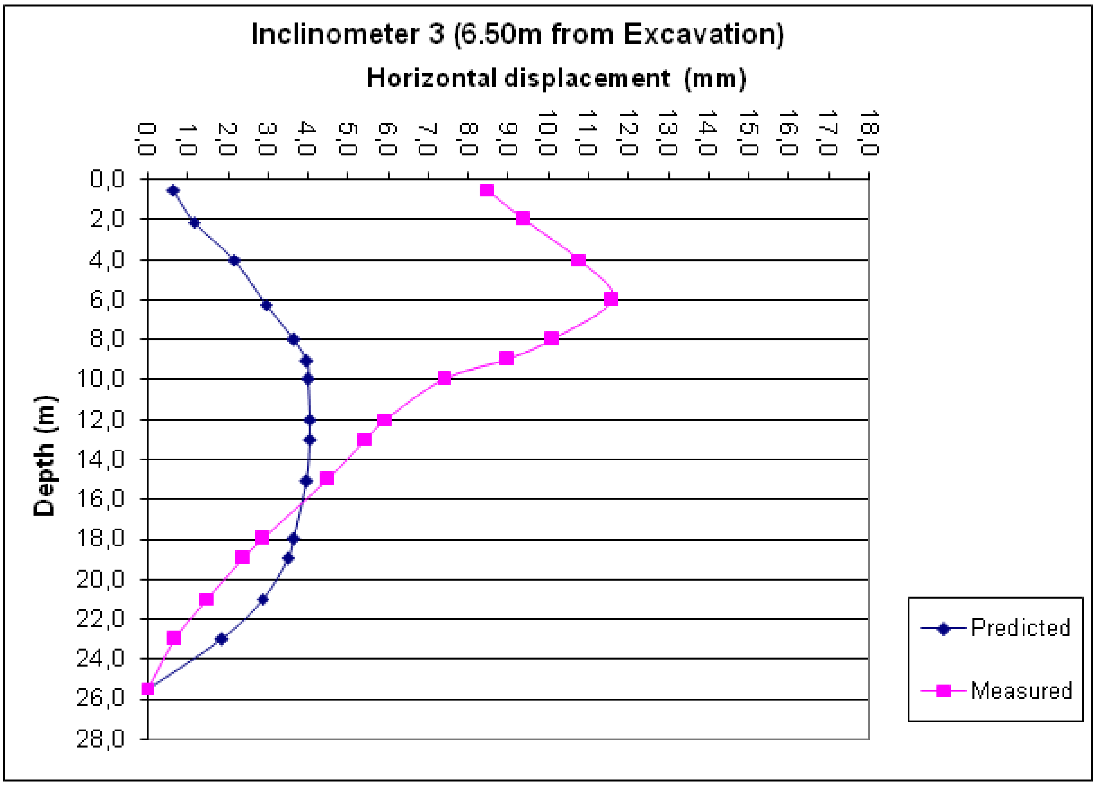

Figure 4.50: Horizontal Displacement vs Depth Graph for Inco 3 when Exc. Depth is 12.80m.

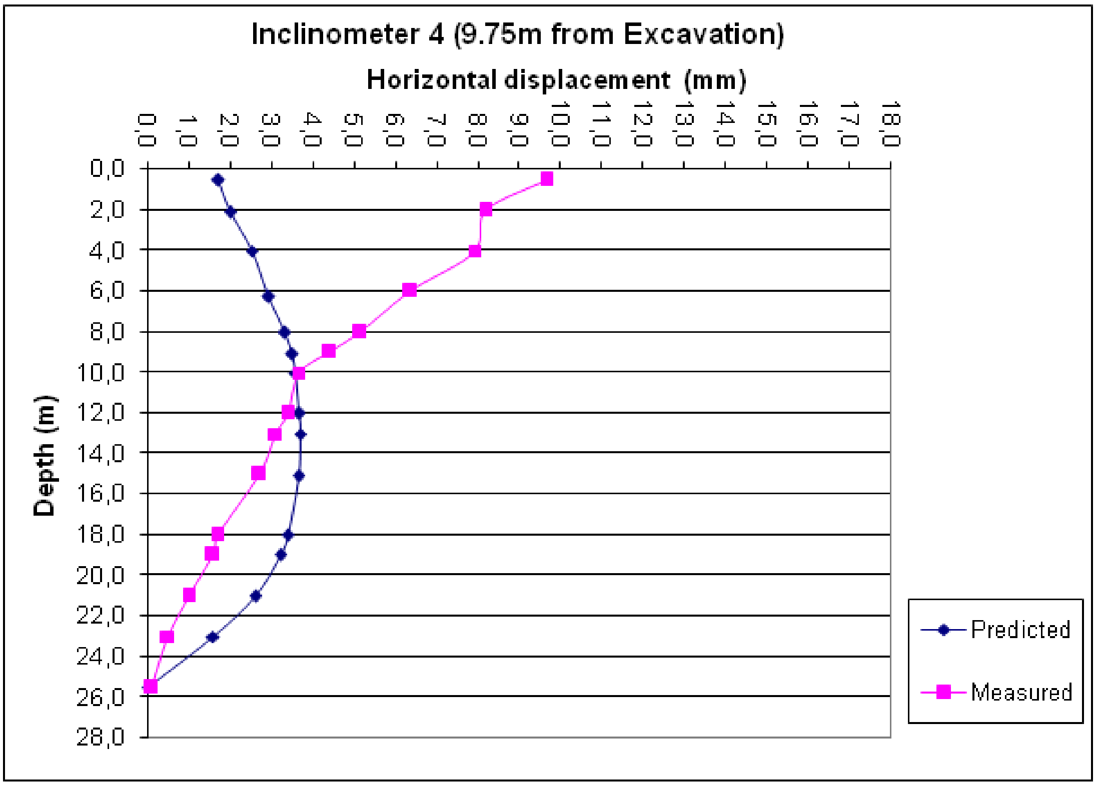

Figure 4.51: Horizontal Displacement vs Depth Graph for Inco 4 when Exc. Depth is 12.80m.

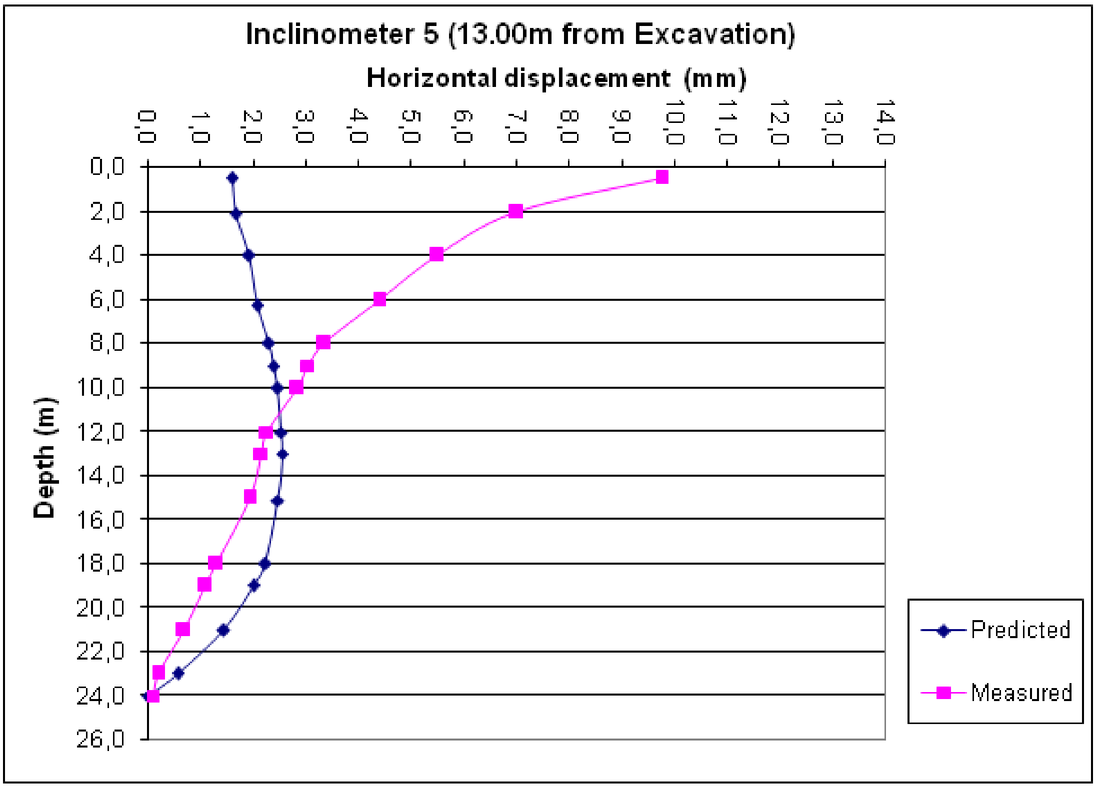

Figure 4.52: Horizontal Displacement vs Depth Graph for Inco 5 when Exc. Depth is 12.80m.

5. RELIABILITY ANALYSES

A system's reliability has to be defined before you create it. In geotechnical engineering structures, as we deal with and build against nature, determining the reliability of a system is necessary and important. Defining the reliability of a geotechnical system means, defining the reliability of its elements against displacements, earth pressures and/or loss of life, that the risk described by authorities.

In order to define the reliability of an individual or a system traditional methods including Monte Carlo simulation, FORM, SORM or the new developments such as AIS, ISAMF, AMV, and AMV+ may be used. Since Monte Carlo requires a large number of simulations to calculate low or high possibilities and is impractical when each simulation involves extensive finite element computations, it is practical to use the approximate fast probability integration (FPI) methods. However, MC is widely known. In this research, Monte Carlo is used to compute the probability of failure.

5.1 Assumptions

While the system reliability analyses are being performed, assumptions are made to simplify the calculations. Such as; the water level behind and in front of the retaining structure has been controlled by pumping, therefore the water pressure behind the system has been accepted to be the same for that excavation step and the effect of permeability coefficient k, on the system reliability has not been taken into consideration. Similarly, Poisson's ratio has also not been used for the reliability analyses, as it is proved to have a smaller relative spatial variability and only a second order importance to settlement statistics (Fenton and Griffiths, 2002).

On the other hand, c, ϕ and E are generally known to be effective in the FE analyses and lateral earth pressures on the retaining system and horizontal and vertical movements on and behind the system, as well. In our research c of clayey layers and ϕ of sand-gravel layers are treated to be random variables in the fault tree equations of the reliability analyses. All other parameters are accepted to be deterministic.

5.2 Distribution Functions of Random Variables

Four random variables of the soil layers have been considered during calculations. They include the friction angle, ϕ, of the 1st and 2nd layers, fill and gravel, respectively and cohesion, c, of 3rd and 5th clayey layers respectively, in the soil profile. ϕ and c are modeled as having log-normal distribution. This is because the normal distribution may have negative values and it is not possible for ϕ and c to have negative values in practice. Therefore, ϕ and c will be treated to have log-normal distribution. In addition to the soil parameters, distance between the adjacent structure and excavation will affect the system reliability. However, distance will be taken into account not as a random variable, but the variation of displacements depending on the distance will be calculated and examined. Main aim is to calculate the horizontal displacement of the pile wall and the settlement behind the retaining system based on the variations of the soil parameters. The mean and standard deviations of the parameters have been summarized in Table 5.1.

Table 5.1: Distribution Function Parameters for Random Variables.

Variable	Distribution	Mean	Standard Deviation	COV (%)
ϕ1 (Friction angle of fill layer)	Log-normal	41,47	4,511	10,88
ϕ2 (Friction angle of sand-gravel layer)	Log-normal	35,77	2,954	8,25
c3 (cohesion of medium stiff clay layer)	Log-normal	45,94	11,743	25,56
c5 (cohesion of stiff clay layer)	Log-normal	66,36	15,641	23,57

Mean and standard deviations of the parameters are calculated by empirical formula with the data obtained from SPT performed during soil borings at the site and laboratory test results. The area of the construction site was 500 000 m^2, so not all borings at the site have been taken into account, but the borings close to the scale pit area representing the soil profile of the scale pit have been. When the COV’s in Table 5.1 are compared to Table 5.2, it is clear that they cover the data in literature.

Table 5.2: Approximate Guidelines for Design Property Variability (Phoon, 1995).

Design Property	Test	Soil Type	Point COV (%)	Spatial Avg COV (%)
s_u(UC)	Direct	Clay	20-55	10-40
s_u(UU)	Direct	Clay	10-35	7-25
s_u(CIUC)	Direct	Clay	20-45	10-30
s_u(field)	VST	Clay	15-50	15-50
s_u(UU)	q_t	Clay	30-40	30-35
s_u(CIUC)	q_t	Clay	35-50	35-40
s_u(UU)	N	Clay	40-60	40-55
s_u	K_D	Clay	30-55	30-55
s_u(field)	PI	Clay	30-55	
ϕ	Direct	Clay, Sand	7-20	6-20
ϕ (TC)	q_t	Sand	10-15	10
ϕ_{cv}	PI	Clay	15-20	15-20
K_0	Direct	Clay	20-45	15-45
K_0	Direct	Sand	25-55	20-55
K_0	K_D	Clay	35-50	35-50
K_0	N	Clay	40-75	
E_{PMT}	Direct	Sand	20-70	15-70
E_D	Direct	Sand	15-70	10-70
E_{PMT}	N	Clay	85-95	85-95
E_D	N	Silt	40-60	35-55

5.3 Point Estimate Method (PEM)

It is well known that depending on the budget and limited time of the projects and knowledge level of the clients, it is not always possible to investigate and monitor every meter of the construction sites. Lack of knowledge may lead insufficient soil parameters, even sometimes wrong solutions; since it gives the full responsibility to engineer’s experience. Besides, even if lots of site investigations are done and numerous parameters are obtained, the uncertainty in the heterogeneity of the soil profile and measurement errors obtained during investigations, also provide uncertainties and errors for the FE analysis. This may also lead to large numbers of finite element analyses, which is not always a useful solution since it requires much more time.

By using point estimate method (PEM), determined by Schweiger et al. (2001), in combination with finite element analysis, the problems explained above can be solved with less FE analyses. They used the approach proposed by Zhou and Nowak, 1988. “The method develops a simple numerical integration to compute the statistical parameters of a function of multiple random variables. The samples of basic variables are obtained by transforming a priori the selected points in standard normal space to basic variable space" [Zhou and Nowak, 1988].

The performance function for standard normal distributed variables can be written as:

$$G(X)= G(X_1, X_2,\ldots..,Xn) \tag{5.1}$$

By evaluating the integral below, the exact k^{th} moment of G, $E[G^k(X)]$ may be obtained as:

$$E[G^k(X)] = \int\ldots\int f_x (x_1, \ldots.., x_n)\, G^k (x_1,\ldots.., x_n)\, dx_1\ldots.dx_n \tag{5.2}$$

Where f_x $(x_1, \ldots.., x_n)$ is the joint probability density function (PDF) of X. It is difficult to integrate equation (5.2) in many complex applications. Zhou and Nowak, 1988, formulated numerical formulas for any joint distributed random vector. The formulas are gathered under several titles for single standard normal variable, single non-normal variable, multiple standard normal variables, variable with joint distribution known and variables with marginal distributions known.

In this research the integration formulas for a function of non-normal variables, non-product integration formula, will be used.

As mentioned in the paragraph above integration of eqn. (5.2) may be difficult so $E[G^k(x)]$ may be obtained by using the transformation below:

$$f_x(X) = \Phi(z) \tag{5.3}$$

$$X=F_x^{-1}(\Phi(z)) \tag{5.4}$$

by evaluating the integral:

$$E[G^k(X)]= \int \Phi(z)\, G^k(z)dz \tag{5.5}$$

where $\Phi(z)$ is the cumulative distribution function of standard normal variable Z.

$$F_x^{-1} (\phi(z)) \cong \Sigma\, w_j\, G^k (F_x^{-1}(\phi(z_j))) \tag{5.6}$$

The integration in eqn. (5.2) becomes;

$$E[G^k(X)] \cong \Sigma\, w_j\, G_k (z_j) \qquad\qquad 1 \leq j \leq m \tag{5.7}$$

where m is the number of points considered, w_j are the weights and z_j are the typical normal points.

Two approaches; product and non-product integration formula, have been developed to evaluate eqn.(5.2) as it becomes

$$E[G^k(Z)] = \int\ldots\int \Phi(z_1) \ldots. \Phi(z_n)\, G^k (z_1,\ldots.., z_n)\, dz_1\ldots.dz_n \qquad \textbf{(5.8)}$$

where;

$$f_x (z_1, z_2, \ldots.., z_n) = \Phi(z_1)\, \Phi(z_2) \ldots. \Phi(z_n) \qquad \textbf{(5.9)}$$

The formulation and details of both integration formulas given in Zhou and Nowak, 1988 will not be repeated here, but the non-product formulation will be explained briefly.

In non-product formula, for a multiple independent standard normal vector Z, the probability density function, eqn. (5.9), can be further expressed as;

$$f_Z (z_1, z_2, \ldots.., z_n) = [1/ (\sqrt{2\pi})^n] \exp (-1/2\, z_1^2-1/2\, z_2^2- \ldots..-1/2\, z_n^2) \qquad \textbf{(5.10)}$$

Substituting eqn. (5.10) into eqn. (5.2) and zi= $\sqrt{2}\, u_i$ (dzi=$\sqrt{2}\, du_i$), eqn. (5.2) can be rewritten as:

$$E[G^k(Z)] = (1/\sqrt{\pi^n}) \int\ldots\int \exp(-u_1^2-u_2^2-\ldots..-u_n^2)\, G^k (\sqrt{2}\, \boldsymbol{U})\, du_1\ldots.du_n \qquad \textbf{(5.11)}$$

The integration of eqn. (5.11) can be evaluated using various Gauss quadrature rules:

$$E[G^k(Z)] \cong (1/\sqrt{\pi^n})\, \Sigma\, \alpha_j\, G^k (\sqrt{2}\, u_{1j}, \ldots.., \sqrt{2}\, u_{nj}) \qquad 1 \le j \le m \qquad \textbf{(5.12)}$$

where α_j and (u_{1j},. . . , u_{nj}) are widely available Gauss quadrature weight factors and points.

Substituting $z_{ij} = \sqrt{2}\, u_{ij}$ and $w_j = \alpha_j / \sqrt{\pi^n}$ into eqn. (5.12) the following non-product integration formula is obtained:

$$E[G^k (Z_1,\ldots..,Z_n)] \cong \Sigma\, w_j\, G^k (z_{1j}, z_{2j}, \ldots. , z_{nj}) \qquad 1 \le j \le m \qquad \textbf{(5.13)}$$

Typical weights w_j and points (z_{1j}, z_{2j},……, z_{nj}) in independent standard normal space are given in Table 5.3.

Table 5.3: Examples of points and weights for non-product integration formula (Zhou and Nowak, 1988).

Formulas m	Points $(z_{1j}, \ldots, z_{ij}, \ldots, z_{nj})$	Weight factors w_j
$n+1$	$Z_1 = (\sqrt{n}, 0, 0, \ldots, 0)$	$w_1 = \frac{1}{n+1}$
	$Z_2 = \left(-\sqrt{\frac{1}{n}}, \sqrt{\frac{(n+1)(n-1)}{n}}, 0, \ldots, 0\right)$	$w_2 = \frac{1}{n+1}$
	$Z_3 = \left(-\sqrt{\frac{1}{n}}, \sqrt{\frac{(n+1)}{n(n-1)}}, \sqrt{\frac{(n+1)(n-2)}{n-1}}, 0, \ldots, 0\right)$	$w_3 = \frac{1}{n+1}$
	$\ldots$	$\ldots$
	$Z_n = \left(-\sqrt{\frac{1}{n}}, -\sqrt{\frac{(n+1)}{n(n-1)}}, -\sqrt{\frac{(n+1)}{(n-1)(n-2)}}, \ldots, \sqrt{\frac{n+1}{2}}\right)$	$w_n = \frac{1}{n+1}$
	$Z_{n+1} = \left(-\sqrt{\frac{1}{n}}, -\sqrt{\frac{(n+1)}{n(n-1)}}, -\sqrt{\frac{(n+1)}{(n-1)(n-2)}}, \ldots, -\sqrt{\frac{n+1}{2}}\right)$	$w_{n+1} = \frac{1}{n+1}$
$2n$	$Z_1 = -Z_{n+1} = (\sqrt{n}, 0, \ldots, 0)$	$w_1 = w_{n+1} = \frac{1}{2n}$
	$Z_2 = -Z_{n+2} = (0, \sqrt{n}, 0, \ldots, 0)$	$w_2 = w_{n+2} = \frac{1}{2n}$
	$\ldots$	$\ldots$
	$Z_n = -Z_{n+n} = (0, 0, \ldots, \sqrt{n})$	$w_n = w_{n+n} = \frac{1}{2n}$
$2n^2+1$	$Z = (0, 0, \ldots, 0)$	$w_j = \frac{2}{n+2}$
	$Z = (\pm\sqrt{n+2}, 0, \ldots, 0)$ [a]	$w_j = \frac{4-n}{2(n+2)^2}$
	$Z = \left(\pm\sqrt{\frac{n+2}{2}}, \pm\sqrt{\frac{n+2}{2}}, \ldots, 0\right)$ [a]	$w_j = \frac{1}{(n+2)^2}$

[a] Points include all possible permutations of coordinates.

In order to determine the required parameters from the FE analysis, by using PEM, following steps have to be performed for practical applications (Schweiger et.al, 2001):

1. Choose the calculation model
2. Decide which of the input parameters are to be taken into account with stochastic properties (number n) in the analysis
3. Determine the mean and standard deviation for all variables and define the distribution function of the parameters
4. Find the sensitivity of the parameters by performing a Taylor-Series-Finite-Difference analysis (TSFD) to identify the parameters that have the most significant influence on certain results, to only treat these as stochastic parameters for further calculations (This step is optional and not used in our case)

5. Calculate the integration points, that is, the mathematically defined parameter combinations depending on the chosen integration method and preparation of the relevant data files for the finite element calculations
6. Perform finite element analysis
7. Define the performance (g) functions that are critical for the problem. Such as, a g function for horizontal displacement of the top of the wall and a g function for settlement behind the retaining system
8. Calculate the first two moments of the required g function parameters and evaluate the performance function. Calculation of the mean value (μ_G) and standard deviation (σ_G) as well as the safety index β_{HL} is also performed by means of MC simulations, or FORM or any other analysis.

5.3.1 Determining the parameter variations

For the excavation problem, whose modeling process is explained in section 4.3, the probability of exceeding a predefined horizontal displacement on the wall and the probability of exceeding a predefined settlement behind the retaining system, are discussed in this section. Plaxis with Mohr-Coulomb Model is used for the FE Analysis. The geometry, the finite element mesh, and the boundary conditions are shown in Figure 5.1.

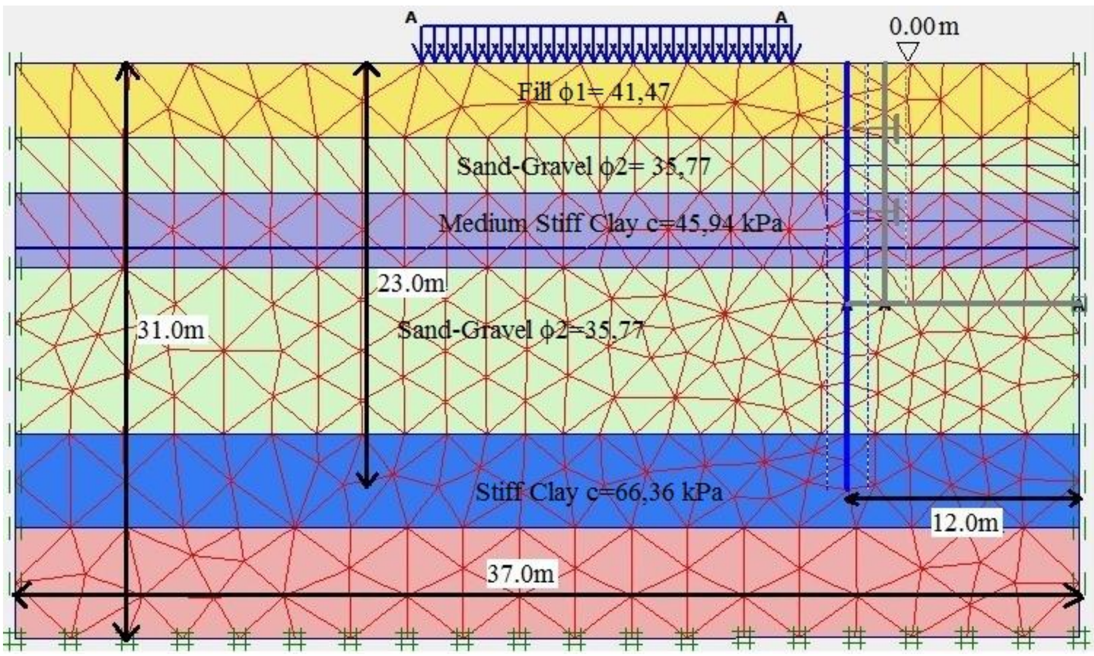

Figure 5.1: Soil Model for FE Analysis.

Four random variables are used for the FE analysis as can be seen from Table 5.1, providing 33 input values for FE calculations according to PEM with a $2n^2+1$ Integration Rule [Zhou and Nowak, 1988].

The z points can be calculated with the matrix below;

$$
\begin{array}{cccc}
z1 & z2 & z3 & z4
\end{array}
$$

$$
\begin{bmatrix}
0 & 0 & 0 & 0 \\
2{,}449 & 0 & 0 & 0 \\
0 & 2{,}449 & 0 & 0 \\
0 & 0 & 2{,}449 & 0 \\
0 & 0 & 0 & 2{,}449 \\
-2{,}449 & 0 & 0 & 0 \\
0 & -2{,}449 & 0 & 0 \\
0 & 0 & -2{,}449 & 0 \\
0 & 0 & 0 & -2{,}449 \\
1{,}732 & 1{,}732 & 0 & 0 \\
1{,}732 & 0 & 1{,}732 & 0 \\
1{,}732 & 0 & 0 & 1{,}732 \\
0 & 1{,}732 & 1{,}732 & 0 \\
0 & 1{,}732 & 0 & 1{,}732 \\
0 & 0 & 1{,}732 & 1{,}732 \\
-1{,}732 & -1{,}732 & 0 & 0 \\
-1{,}732 & 0 & -1{,}732 & 0 \\
-1{,}732 & 0 & 0 & -1{,}732 \\
0 & -1{,}732 & -1{,}732 & 0 \\
0 & -1{,}732 & 0 & -1{,}732 \\
0 & 0 & -1{,}732 & -1{,}732 \\
1{,}732 & -1{,}732 & 0 & 0 \\
1{,}732 & 0 & -1{,}732 & 0 \\
1{,}732 & 0 & 0 & -1{,}732 \\
-1{,}732 & 1{,}732 & 0 & 0 \\
-1{,}732 & 0 & 1{,}732 & 0 \\
-1{,}732 & 0 & 0 & 1{,}732 \\
0 & 1{,}732 & -1{,}732 & 0 \\
0 & 1{,}732 & 0 & -1{,}732 \\
0 & 0 & 1{,}732 & -1{,}732 \\
0 & -1{,}732 & 1{,}732 & 0 \\
0 & -1{,}732 & 0 & 1{,}732 \\
0 & 0 & -1{,}732 & 1{,}732
\end{bmatrix}
$$

$$S_{QN}^2 = \ln(1+(\sigma/\mu)^2) \quad \textbf{(5.14)}$$

$$\mu_{QN} = \ln(m) - (S_{QN}^2/2) \quad \textbf{(5.15)}$$

$$x_j = F_x^{-1}(\phi(z_j)) = \exp\,(\mu_{QN} + S_{QN}*z_j) \quad \textbf{(5.16)}$$

where, μ_{QN} and S_{QN} are equivalent normal second and third moments, respectively. The soil parameter variations used in FE calculations are given in Table 5.4.

The analysis has been performed as staged construction with an excavation depth simulated in 3.80m intervals, and for each excavation depth, calculations have been made with the parameters in Table 5.4.

Table 5.4: Parameters determined by PEM (ϕ and c are random).

Layer	Fill	Sand Gravel	Medium Stiff Clay	Stiff Clay	Layer	Fill	Sand Gravel	Medium Stiff Clay	Stiff Clay
Parameter	ϕ1	ϕ2	c3	c5	Parameter	ϕ1	ϕ2	c3	c5
Step	x1	x2	x3	x4	Step	x1	x2	x3	x4
1	41,23	35,66	44,52	64,59	18	34,17	35,66	44,52	43,18
2	53,77	35,66	44,52	64,59	19	41,23	30,91	28,79	64,59
3	41,23	43,63	44,52	64,59	20	41,23	30,91	44,52	43,18
4	41,23	35,66	82,44	64,59	21	41,23	35,66	28,79	43,18
5	41,23	35,66	44,52	114,16	22	49,75	30,91	44,52	64,59
6	31,61	35,66	44,52	64,59	23	49,75	35,66	28,79	64,59
7	41,23	29,14	44,52	64,59	24	49,75	35,66	44,52	43,18
8	41,23	35,66	24,04	64,59	25	34,17	41,13	44,52	64,59
9	41,23	35,66	44,52	36,54	26	34,17	35,66	68,82	64,59
10	49,75	41,13	44,52	64,59	27	34,17	35,66	44,52	96,62
11	49,75	35,66	68,82	64,59	28	41,23	41,13	28,79	64,59
12	49,75	35,66	44,52	96,62	29	41,23	41,13	44,52	43,18
13	41,23	41,13	68,82	64,59	30	41,23	30,91	68,82	64,59
14	41,23	41,13	44,52	96,62	31	41,23	30,91	44,52	96,62
15	41,23	35,66	68,82	96,62	32	41,23	35,66	68,82	43,18
16	34,17	30,91	44,52	64,59	33	41,23	35,66	28,79	96,62
17	34,17	35,66	28,79	64,59					

Finite element analyses results depending on the change in the parameters determined by PEM will be explained in clause 5.4. But, it is important to mention that when the variation in the horizontal displacement of the retaining system due to excavation depth and settlement behind the excavation varying by the distance from excavation have been examined, the variation in ϕ and c with the original COV of the parameters, seemed not to affect the probability of failure of the system. So, ϕ and c are changed by the maximum COV determined in the literature (Table 5.2). The results of the parameter variations are given in Table 5.5. This change in the COV also helped to understand the variation in displacements, in case the geological profile of the in the field vary on the edge or the soil parameters may be incorrect.

Table 5.5: Parameters determined by PEM (ϕ and c with COVmax).

Layer	Fill	Sand Gravel	Medium Stiff Clay	Stiff Clay	Layer	Fill	Sand Gravel	Medium Stiff Clay	Stiff Clay
Parameter	ϕ1	ϕ2	c3	c5	Parameter	ϕ1	ϕ2	c3	c5
Step	x1	x2	x3	x4	Step	x1	x2	x3	x4
1	40,67	35,08	43,37	62,63	18	28,86	35,08	43,37	34,76
2	66,06	35,08	43,37	62,63	19	40,67	24,90	24,07	62,63
3	40,67	56,99	43,37	62,63	20	40,67	24,90	43,37	34,76
4	40,67	35,08	99,72	62,63	21	40,67	35,08	24,07	34,76
5	40,67	35,08	43,37	144,03	22	57,31	24,90	43,37	62,63
6	25,04	35,08	43,37	62,63	23	57,31	35,08	24,07	62,63
7	40,67	21,60	43,37	62,63	24	57,31	35,08	43,37	34,76
8	40,67	35,08	18,86	62,63	25	28,86	49,44	43,37	62,63
9	40,67	35,08	43,37	27,24	26	28,86	35,08	78,14	62,63
10	57,31	49,44	43,37	62,63	27	28,86	35,08	43,37	112,86
11	57,31	35,08	78,14	62,63	28	40,67	49,44	24,07	62,63
12	57,31	35,08	43,37	112,86	29	40,67	49,44	43,37	34,76
13	40,67	49,44	78,14	62,63	30	40,67	24,90	78,14	62,63
14	40,67	50,82	43,37	112,86	31	40,67	24,90	43,37	112,86
15	40,67	35,08	78,14	118,31	32	40,67	35,08	78,14	34,76
16	28,86	24,90	43,37	62,63	33	40,67	35,08	24,07	112,86
17	28,86	35,08	24,07	62,63					

While changing the ϕ and c of the system Young's Modulus (E) was also changed, not as a random variable but a dependent variable on ϕ and c. E has been determined by using the empirical formula in the literature.

As it is known, Young's Modulus differs for drained and undrained conditions. In initial quick loading conditions, like in excavation problems, response of the cohesive soils is undrained. For undrained modulus of cohesive soils (E_{ut}), Kulhawy, and Mayne, 1990, suggested use of a hyperbolic model, as given below:

$$E_{ut} = \kappa\, p_a\, (\sigma_c / p_a)^n\, [1 - R_f\, (\sigma_1 - \sigma_3) / (2\, s_u)]^2 \qquad \textbf{(5.17)}$$

where σ_c=isotropic confining pressure, σ_1=total major principal stress, σ_3=total minor principal stress and κ, n, R_f = modulus parameters (Table 5.6). For UU test conditions, σ_c would equal σ_3.

Table 5.6: Typical Undrained Hyperbolic Modulus Parameters (Kulhawy and Mayne, 1990).

Unified Soil Classification	κ	n	R_f
CL	100 to 200	1	0.9
CH	100 to 300	1	0.9

On the other hand, cohesionless soils do not exhibit time-dependency to loading caused by excess pore pressure dissipation and therefore the modulus under undrained conditions exists only briefly (Kulhawy and Mayne, 1990). For drained conditions, Duncan and Chang, 1970 suggested a hyperbolic model to estimate the drained tangent modulus, as below:

$$E_t = \kappa\, p_a\, (\sigma'_3 / p_a)^n \left[1 - R_f\, (1 - \sin\phi'_{tc})\, (\sigma'_1 - \sigma'_3) / (2\, \sigma_3 \sin\phi'_{tc})\right]^2 \quad \textbf{(5.18)}$$

where σ'_1 = effective major principal stress, σ'_3 = effective minor principal stress, ϕ'_{tc}= effective stress friction angle in triaxial compression and κ, n, R_f = modulus parameters given in Table 5.7.

Table 5.7: Typical Drained Hyperbolic Modulus Parameters (Kulhawy and Mayne, 1990).

Unified Soil Classification	κ	n	R_f
GW	300 to 1200	1/3	0.7
GP	500 to 1800	1/3	0.8
SW	300 to 1200	1/2	0.7
SP	300 to 1200	1/2	0.8
ML	300 to 1200	2/3	0.8

In our case it had not been possible to use the formula above, since there should be triaxial test results for each ϕ and c in the profiles. Whereas, our profiles used in the analyses are generated by PEM. Thus, equations in the literature are used to calculate elasticity modulus.

Early correlations in literature related E for sands directly to the standard penetration test N value (Figure 5.2 and Table 5.8). However, all attempts to date which correlate a modulus with N show considerable scatter, this is because SPT N value varies with many factors. Therefore, as a first order estimator, the following may be used:

$$E/Pa = 5\ N_{60} \text{ (sand with fines)} \qquad \textbf{(5.19-a)}$$

$$E/Pa = 10\ N_{60} \text{ (clean NC sands)} \qquad \textbf{(5.19-b)}$$

$$E/Pa = 15\ N_{60} \text{ (clean OC sands)} \qquad \textbf{(5.19-c)}$$

where N_{60} is the corrected N value and Pa is atmospheric pressure.

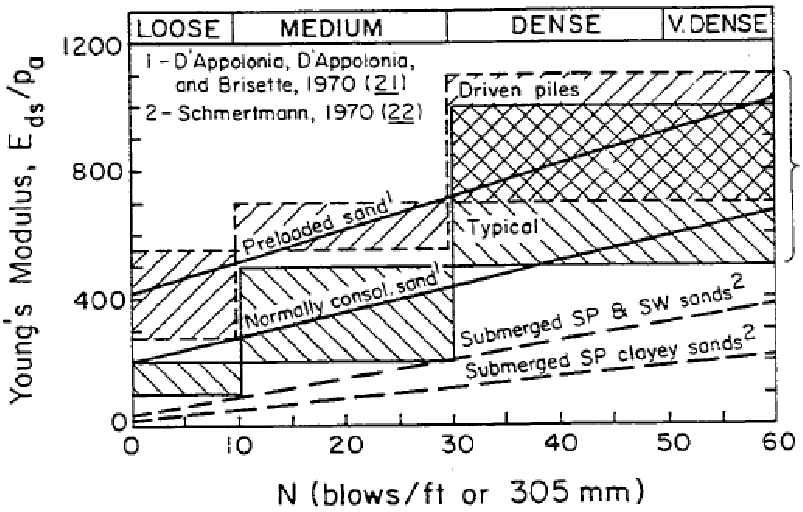

Figure 5.2: Comparative Plot of Drained Modulus Correlations for Sand (Kulhawy and Mayne, 1990).

For undrained modulus of cohesive soils the range below is appropriate to use as shown in Figure 5.3 and given in Table 5.8.

$$E = 750\ cu \sim 2000\ cu \text{ (kPa)} \qquad \textbf{(5.20)}$$

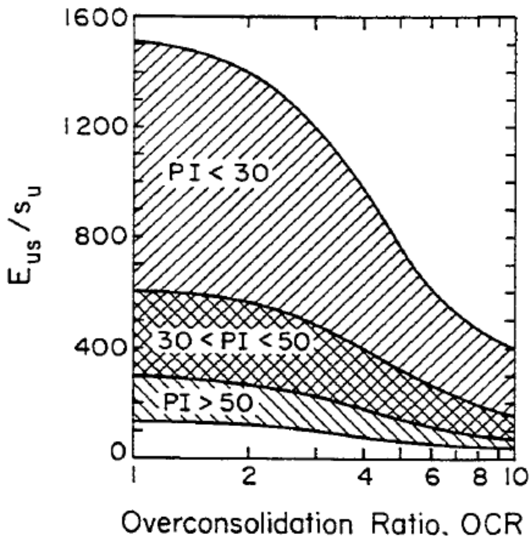

Figure 5.3: Generalized Undrained Modulus Ratio versus OCR and PI (Kulhawy and Mayne, 1990).

The Elasticity Modulus is calculated for lower and upper limits of the equations and the FE analyses are performed for both values to see the difference between.

Table 5.8: Equations for stress-strain modulus Es.

Soil	**SPT**	**CPT**
Sand (normally consolidated)	Es=500(N+15) =7000√N =6000N	Es=(2to4)qu =8000√qc =1.2(3Dr^2+2)qc
Sand (saturated)	Es=250(N+15)	Es=F*qc e=1.0 F=3.5 e=0.6 F=7.0
Sands, all (norm. consol.)	Es=(2600 to 2900)N	
Sand (overconsolidated)	Es=40000+1050N	Es=(6 to 30)qc
Garvelly Sand	Es=1200 (N+6) =600(N+6) N≤15 =600(N+6)+2000 N>15	
Clayey Sand	Es=320(N+15)	Es= (3 to 6)qc
Silts, sandy silt or clayey silt	Es=300(N+6)	Es= (1 to 2)qc If qc<2500kPa use Es`=2.5qc 2500<qc<5000kPa use Es`= 4qc + 5000 Where Es`= 1/mv
Soft clay or clayey silt		Es= (3 to 8)qc

	Ip	**Es**
Clay and silt	Ip>30 or organic	Es= (100 to 500) su
Silty or sandy clay	Ip<30 or stiff	Es= (500 to 1500)su

5.4 Finite Element Analyses

FE analysis results give the variation of horizontal displacement (Sh) and settlement (Sv) due to depth of and distance from excavation. When the maximum horizontal displacement on and settlement behind the retaining wall is calculated for each soil profile given in Table 5.4, some of the profiles come out as critical, since the displacement results make a peak at these profiles.

Clearly, it can be seen from Figure 5.4, profiles 7, 16, 20, 22, 30, 31 may be called as critical profiles. In profile 16, friction angle of the fill layer, ϕ_1, is smaller than mean value and is the smallest parameter. In profile 20, cohesion of the stiff clay layer (c_5) at the bottom of the piles, is smaller than mean value, but not the smallest one. In profile 22, friction angle of the fill layer is greater than mean value, which gives a smaller displacement than profile 20. For profile 30, cohesion of the medium stiff clay layer (c_3) and for profile 31 cohesion of the stiff clay layer is greater than the other profiles. In every critical profile, friction angle of the sand-gravel layer (ϕ_2) is the common difference and ϕ_2 in these profiles are smaller than the other profiles and mean value.

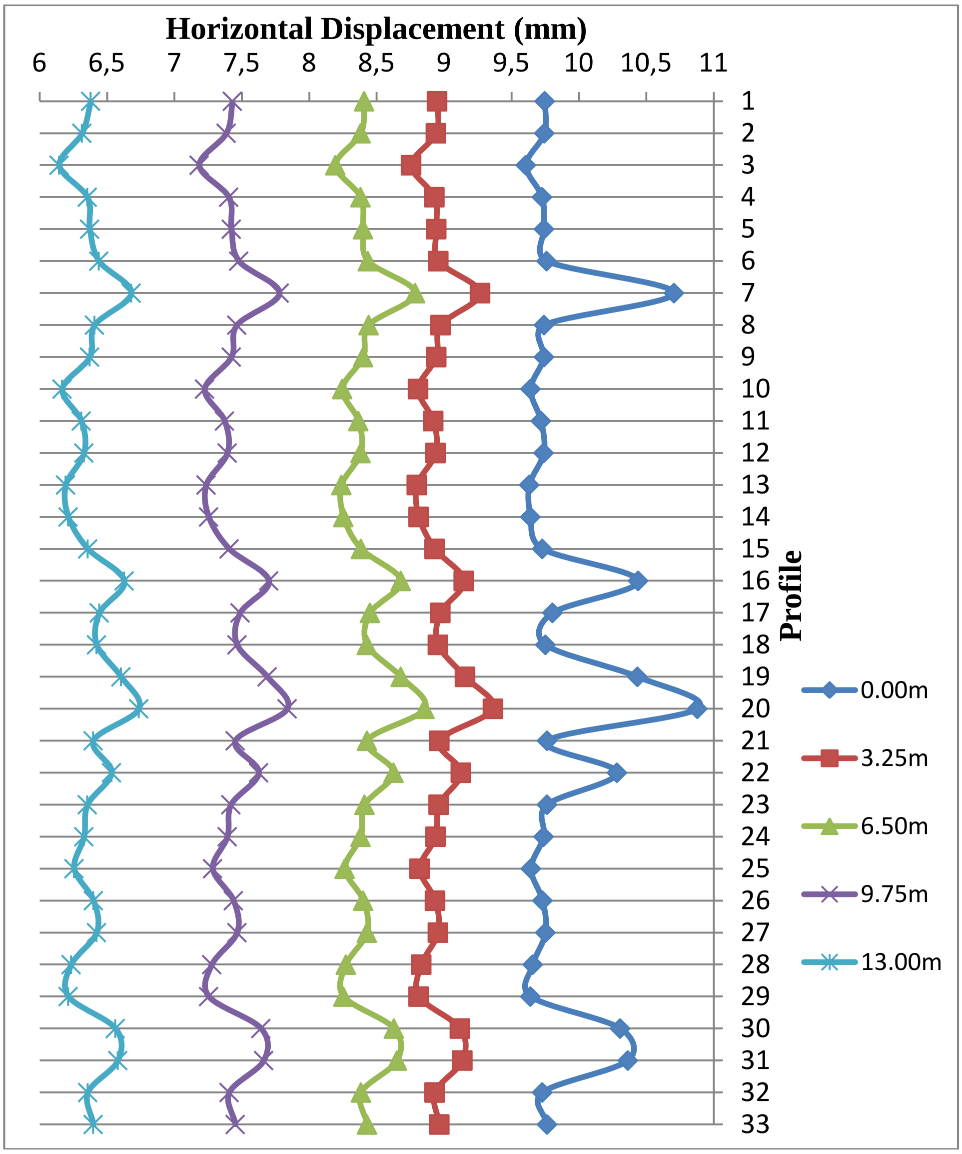

Figure 5.4: Maximum Horizontal Displacement vs Profile at 12.80m Exc. Depth. due to Distance from Excavation (E does not vary).

As a result, even by looking at Figure 5.4 we can say that;

1. ϕ_2 is more effective than other parameters on the displacement of the system, when maximum excavation depth is reached.
2. ϕ_1 is more effective than c_3 and c_5.
3. ϕ_1, c_3 and c_5 are not effective when single change is applied.

As explained in Clause 5.3.1, the parameter variations are changed depending on the COV limits and Young's modulus limits. Finite element analysis has been performed with these parameter variations. As known in general horizontal displacement on the piles and settlement behind the retaining system gets larger as the excavation gets deeper (Appendix A).

Table 5.9: Horizontal Displacement Due to Excavation Depth.

Variables	c, ϕ and E_{lower}		c, ϕ and E_{upper}		c, ϕ and E_{lower} with COVmax		c, ϕ and E_{upper} with COVmax	
Excavation Depth(m)	Mean	Std. Dev.	Mean	Std. Dev.	Mean	Std. Dev.	Mean	Std. Dev.
3,80	4,30	0,860	1,72	0,426	4,98	3,024	2,03	1,269
7,80	8,75	1,833	3,39	0,844	10,34	5,526	4,46	2,872
12,80	14,14	2,978	4,95	1,299	13,58	6,903	6,49	4,184

Table 5.10: Settlement Values Due to Excavation Depth and Distance from Excavation.

	Variables	c, ϕ and E_{lower}		c, ϕ and E_{upper}		c, ϕ and E_{lower} with COV max		c, ϕ and E_{upper} with COV max	
Exc. Depth (m)	Distance from Excavation (m)	Mean	Std. Dev.	Mean	Std. Dev.	Mean	Std. Dev.	Mean	Std. Dev.
3.80	3.25	2,67	0,457	1,99	0,027	2,92	1,128	2,31	0,636
	6.50	1,43	0,310	0,85	0,010	1,66	0,867	1,61	0,515
	9.75	0,51	0,210	0,06	0,005	0,67	0,549	1,00	0,315
	13.00	-0,11	0,179	-0,46	0,004	0,17	0,993	0,61	0,439
7.80	3.25	3,45	0,505	3,17	0,229	3,15	0,754	3,28	0,464
	6.50	1,34	0,521	1,01	0,072	0,74	1,736	1,96	0,937
	9.75	-0,12	0,498	-0,41	0,095	-0,81	2,226	0,98	1,209
	13.00	-1,06	0,504	-1,31	0,152	-1,55	1,603	0,36	0,922
12.80	3.25	2,51	0,306	2,21	0,117	2,22	1,007	3,08	0,615
	6.50	-0,26	0,616	-0,14	0,122	-0,59	2,446	1,42	1,499
	9.75	-2,00	0,806	-1,59	0,112	-2,28	3,089	0,30	1,919
	13.00	-2,99	0,875	-2,43	0,097	-2,98	2,483	-0,35	1,621

The horizontal displacement and settlement on the system has been determined during FE analyses. The displacement and settlement values are summarized in Table 5.9 and Table 5.10, respectively. When the ratio between Sh and Sv is created the range becomes 0,4Sh < Sv < 1.0Sh for the idealized soil profile determined by PEM (Figure 5.5a and Figure 5.5b). However, the range was obtained as 0.25Sh < Sv < 0.5Sh, during the measurements at the research site.

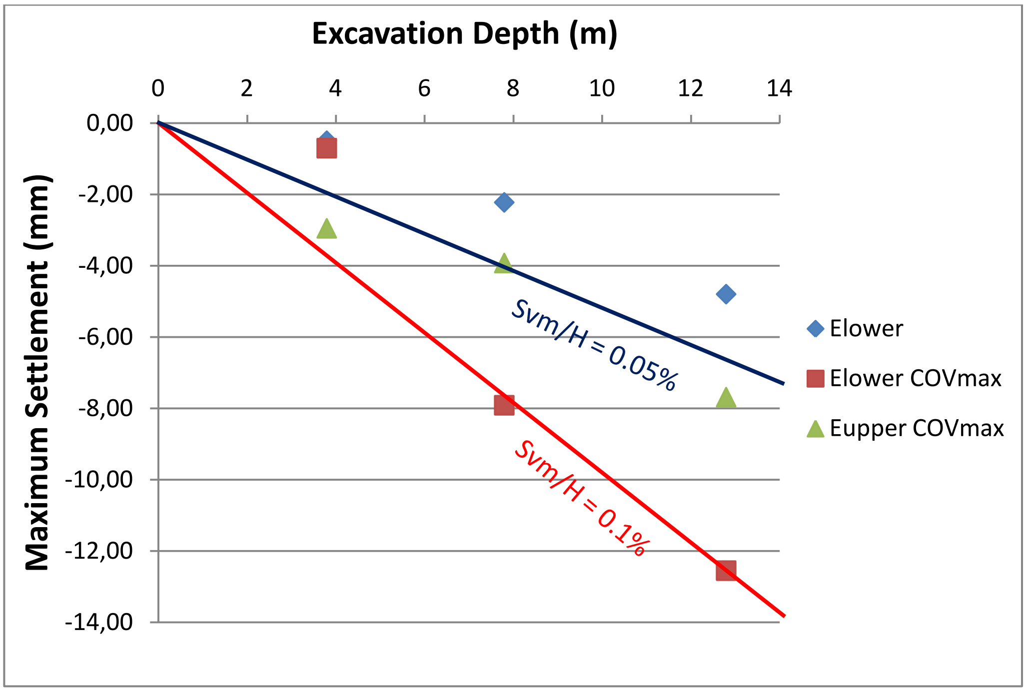

Figure 5.5a: Maximum Settlement vs Excavation Depth.

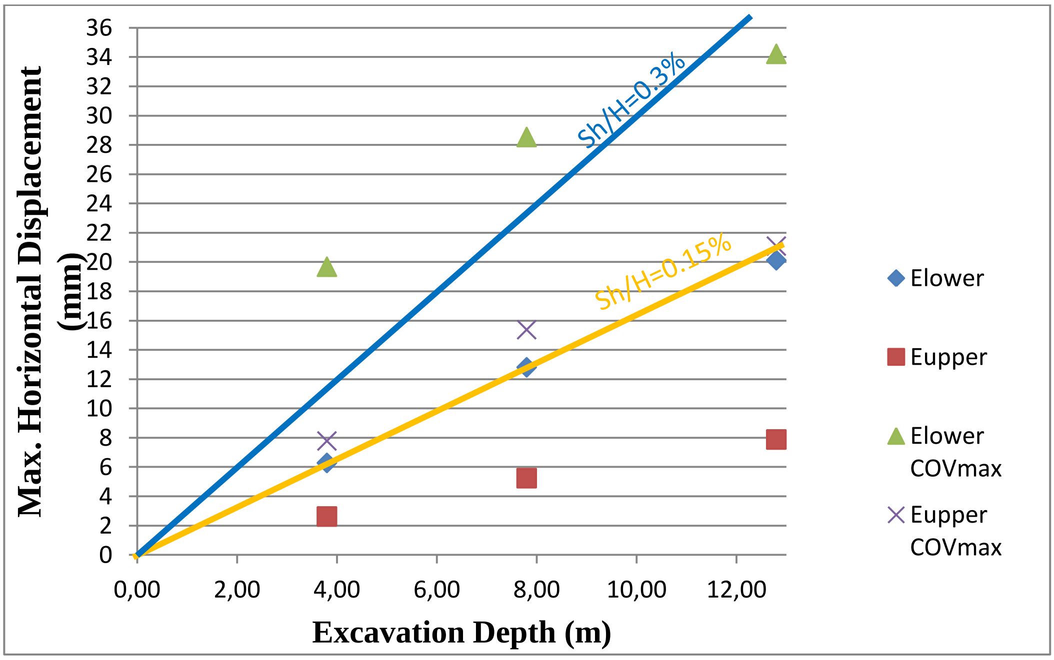

Figure 5.5b: Maximum Horizontal Displacement vs Excavation Depth.

This ratio is about 0.4Sh < Sv < 0.5Sh due to Liu et al., 2005 and 0.5Sh < Sv < 1.0Sh in Mana and Clough, 1981, which satisfy the predicted results. In Clough and O'Rourke, 1990, it is shown that the horizontal movements tend to average about 0.2% of maximum excavation depth, Hmax and vertical movements about 0.15% of Hmax in excavations in stiff clays, residual soils and sands, as shown in Figure 5.6a and Figure 5.6b, respectively. Therefore, we can say that the Sv/Sh ratio is 0.75 (0.75Sh=Sv).

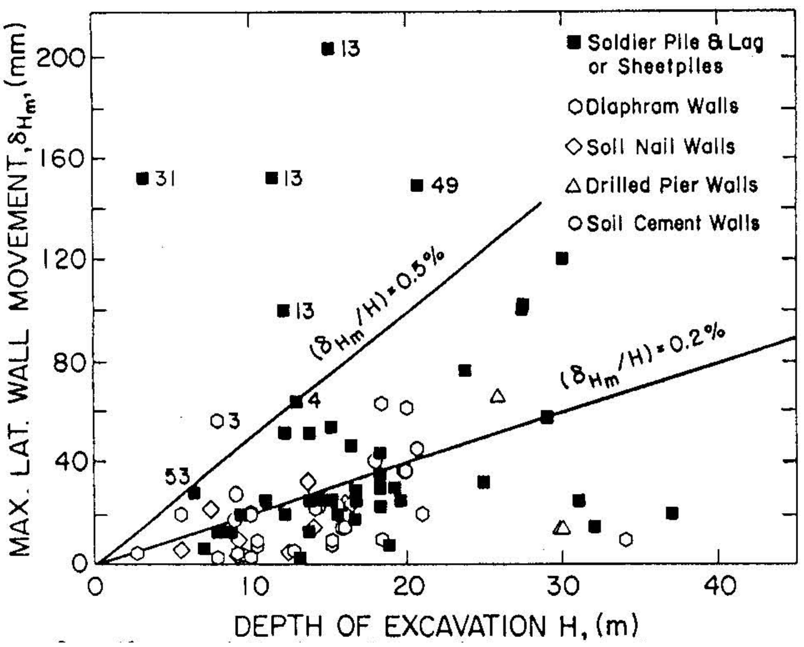

Figure 5.6a: Maximum Horizontal Displacement vs Excavation Depth (Clough&O'Rourke, 1990).

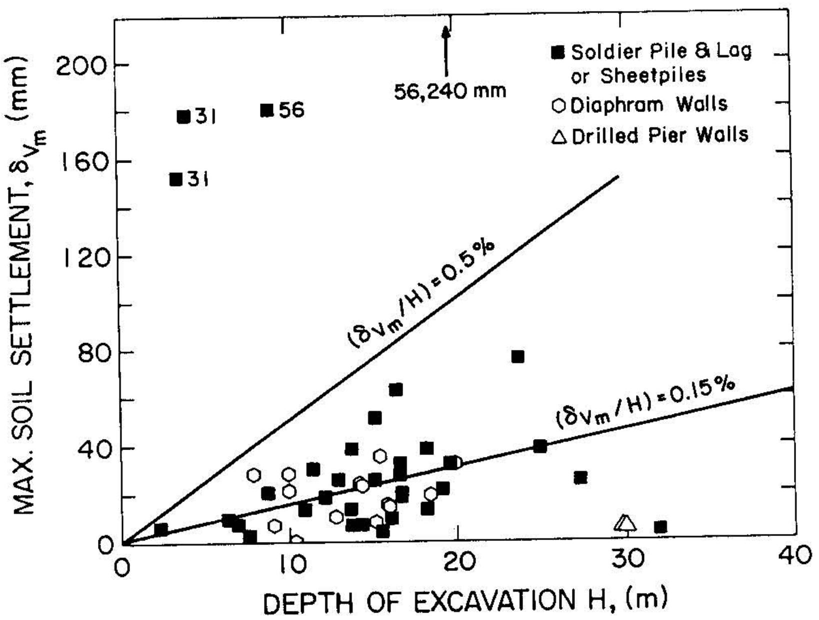

Figure 5.6b: Maximum Settlement vs Excavation Depth (Clough&O'Rourke, 1990).

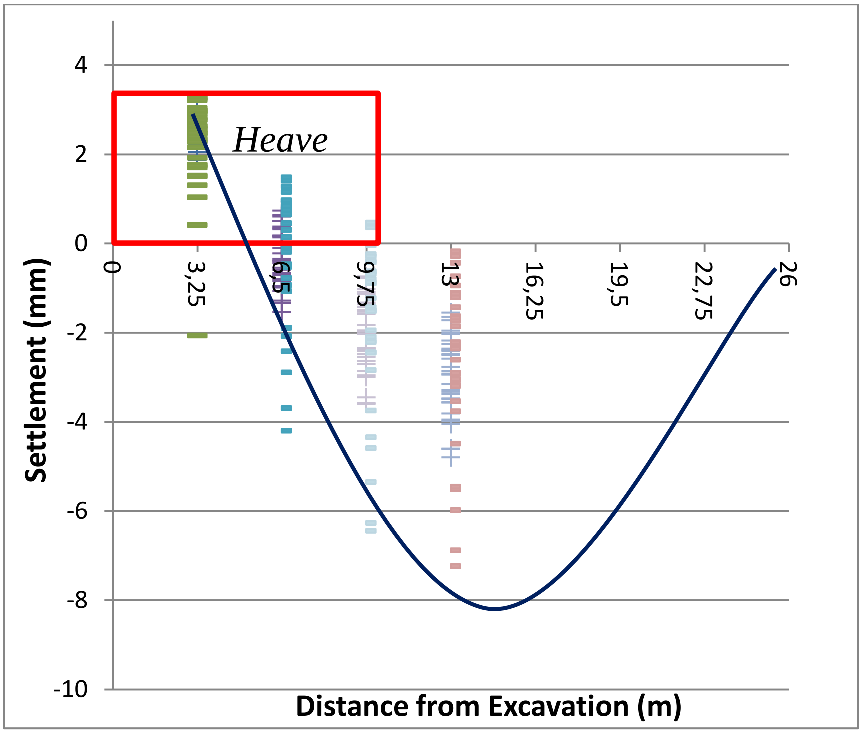

Figure 5.7: Settlement vs Distance from Excavation.

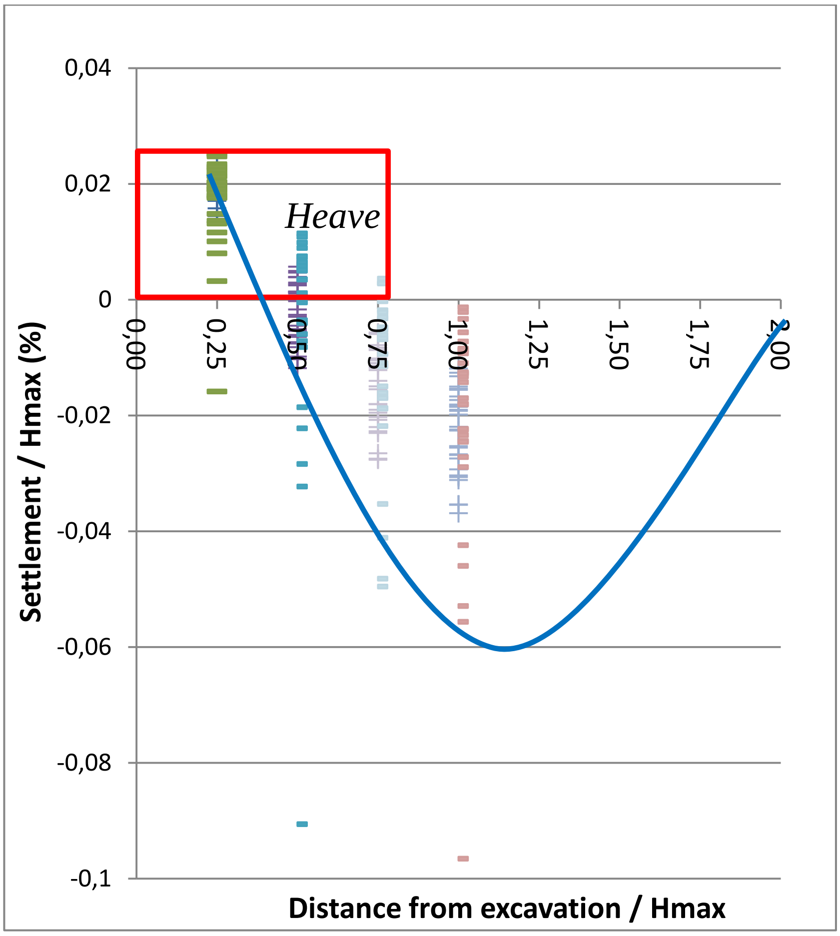

Figure 5.8: Settlement / Hmax (%) vs Distance from Excavation / Hmax.

Figure 5.7 and Figure 5.8 summarize the settlements adjacent to excavation as a function of distance from excavation. There is heave at the edge of the excavation and heave neutralizes at distance 0.5Hmax. It is clear that the settlements are low at the closest distance and increases by distance first then decreases as the distance goes to 2Hmax, where the settlements decrease to zero. This path has proved the soil profile diagram given by Peck (1969) in Figure 4.3 and the path modified by Liu et al., (2005) in Figure 4.2.

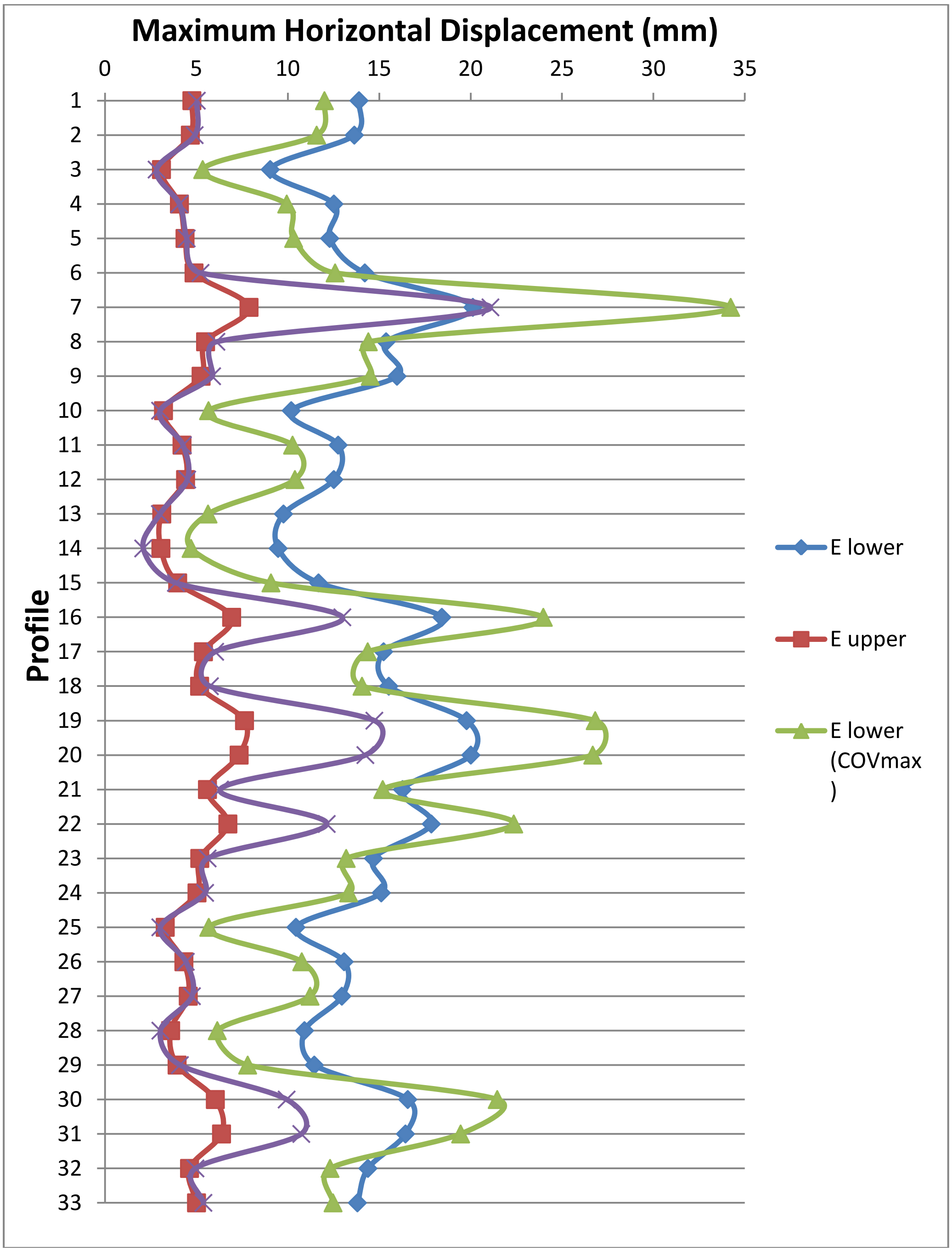

Figure 5.9: Maximum Horizontal Displacement on Pile vs Profile at 12.80m Exc. Depth due to Variation of E.

As indicated in Table 5.9 and Table 5.10, when E is used in its upper limits, the horizontal displacement and settlement values become almost three times less than the results with E_{lower}. Also, when the FE analyses are performed with the parameter variations with maximum COV in the literature (Table 5.2), the maximum displacements on and behind the system reduces (Figure 5.9). Before the reliabilty analyses, we can also say that using the COVmax in the literature, meaning the variaton in the soil parameters; choosing the parameters wrongly or the geologic structure of the soil profile changes on the edges, affects the system notably. This may lead to over design or poor design, which may cause loss of money, loss of life.

In order to determine the most effective soil parameter on the system deformations, sensitivity analyses were also performed by using VIPlaxis 9.2 software. The results of the analyses with different variations of soil parameters also showed that the most important soil parameter is the Young's Modulus, E. The most sensitive E is the Medium Stiff Silty Clay's, with an average 40-50% sensitivity, on the horizontal displacements on the pile. For vertical displacements behind the retaining system we can also say that E of medium stiff silty clay is most effective for the distances where heave occurs and E of dense sand-gravel layer is effective at the distance far from 0.75Hmax from the system where settlement occurs. The results of the sensitivity analyses are given in the diagrams in Appendix B.

In addition to the geotechnical influences on movements on the retaining system and behind, the retaining system itself is also important on the displacements. It is significant, since it can be controlled by the designer, its limits can be defined and the behavior of the system may be improved.

Stiffness of the wall helps to reduce movements. But, in conditions where the clay is inherently stable, stiffness of the wall is much less effective in reducing movements than in conditions where there is a basal heave. In presence of a stable base, increasing the wall stiffness theoretically does not significantly reduce wall system movements in cohesionless soils. Whereas, with a low FS condition of the soil profile (Figure 5.10), a stiff wall is also subject to movements due to extraneous construction factors as a flexible wall (Clough and O'Rourke, 1990). The support spacing is more important than wall stiffness. The support spacing is raised to the forth power in system stiffness across wall stiffness. The smaller the support spacing, the stiffer the support system.

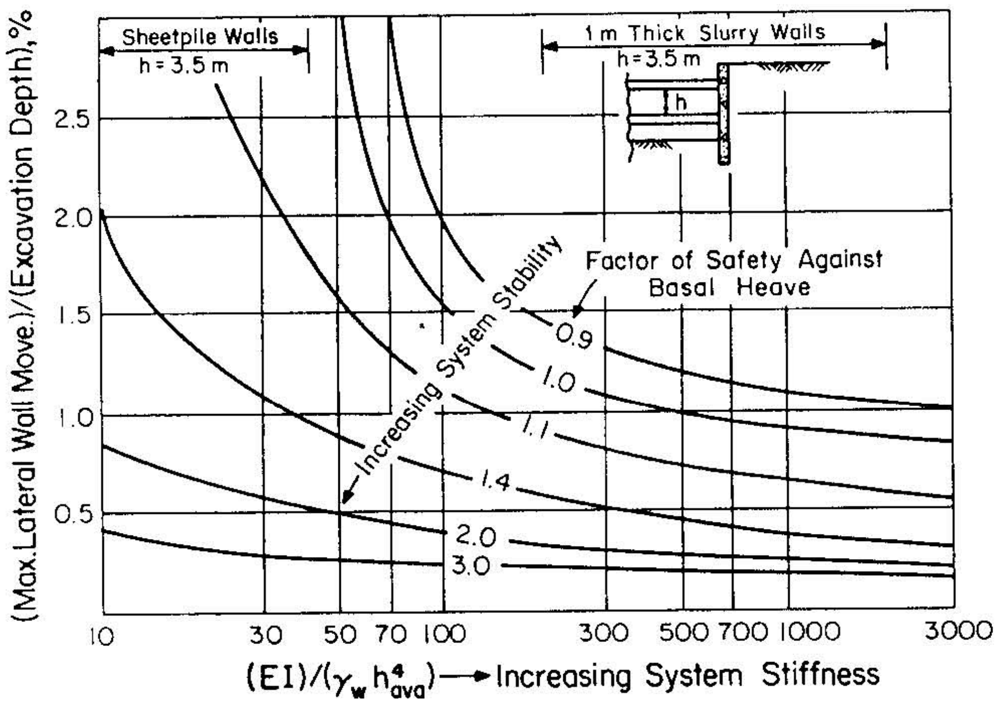

Figure 5.10: Design Curves to Obtain Maximum Lateral Wall Movement (or Soil Settlement) for Soft to Medium Clays (Clough et al.,1989).

As it is clear in Figure 5.11, the vertical spacing of struts is very important. In cases in Figure 5.11, both excavations are performed in similar soil conditions and both used diaphragm walls. Although the shallower excavation was half of the deeper excavation, the lateral displacement on the shallower wall was one fourth of the other since the support vertical spacing for shallower one was twice the deeper one. A primary factor in the difference in response was the much smaller support spacing used in the deeper excavation.

In our case horizontal spacing of the struts is 4.0m and vertical spacing is 3.50m, which are maximum spacing that could be provided according to excavation steps and depending on the maximum excavation depth. In a system with wider horizontal support spacing, there would be increase in moment at the bored piles, which would require more reinforcement or increase in pile diameters and would not be economical. Penetrating the wall to a more bearing layer can be a solution, where possible, however, it may be uneconomical to extend the entire wall perimeter to a hard layer to increase the cantilever capacity of the wall or prevent settlement or horizontal displacements, while a great depth may be required.

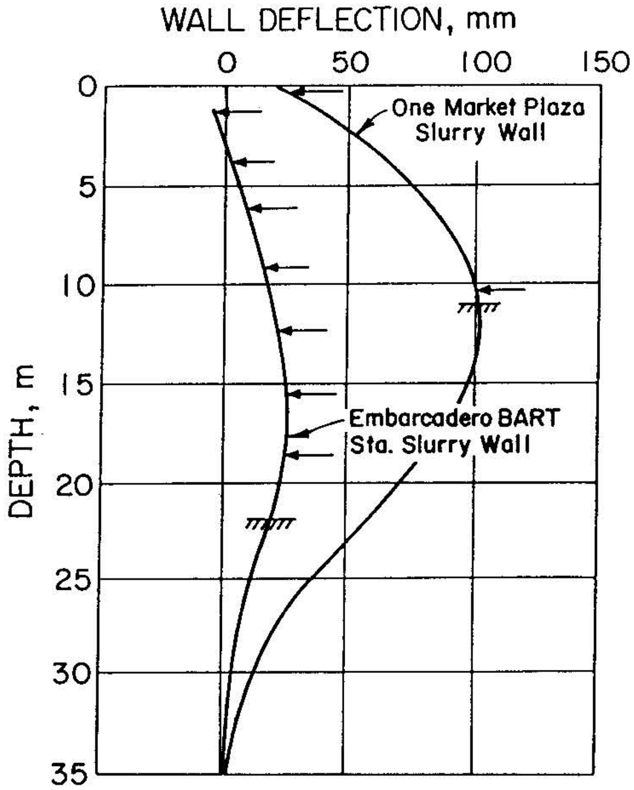

Figure 5.11: Comparative Braced Wall Case Histories in Soft Clay Illustrating Effects of Support Vertical Spacing (Clough & O'Rourke,1990).

5.5 Reliability Analyses

5.5.1 Target reliability

It is an important part of the process to determine the target reliability or target probability of failure, during Reliability Based Design of a system. Target reliability can be expressed as the mean reliability established by research and in-situ experience during engineering works. Various charts are used during design of various engineering structures. These charts are used to estimate the acceptable risk. An example of these charts, depicting the average annual probability of failure for different types of civil engineering structures, is given in Figure 5.12.

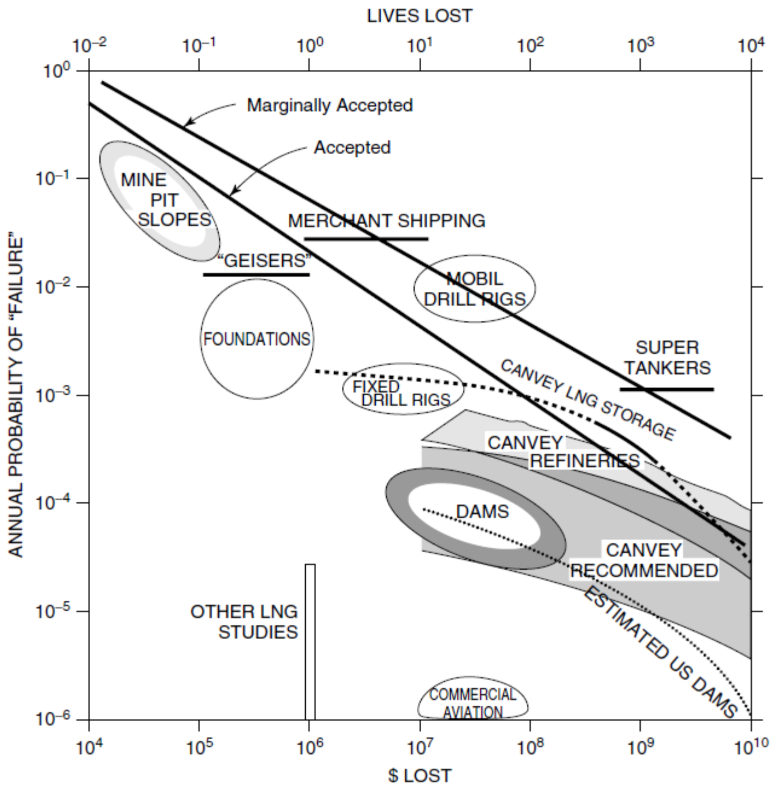

Figure 5.12: Chart Showing Average Annual Risks Posed by a Variety of Traditional Civil Facilities and Other Large Structures or Projects (Baecher and Christian, 2003).

As can be seen from Figure 5.12 the probability of failure changes depending on the type of structure. There is a unique relationship between probability of failure and reliability index as given in Table 5.11.

Table 5.11: Relationship between the Reliability Index and Probability of Failure (Akbaş, 2007).

Reliability Index (β)	Probability of Failure Pf= Φ(-β)
1.0	0.159
1.5	0.0668
2.0	0.0228
2.5	0.00621
3.0	0.00135
3.5	0.000233
4.0	0.0000316

Table 5.11 shows the relationship between reliability index and probability of failure. "There is a unique relationship between the reliability index and probability of failure, with β increasing as pf decreases" (Akbaş, 2007). For engineering structures both probability of failure and reliability index can be used to calculate the risk in the

design; however in geotechnical engineering works, where reliability against earth pressures are very important, P_f values can take very small values for usual applications. Therefore, it is preferable to use β.

Beside, different references give different reliability indices based on structure types. For example, for transmission line structures Criswell and Vanderbilt, 1987 suggests target reliability index from 2.7 to 3.2, while ASCE Task Committee on Structural Loadings, 1991 suggest values between 2.3 and 3.4. On the other hand, for foundation design the reliability index was proposed to be 2.3 to 3.7 by Meyerhof, 1994, while it is 3.5 in the National Building Code of Canada 1995. Similarly, for temporary retaining systems of deep excavations target reliability index may be chosen as 2.2, which allows a 0.011 probability of failure in the system.

5.5.2 Probability of failure due to settlement and horizontal displacement criteria

Reliability of the elements of the system and the system as a whole should be investigated separately while determining the reliability of the system. This is because, weak points of each element, independently or by effecting each other may cause collapse of the system or the system to be accepted as non-serviceable. In this research, reliability of the retaining system of a deep excavation has been investigated by examining the reliability of each element affecting the retaining system separately and connected.

The effective elements of system reliability that are investigated in this research are the horizontal and vertical displacements and earth pressures depending on the variations in the engineering parameters of layers in soil profile. Limiting values for horizontal displacements and settlements are classified depending on the properties of the layers in the soil profile, excavation depth, characteristics of adjacent structures, etc., by national and international standards and manuals.

For example, as described in NAVFAC DM-7.2 “Foundation and Earth Structures Design Manual 7.2”, magnitude of wall rotation (Sh/H) for failure is 0.002, for loose cohesionless soils. On the other hand, 5mm of total settlement is determined as the limit value for steel structures, for crane ways in the Canadian Steel Structures Manual. These limit values are summarized in Table 5.12.

Table 5.12: Limit Values for Total Settlement Depending on the Structure Type.

Structure Type	Total Settlement	References
Reinforced Concrete	100 mm	Turkish Building Code
Brick	80 mm	USSR Building Code 1995
Rail to Rail Elevation	5 mm for L≤15m	Canadian Steel Structures
Vertical Deformation on Runway Beam	L/800, max.12mm	Canadian Steel Structures
	L/600	TS EN 1993-6
Difference between vertical deformations of two beams	L/600	TS EN 1993-6

L: span between crane runway beams (12m in our case).

It is clear from Table 5.12 that choosing the limit values at the beginning of the design, wil give the criteria that the system reliability would be investigated against.

A performance function can be specified with respect to the displacement of the wall, thus representing a criterion for the serviceability of the structure. When H*0.2% mm horizontal displacement for deep excavations in sand, clay layers, defined as limiting values by NAVFAC 7.2, 1982, Clouterre, 1991 or Puller, 2003 and 5 mm settlement for crane runways, defined as limiting values by the Canadian Steel Structures (2005). The performance functions are;

$$g(X) = H*0.2\% - S_{h,FE} \quad \textbf{(5.21)}$$

$$g(X) = 5 - S_{v,FE} \quad \textbf{(5.22)}$$

$S_{h,FE}$ and $S_{v,FE}$ are the mean values of the displacements obtained from the finite element analyses.

Following the procedure described above and in Schweiger et al. (2001), after obtaining the mean and standard deviation of the $S_{h,FE}$ and $S_{v,FE}$ for each excavation depth and by an assumption of a normal distribution for displacements, the reliability index is obtained and summarized in Table 5.13.

Table 5.13: Reliability Index (β) of Sh and Sv.

		COVnormal		COVmax	
	Excavation Depth (m)	ϕ+c+$E_{(lower)}$	ϕ+c+$E_{(upper)}$	ϕ+c+$E_{(lower)}$	ϕ+c+$E_{(upper)}$
S_h	3.80	3,810	11,25	0,866	4,289
	7.80	3,720	11,25	0,952	3,842
	12.80	3,940	11,25	1,800	4,612
S_{vmax} (5mm)	12.80	2,300	11,25	0,814	3,120

As explained in section 5.5.1, target reliability of a temporary retaining system for a deep excavation can be chosen as 2.2. From the data given in Table 5.13, we can say that the reliability of the system is over target reliability, where soil parameters vary at lower and upper limits of E. However, the reliability of the system is under target reliability when COV is maximum with lower limit of E. This is because; fluctuations in the soil parameters vary on the edges and its affect doubles when E is in the lower limits.

5.5.3 Fault tree for system reliability

Soil parameters and dimensions of the retaining system have been taken into account while creating the Fault Tree. The rigidity and parameters of the retaining system elements have not been taken into consideration. This is done in order to make parameter-controlled tests, by limiting the unknowns.

The active earth pressure coefficient has been used during the calculation of lateral earth pressure, to allow displacements. However, the equations in the fault tree have been created with the assumption that, there will be no cracks on the retaining system and the displacements will be within the allowable limits.

Fault Tree for the system failure has been created with the acceptance that the horizontal displacements of the vertical elements of retaining structure, total/differential settlement of adjacent structure and the bearing capacity of vertical elements of retaining system against lateral earth pressure limits the system choice and defines the reliability of the system (Figure 5.13). Because, although the factor of safety (FOS) of the retaining system is greater than one, the horizontal movements may exceed the limits and the structure can be called to be non-serviceable, or the settlements behind the retaining system may cause differential settlements over limits that the adjacent structure has to be repaired or even evacuated. The system, itself, may fail when it is designed at the limits that do not allow any cracks, even without any horizontal displacement or settlement on and behind the system. This may be caused by exceeding the moment or shear strength capacity of the piles.

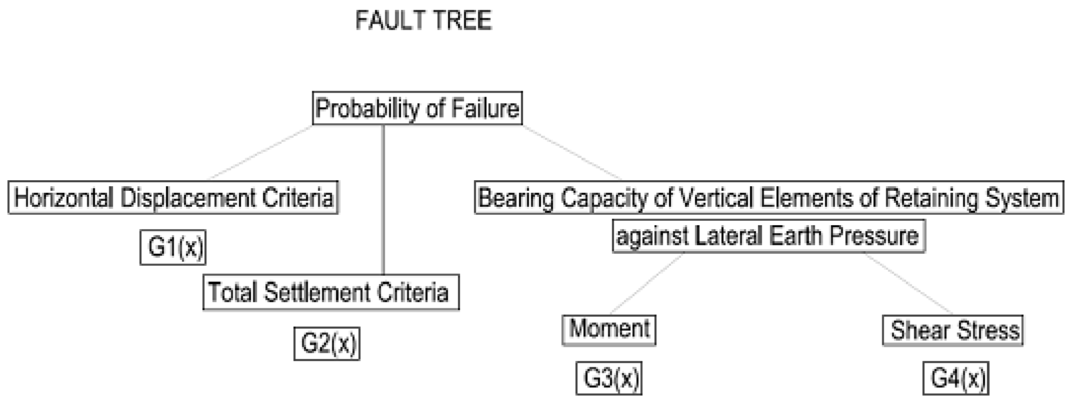

Figure 5.13: Fault Tree for System Failure.

5.5.4 System reliability analyses via NESSUS

The system reliability analysis in this research was performed by using NESSUS. As an ability of NESSUS, results of some commercial finite element models can directly be adapted to the program with an interface that is already installed; in order to reduce the time elapsed for modeling and running the probability analysis. However, as NESSUS does not have an interface with Plaxis, the model in this research has been created and run in Plaxis and then the results have been used in the fault tree (Figure 5.14) and analytical equations below.

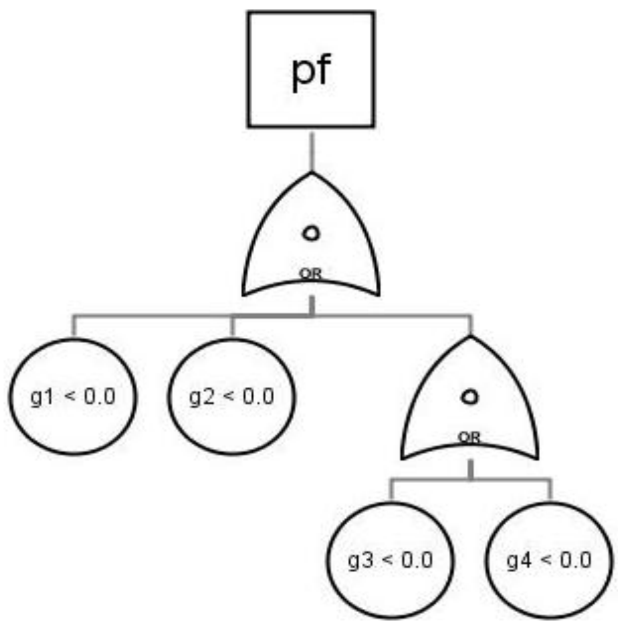

Figure 5.14: Fault Tree Used for reliability Analyses in NESSUS.

$$pf = P\{(g1 < 0.0 \text{ OR } g2 < 0.0 \text{ OR } (g3 < 0.0 \text{ OR } g4 < 0.0))\} \quad \textbf{(5.23)}$$

$$g1 = H*0.0020-Sh \quad \textbf{(5.24)}$$

$$g2 = 5-Sv \quad \textbf{(5.25)}$$

$$g3 = Md-Mp \quad \textbf{(5.26)}$$

$$g4 = Nd-Np \quad \textbf{(5.27)}$$

where;

p_f : probability of failure

g1 : probability function of horizontal displacement

g2 : probability function of settlement

g3 : probability function of moment on piles

g4 : probability function of shear stress on piles

M_d : design moment

M_p : moment from earth pressure

N_d : design shear stress

N_p : shear stress from earth pressure

Sh : horizontal displacement at the construction stage

Sv : total settlement at the construction stage

H : depth of excavation at the construction stage

The system has been analyzed by using the fault tree in Figure 5.13. The variations in the lateral displacement on the piles and settlement on the surface behind the piles, total moment and shear stress on the piles were considered as effective elements on the system reliability. The results of the analyses due to excavation depth and soil parameter variations have been summarized in Table 5.14 and the sensitivity diagrams are given in Appendix B and Appendix C, for Sv=5mm and Sv=10mm, respectively.

Table 5.14: Reliability Index of the System due to Excavation Depth and Soil Parameter Variations

Soil Parameter Variation	Sv=5mm			Sv=10mm		
	3.80m	**7.80m**	**12.80m**	**3.80m**	**7.80m**	**12.80m**
$\phi + c + E_{(lower)}$	3.830	3.034	2.299	3.834	3.714	3.951
$\phi + c + E_{(upper)}$	11.25	11.25	11.25	11.25	11.25	11.25
$\phi + c + E_{(lower)}$ [COVmax]	0.775	0.931	0.716	0.867	0.953	1.769
$\phi + c + E_{(upper)}$ [COVmax]	4.096	3.589	3.114	4.325	3.859	4.465

β=2,2 target reliability can be taken into account for the system as well and from the data given in Table 5.14, we can say that the reliability of the system is over target reliability, where soil parameters vary at lower and upper limits of E (Figure 5.15 and 5.16). However, the reliability of the system is under target reliability when COV is maximum with lower limit of E. This is because; fluctuations in the soil parameters vary on the edges and its effect doubles when E is also in the lower limits.

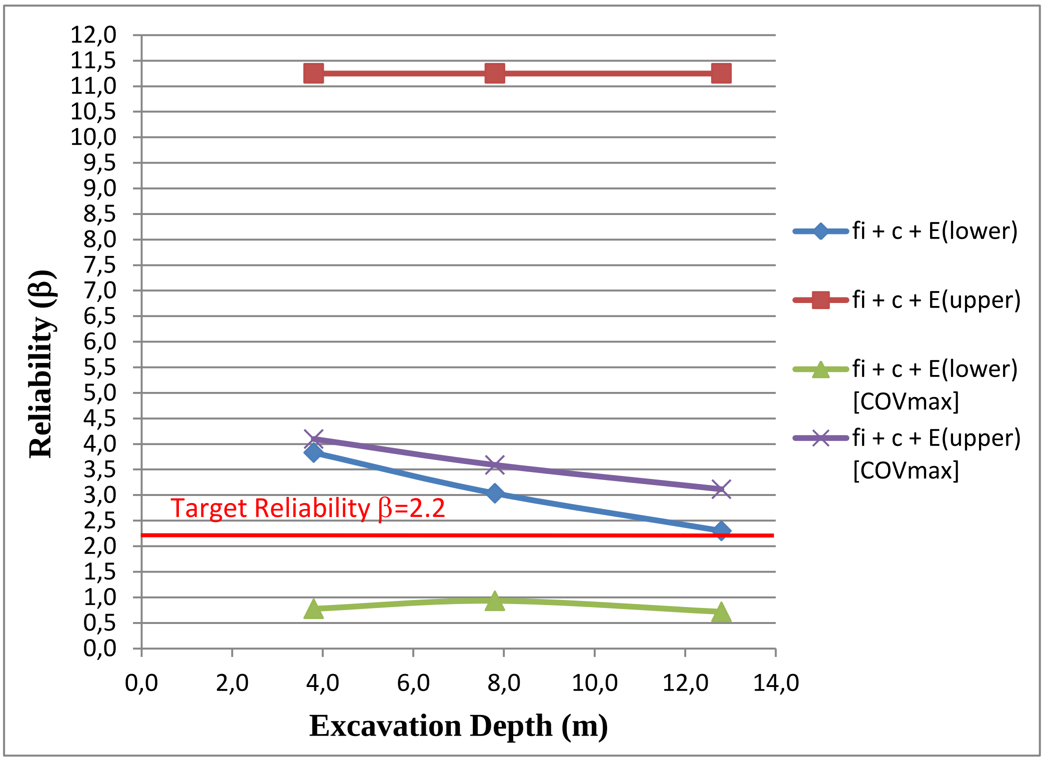

Figure 5.15: System Reliability vs Excavation Depth Diagram for Sv=5mm.

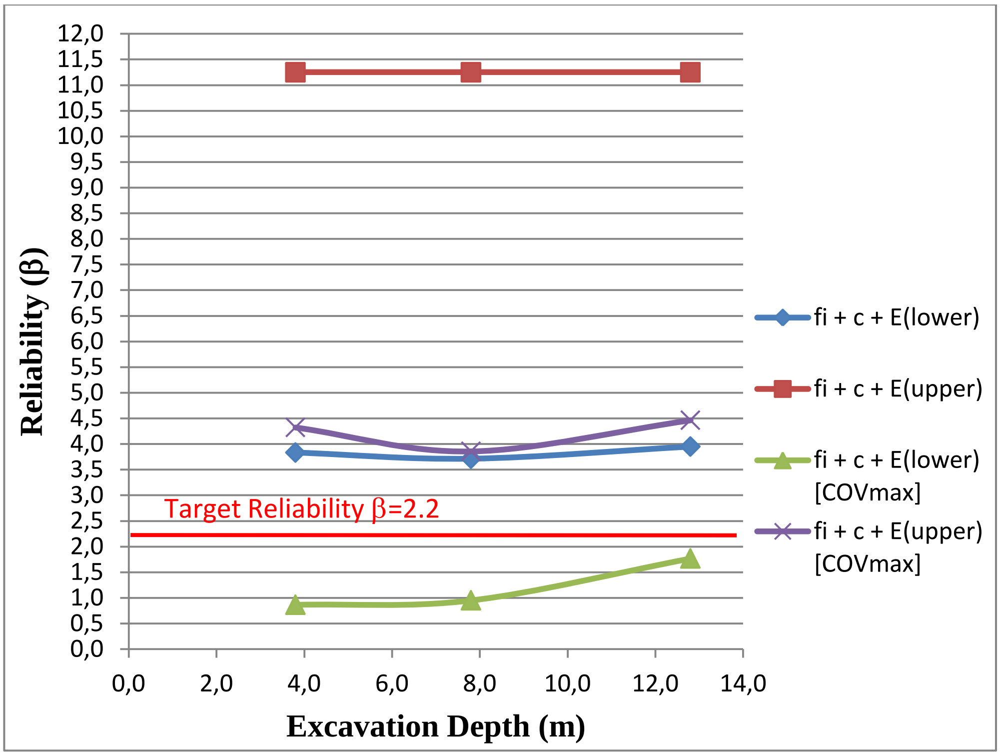

Figure 5.16: System Reliability vs Excavation Depth Diagram for Sv=10mm.

When the reliabilities due to δh and δv have been compared to the reliability of the system, it is clear that δv is the significant criteria for the system reliability and system is weak when the lower limit of E is chosen while the COV of soil parameters is at maximum.

5.6 Soft Soil Conditions

In order to see the effect of E variations with mean COV and maximum COV, on the reliability of the system, an imaginary soft soil condition with the same retaining system has been created and investigated. The soil profile consists of one layer, soft clay. The undrained cohesion of soft clay has been treated as a random variable and its mean and standard deviation has been determined by using the SPT numbers of the soft clay layers at the site. The mean value for c is μ=37.45 kN/m^2 and σ=7.63 (COV=21%). For the analyses with COVmax, COV has also been taken from the literature as COVmax=35% (Table 5.2).

Following the same steps in PEM, $2n^2+1=3$ soil profiles has been created for each E variation; $E_{(lower)}$, $E_{(upper)}$, $E_{(lower)\_COVmax}$, $E_{(upper)\_COVmax}$. Therefore, twelve FE analyses have been performed and the results for the horizontal displacement and settlements have been shown in Figure 5.17 and 5.18, respectively.

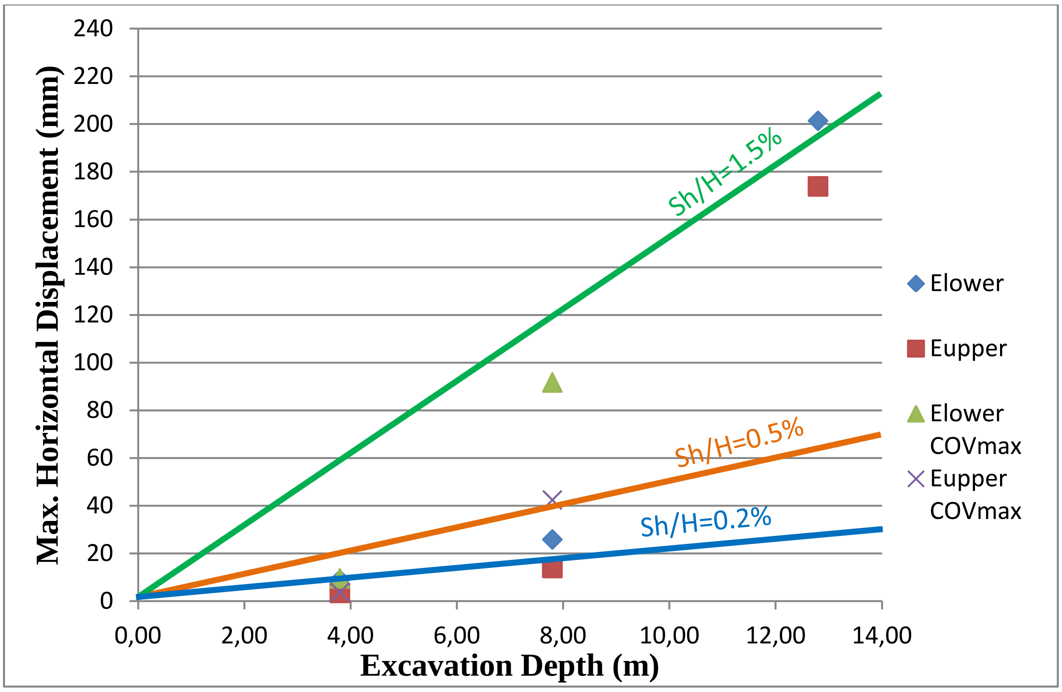

Figure 5.17: Maximum Horizontal Displacement vs Excavation Depth.

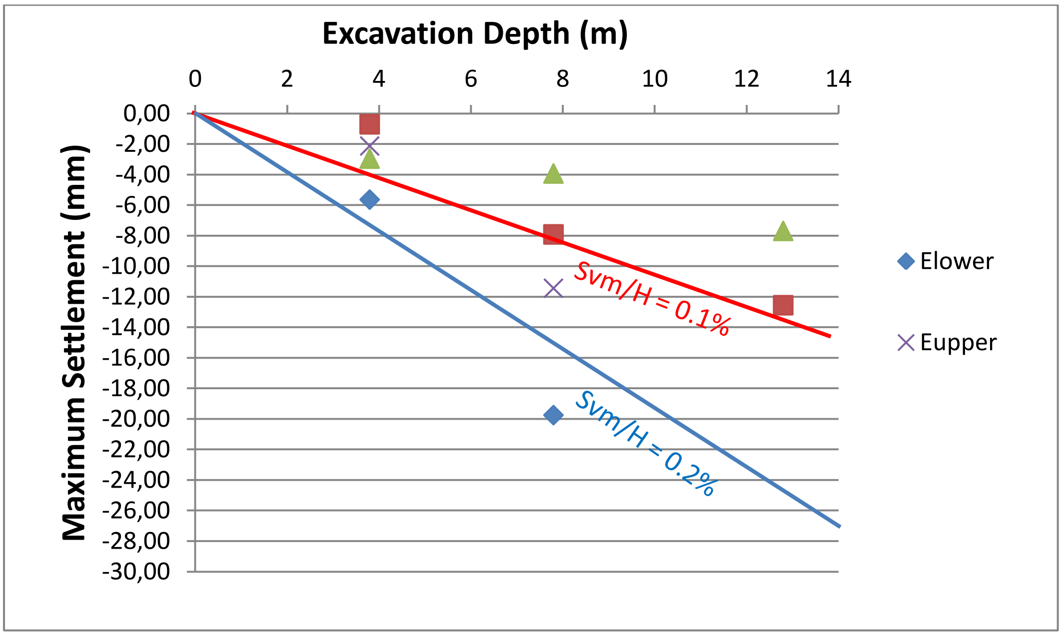

Figure 5.18: Maximum Settlement vs Excavation Depth.

The displacement values are summarized in Table 5.15 and Table 5.16. When the ratio between S_h and S_v is determined the range becomes $1.0S_h < S_v < 2.0S_h$ for the profile determined by PEM (Figure 5.17 and Figure 5.18).

Peck, 1969 showed that vertical movements in soft clays are between 1% to 3% of H_{max}. In our soft clay case, the vertical movements tend to average about 1.2% of H_{max}, when reached to maximum excavation depth.

Table 5.15: Horizontal Displacement Due to Excavation Depth for Soft Clay.

Variables	c, ϕ ve E_{lower}		c, ϕ ve E_{upper}		c, ϕ ve E_{lower} with COVmax		c, ϕ ve E_{upper} with COVmax	
Excavation Depth(m)	Mean	Std. Dev.	Mean	Std. Dev.	Mean	Std. Dev.	Mean	Std. Dev.
3,80	8,04	0,704	3,11	0,272	7,87	1,44	3,04	0,56
7,80	20,68	3,82	10,24	2,69	41,46	35,45	19,27	16,41
12,80	107,34	69,03	80,89	67,18	176,73	176,31	142,45	157,17

Table 5.16: Maximum Settlement Values Due to Distance from Excavation and Excavation Depth for Soft Clay.

	c, ϕ ve E_{lower}		c, ϕ ve E_{upper}		c, ϕ ve E_{lower} with COV max		c, ϕ ve E_{upper} with COV max	
Exc. Depth (m)	Mean	Std. Dev.	Mean	Std. Dev.	Mean	Std. Dev.	Mean	Std. Dev.
3.80	5,39	0,42	2,03	0,16	5,29	0,86	1,99	0,33
7.80	14,81	3,64	7,70	2,75	29,94	26,92	16,13	15,83
12.80	82,54	50,33	66,05	54,79	137,52	140,23	115,59	127,35

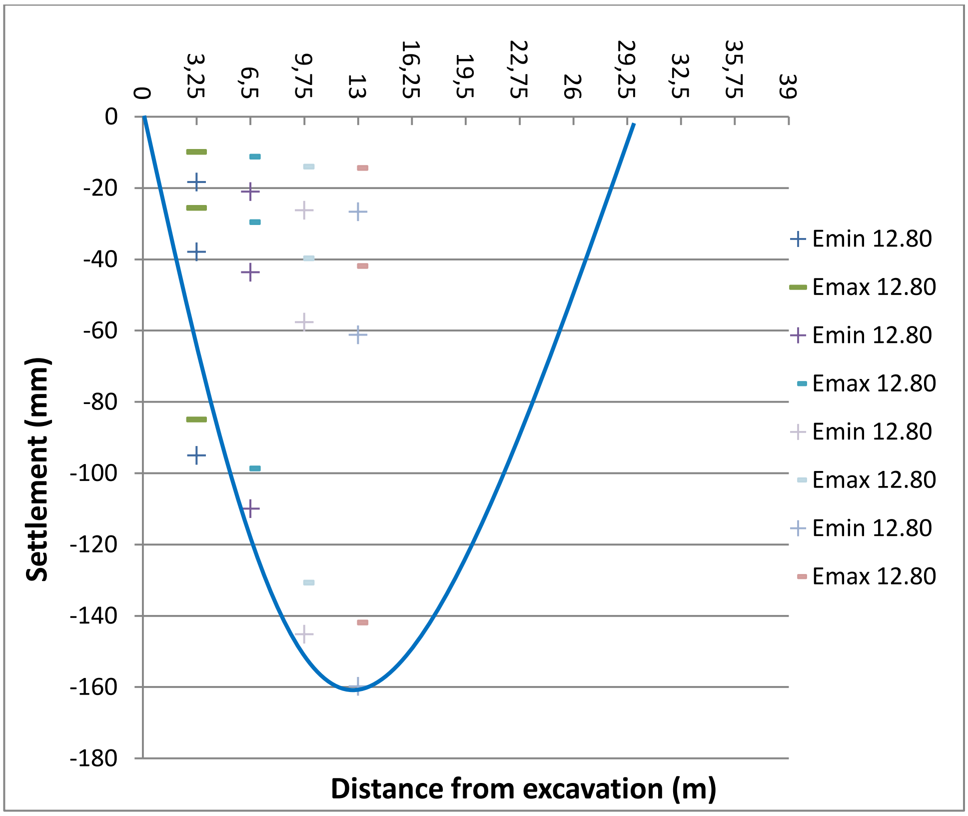

Figure 5.19: Settlement vs Distance from Excavation.

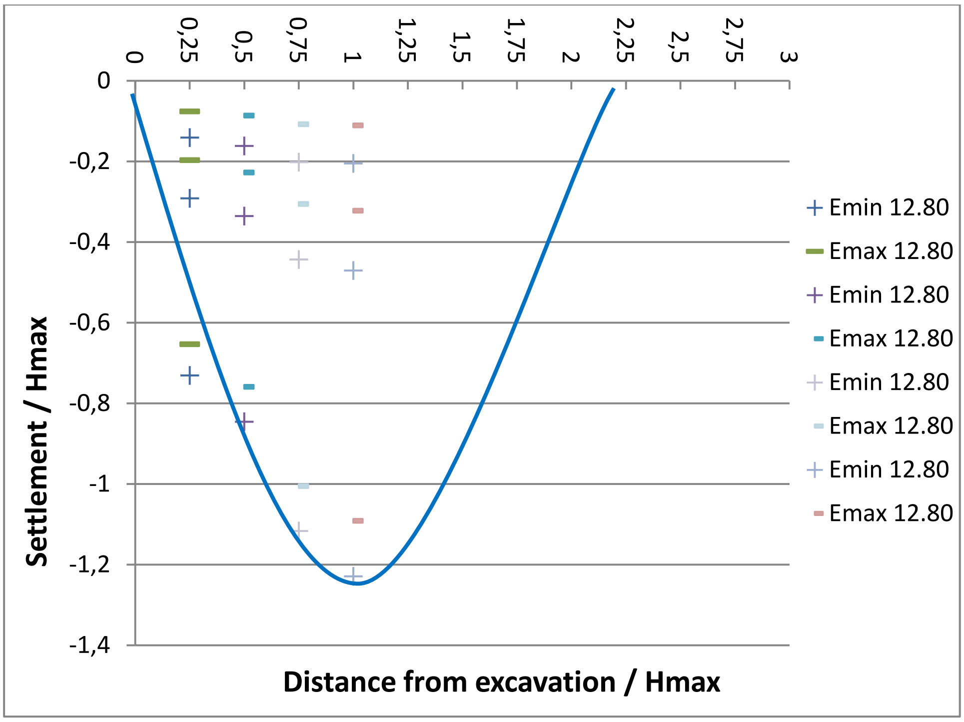

Figure 5.20: Settlement / Hmax (%) vs Distance from Excavation / Hmax.

Figure 5.19 and Figure 5.20 summarize the settlements adjacent to excavation as a function of distance from excavation. It is clear that the settlements are low at the closest distance and increases by distance first then decreases as the distance goes to $2H_{max}$, where the settlements decrease to zero. This path has proved the soil profile diagram given by Peck (1969) for soft clays in Figure 4.3 and the path modified by Liu et al., (2005) in Figure 4.2.

For the reliability analyses for soft clay condition, the performance functions in Equation 5.18 and 5.19 have also been used, with the $S_{h,FE}$ and $S_{v,FE}$ whose the mean values have been obtained from the finite element analyses. The results of the reliability analyses for each element and the system are summarized in Table 5.17 and 5.18, respectively.

Table 5.17: Probability of Failure (%) of Sh and Sv.

		COVnormal		COVmax	
	Excavation Depth (m)	ϕ+c+$E_{(lower)}$	ϕ+c+$E_{(upper)}$	ϕ+c+$E_{(lower)}$	ϕ+c+$E_{(upper)}$
Sh	3.80	73,26	0	57,51	0
	7.80	90,82	12,96	76,94	65,54
	12.80	88,06	82,08	80,40	77,95
Svmax (5mm)	12.80	93,83	88,00	82,95	81,33
Svmax (100mm)	12.80	36,45	29,27	60,78	56,26

Table 5.18: Probability of Failure (%) of the Retaining System.

Soil Parameter Variation	Sv=5mm	Sv=100mm
$\phi + c + E_{(lower)}$	99,29	94,74
$\phi + c + E_{(upper)}$	97,97	88,76
$\phi + c + E_{(lower)}$ [COVmax]	98,49	96,55
$\phi + c + E_{(upper)}$ [COVmax]	96,63	92,09

As the reliability index for temporary retaining systems of deep excavations has been accepted to be β=2,2, which corresponds to a pf of 0.011, from the data given in Table 5.17 and Table 5.18, we can say that the reliability of the system is under target reliability, for soft clay conditions and probability of failure of the system is about 90%. For such soft clay conditions, rigidity of the system should be increased and the strut spacing should be closer at the horizontal and vertical directions. Also, from the FE analyses diagrams, we can say that the base of the excavation in front of the piles should be strengthened against heave and opening in the socket of the pile.

5.7 Results of the Research

Aim of this research was to investigate the reliability of a deep excavation and its retaining system depending on the soil parameter variations and due to the settlement of neighboring structures. A correlation between the settlement of adjacent structures and the excavation system reliability has been examined. Therefore, more than 200 finite element and reliability analyses has been performed.

The results obtained from the analyses are presented below:

- Increasing wall stiffness tends to reduce system movements, but this is most effective in soft to medium clays. On the other hand, support spacing is more important than wall stiffness in defining system stiffness and helping control movements. It is important because movements in strutted systems occur just after the excavation phase and cannot be reduced after the placement of struts.
- Horizontal displacements on piles of excavations, which are laterally supported with struts, occur on the excavation stage at the excavation level. Thus, the settlement behind the retaining system occurs in a hyperbolic shape. The settlement increases with distance from excavation at first and lasts at a distance of about twice the maximum excavation depth.

- It was observed that the variation in ϕ and c with the calculated COV of the parameters is not that effective on the probability of failure of the system. Changing the ϕ and c and dependently E with the maximum COV in the literature, which represents the case that the geological profile in the field vary on the edge or the insufficient soil exploration, helped to understand the effect of parameter fluctuations on the system displacement and reliability.
- Using point estimate method (PEM), developed by Schweiger et al. (2001), in combination with finite element analysis can help reducing budget of site investigations by creating realistic artificial models, reducing time for modeling, and can allow optimal decisions with less certainty in the properties of the layers in the soil profile.
- The magnetic column readings at the site confirmed that the ground movement lie in between $\delta v(max) = 0.25\delta h(max)$ and $\delta v(max) = 0.5\delta h(max)$ for the soil profile of Scale Pit, while it is $\delta v(max) = 0.5\delta h(max)$ and $\delta v(max) = \delta h(max)$ according to Mana and Clough (1981). The ground movements are substantially small probably because of the dimensions of the excavation is small and the soil profile behind the retaining system is stiff.
- The horizontal displacements and settlements conducted during analyses are less that 0.1% and 0.3% of the maximum excavation depth, respectively and are related with a ratio of $0.4\delta h<\delta v<1\delta h$. While, the same range was obtained as $0.25\delta h< \delta v < 0.5\delta h$, during the measurements on the site.
- For temporary retaining systems of deep excavations target reliability index may be chosen as 2.2, which allows a 1.1% probability of failure in the system.
- It can be said that the reliability of the system is over target reliability, where soil parameters vary at lower and upper limits of E. However, the reliability of the system is under target reliability when COV is maximum with lower limit of E. This is because; fluctuations in the soil parameters vary on the edges and its effect doubles when E is also in the lower limits.
- When the reliabilities due to δh and δv have been compared to the reliability of the system, it is clear that δv is the significant criteria for the system reliability and system is weak when the lower limit of E is chosen while the COV of soil parameters is at maximum.

- When E modulus is calculated with its upper limits and average COV the system becomes over reliable. When it is calculated with COV max in the literature, the reliability decreases sharply. This is because the uncertainties in the system increases sharply, as the fluctuations, variations in the soil conditions and soil parameters increase, causing the reliability of the parameters and system to decrease.
- In order to determine the most effective soil parameter on the system deformations, sensitivity analyses were performed by using finite element software. The results of the analyses with different variations of soil parameters also showed that the most important soil parameter is the Young's Modulus, E. The most sensitive E is the Medium Stiff Silty Clay's, with an average 40-50% sensitivity, on the horizontal displacements on the pile. For vertical displacements behind the retaining system we can also say that E of medium stiff silty clay is most effective for the distances where heave occurs and E of dense sand-gravel layer is effective at the distance far from 0.75Hmax from the system where settlement occurs.
- In soft clay conditions the horizontal movements tend to average about 1.5% of maximum excavation depth, Hmax and vertical movements about 1.2% of Hmax, when reached to maximum excavation depth.
- The reliability of the system in soft clay, is under target reliability and probability of failure of the system is about 90%, depending on the soft soil conditions and low, c and E values. For such soft clay conditions, rigidity of the system should be increased and the strut spacing should be closer at the horizontal and vertical directions. Also, from the FE analyses diagrams, we can say that the base of the excavation in front of the piles should be strengthened against heave and opening in the socket of the pile.
- Limit conditions, such as settlement, horizontal displacement, angular distortion limits for retaining walls or crack width limits for superstructures may be differ from site to site and even from employer to employer, of course to be under limits that are specified by the standards. The limit values for each element affecting the system reliability should be determined precisely before starting the design. This is because the limit values affect the reliability conditions and systems are specified as reliable or unreliable due to those limits.

6. CONCLUSIONS

The main objective of this research was to determine the effect of parameter variations on the reliability of a retaining system for deep excavations. The reliability of the system has been investigated considering the settlement of neighboring structures. A correlation between the settlement of adjacent structures and the excavation system reliability has been examined.

For this purpose, a detailed monitoring has been conducted on a scale pit excavation, in a steel complex and the excavation has been monitored from the beginning of the excavation until the last level of the struts were removed. The measured and predicted horizontal and vertical displacements and pipe loads are compared to varify the model accuracy. Following this varification, the soil profile has been idealized and the system has been modeled again in this soil profile. For the FE analysis the soil profile has been varied by the soil parameters created by point estimate method (PEM), suggested by Schweiger et al. (2001). 132 analysis were performed in order to determine the lateral displacement of the retaining structure and settlement behind it and analyze the effect of soil parameter variations on the system reliability.

The target reliability index (β) has been established according to the monitoring results and data in literature for service limit state. The system has been investigated as a whole for the reliability analyses.

Based on the FE and reliability analyses we can say that settlement criteria is more effective on the system reliability with increasing depth of excavation, for retaining systems built in stiff-hard soil conditions. This is because, the horizontal displacement criteria gets larger as the excavation gets deeper. Thus, the horizontal displacement values in stiff-hard soil layers does not reach the limit values.

Additionally, the results showed that the reliability of a retaining system decreases where the COV increases, depending on the increase in uncertainties, insufficient soil explorations, lack of knowledge or heterogeneous structure of the soil profile. We can say that the larger the coefficient of variation becomes, the higher the porbability of failure of the system is.

The analysis performed in two different soil types showed that the same retaining system has higher reliability in stiff soil conditions than soft soil conditions.

This study is an important step to extend the reliability based design methodology to deep excavations in multi layered soil profile, with strutted retaining systems. This task was accomplished by examining lateral displacement and settlement behind the retaining system depending on soil parameter variations, in terms of serviceability limit state, by using point estimate method for parameter variations. In classical factor of safety (FOS) calculations it is easier to design the system with a given FOS in the literature, with ϕ/c reduction, based on failure limit state calculations. On the other hand, a system can be called as non-serviceable before it reaches its failure limit state, before it collapses. However, especially for systems neighboring buildings, underground facilities, tunnels, etc., the system should be examined for its service limit state. Therefore, a performance based design should be performed.

It requires a lot of analysis to determine the reliability index of a system and not as easy as the determination of FOS. In this research, we proved that the number of analyses for determination of reliability index can be reduced also for multi-layered soil profiles, by using PEM. We also proved that such retaining systems next to existing structures, should be designed with reliability based design, performance based design, since it gives more accurate information about the safety and reliability of the system.

In this research we examined the critical excavation phases against reliability. For researches in the future, all excavation and construction stages may be examined. Also, additonal limit state functions, such as water pressure, vertical loads on retaingn system, might be added to fault tree. Different type of existing structures (tunnels, transmission line structures, etc.) might be modeled, retaining structure’s elements or type of random soil parameters can be changed in constant soil profile.

REFERENCES

Akbaş, S.O. (2007). *Deterministic and Probabilistic Assessment of Settlements of Shallow Foundations in Cohesionless Soils*, (PhD Thesis), Faculty of the Graduate School of Cornell University, NY, USA.

Akbaş, S.O. (2008). Characterization of geotechnical variability for Ankara clay, *Proc.*, 8th International Congress on Advances in Civil Engineering, Famagusta, North Cyprus.

Australian Geomechanics Society. (2000). *Landslide Risk Management Concepts and Guidelines*, Australia.

Baecher, G.B. and Christian, J.T. (2003). *Reliability and Statistics in Geotechnical Engineering*, John Wiley & Sons, New York.

Bourdeau, P.L. and Amundaray, J.I. (2006). Non-parametric simulation of geotechnical variability, *Risk and Variability in Geotechnical Engineering*, In M.A. Hicks (Ed.), ICE, 33-46.

Boscardin, M.D. and Cording, E.J. (1989). Building Response to Excavation-Induced Settlement, *Journal of Geotechnical Engineering*, ASCE, January 1989, Vol. **115**, no.1, pp.1-21.

Bowles, J.E. (1997). *Foundation Analysis and Design* (5th Ed.), McGraw-Hill, Singapore.

Brinkgreve, R.B.J., Broere, W. and Waterman, D. (2009). Plaxis 2D V9, *Tutorial Manual and Material Models Manual*, Plaxis bv.

BS:8002-1994. (1994). Code of Practice for Earth Retaining Structures, *British Standard Institute*, UK.

Coduto, D. P., (2001). *Foundation Design: Principles and Practices* (2nd Ed.), Prentice Hall, USA.

Chen, S., Nikolaidis, E. and Cudney, H.H., (1999) Comparison of probabilistic and fuzzy set methods for designing under uncertainty, **AIAA-99-1579**, American Institute of Aeronautics and Astronautics.

Chen, L, Gu, X. and Long, X. (2009). Safety Assessment of Excavation with Fault Tree Analysis, *Georisk*, Vol. **3**, Issue 3, pp. 126-133.

Clough, G.W. and O'Rourke, T.D. (1990). Construction Induced Movements of In-Situ Walls, *Geotechnical Special Publications, no. 25*, p. 439-470, ASCE.

Clough, G.W., Smith E.M., and Sweeney, B.P. (1989). Movement Control of Excavation Support Systems by Iterative Design, *Proceedings*, Congress on Foundation Engineering, Issue. 11, 869-884, ASCE.

Clouterre. (1991). *FHWA Reccommendations Clouterre 1991*, Federal Highway Administration.

Criswell, M.E. and Vanderbilt, M. (1987). Reliability-Based Design of Transmission Line Structures: Methods, **Report EL-4793(1)**, Electric Power Research Institute, Palo Alto.

Das, M.B. (1995). *Principles of Foundation Engineering*, New York: PWS Publishing Company.

El-Ramly, H., Morgenstern, N.R., and Cruden, D.M. (2006). Lodalen slide: a probabilistic assessment, *Canadian Geotechnical Journal*, **43**, 956-968.

ENAR Eng. Arch. Cons. (2009a). *MMK-Atakas, Dortyol Steel Plant Hot Mill Scale Pit, Calculation Report for Retaining Structure, Rev.1*, MMK-Atakaş inner report, (Turkish).

ENAR Eng. Arch. Cons. (2009b). *MMK-Atakas, Dortyol Steel Plant Hot Mill Scale Pit, Retaining Structure Drawings*, enar-atkdy-geo-st-p01_p02-rev5.

ENAR Eng. Arch. Cons. (2009c). *MMK-Atakas, Dortyol Steel Plant Hot Mill Scale Pit, Retaining Structure Drawings*, enar-atkdy-geo-st-p04.

ENAR Eng. Arch. Cons. (2009d). *MMK-Atakas, Dortyol Steel Plant Hot Mill Scale Pit, Evaluation Report for Structural Elements and Retaining System*, MMK-Atakaş inner report, (Turkish).

Fenton, G. A. and Griffiths, D. V. (2002). Probabilistic Foundation Settlement on a Spatially Random Soil, **128** (5), p. 381–390, ASCE.

Fenton, G.A. and Griffiths, D.V. (2008). *Risk Assessment in Geotechnical Engineering*, John Wiley & Sons., USA.

Ferris, G., Samchek, A. and Isherwood, A. (2003). *Geotechnical Risk Assessment: Estimating Slope Failure Probability*, BGC Engineering Publications, Calgary, Canada.

FHWA-HI-97-021 (1997). *Training Course in Geotechnical and Foundation Engineering: NHI Course No. 13231 – Module 1; Subsurface Investigations*, Federal Highway Administration.

FHWA-IF-99-015 (1999). *Geotechnical Engineering Circular No.4, Ground Anchors and Anchored Systems*, Federal Highway Administration.

Finno, R.J. and Roboski, J.F., (2005). Three Dimensional Responses of a Tied-Back Excavation through Clay, *J. Geotechnical and Geoenvironmental Engineering. Mech.*, **131**, 3, pp.273-282.

Finno, R.J., Voss Jr., F.T., Rossow, E. and Blackburn, J.T. (2005). Evaluating Damage Potential in Buildings Affected by Excavations, *J. Geotechnical and Geoenvironmental Engineering. Mech.*, **131**, 10, pp.1199-1210.

Goh, A.T.C. and Kulhawy, F.H. (2005). Reliability Assessment of Serviceability Performance of Braced Retaining Walls Using A Neural Network Approach, *International Journal For Numerical And Analytical Methods In Geomechanics*, **29**, pp.627–642.

Goldsworthy, J.S., Jaksa, M.B., Fenton, G.A., Kaggwa, W.S., Griffiths, V. and Poulos, H.G. (2007). Effect of Sample Location on the Reliability based Design of Pad Foundations, *Georisk*, Vol. **1**, Issue 3, 155-166.

Haldar, A. and Mahadevan, S. (2006). *Reliability Assessment Using Stochastic Finite Element Analysis*, John Wiley&Sons, USA.

Hashash, Y.M.A., Osouli, A. and Marulanda, C. (2008). Central Artery / Tunnel Project Excavation Induced Ground Deformations, *J. Geotech. And Geoenv. Eng.*, **134**:9, 1399-1406, ASCE.

Horelli, J.A. (2005). *Landslides in Hong Kong*, (Master Thesis), University of Helsinki.

Hick, M.A. (2006). *Risk and Variability in Geotechnical Engineering*, ICE, Thomas Telford.

Il'ichev, V.A., Konovalov, P.A. and Nikiforova, N.S. (2001). Effect of Construction of Deep Seated Structures on Existing Historic Buildings in Moscow, *Soil Mech. and Foundation Eng.*, Vol. **38**, no.4, pp.130-136.

Il'ichev, V.A., Nikiforova, N.S. and Koreneva, E.B. (2004). Prediction of Deformations of Buildings Situated Near Pits Opened in Cramped Urban Settings within Moscow, *Soil Mech. and Foundation Eng.*, Vol. **41**, no.4, pp.133-137.

Il'ichev, V.A., Nikiforova, N.S. and Koreneva, E.B. (2006). Method for Calculating Bed Deformations of Buildings Near Deep Excavations, *Soil Mech. and Foundation Eng.*, Vol. **43**, no.6, pp.189-196.

Institute for Research in Construction. (1995). *National Building Code of Canada*, National Research Council of Canada, Ottawa, (as cited in Akbaş, 2007).

Kiureghian, A.D., and Liu, P. (1986). Structural reliability under incomplete probability information, *J. Engrg. Mech.*, Vol. **112**, Issue 1, pp.85-104, ASCE.

Kulhawy, F.H., and Mayne, P.W. (1990). Manual on Estimating Soil Properties for Foundation Design, **Report EL-6800**, Electric Power Research Institute, Palo Alto, 308 p.

Kulhawy, F.H., Trautmann, C.H., Beech, J.F., O'Rourke, T.D. and McGuire, W. (1983). Transmission Line Structure Foundations for Uplift-Compression Loading, **Report EL-2780**, Electric Power Research Institute, Palo Alto, 412 p.

Lacasse, S. and Nadim, F. (2007). Probabilistic Geotechnical Analyses for Offshore Facilities, *Georisk*, March, Vol. **1**, Issue 1, pp.21-42.

Lambe, T.W. and Whitman, R.V. (1996). *Soil Mechanics*, John Wiley & Sons, USA.

Liao, S.S.C., Druss, D.L., Neff, T.L. and Brenner, B.R. (1996). Just One More Boring, And We'll Know for Sure, Proc., Uncertainty in the Geologic Environment: From Theory to Practice, Uncertainty '96, *Geotechnical Special Publication No.58*, Vol.**1**, 119-133.

Liu, G.B., Ng, C.W.W. and Wang, Z.W. (2005). Observed Performance of Deep Multistrutted Excavation in Shanghai Soft Clays, *Journal of Geot. and Geoenv. Eng.*, **131**:8, pp. 1004-1013.

MacCrimmon, R.A., Acres International Limited (2005). *Crane-Supporting Steel Structures Design Guide*, Canadian Institute of Steel Construction, Ontario.

Mana, A.I. and Clough, G.W. (1981). Prediction of Movements for Braced Cuts in Clay, *Journal of Geotechnical Devision*, **107**(6), 759-777, ASCE.

Meyerhof, G.G. (1994). Evolution of Safety Factors and Geotechnical Limit State Design, *Spencer J. Buchanan Lecture*, Texas A&M University, College Station.

Modarres, M., Kaminskiy, M., and Krivtsov, V. (1999). *Reliability Engineering and Risk Analysis*, Marcel Decker.

NAVFAC DM-7.2 (1982). *Foundation and Earth Structures Design Manual 7.2*, Department of the Navy, Naval Facilities Engineering Command, USA.

Ng, C.W.W. (1999). Stress Path Relation to Deep Excavations, *Journal of Geot. and Geoenv. Eng.*, Vol. **125**, no. 5, 357-363.

O'Rourke, T. D. (1981). Ground movements caused by braced excavations, *Geotech. Engrg. Div.*, **107**(9), 1159-1178.

O'Rourke, T.D. (1989). Predicting displacements of lateral support systems, design, construction and performance of deep excavations in urban areas, *Proceedings of the 1989 Seminar*, Boston Society of Civil Engineers.

Park, J.K., Blackburn, J.T. and Gardoni, P. (2007). Reliability Assessment of Excavation Systems Considering Both Stability and Serviceability Performance, *Georisk*, Vol. **1**, Issue 3, pp.123-141.

Peck, R. (1969). Deep excavations and tunneling in soft ground, state-of-the-art report, Proc. of 7th Int. Conf. Soil Mechanics Foundation Engineering, Mexico.

Peschl, G.M., Schweiger, H.F. (2003). Reliability Analysis in Geotechnics with Finite Elements – Comparison of Probabilistic, Stochastic and Fuzzy Set Methods, ISIPTA.

Phoon, K-K., Kulhawy, F. H., & Grigoriu, M. D. (1995). Reliability-Based Design of Foundations for Transmission Line Structures, **Report TR-105000**, Electric Power Research Institute, Palo Alto, CA, 380 p.

Phoon, K.K., and Kulhawy, F.H. (2006). Characterization of Model Uncertainties for Laterally Loaded Rigid Drilled Shafts, *Risk and Variability in Geotechnical Engineering*, pp.101-110, ICE.

Phoon, K.K., and Kulhawy, F.H. (1999). Evaluation of Geotechnical Property Variability, *Canadian Geotechnical Journal*, Vol. **36**, pp.624-639.

Phoon, K.K., and Kulhawy, F.H. (1999). Characterization of Geotechnical Variability and Evaluation of Geotechnical Property Variability: Reply, *Canadian Geotechnical Journal*, Vol. **38**, pp.214-215.

Preene, M. (2000). Assessment of Settlements Caused by Groundwater Control, *Proc.*, Instn. Civil Engineers Geotechnical Engineering, **143**, 4, 177-190.

Puller, M. (2003). *Deep Excavations: A Practical Manual (2^{nd} Ed.)*, Thomas Telford, UK.

Reznik, Y. M. (1996). Minimizing Uncertainties in Geotechnical Investigations, Proc., Uncertainty in the Geologic Environment: From Theory to Practice, Uncertainty'96, *Geotechnical Special Publication No.58*, Vol. **1**, 149-166.

Riha, D.S., Thacker, B.H., Enright, M.P., Huyse, L. and Fitch, S.H.K. (2002). Recent Advances Of The Nessus® Probabilistic Analysis Software For Engineering Applications, *43rd AIAA/ASME/ASCE/AHS/ASC Structures, Structural Dynamics, and Materials Conference and Exhibit Non-Deterministic Approaches Forum April 22-25*, Denver, Colorado.

Riha, D.S., Thacker, B. H., Millwater, H.R., Wu, Y.T. and Enright, M. P. (2000). Probabilistic Engineering Analysis Using The Nessus Software, *AIAA-2000-1512***,** American Institute of Aeronautics and Astronautics.

Roboski, J. and Finno, R.J. (2006). Distribution of Ground Movements Parallel to Deep Excavations in Clay, *Canadian Geotechnical Journal*, **43**, pp.43-58.

Sağlamer, A. (1996). Arazi Deneylerinin Geoteknik Tasarımda Kullanılması, *Ord. Prof. Dr. Hamdi Peynircioğlu Conference*, İstanbul.

Salzer, H. E., Zucker, R., and Capuano, R. (1952). Table of the zeros and weight factors of the first twenty hermite polynomials, *Journal of Research of the National Bureau of Standards*, February, Vol. **48**, no.2, Research Paper 2294.

Schuster, M. and Juang, C.H. (2009). Reliability assessment of damage potential of buildings caused by excavation, Proc. 2009 International Foundation Congress and EXPO, Contemporary Topics in In-situ Testing, Analysis, and Reliability of Foundations, *Geotechnical Special Publication No.186*, 286-291.

Schweiger, H.F., Thurner, R., and Pöttler, R. (2001). Reliability Analysis in Geotechnics with Deterministic Finite Elements: Theoretical Concepts and Practical Application, *International Journal of Geomechanics*, Vol. **1**, no.1, pp.389-413.

Singh, V.P., Jain, S.K. and Tyagi, A. (2007). *Risk and Reliability Analysis*, ASCE, USA.

Southwest Research Institute (1995). Probabilistic Structural Analysis Methods (PSAM) for Select Space Propulsion System Components, *Final Report NASA Contract NAS3-24389*, NASA Lewis Research Center, Cleveland, Ohio.

Southwest Research Institute (2011). *NESSUS Theoretical Manual Version 9.6.2*, Southwest Research Institute, Texas, USA.

Southwest Research Institute (2011). *NESSUS Getting Started Manual Version 9.6.2*, Southwest Research Institute, Texas, USA.

Task Committee on Structural Loadings (J.D. Mozer, Chair) (1991). Guidelines for Electrical Transmission Line Structural Loading, *Manual and*

Report on Engineering Practice, **74**, New York.

Timoshenko, S. and Goodier, J.N. (1951). *Theory of Elasticity*, McGraw-Hill, New York.

Thorley, C.B.B. and Forth, R.A. (2002). Settlement Due to Diaphragm Wall Construction in Reclaimed Land in Hong Kong, *Journal of Geot. and Geoenv. Eng.*, **128**:6, 473-478, ASCE.

TS 500 (2000). Betonarme Yapıların Tasarım ve Yapım Kuralları, *Türk Standartları Enstitüsü*, Ankara, Turkey.

TS EN 1993-6 (2007). Eurocode 3 – Design of Steel Structures – Part 6: Crane Supporting Structures, *Türk Standartları Enstitüsü*, Ankara, Turkey.

Von Thun, J.L. (1996). Risk Assessment of Nambe Falls Dam, Proc., Uncertainty in the Geologic Environment: From Theory to Practice, Uncertainty '96, *Geotechnical Special Publication No.58*, Vol. **1**, 604-635, ASCE.

Westergaard, H.M. (1938). *A Problem of Elasticity Suggested by a Problem in Soil Mechanics: Soft Material Reinforced by Numerous Strong Horizontal Sheets*, Macmillan, New York.

Whittlestone, A.P., Johnson J.D., Rogers, M.E. and Pine, R.J. (1995). Probabilistic Risk Analysis of Slope Stability, *Transaction Institution of Mining and Metallurgy Section – Mining Industry*, **104**, A19-A24.

Wirsching, P.H., Riha, D.S., Thacker, B. H., Enright, M.P. (2008). Lecture Notes of 19th Annual Short Course on Probabilistic Analysis and Design, Southwest Research Institute, September 8-12.

Wislocki, A.P. and Bentley, S.P. (1991). An Expert System for Landslide Hazard and Risk Assessment, *Journal of Computers and Structures*, Vol. **40**, no. 1, pp.169-172.

Zhou, J. and Nowak A.S. (1988). Integration formulas to evaluate functions of random variables, *Structural Safety*, **5**, 267-284, Elsevier Science Publishers B.V., Amsterdam.

APPENDICES

APPENDIX A : Diagrams for Sensitivity Analyses with Plaxis
APPENDIX B : System Sensitivity Results for S_v=5mm Criteria
APPENDIX C : System Sensitivity Results for S_v=10mm Criteria

APPENDIX A : Diagrams for Sensitivity Analyses with Plaxis

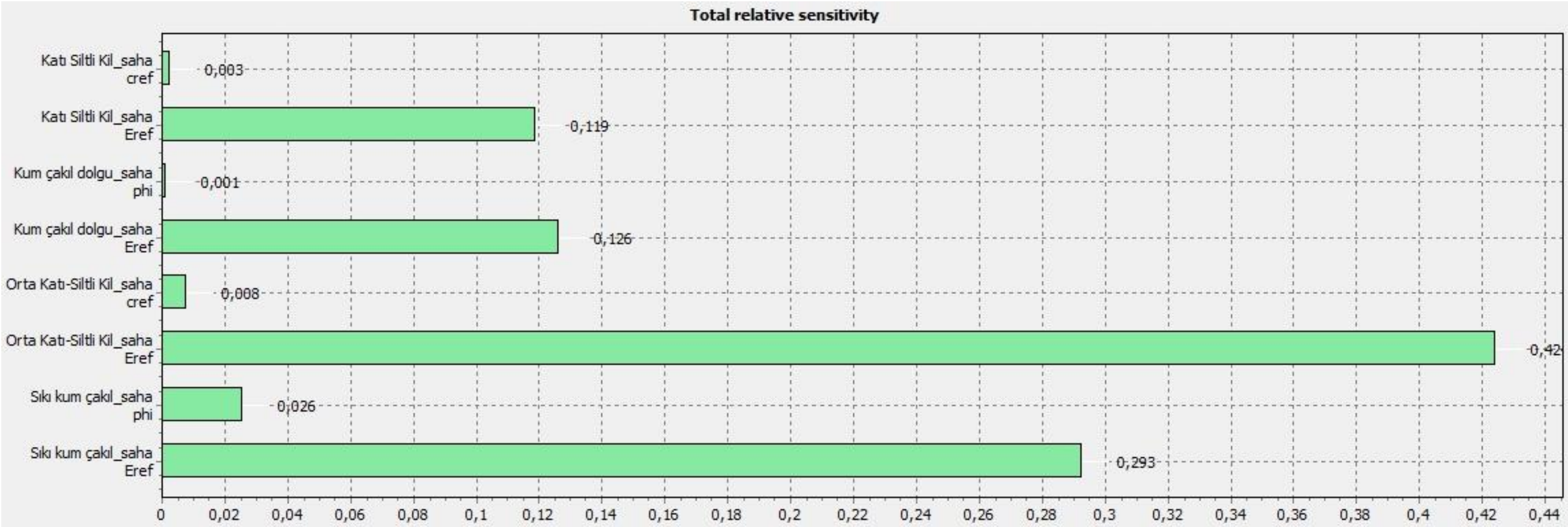

Figure A.1 : Sensitivity of parameters on the horizontal displacement at pile cap at an excavation depth of 12.80m.

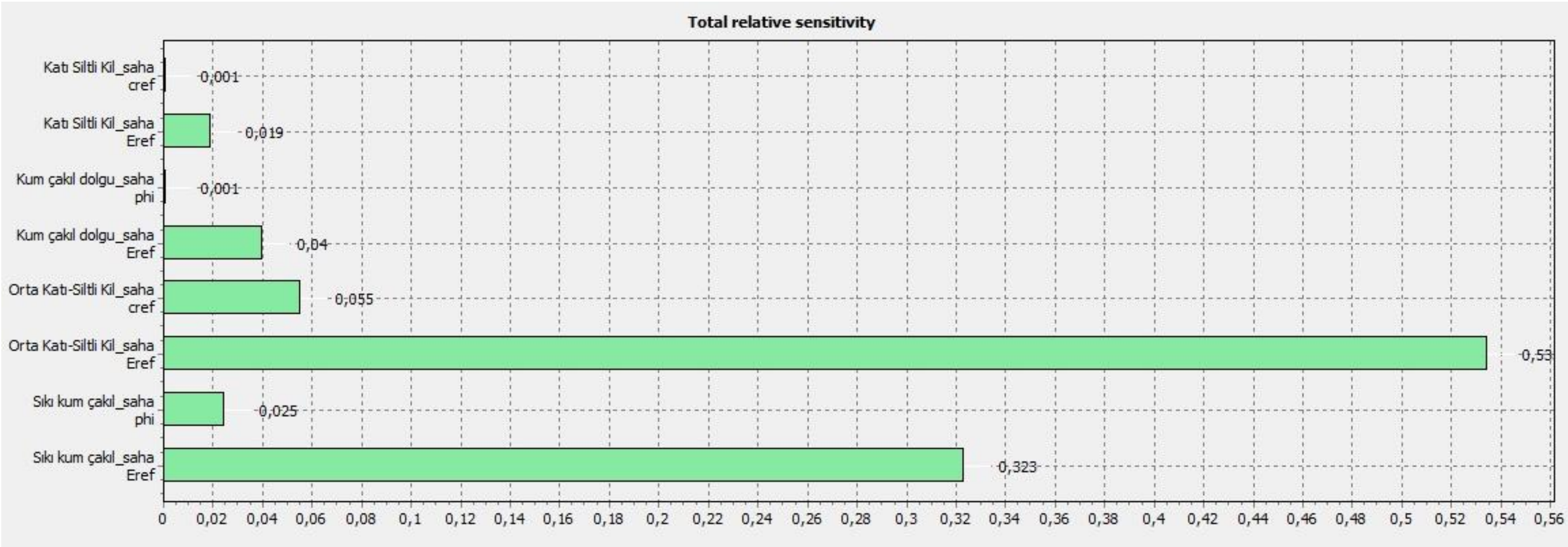

Figure A.2 : Sensitivity of parameters on the horizontal displacement between 1st and 2nd strut level at an excavation depth of 12.80m.

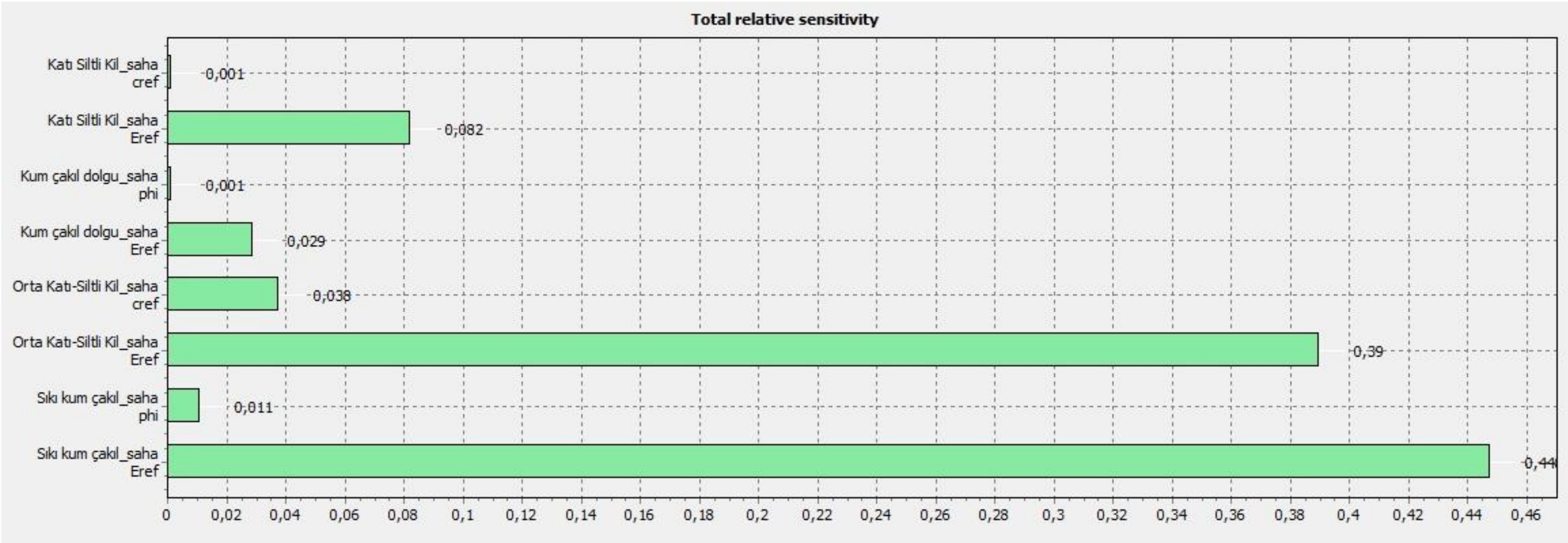

Figure A.3 : Sensitivity of parameters on the horizontal displacement between 2nd strut level and foundation at an excavation depth of 12.80m.

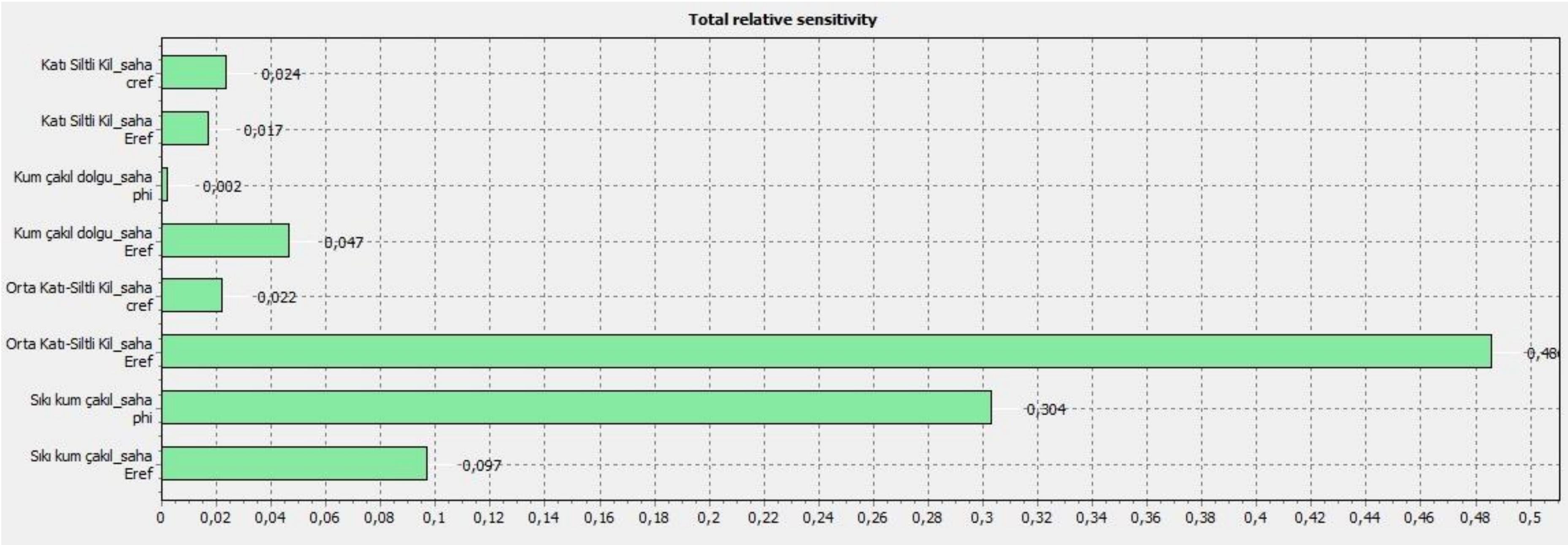

Figure A.4 : Sensitivity of parameters on the vertical displacement at 3.25m away from the excavation at an excavation depth of 12.80m.

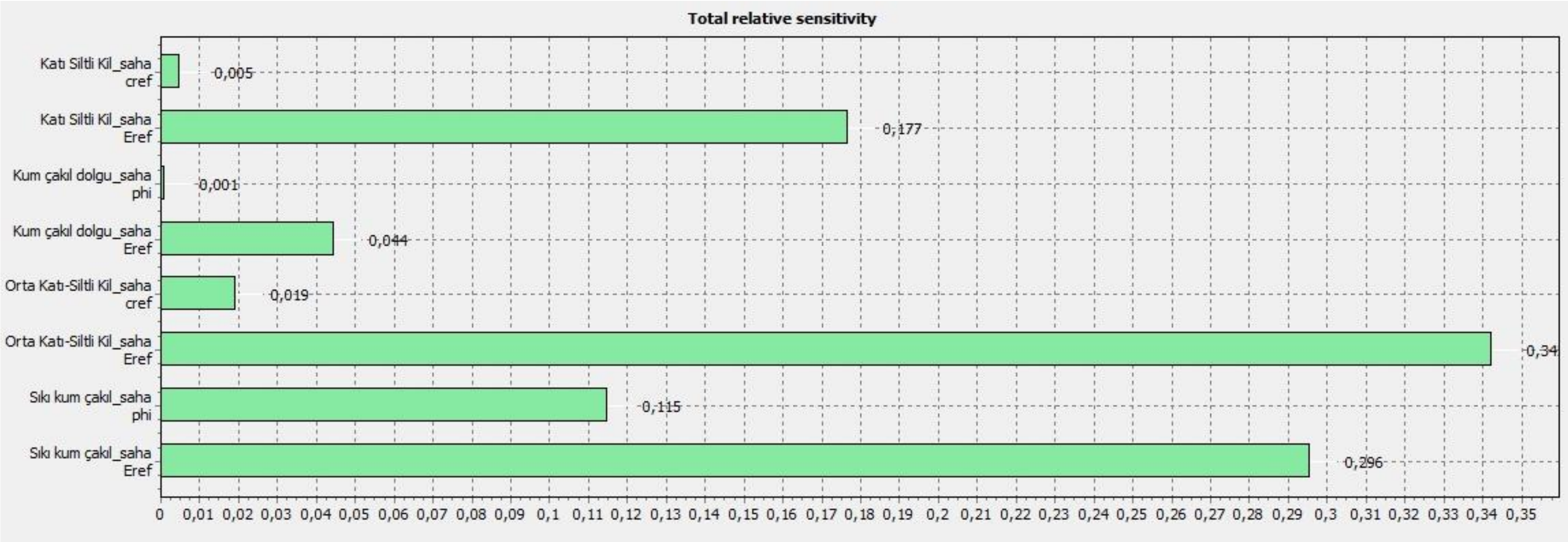

Figure A.5 : Sensitivity of parameters on the vertical displacement at 6.50m away from the excavation at an excavation depth of 12.80m.

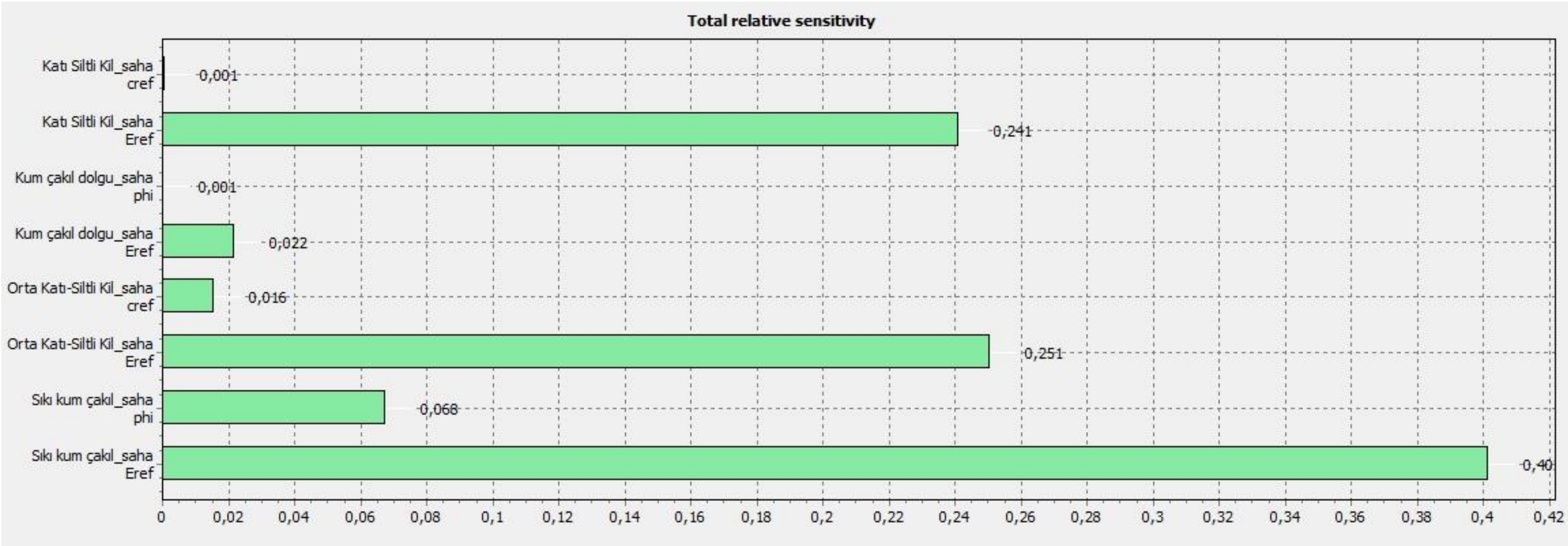

Figure A.6 : Sensitivity of parameters on the vertical displacement at 9.75m away from the excavation at an excavation depth of 12.80m.

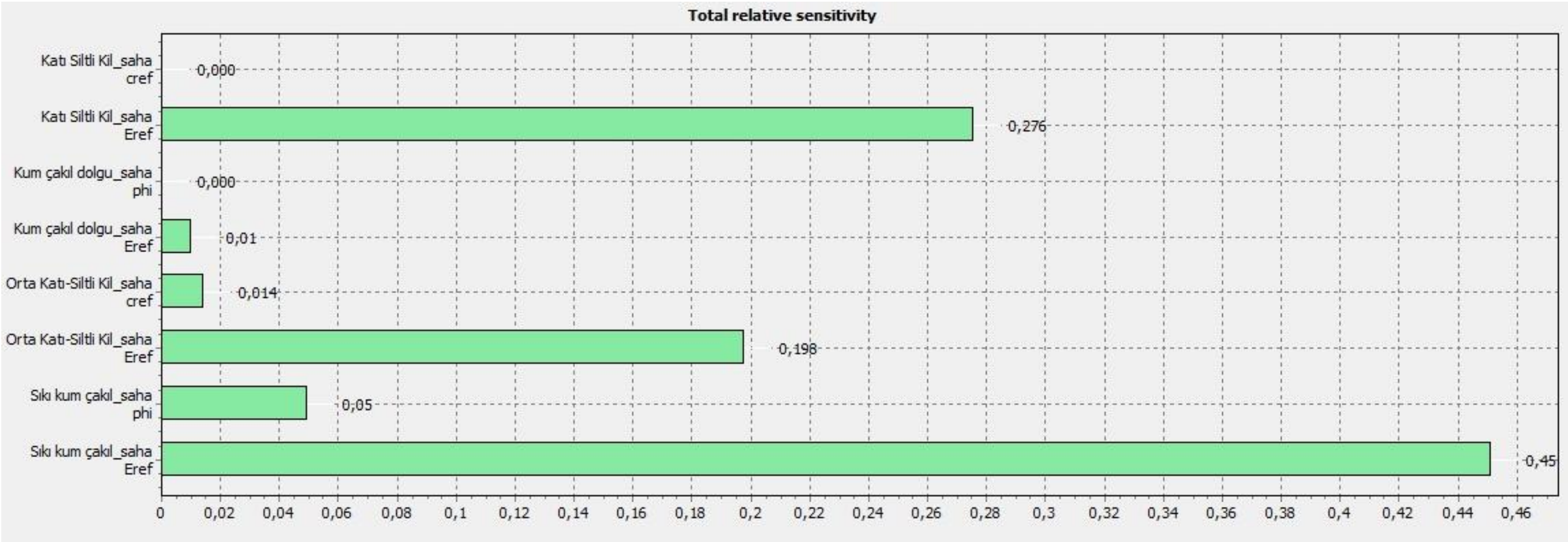

Figure A.7 : Sensitivity of parameters on the vertical displacement at 13.00m away from the excavation at an excavation depth of 12.80m.

APPENDIX B : System Sensitivity Results for S_v=5mm Criteria

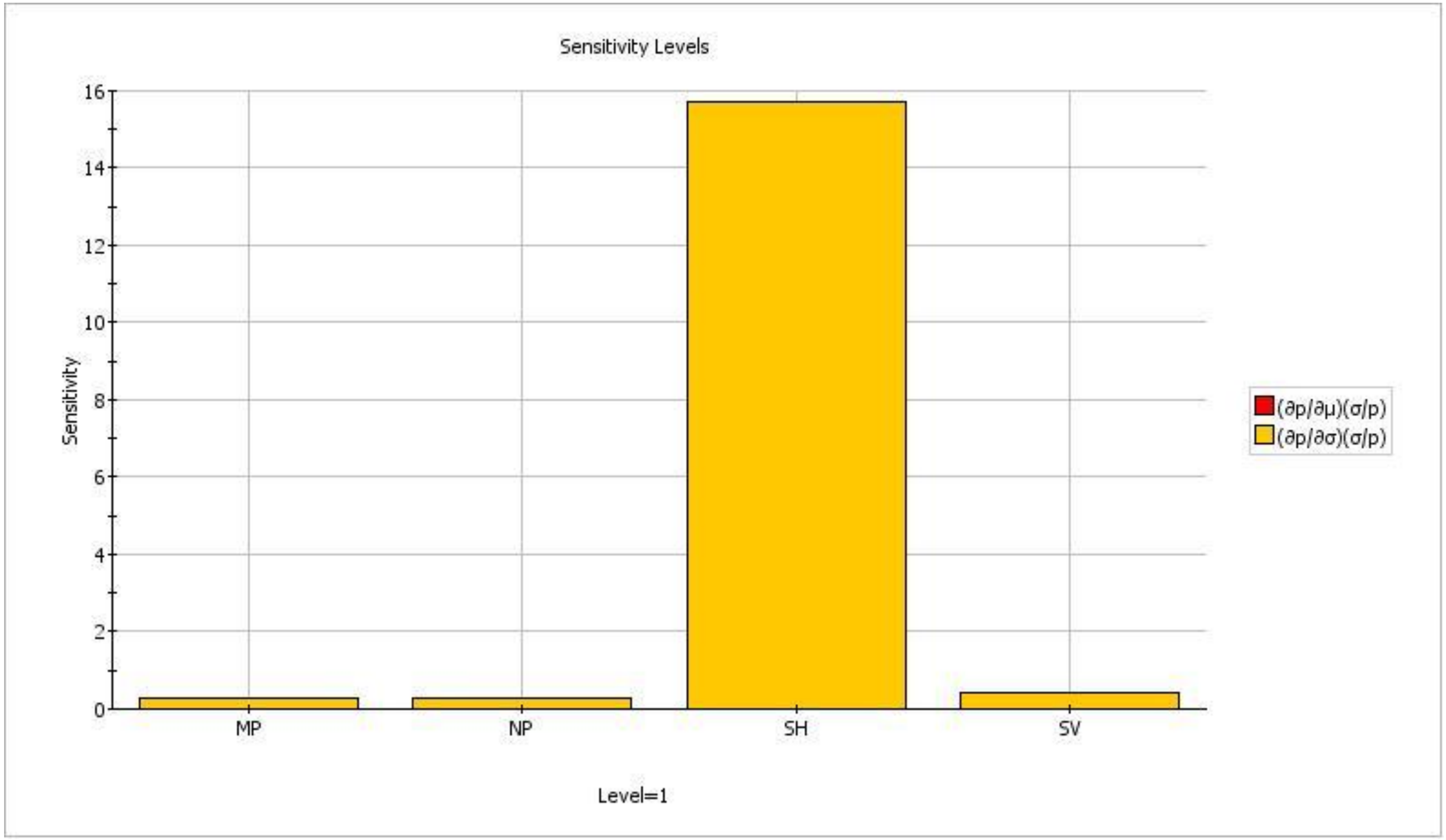

Figure B.1: System Sensitivity at Excavation Depth 3.80m with Elower

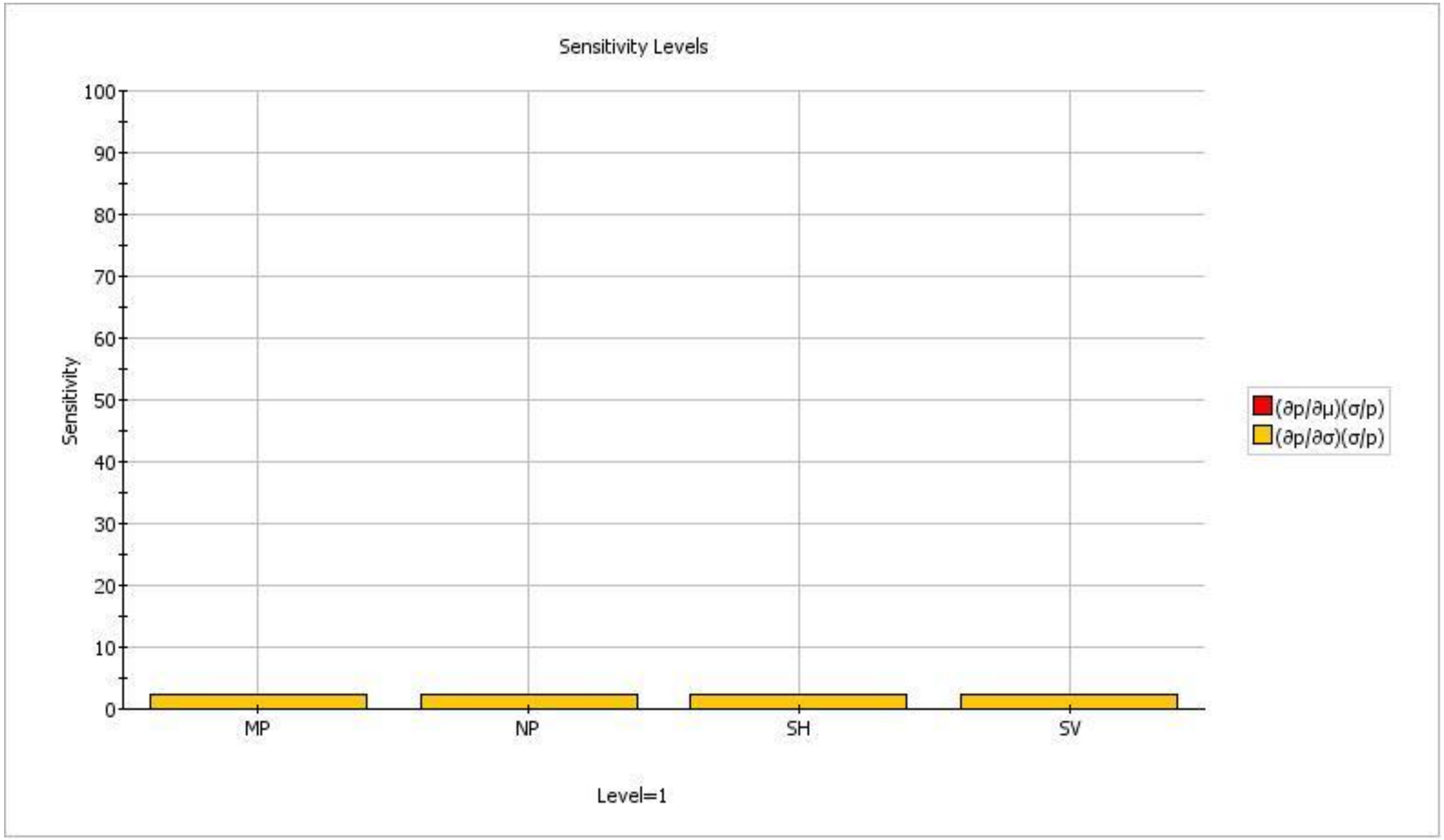

Figure B.2: System Sensitivity at Excavation Depth 3.80m with Eupper

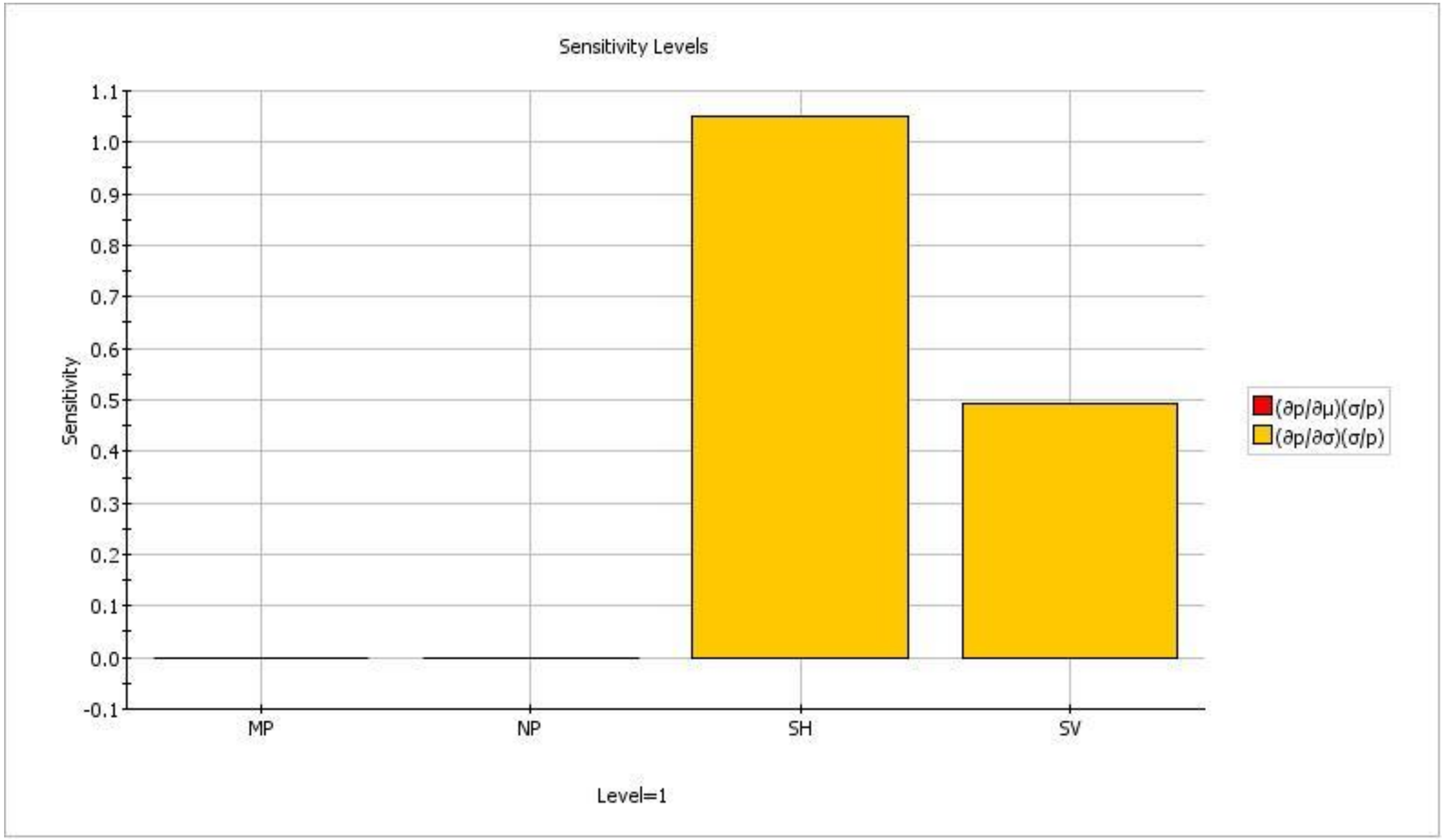

Figure B.3: System Sensitivity at Excavation Depth 3.80m with COVmax Elower

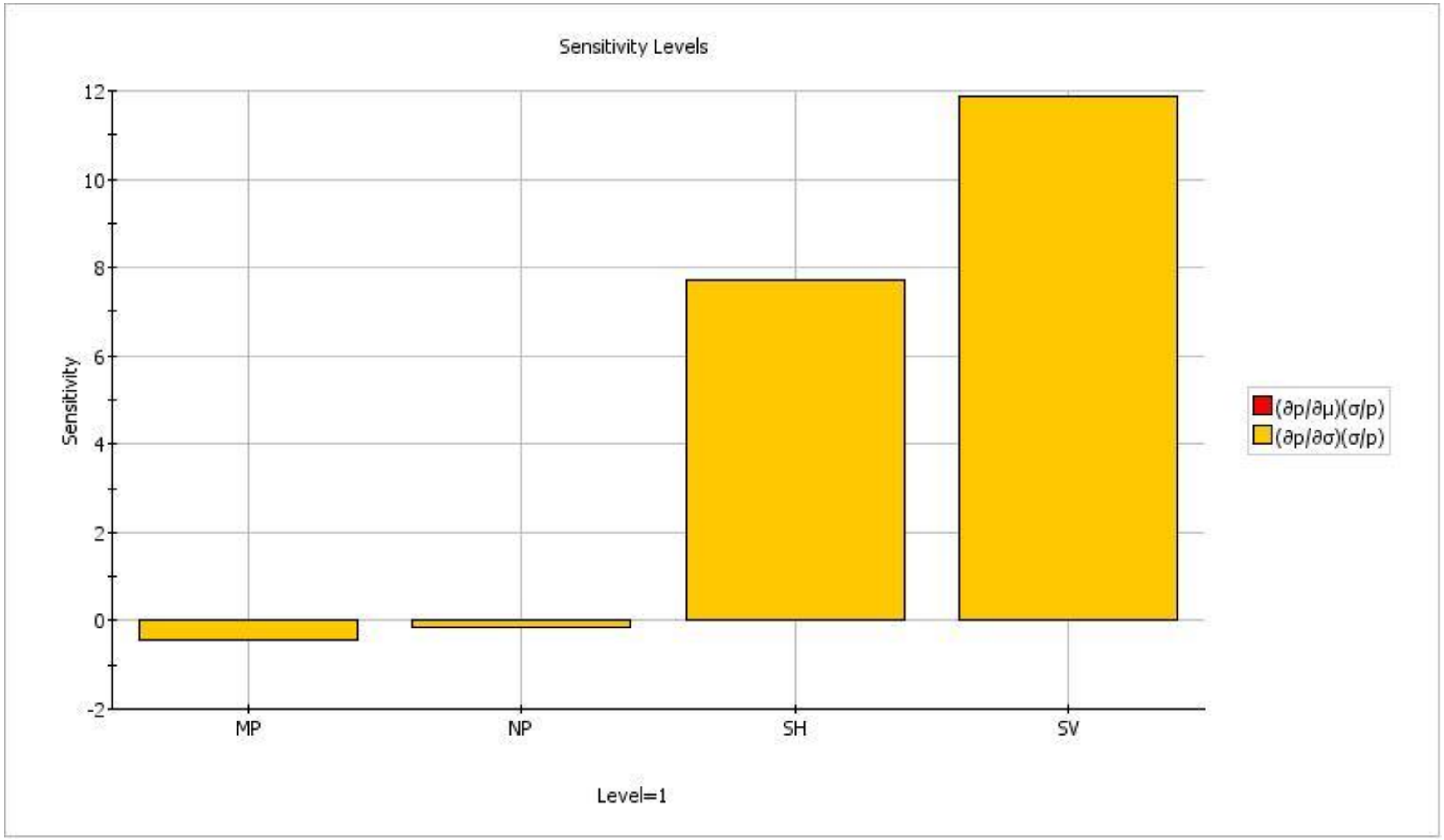

Figure B.4: System Sensitivity at Excavation Depth 3.80m with COVmax Eupper

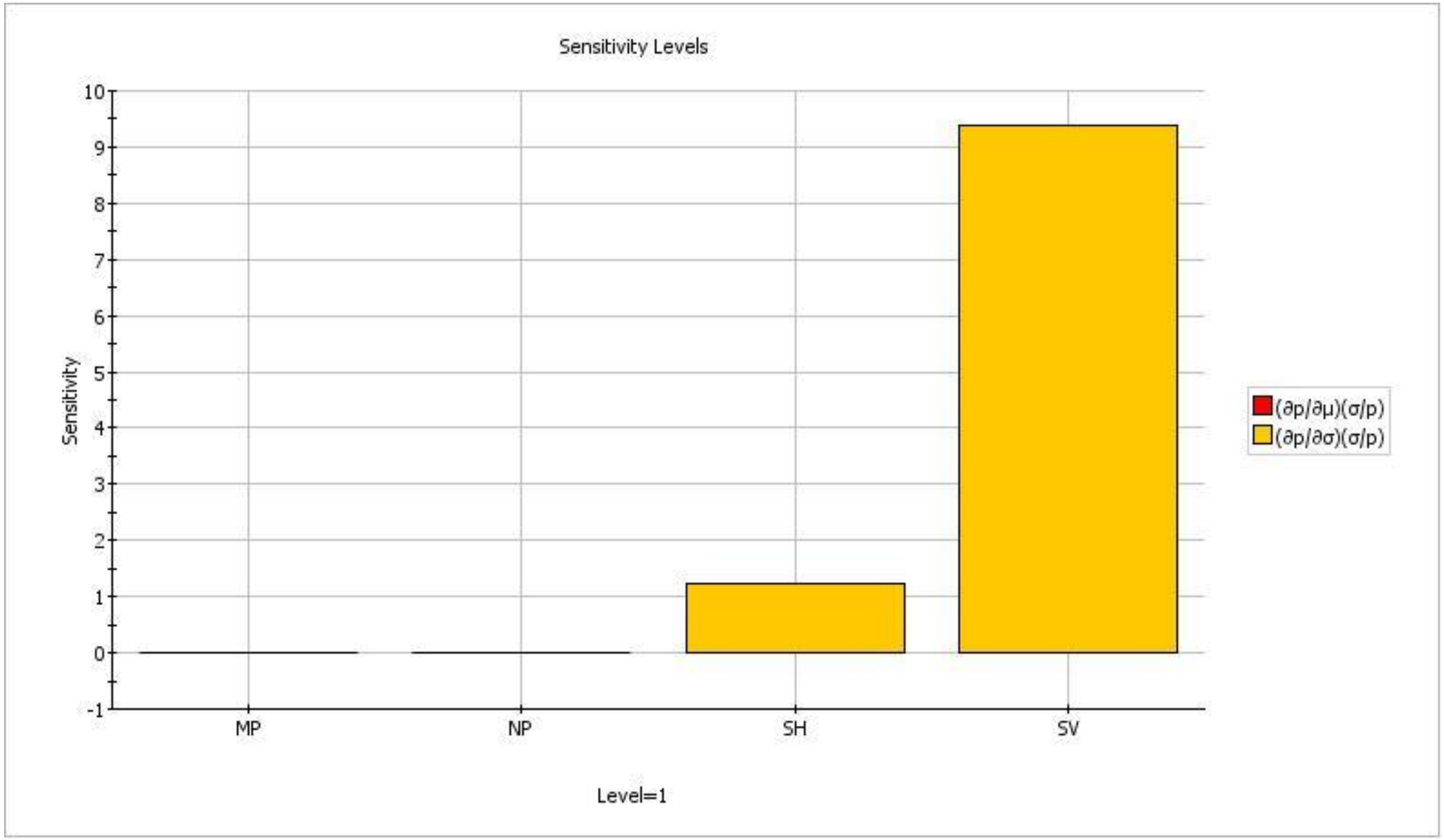

Figure B.5: System Sensitivity at Excavation Depth 7.80m with Elower

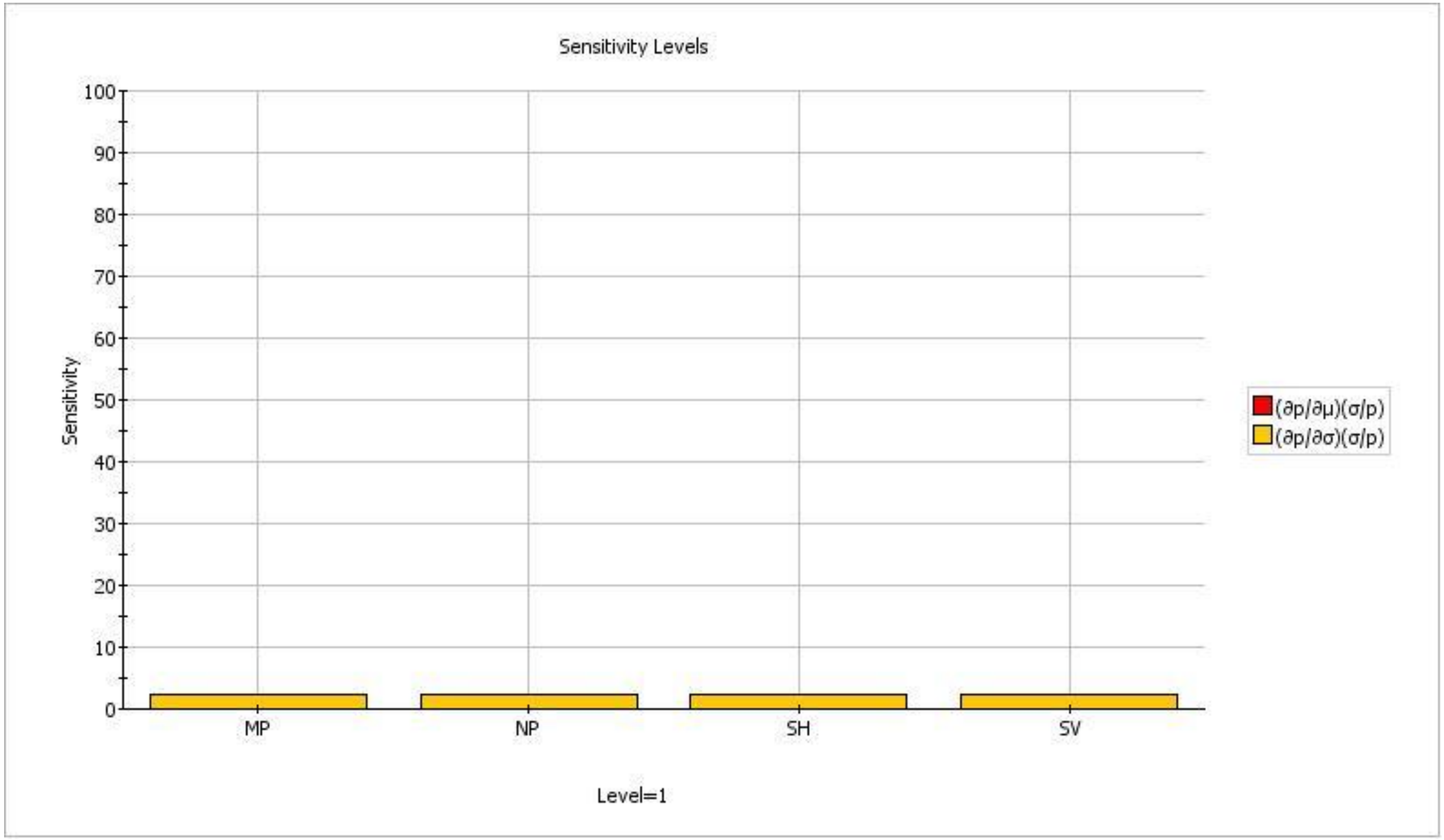

Figure B.6: System Sensitivity at Excavation Depth 7.80m with Eupper

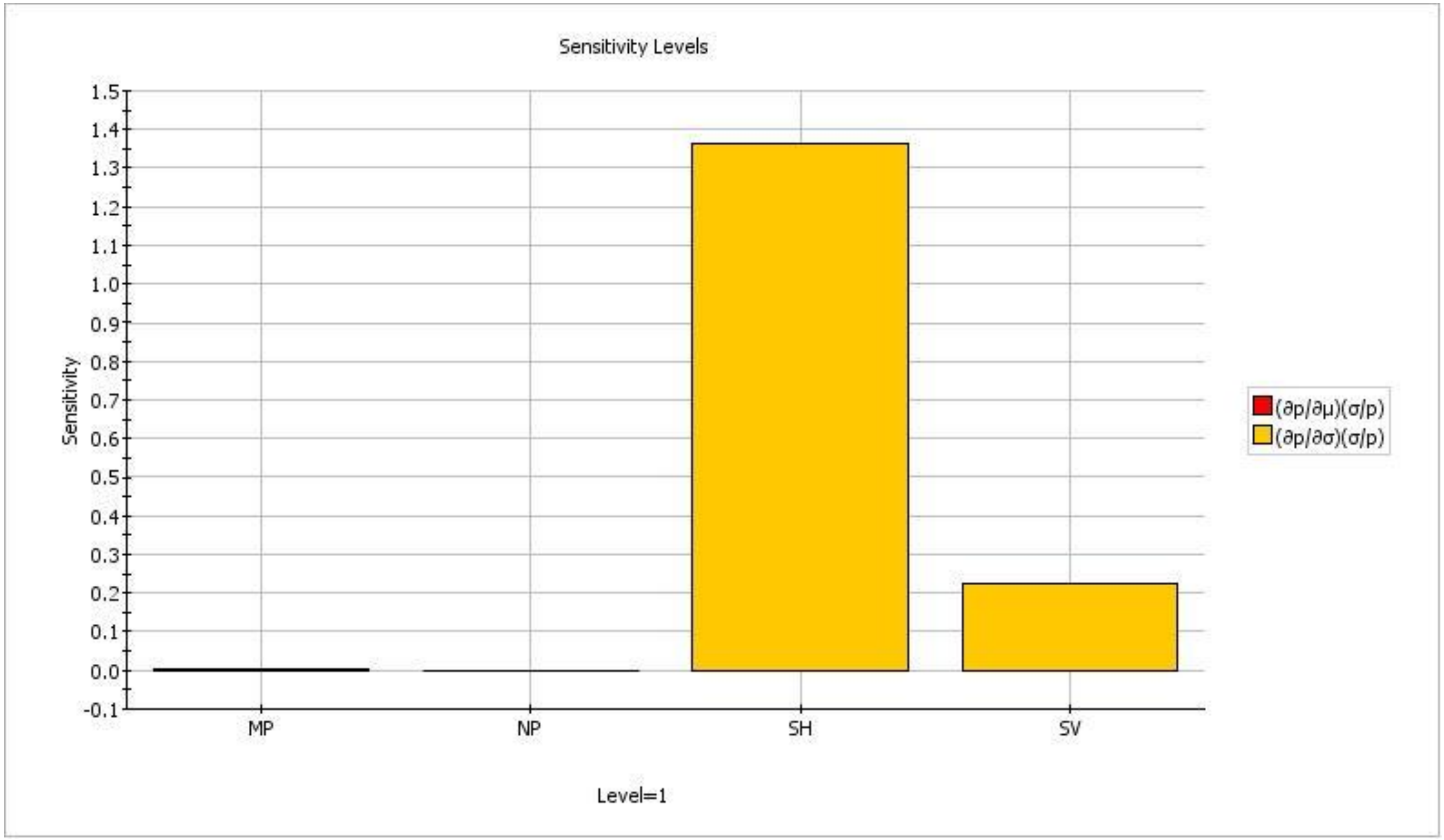

Figure B.7: System Sensitivity at Excavation Depth 7.80m with COVmax Elower

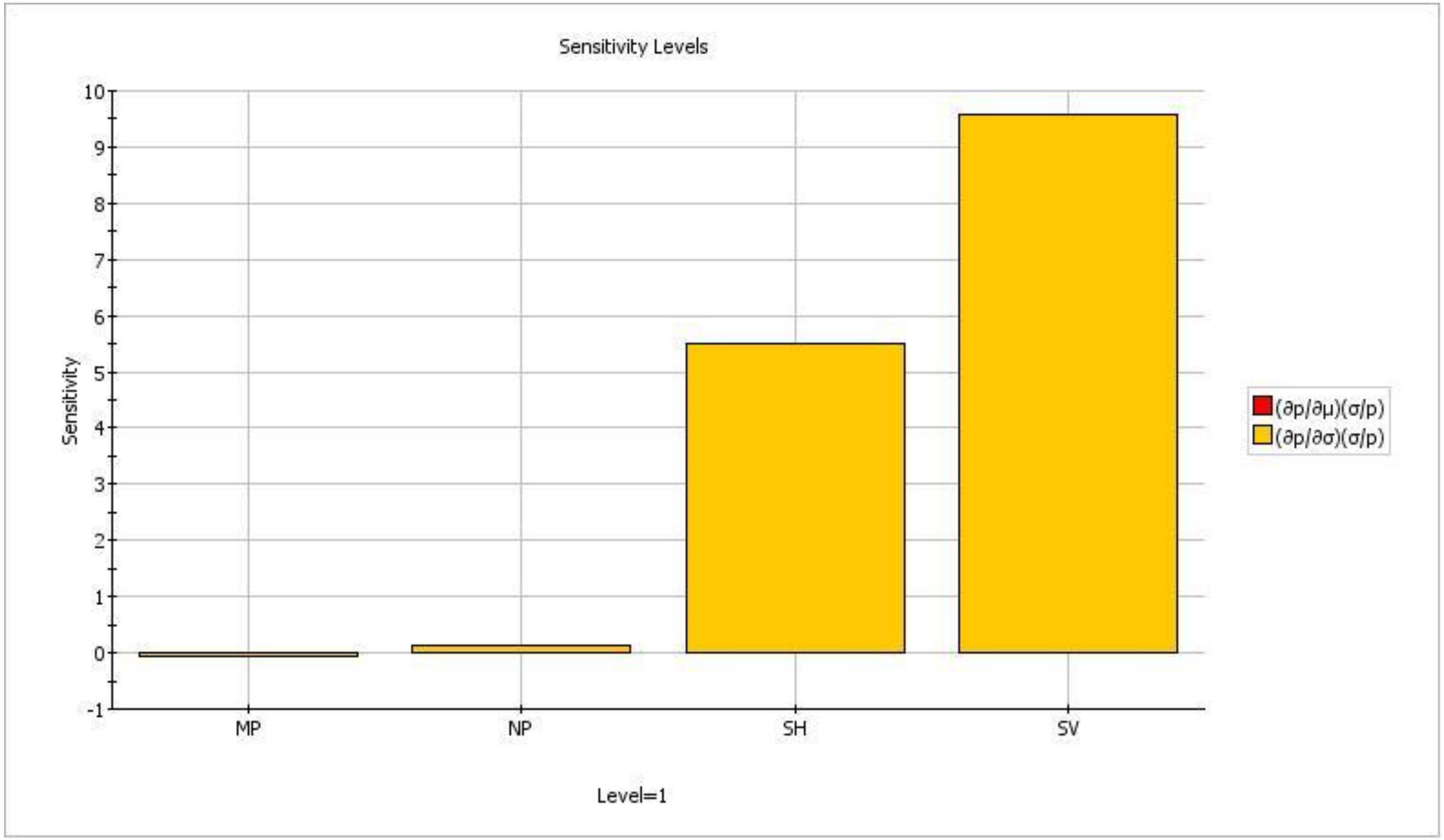

Figure B.8: System Sensitivity at Excavation Depth 7.80m with COVmax Eupper

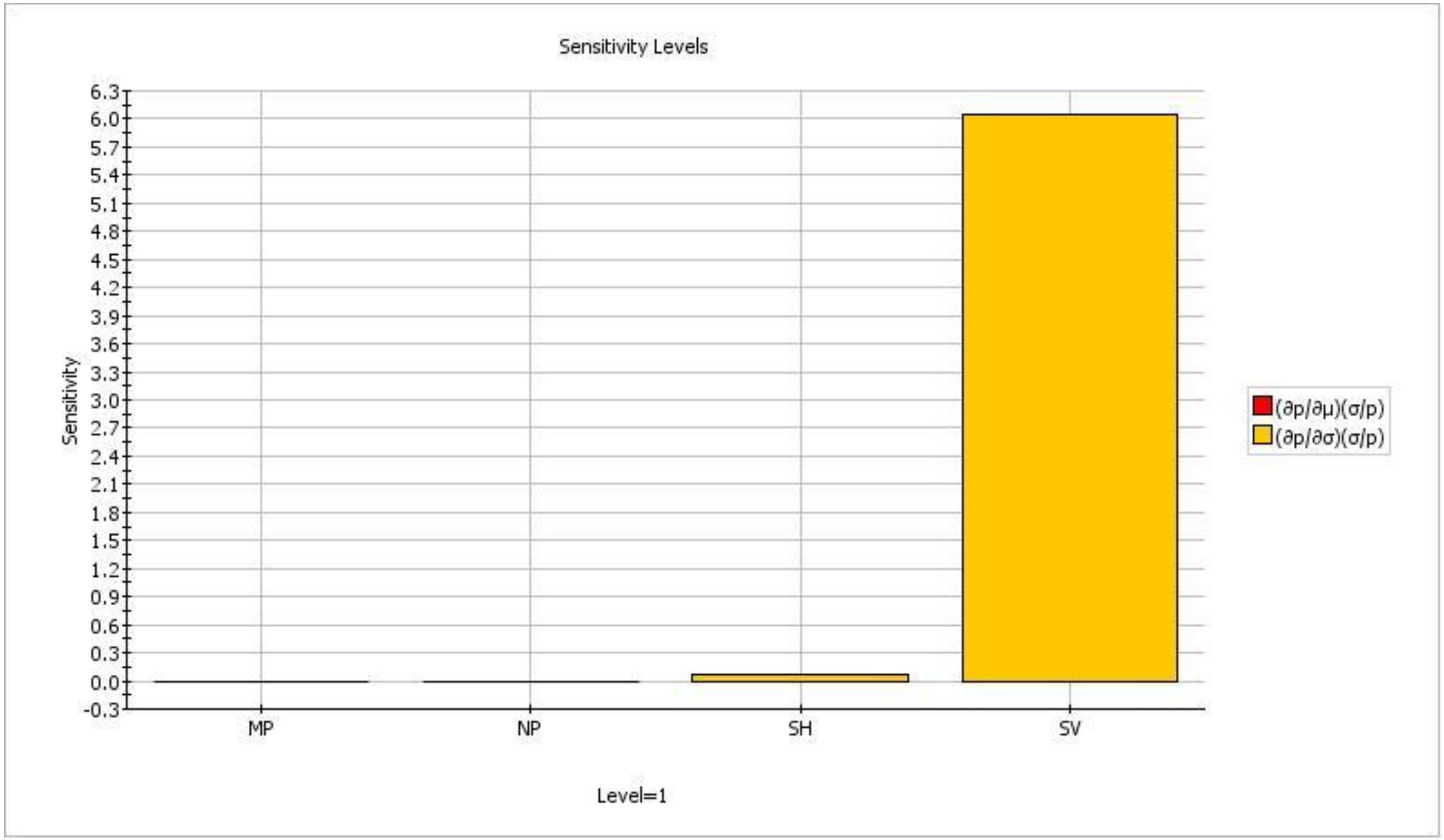

Figure B.9: System Sensitivity at Excavation Depth 12.80m with Elower

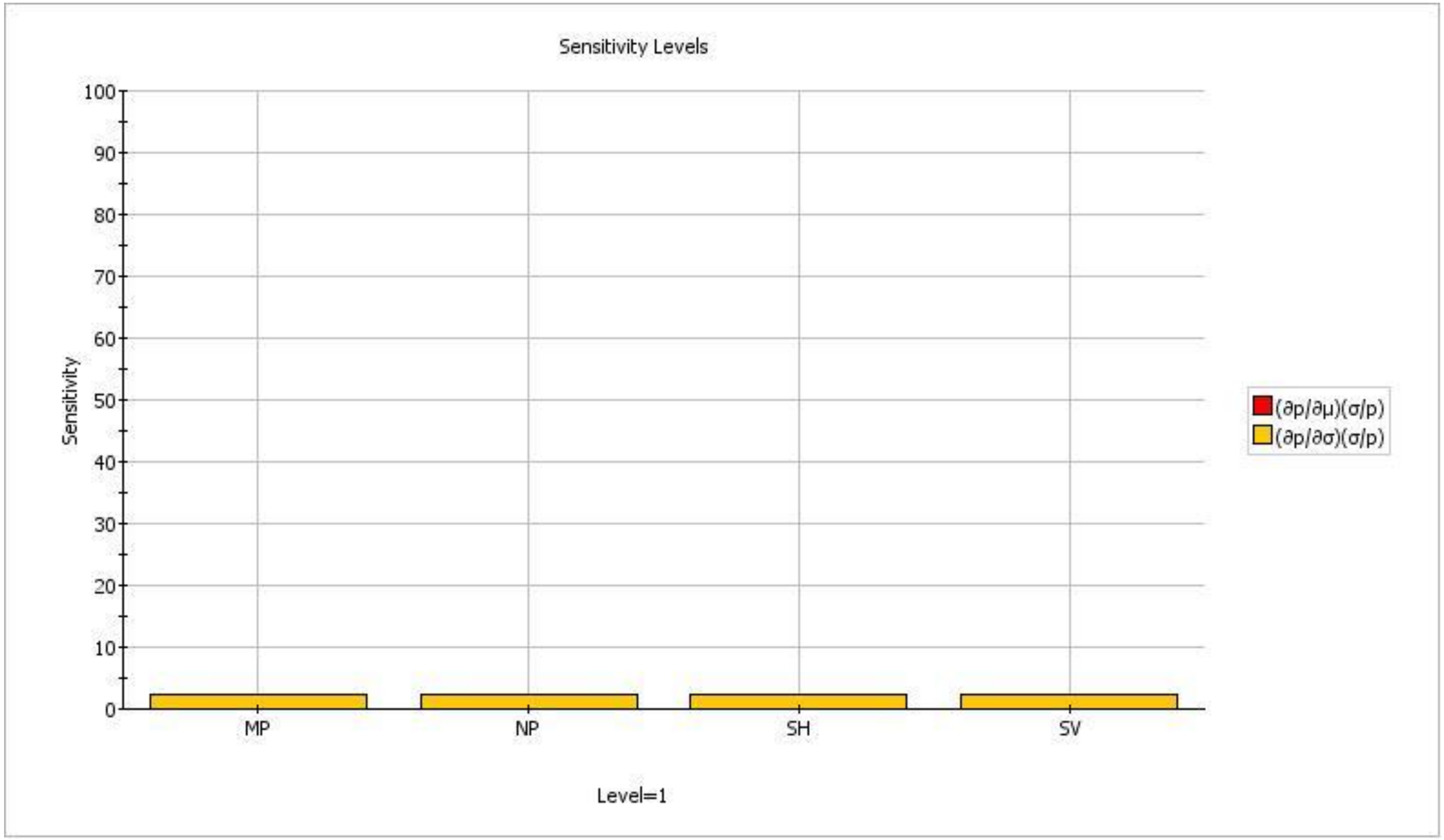

Figure B.10: System Sensitivity at Excavation Depth 12.80m with Eupper

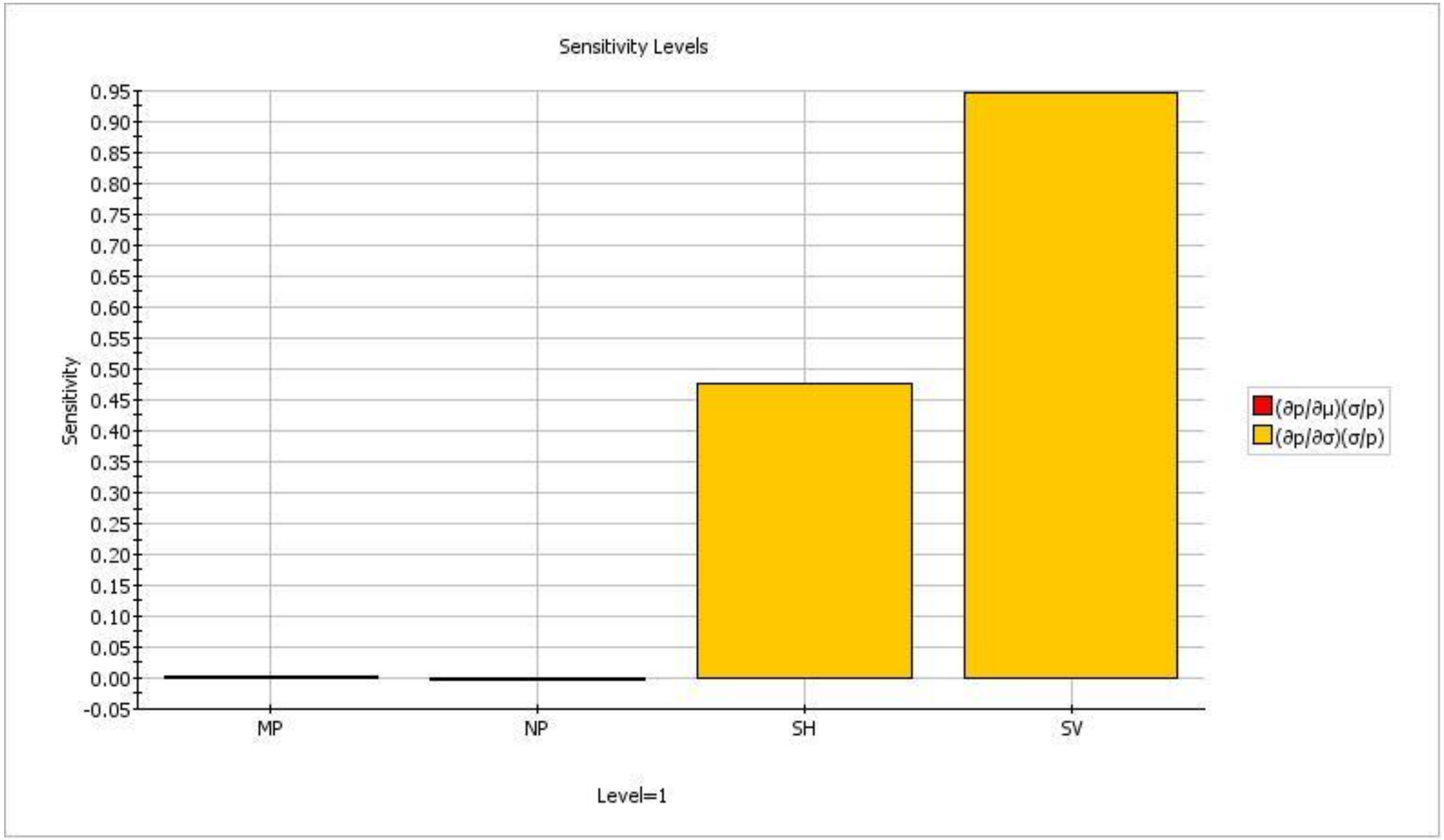

Figure B.11: System Sensitivity at Excavation Depth 12.80m with COVmax Elower

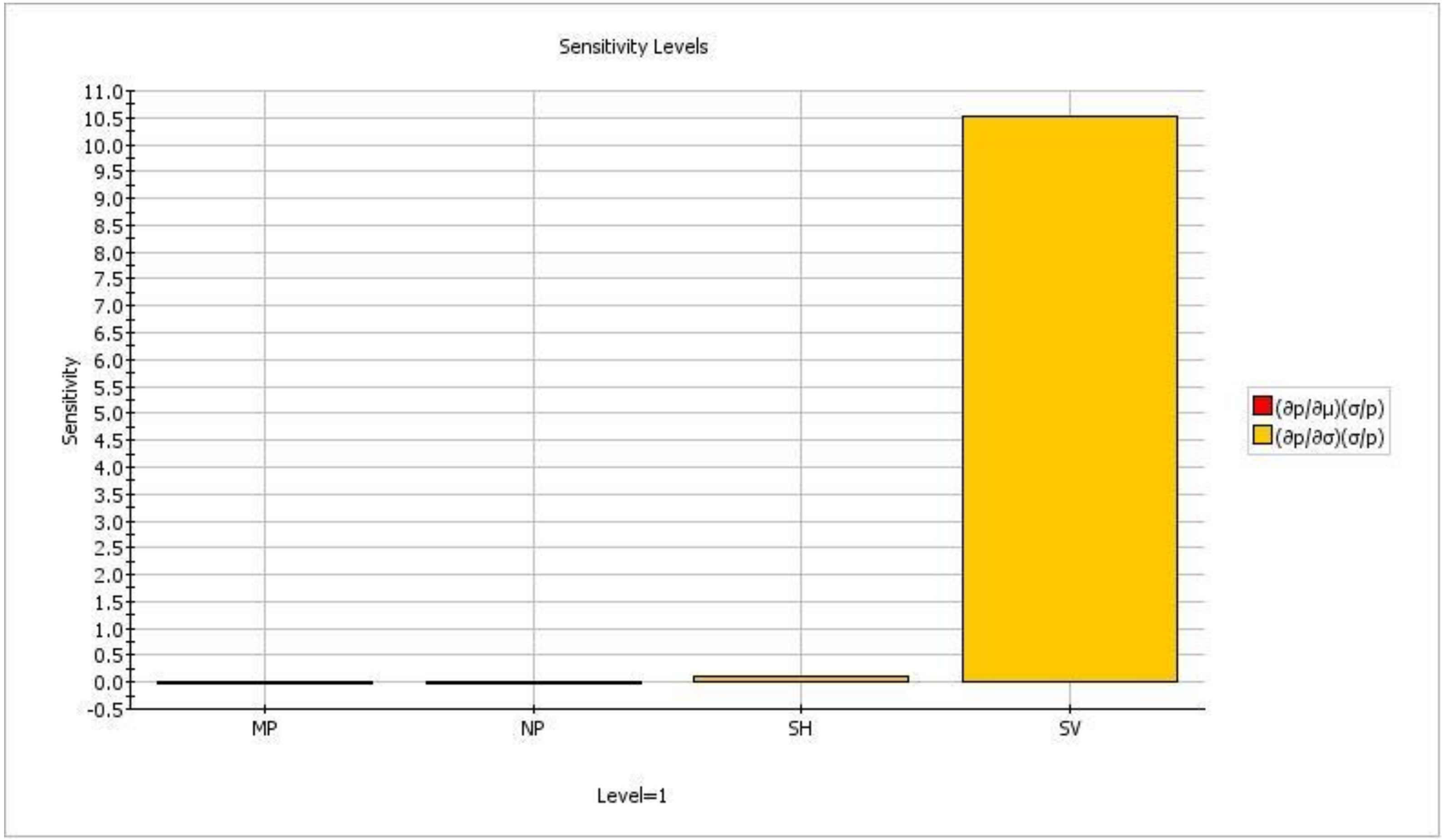

Figure B.12: System Sensitivity at Excavation Depth 12.80m with COVmax Eupper

APPENDIX C : System Sensitivity Results for S_v=10mm Criteria

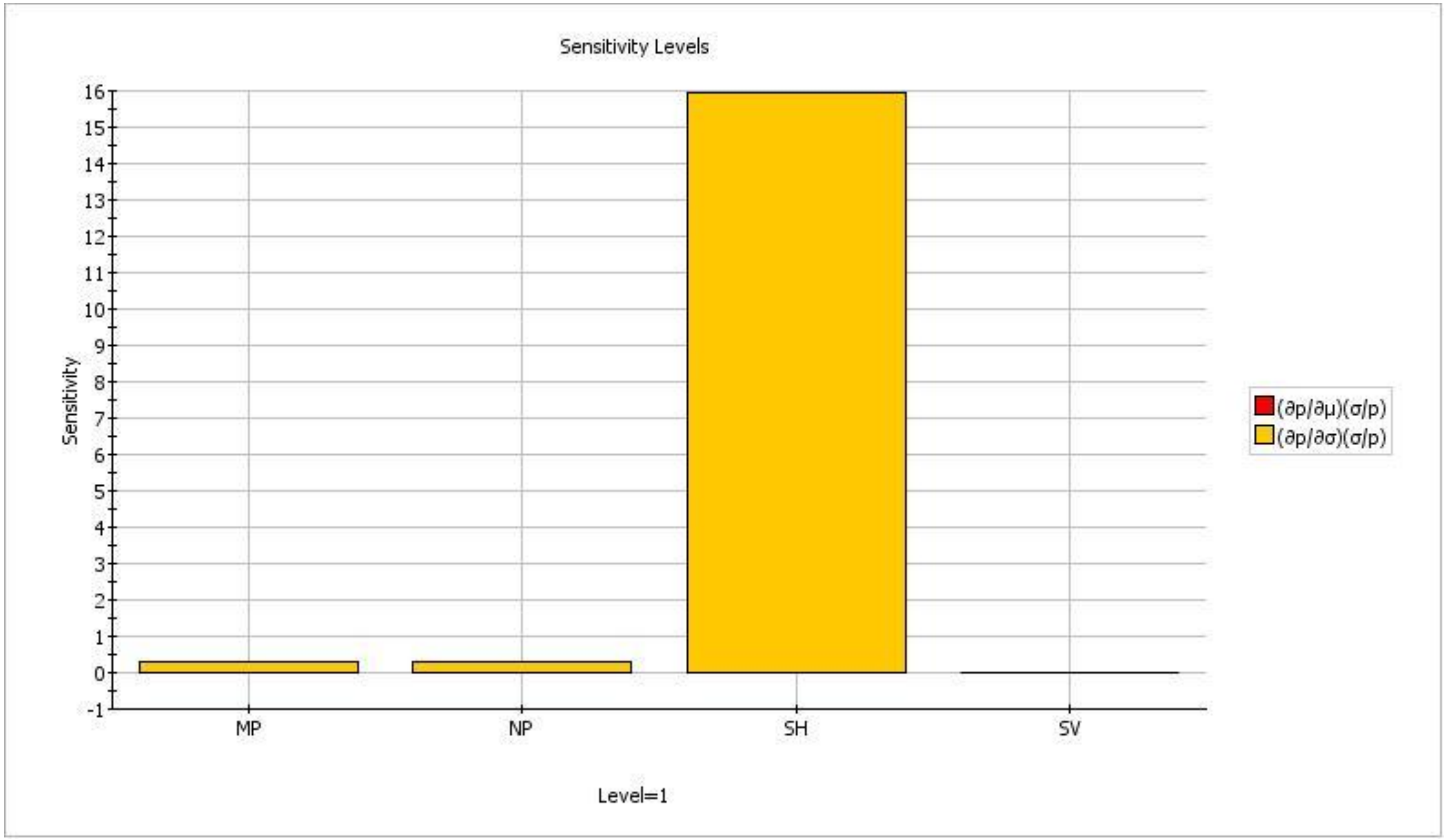

Figure C.1: System Sensitivity at Excavation Depth 3.80m with Elower

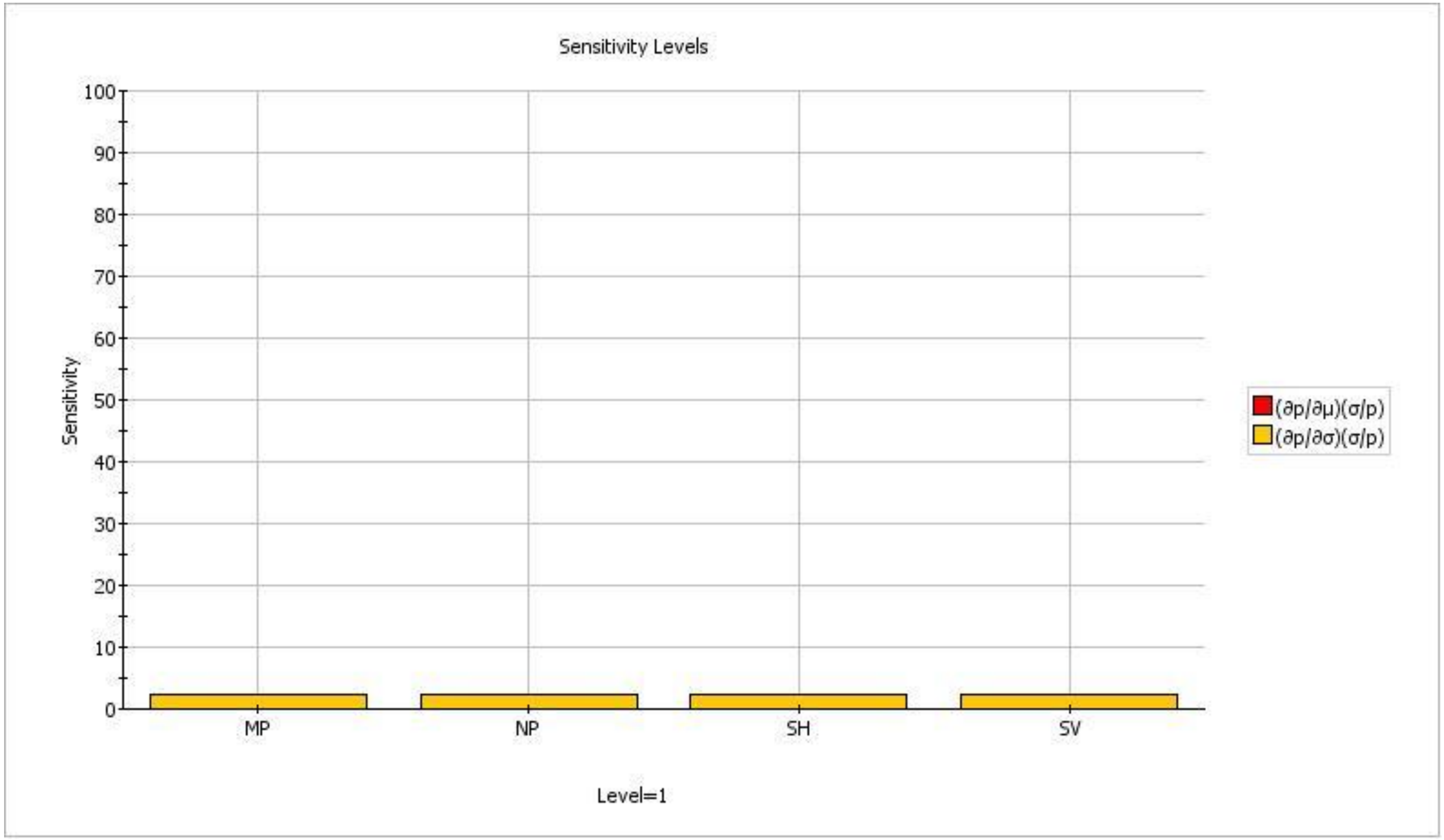

Figure C.2: System Sensitivity at Excavation Depth 3.80m with Eupper

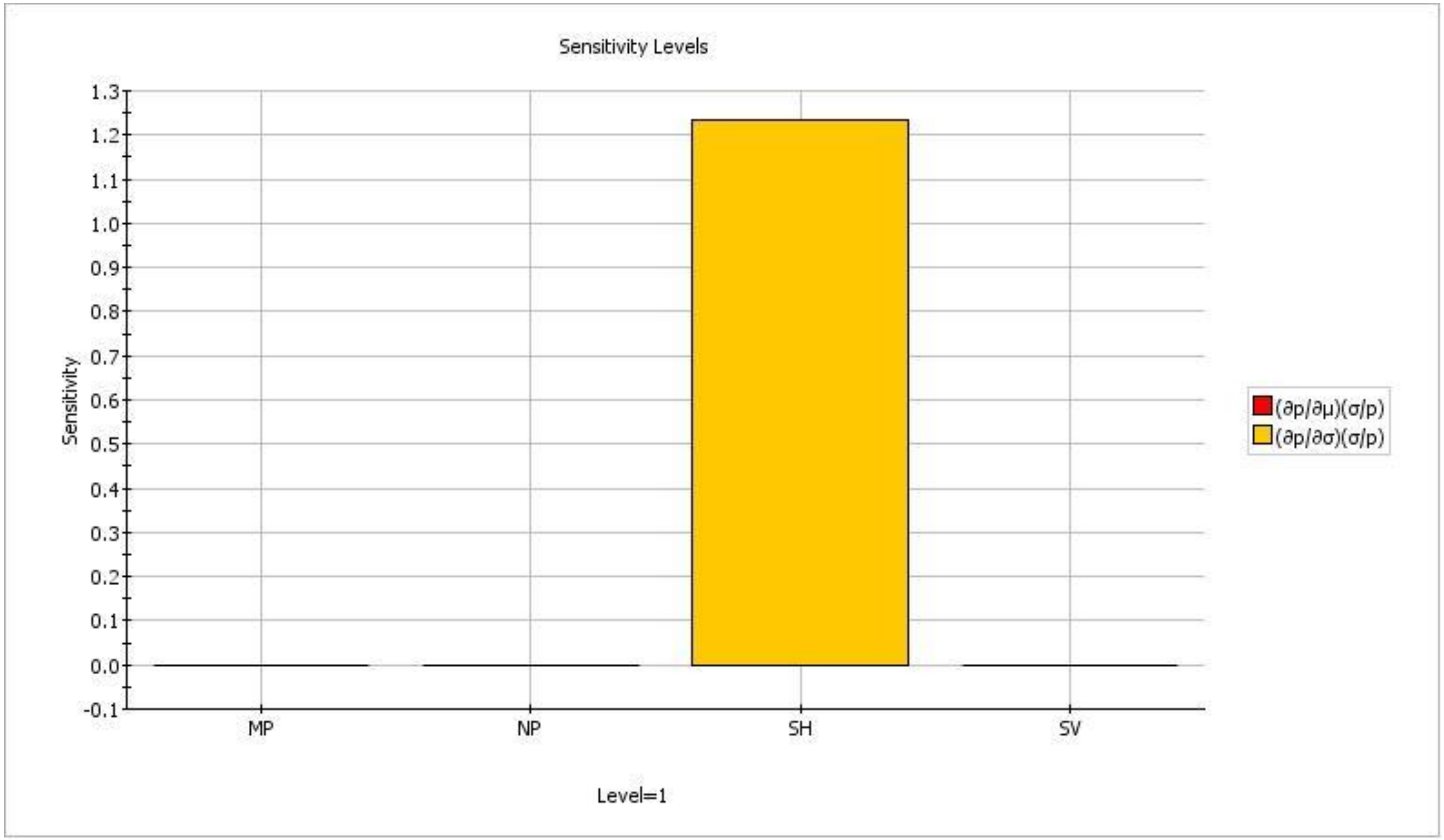

Figure C.3: System Sensitivity at Excavation Depth 3.80m with COVmax Elower

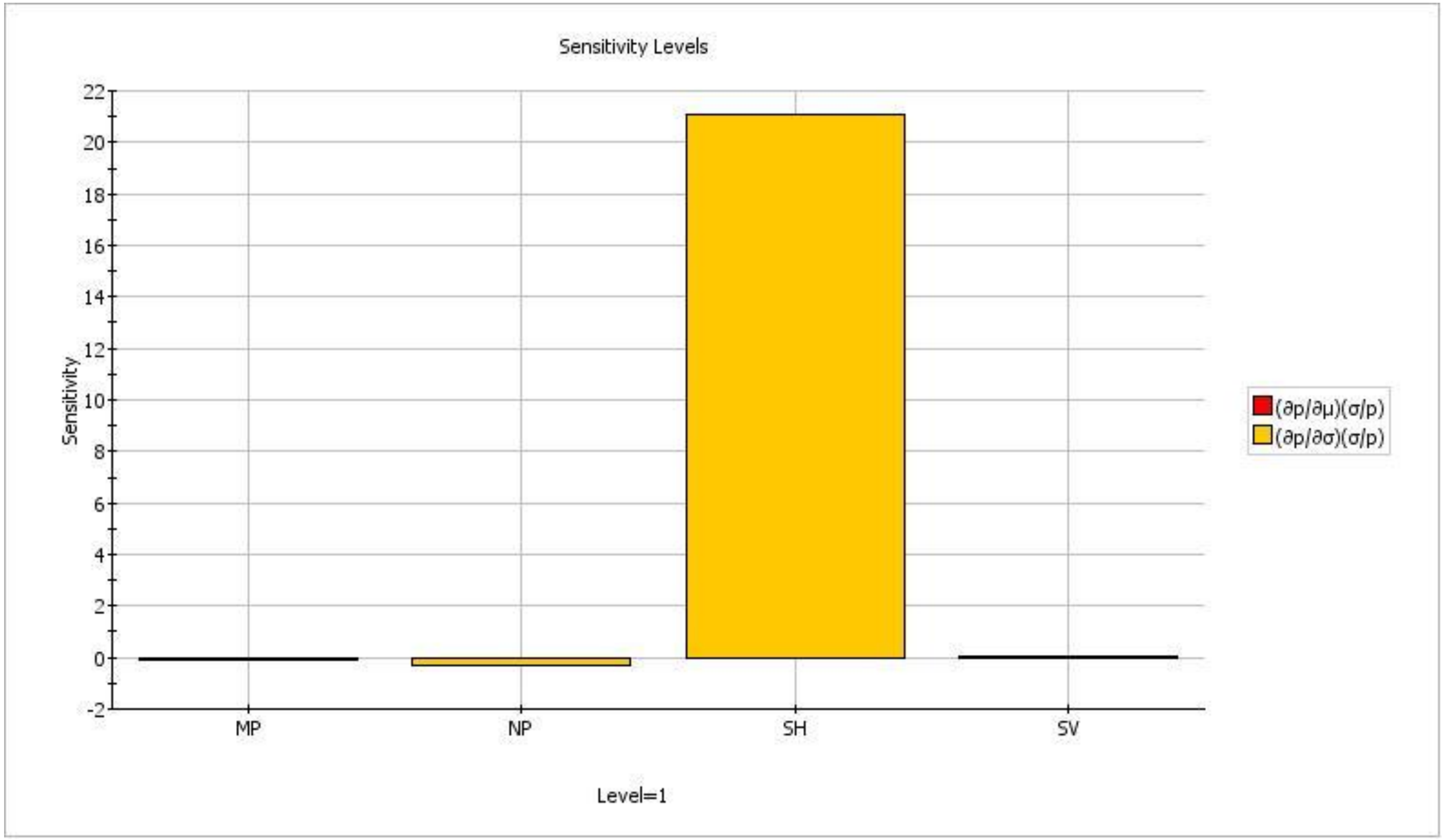

Figure C.4: System Sensitivity at Excavation Depth 3.80m with COVmax Eupper

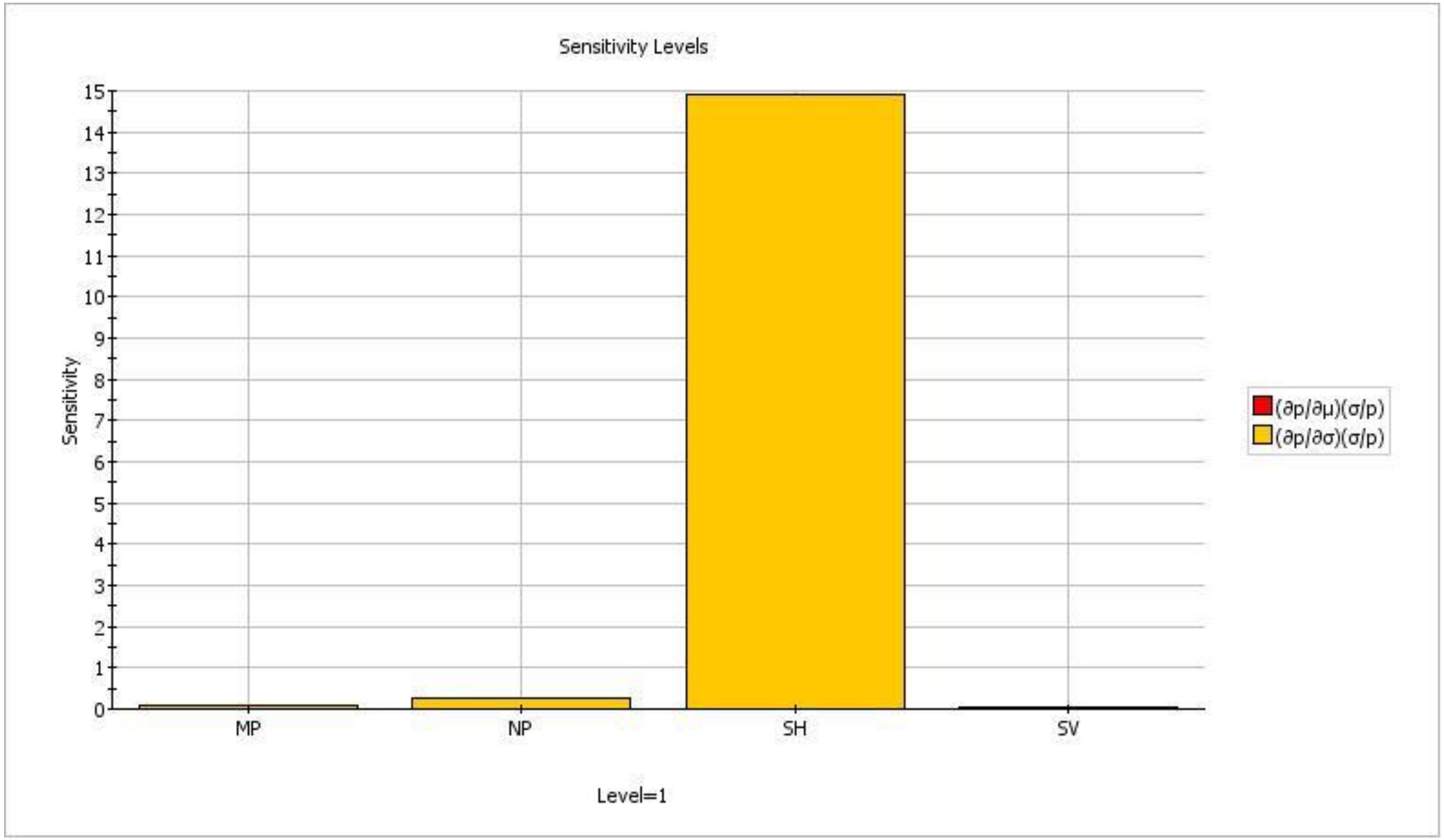

Figure C.5: System Sensitivity at Excavation Depth 7.80m with Elower

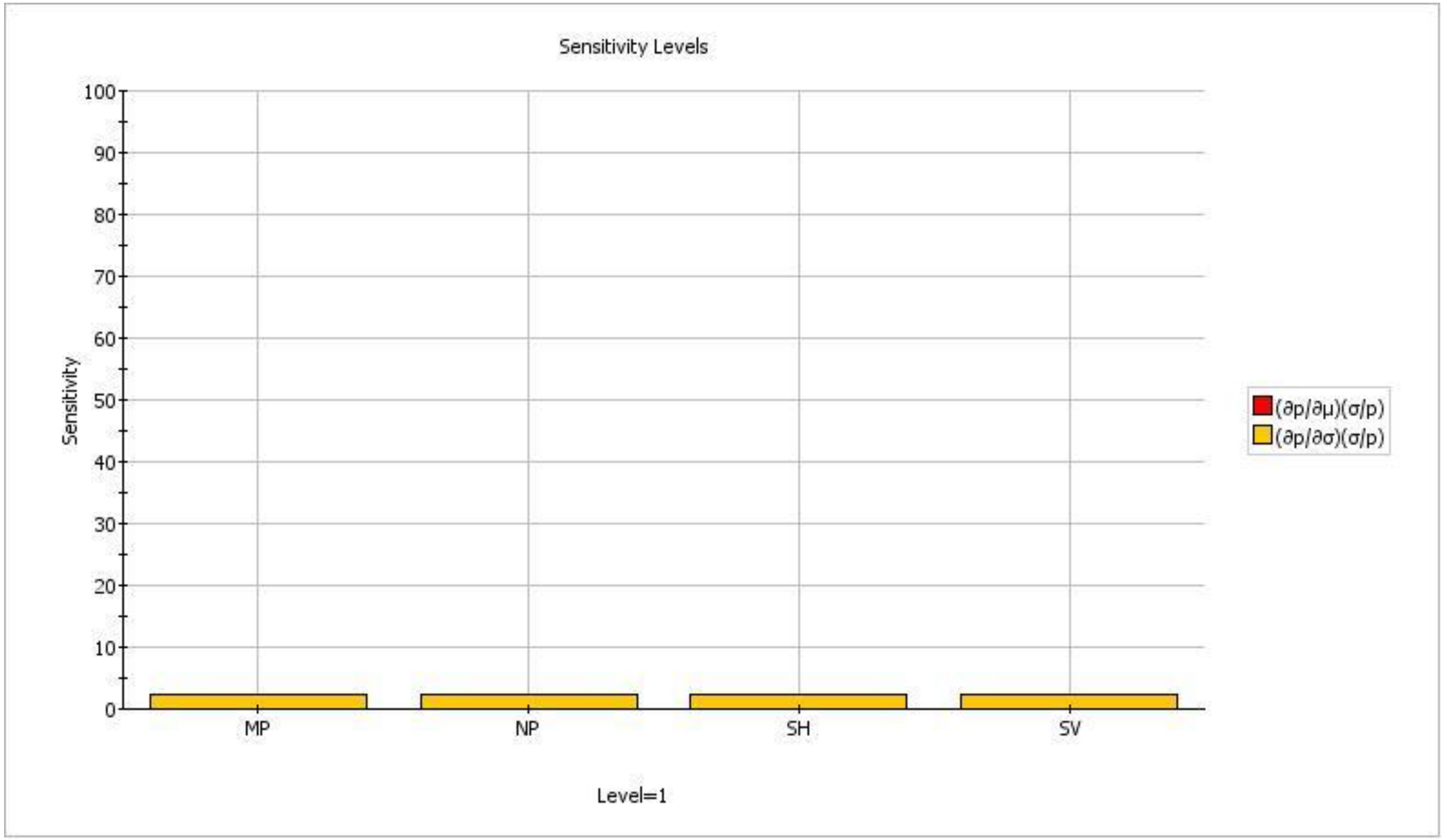

Figure C.6: System Sensitivity at Excavation Depth 7.80m with Eupper

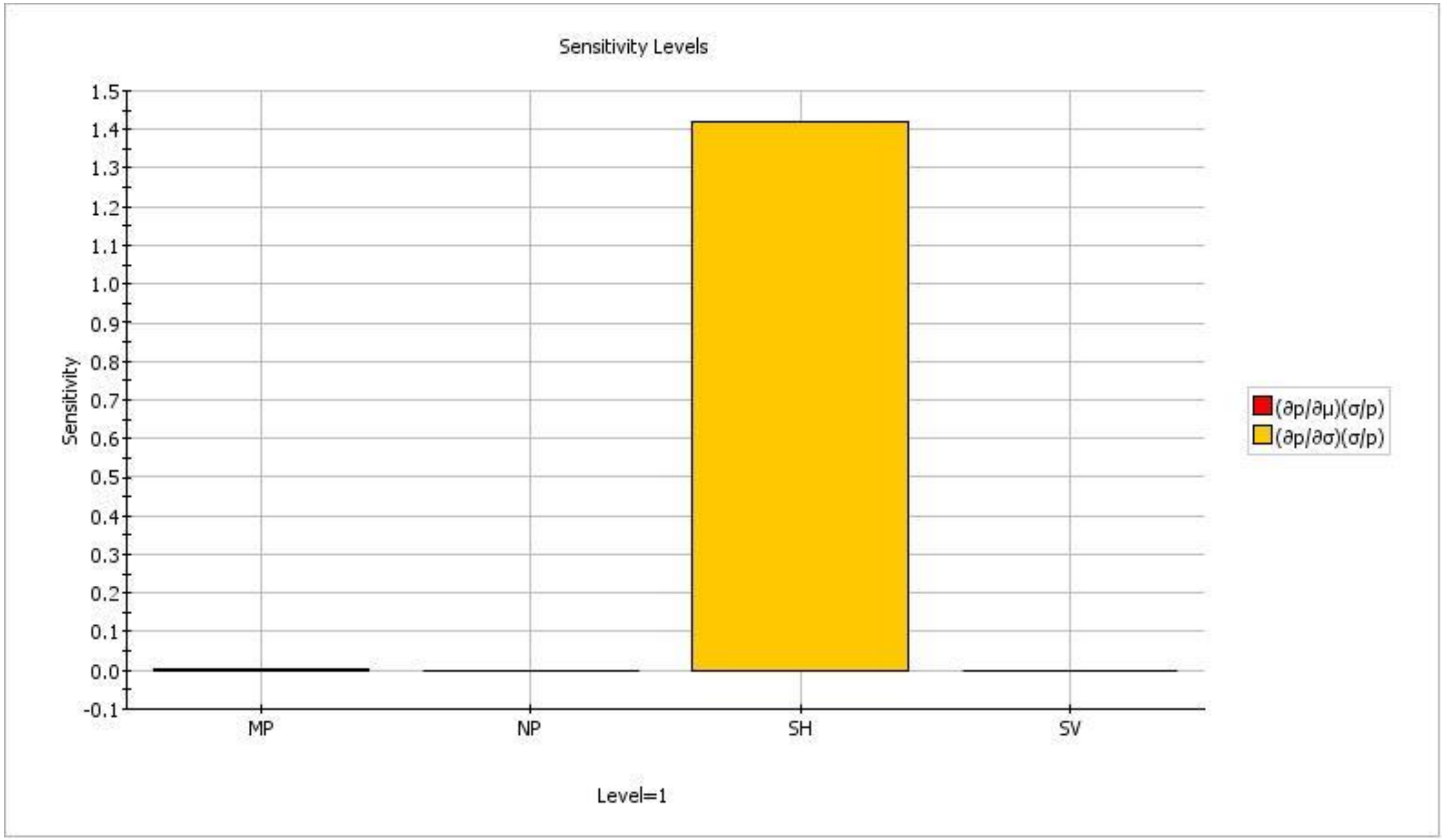

Figure C.7: System Sensitivity at Excavation Depth 7.80m with COVmax Elower

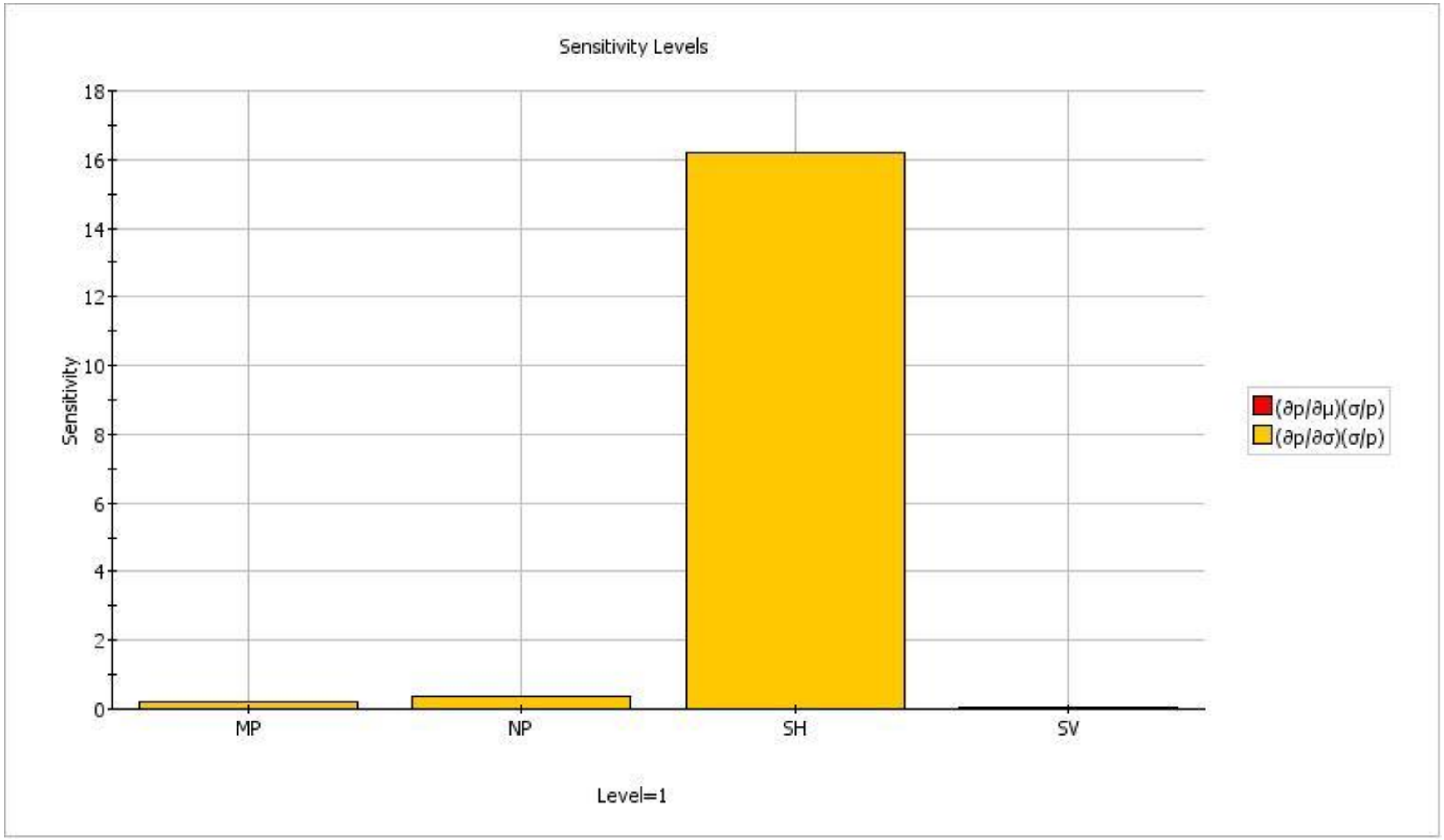

Figure C.8: System Sensitivity at Excavation Depth 7.80m with COVmax Eupper

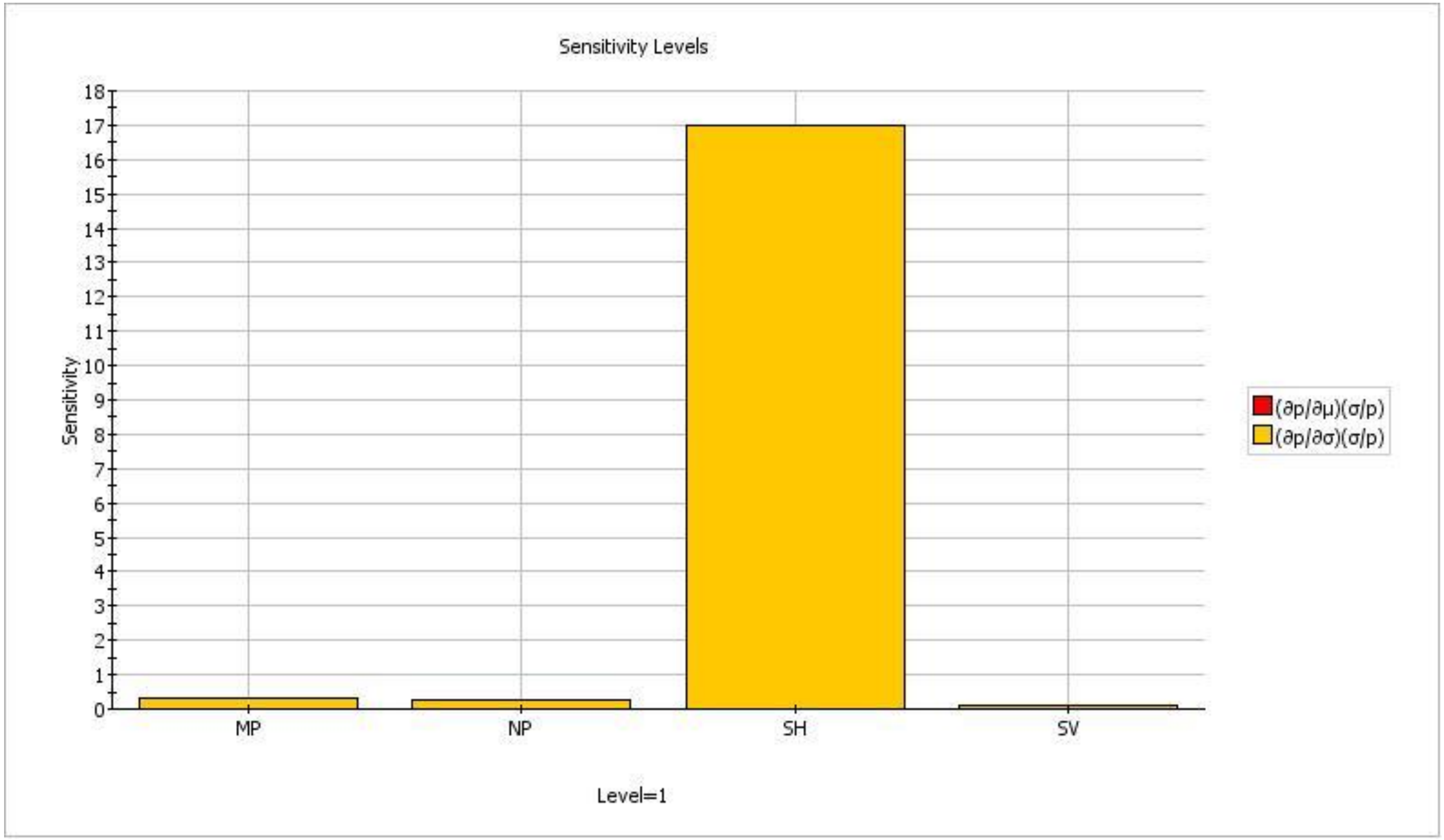

Figure C.9: System Sensitivity at Excavation Depth 12.80m with Elower

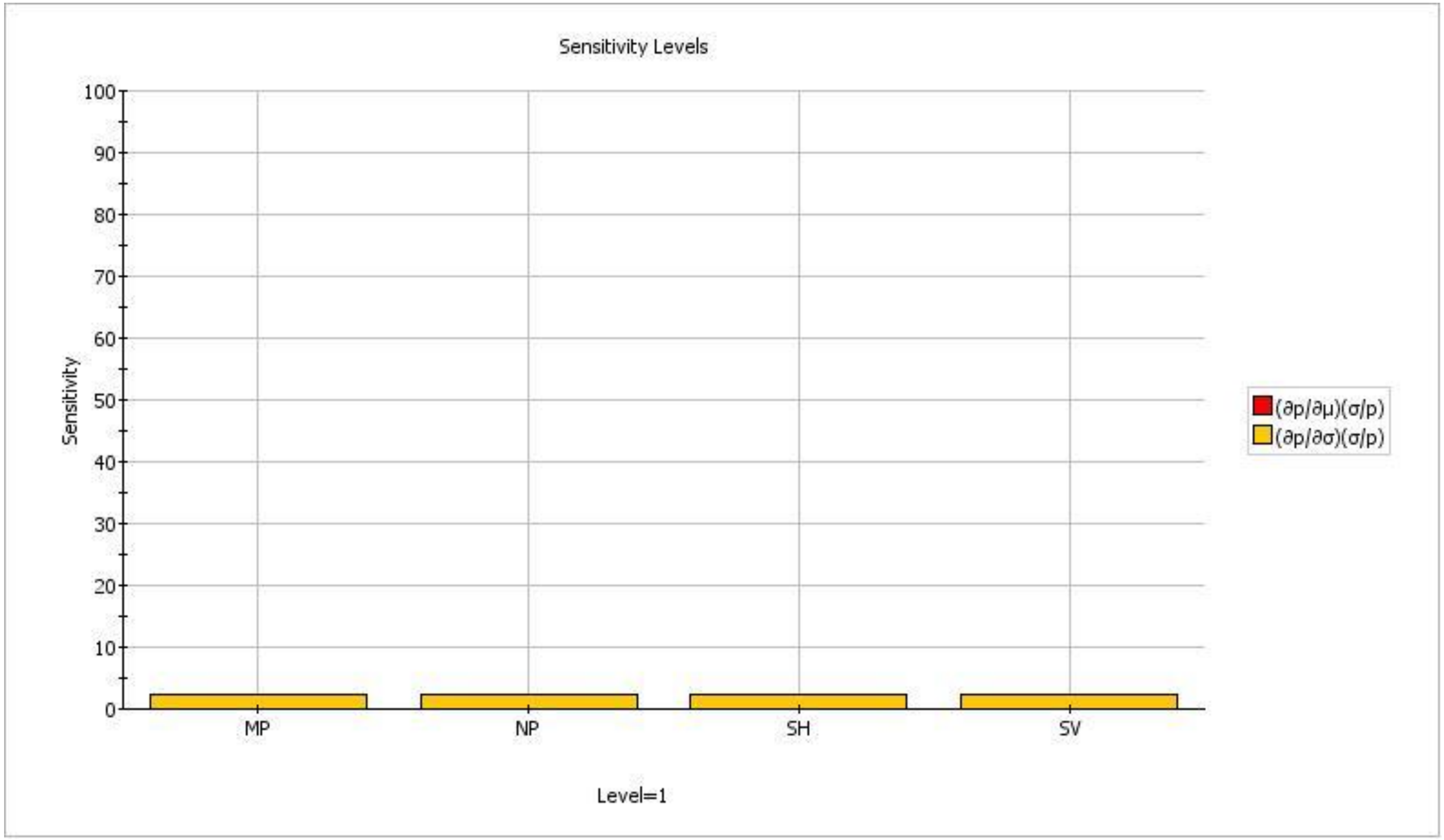

Figure C.10: System Sensitivity at Excavation Depth 12.80m with Eupper

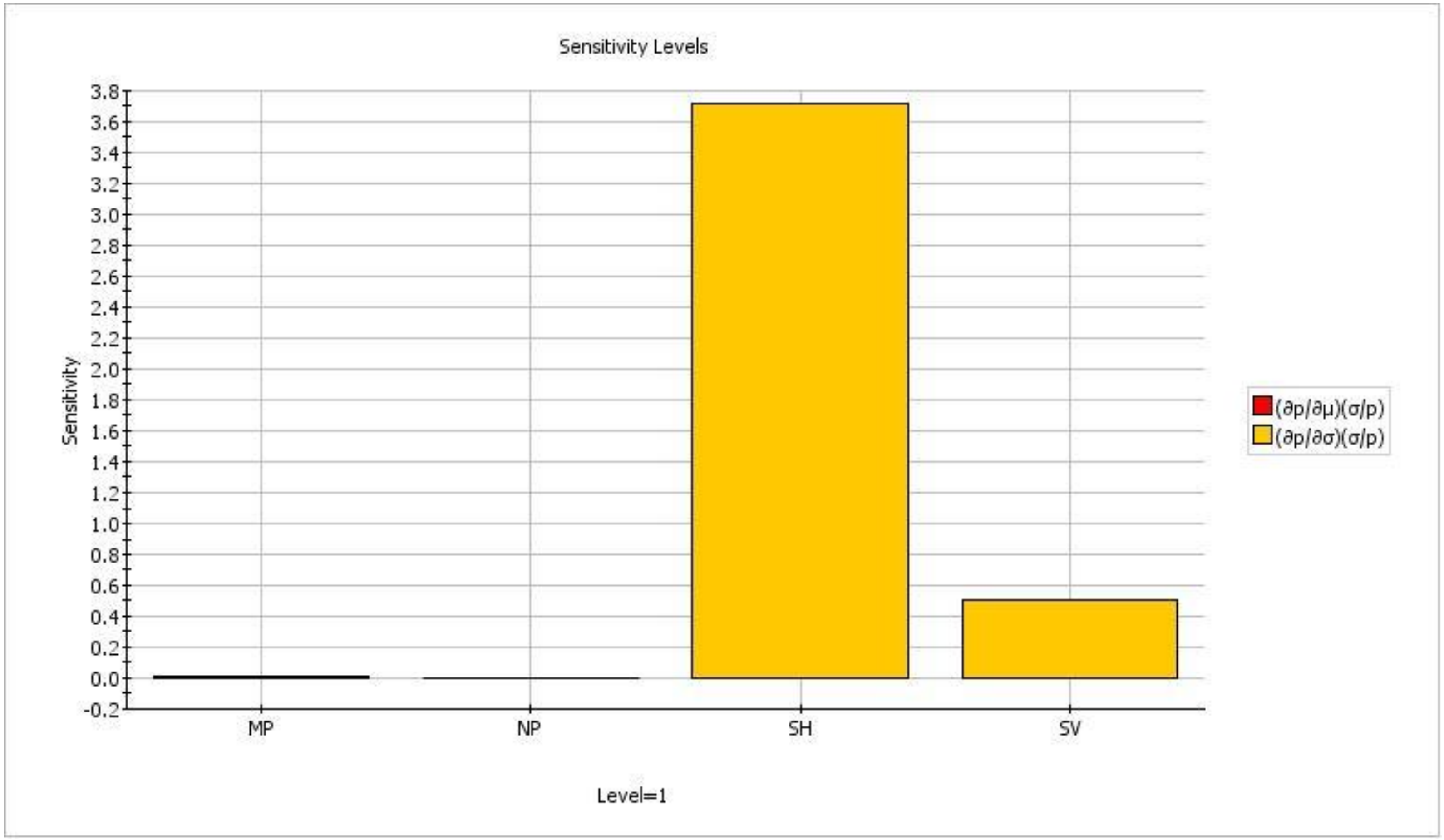

Figure C.11: System Sensitivity at Excavation Depth 12.80m with COVmax Elower

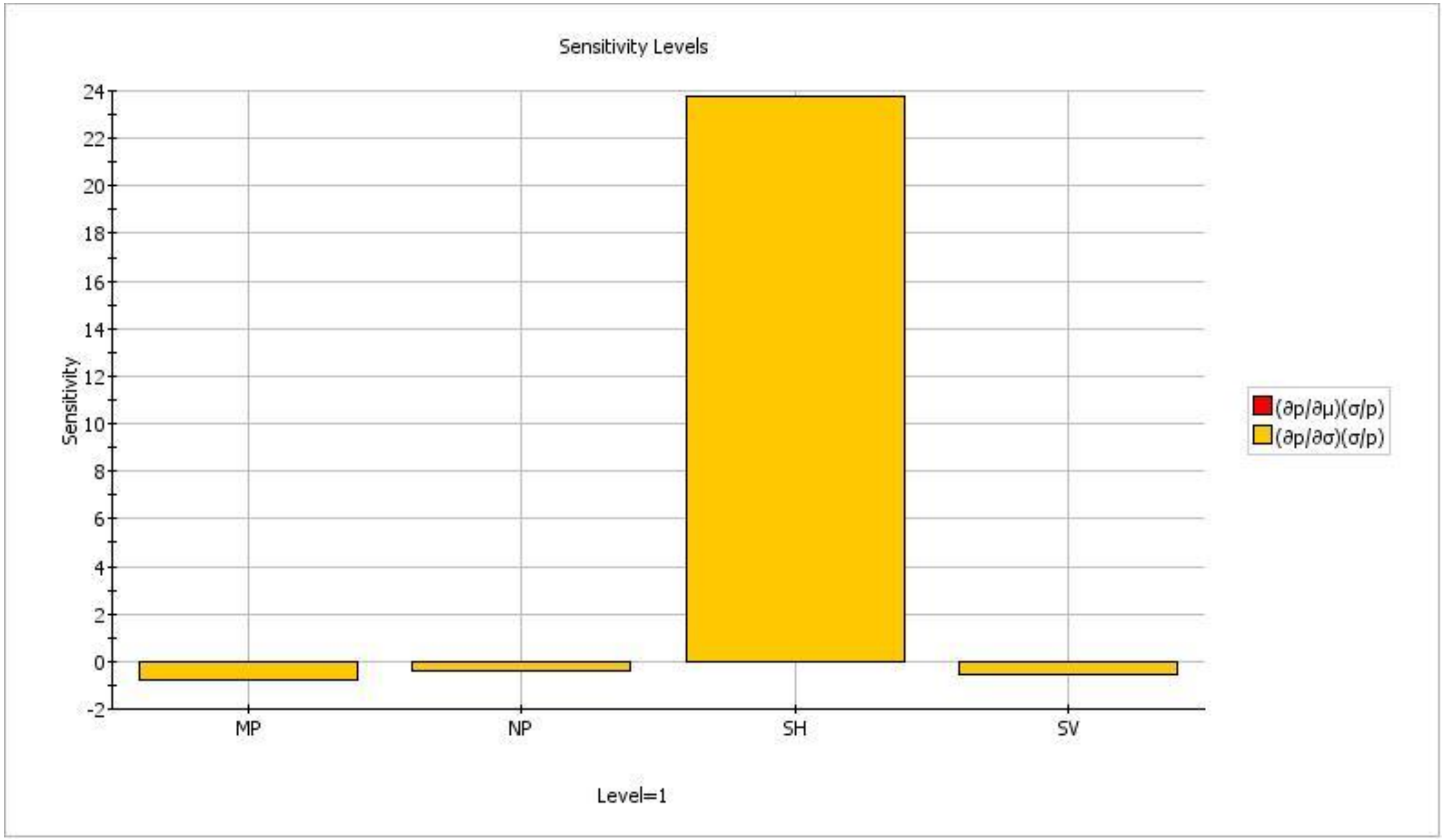

Figure C.12: System Sensitivity at Excavation Depth 12.80m with COVmax Eupper

CURRICULUM VITAE

Name Surname: Zeynep ASLAY

Place and Date of Birth: Istanbul / 1980

Address: Tola Sok. No.4 Küçükyalı, Maltepe / İstanbul

E-Mail: aslay@itu.edu.tr

B.Sc.: Civil Engineering (ITU)

M.Sc.: Geotechnical Engineering (ITU)

IT Based Construction Management (ITU)

List of Publications and Patents:

- **Aslay, Z.** (2004). Structural and Geotechnical Damages on Historical Structures and Strengthening of Their Foundations. MSc Thesis, Istanbul Technical University, 2004, Istanbul, Turkey.
- **Aslay, Z.** (2006). An Industrial Heritage: Silahtar, the First Thermoelectric Power Plant of Turkey. *17th European Young Geotechnical Engineers Confrence*, July 2006, Zagreb, Croatia.
- Sağlamer, A., Balık, E., Özalp, H.K., and **Aslay, Z.** (2007). A Deep Excavation for the Construction of a Hotel Building in Istanbul. *14th European Conference on Soil Mechanics and Geotechnical Engineering*, September 2007, Madrid, Spain.
- **Aslay, Z.** (2007). Underpinning the Historical Heritage. *14th European Conference on Soil Mechanics and Geotechnical Engineering*, September 2007, Madrid, Spain (Panelist).
- Sağlamer, A., and **Aslay, Z. (**2009). Soil Improvement Under the Foundations of a Steel Plant. *3rd Geotechnical Symposium*, December 2009, Adana, Turkey (in Turkish)
- Sağlamer, A., and **Aslay, Z.** (2009). Monitoring Deep Excavations in Istanbul. *17th International Conference on Soil Mechanics and Geotechnical Engineering*, October 2009, Alexandria, Egypt.

PUBLICATIONS/PRESENTATIONS ON THE THESIS

- **Aslay, Z.,** and Ural, D. (2012). Underground Space Use in Urban Areas. *IAHS 38th World Congress on Housing*, April 16-19, 2012, Istanbul, Turkey.